



City Research Online

City, University of London Institutional Repository

Citation: Travers, M.J. (1990). Structural correlates of shape change in the primate crystalline lens. (Unpublished Doctoral thesis, City University London)

This is the accepted version of the paper.

This version of the publication may differ from the final published version.

Permanent repository link: <https://openaccess.city.ac.uk/id/eprint/7669/>

Link to published version:

Copyright: City Research Online aims to make research outputs of City, University of London available to a wider audience. Copyright and Moral Rights remain with the author(s) and/or copyright holders. URLs from City Research Online may be freely distributed and linked to.

Reuse: Copies of full items can be used for personal research or study, educational, or not-for-profit purposes without prior permission or charge. Provided that the authors, title and full bibliographic details are credited, a hyperlink and/or URL is given for the original metadata page and the content is not changed in any way.

STRUCTURAL CORRELATES OF SHAPE CHANGE IN THE PRIMATE
CRYSTALLINE LENS

A Thesis
Submitted by

MARGARET J. TRAVERS

For the degree of
DOCTOR OF PHILOSOPHY

Department of Optometry and Visual Science
The City University

June 1990

CONTENTS

	<u>Page</u>
<u>CONTENTS</u>	2
<u>LIST OF TABLES AND ILLUSTRATIONS</u>	5
<u>ACKNOWLEDGEMENTS</u>	9
<u>ABSTRACT</u>	10
 <u>CHAPTER ONE</u>	 11
1. <u>INTRODUCTION</u>	11
1.1 FINE STRUCTURE OF THE LENS	15
1:1.1 The Capsule	15
1:1.2 The Epithelium	16
1:1.3 Formation of Lens Fibres	17
1:1.4 Lens Fibres	18
1.2 LENS SHAPE CHANGES IN ACCOMMODATION	22
1.3 CAPSULAR THEORY OF ACCOMMODATION	25
1.4 INTRA-LENTICULAR CHANGES IN ACCOMMODATION	29
1.5 EXTRA LENTICULAR CONSIDERATIONS	31
1:5.1 The Vitreous	31
1:5.2 The Zonular Fibres	33
1.6 NON PRIMATE AND PRIMATE ACCOMMODATION	33
1.7 AIMS OF THIS STUDY	37
 <u>CHAPTER TWO</u>	 38
2 <u>EXPERIMENTAL DESIGN</u>	
 <u>CHAPTER THREE</u>	 40
3. <u>LENS FIBRE MORPHOLOGY IN THE CYNOMOLGUS MONKEY</u>	
3.1 MATERIALS	40
3.2 METHODS	
	41
3:2.1 Preparation For Scanning Electron Microscopy	41

	<u>Pag</u>
3.2.2 Preparation for Light Microscopy	43
3.3 OBSERVATIONS AND RESULTS	44
3:3.1 Scanning Electron Microscopy of Natural Fracture Plains	45
- Features of the Lens Fibre Interface	47
- Changes in Lens Fibre Form with Lens Depth	52
3:3.2 Scanning Electron Microscopy of Forced Fracture Faces	56
3:3.3 Comparison of Forced and Natural Fracture Faces	57
3:3.4 Observations with Light Microscopy	58
3.4 DISCUSSION	60
<u>CHAPTER FOUR</u>	73
4 <u>EVIDENCE FOR CYTOPLASMIC FLOW IN THE ACCOMMODATED LENS</u>	
4.1 INTRODUCTION: HYPOTHESIS OF CYTOPLASMIC FLOW	73
4.2 MATERIALS TO TEST THE HYPOTHESIS OF CYTOPLASMIC FLOW	74
4:2.1 Induction of Accommodative Spasm	74
4:2.2 Unilateral Lens Dislocation	77
4.3 METHODS TO TEST FOR CYTOPLASMIC FLOW	78
4:3.1 Measurement of Surface Lens Fibres	79
4:3.2 Lens Fibre Morphology and Width Measurements using Scanning Electron Microscopy	80
4:3.3 Preparation of Sections to Test for Local Volume Changes	82
4:3.4 Methods for Counting Lens Fibre Density, and Lens Fibre Mean Cross-Sectional Area	85
- Lens Fibre Density	85
- Lens Fibre Cross Sectional Area	86
4.4 RESULTS	88
4:4.1 Comparison of Lens Fibre Morphology in Control and Drug-treated Lenses, using Scanning Electron Microscopy	8
4:4.2 Measurement of Surface Lens Fibre Width Using Light Microscopy	90

	<u>Page</u>
4:4.3 Local Volume Changes	92
- In the Dislocated/Control Pair	92
- In the Phospholine Iodide Treated Control Pair	96
4.5 DISCUSSION	98
 <u>CHAPTER FIVE</u>	 10
<u>LENS CAPSULE THICKNESS AND LENS SHAPE</u>	
5.1 MATERIALS	110
5.2 METHODS	111
5.2.1 Measurement of Monkey Capsule Thickness	111
5.2.2 Human Capsule Thickness	112
5.2.3 Experiments to Investigate the Affects of Decapsulation on Lens Shape and Capsule Thickness.	115
5.3 RESULTS	119
5.3.1 Monkey Lens Capsule Thickness	119
- Capsule Thickness in Perfuse-Fixed Lenses	119
- Capsule Thickness in Lenses Fixed in Accommodated States	120
- Thickness of Dislocated lens and Detached Capsules in the Monkey	121
5.3.2 Human lens Capsule Thickness	122
5.3.3 Lens Shape in the Monkey, With and Without the Capsule	124
5.4 DISCUSSION	127
 <u>CHAPTER SIX</u>	 137
<u>DISCUSSION AND CONCLUSIONS</u>	
 <u>APPENDIX</u>	 142
<u>REFERENCES</u>	158

LIST OF TABLES AND ILLUSTRATIONS

This list is to help locate the many figures and tables referred to in the text. It is recommended that the reader refers to the legends which accompany each figure.

S.E.Mg. = Scanning Electron Micrograph

L.Mg. = Light Micrograph

S.P = Stereo Pair

	FOLLOWS PAGE
Figure 3.1 S.E.M.: Intermediate lens fibres	44
Figure 3.2 Diagram: Definitions	45
Figure 3.3 S.E.Mg. (S.P):Nuclear fibres	46
Figure 3.4 S.E.Mg. Equatorial nuclear fibres	46
Figure 3 5 " Cortical fibres.	47
Figure 3.6 Illustration: Junctional Structures	47
Figure 3.7 S.E.Mg. Superficial cortical fibres	47
Figure 3.8 Diagram: Ball and Sockets	48
Figure 3.9 S.E.Mg. (S.P): Junctional structures	48
Figure 3.10 Diagram: Angle Processes	49
Figure 3.11 S.E.Mg. (S.P): Intermediate fibres	49
Figure 3.12 S.E.Mg. Nuclear junctional structures	50
Figure 3.13 S.E.Mg. Tongue and groove junctions	50
Table 3.1 Lens Fibre Width	51
Figure 3.14 S.E.Mg. A cortical suture	51
Figure 3.15a and b S.E.Mg: Fibres close to sutures	52
Figure 3.16 S.E.Mg: Fibre extensions at suture	52
Figure 3.17 S.E.Mg: Superficial lens fibres	52

	FOLLOWS PAGE
Figure 3.18 S.E.Mg: Development of processes	53
Figure 3.19 S.E.Mg. (S.P): Deep cortical fibres	53
Figure 3.20 S.E.Mg: Fibres, level e/f	5
Figure 3.21 S.E.Mg: Pre-axial fibres, level e/f	53
Figure 3.22 a,b and c S.E.Mgs: Fibre level d	4
Table 3.2 Junctional Structures	55
Figure 3.23 S.E.Mg: Forced fracture plane	56
Figure 3.24 S.E.Mg: Opposing forced fibre faces	56
Figure 3.25 S.E.Mg: Natural and forced fracture faces	7
Figure 3.26 L.M: Lens fibre shape	58
Figure 3.27 L.M: Change in lens fibre shape	58
Figure 3.28 L.M: Cortical fibres	59
Figure 3.29 L.M: Deep cortical fibres	59
Figure 3.30 L.M: Equatorial fibres	59
Figure 3.31 L.M: Deeper lens fibres	59
Figure 3.32 L.M: Deep nuclear lens fibres	60
Figure 3.33 L.M: Processes	60
Figure 3.34 L.M. Long section of processes	60
Figure 3.35 Illustration: Effect of Lens Fibre Shape	70
 Figure 4.1 Lens profiles (drug-treated and control)	 7
Figure 4.2 Lens profiles (dislocated and control)	77
Figure 4.3 L.M: Lens fibre paths	82
Figure 4.4 Diagram: To test for cytoplasmic flow	83
Figure 4.5 Photograph of counting equipment	8
Figures 4.6a and b: Image processing and counting.	86
Figures 4.7a and b S.E.Mg: Undulation across fibres.	88

	F L L O W	P G E
Figure 4.8 Graph: Tongue and groove orientation		89
Figure 4.9 Graph: Fibre broad face width		8
Table 4.3: Surface equatorial fibre width		90
Figure 4.10 L.M: Surface lens fibres under equator		91
Figure 4.11 Graph: Surface fibre width		91
Figure 4.12 " : Lens fibre density in the nucleus		92
Figure 4.13 Fibre thickness in the nucleus		93
Figure 4.14 " Fibre cross-sectional area - control		94
Figure 4.15 " " " - drug-treated		94
Figure 4.16 " " " - nucleus		94
Figure 4.17 L.M: Deep cortical fibres control/treated		95
Figure 4.18 Graph: Cross-sectional area, - control		96
Figure 4.19 " " " dislocated		96
Figure 4.20 Graph " " - nucleus		96
Figure 4.21 " " " - cortex		96
Table 5.1 Monkey Capsule Thickness		119
Figure 5.1 Scale drawings of capsule thickness		120
Figure 5.2 Graph: Capsule thickness in monkey		120
Figure 5.3 Graph: Capsule thickness, - accommodated		120
Table 5.2 Capsule Thickness - attached/detached		121
Figures 5.4 to 5.8 Graphs of capsule thickness		121
Figure 5.9 L.M: Monkey lens capsule (age 3 months)		122
Figure 5.10 " " " (age 11 months)		122
Figure 5.11 " " " (age 10 years)		122
Table 5.3 Human Capsule Thickness		124
Figure 5.12 Scale drawings - human capsule thickness		124

ACKNOWLEDGEMENTS

I would like to thank Professor G.L Ruskell, for all his supervision, advice and help through every stage of this study.

I am also indebted to Mr Mike Phillips, of the Department of Physics, for his instruction and help with the use of the electron microscope; Mr Darrel De Cunha of the Applied Vision Research Unit, Department of Optometry and Visual Science, for writing the image processing and cell counting program; Mr Fred Taylor and Mr. Chris Milner who produced the photographs; and Dr. A.E. Renshaw, Department of Mathematics, for his statistical advice.

I would also like to thank Dr. M. Bolton, of the Institute of Ophthalmology, London; Mr. M. Kerr Muir F.R.C.S. of St.Thomas' Hospital, London; Mr. J. Cooper of the Royal College of Surgeons, Downe, who all went to considerable trouble to assist with supply of materials.

Sincere thanks are also due to my parents, for their encouragement and to my husband, Gary Stafford, who wrote the software for our home computer, for his support and patience.

DECLARATION

I grant powers of discretion to the University Librarian to allow the copying of this thesis, in whole or part, without further reference to myself.

ABSTRACT

Cytological changes associated with accommodation in macaques and man were investigated using light and scanning electron microscopy to examine lenticular fibre modification and the role of the lens capsule.

Accommodation was simulated monocularly in one animal with local administration of 1/4% phospholine iodide and by dislocation in another followed by fixation by perfusion.

Three types of junctional structures were observed: angle processes were found at all depths, ball and sockets in outer lens zones, and tongue and grooves in the deeper lens. Interfaces lacking junctional structures were not present and the concept of sliding between fibre layers to permit curvature changes was rejected.

The hypothesis of intracellular redistribution of cytoplasm within lens fibres was tested, by comparing fibre cross sectional area throughout the posterior half of accommodated and unaccommodated lenses. In one animal evidence for cytoplasmic flow was found throughout the lens but was greatest in the nucleus. In the other, showing less curvature difference, evidence was restricted to the nucleus and superficial cortex. The thin superficial cortex is probably of little significance in effecting shape change. Consequently the results support the notion of greater nuclear than cortical action in accommodative shape changes. The fibres of the intermediate and deep cortex are remarkably thin and indented and are arguably less conducive to cytoplasmic flow.

Lens capsule thickness was measured in 23 monkey and 11 human lenses in situ and detached, giving similar results. Profiles were recorded of unfixed monkey lenses with and without capsules. An annular zone of flattening, nearly coincident with maximum capsular thickness, giving the classical "lenticonus" form, reduced on decapsulation. The young human and monkey capsule thickness variation was consistent with classical rather than more recent data thinnest at the posterior pole and thickest near, not at the equator.

The results demonstrate a role for capsular shaping of the accommodated lens (with or without local moulding), effected by cytoplasmic flow most marked in the nucleus.

INTRODUCTION

Reading, writing, and written language - all fundamental to human civilisation - depend on near vision.

The young human eye has a flexible optical system enabling clear vision from infinity down to the near point. This accommodation is achieved by increased curvature of the crystalline lens, resulting in an increase in dioptric power. This lens is a transparent, optically dense, flexible biconvex living lens located between the primary fixed refracting surface of the cornea and the light sensitive retina.

Unfortunately this accommodative power reduces with age and by middle age, reading glasses are required to assist clear focus of near objects.

The crystalline lens is suspended radially from the ciliary body by the zonula fibres attached on either side of its equator. The ciliary body encircles the lens and is roughly triangular in cross section. It forms a separated ring roughly concentric with the lens, being attached anteriorly in the scleral spur, and posteriorly at the Ora Serrata. When the muscle within this ciliary body contracts, the body swells radially and reduces the ciliary annulus which via the zonules, allows the elastic lens to take up its preferred accommodated (and more spherical) state. Tension is returned to the lens zonule system by relaxation

of the ciliary muscle, causing the lens to flatten ready for distance focusing.

Lens fibres are arranged in layers like an onion around the embryonic primary lens fibres and are surrounded by an elastic capsule which is a thickened basement membrane secreted by the lens epithelium. New lens fibres are continually formed by the epithelium, so that the lens increases in size throughout life. Lens fibres appear to be tightly joined by a network of junctional structures and membrane modifications, with little intracellular space. The vitreous humour lies behind the lens, the aqueous in front with the lens itself having the higher refractive index.

Accommodation has been the subject of many studies and theories but relatively little is known of intra lenticular changes in accommodation. By contrast, much has been written on lenticular shape changes and the role of the ciliary body, zonules, vitreous, and capsule, etc. but most details of the accommodative mechanism remain controversial.

Descartes (1596-1650) first suggested that accommodation could be achieved by a change of crystalline lens shape and Thomas Young (1801), after discrediting the alternatives, (corneal steepening, globe elongation, etc. showed that the lens did indeed steepen to achieve the power increase of accommodation. The missing link for Young, the ciliary muscle within the ciliary body, was demonstrated by Brucke and Bowman in 1848 and this opened a flood-gate o

speculation on the accommodative mechanism.

Our present understanding of the accommodative process is based on the ideas of Helmholtz (1858) who first suggested that contraction of the ciliary muscle and reduction of the ciliary annulus, relaxed tension in the zonules. Hence a shape change occurs in the elastic crystalline lens. Conversely, relaxation of the ciliary muscle, increased the tension on the zonules, flattening the lens and decreasing its axial thickness. Helmholtz's theory was opposed because it did not explain the loss of accommodation with age, or the more conical or hyperbolic shape of the anterior and posterior surfaces reported during accommodation by Tscherning (1895,1909) and Von Pflugk (1935).

The Problem

How does the internal lens react to the shape change during accommodation? This question was posed at a Ciba conference (in 1973) and met with divided opinion amongst the leading authorities who had gathered to discuss progress in cataract research. Brown (1973b), who had just completed his experiments on the change in lens shape and internal form during accommodation, suggested two possibilities: either redistribution of lens fibres or redistribution of cell matrix within lens fibres. Fisher (1973b) favoured the idea of fibres sliding and thus redistributing the lens fibres, because the Young's modulus of elasticity of the

whole lens was low compared with that of individual fibres. Philipson (1973), suggested that the prevalence of junctional complexes fusing the adjacent lens fibres would inhibit sliding but the great length of lens fibres would facilitate movement within them.

It was this discussion that inspired the present study. What does happen at lens fibre level during accommodative shape changes? Are there areas of absent or reduced junctional structures? Is sliding a possibility, or do the lens fibres change shape? Scanning electron microscopy methods, in addition to conventional light microscopy, were chosen because of the three-dimensional visualisation of surfaces .

Current researchers into the cytology of the human lens have centred on trying to understand its loss of clarity in cataractogenesis. The other important property of the crystalline lens, that of dioptric power changes to allow the eye to focus from far to near, receives much less attention. There is interest still in the full accommodative mechanism, but in recent years the lenticular role has come under scrutiny, with the function of the lens capsule, geometry of zonular attachments and vitreous effects on the posterior form (if any), attracting attention. Very little is known of the intra-lenticular reaction in accommodation. Brown (1973a) using Scheimpflug slit lamp photography (Brown 1972a and b) in a greatly refined version of

Patnaik's (1967) earlier study, illustrated greater nuclear than cortical axial thickening in accommodation. This has since been confirmed by Koretz et al. (1984). Fisher's (1971) work on lens elastic properties also suggests the nucleus has a more active role than the cortex in lens shape changes.

1:1 FINE STRUCTURE OF THE LENS

Theories of accommodation tend to consider the lens as an obliging transparent bag, but it has a highly organised structure.

1:1.1 Lens Capsule

The lens capsule encases the lens. It is a highly elastic, replicated basal lamina (Rafferty 1985), formed from the basement membrane of the epithelium. With the light microscope, the capsule appears homogeneous, but a laminar nature is revealed with electron microscopy. Each lamina consists of sheets of tiny parallel collagen filaments (Seland 1974). The capsule's elasticity may be due to a superhelical arrangement of filament strands, (Fisher and Wakely, 1976,- cat, and Fisher and Hayes, 1979,- rat). There is a denser outer layer, which is believed to contain a mixture of capsular collagen filaments and zonular elastic microfibrils (Cohen 1965).

Zonular fibrils run tangentially to the lens surface at

their attachment into the capsule (Seland 1974). Most penetrate only a short distance into the capsule, but some bundles of these fibrils are found as deep as the epithelial surface.

The human lens capsule is a fairly even thickness at birth, about $4\mu\text{m}$ around the anterior and equatorial lens, thinning slightly at the posterior pole to $3.5\mu\text{m}$ (Seland, 1974). As the lens volume increases, the capsule has to grow (Fisher and Pettet, 1972) and it continually thickens anteriorly and equatorially (Salzmann, 1912). The capsule increases in thickness, by deposition of new lamellae, either on the inside of new lamellae, (Lerche and Wulle, 1969) or added at the inner surface and pushed through towards the outer surface (Rafferty and Goosens, 1978a).

1:1.2 The Epithelium

The epithelium is of interest here, because lens fibres are formed from these cells.

The lens epithelium is derived from the original cells of the lens vesicle. In the mature lens, it forms a monolayer beneath the anterior and equatorial capsule. Except at the equator, where differentiation and elongation occur, cells appear cuboidal in section, and roughly hexagonal in flat mount. Neighbouring cells, have complex interdigitations with each other, (Wanko and Gavin, 1958; Cohen, 1965; Kuwabara, 1975; Farnsworth et al., 1976), but

are smoother along their basal faces underlying the capsule, and their apical interface with the lens fibres. The basal surface of the epithelial cells, although fairly smooth, does show interdigitation with the basal lamina, at each lateral cell border, and this attachment appears tightest centrally, (anterior pole) where crater-like structures are also found (Farnsworth et al., 1976b). The lateral and apical plasma membranes also have junctional specialisations, desmosomes, and gap junctions (Kuwabara 1975). Tight junctions have been also found close to the capsule, between epithelial cells in the chick (Maisel et al., 1981) and may occur in the human (Cohen, 1965).

Epithelial cells have a role not only in lens fibre production, but in synthesis of lens crystallins, ion transport, and secretion of capsular precursors, and are rich in cytoplasmic organelles. Desmosomes are consistent with cell adhesion, tight junctions with sealing off, and gap junctions with metabolic communication and adhesion.

1:1.3 Formation of Lens Fibres

Epithelial cells divide, pre-equatorially, the new cells moving outwards, to the posterior equator, where they elongate and differentiate into lens fibres. The apical end of the cell pushes forwards, under the epithelium and over the next youngest cortical lens fibres, to terminate eventually forming an anterior suture, whilst the basal process moves backwards, beneath the posterior capsule until

they meet at posterior sutures. As they elongate, cytoplasmic organelles decrease and with the exception of occasional mitochondria, disappear. The nucleus breaks down about the same time as the basal end terminates (Kuwabara, 1975). Interdigitation increases and at the sutural ends, bispheroid terminal bodies (of unknown significance) form from aggregations of ribosomes (Worgul et al., 1977). Desmosomes become rarer and disappear, but gap junctions proliferate as the membrane enlarges (Benedetti et al., 1974). Cohen (1965) reported tight junctions between cortical lens fibres, but Benedetti et al., (1976) suggest that these may have been gap junctions. There is an increase in density of the cytoplasm, which becomes more fibrillar and there are also changes in the cytoskeleton (Kuwabara, 1968).

1:1.4 Lens Fibres

The great bulk of the lens is composed of lens fibres. The lens nucleus contains the original embryonic (primary) lens fibres, surrounded by the fibres of the foetal nucleus, which join at the Y sutures, and then in turn the postnatal lens fibres of the adult nucleus. These latter and those of the cortex, terminate at more complex branching sutures.

Cortical fibres are very thin, roughly hexagonal in cross section, and very long. They are slightly spindle shaped, being wider as they cross the equator (Hogan et al.,

1971; Kuszak & Rae, 1982; Brown et al., 1987). Though lens fibres of different species vary in size and shape, they are cytologically similar (Wanko and Gavin, 1961).

Ultrastructural studies of the human lens are hampered by difficulties with fixation. Fixatives do not penetrate well beyond the most superficial cortex.

Lens fibres from the cortex of the young human, are approximately 7-10 mm in length, roughly hexagonal in section, and appear tightly joined by complex interconnections (Cohen, 1965; Hogan et al., 1971; Jongebloed et al., 1987 and others). Specialised gap junctions are abundant, and often associated with processes. In chicks gap junctions have been reported to involve up to 60% of the membrane (Kuszak et al., 1978). It is thought that the gap junctions allow metabolic communication throughout the avascular lens, and these seem to be adapted to their unusual environment (Goodenough, 1979; Benedetti et al., 1981; Costello et al. 1984). However electrical coupling by lens gap junctions, has still to be demonstrated in primates.

Using scanning electron microscopy (SEM), three types of fibre surface structures have been identified. Interlocking protrusions (Willekens and Vrensen, 1982, - human) along the six edges of the lens fibre, appear to join adjacent fibres. There is some variation in their size, shape and frequency between species, as can be guessed at from the variety of descriptive terms used in the literature. They have variously been described as a zipper

system (Jongebloed et al., 1987,- human), knobs and sockets (Kuwabara, 1975 -human), ball and sockets (Dickson and Crock, 1972 -monkeys), jigsaw interlocking processes (Leeson, 1971 rat), ball and sockets, flaps and imprints (Kuszak et al., 1980,- chick; Kuszak and Rae 1982,- frog). Wanko and Gavin (1961) noted that these interdigitating processes are more common in the areas of greatest shape change, - the equator and periaxial zones, speculating that they may have a role in accommodation. Dickson and Crock (1972) noted that these processes (which they also called ball & sockets) became more prominent in the deeper cortical and nuclear zones of the monkey lens.

A second type of 'ball and socket' junction was described as occurring on the lateral faces, of human lens fibres, by Willekens and Vrensen (1982). These only connect two lens fibre faces, (whereas the edge processes interconnect three fibres) and are most profuse in the cortex, para equatorially, where perhaps zonular forces are most evident. Gap junctions have been observed in association with ball and sockets, (Cohen, 1965; Goodenough et al., 1980; Kuwabara, 1975 etc.) Only the more recent work using SEM (Willekens and Vrensen, 1981,1982; Carhart, 1981) have distinguished between ball and sockets processes and the interdigitating angle processes, since with transmission electron microscopy (TEM) these protrusions present a similar appearance.

In the deep cortex and nucleus, all six surfaces can

display linear folds (Kuwabara, 1975- man), sometimes called tongue and groove junctions (Dickson and Crock, 1972- monkey), or micro-*plique* (Willekens & Vrensen, 1982- man). Their distribution and form varies between species and their function is unclear, but Dickson and Crock wondered if they aid in reducing lateral sliding between lens fibres. Kuszak et al. (1988) in a recent study, using stereopair SEM and thick section TEM micrographs, have described the areas of furrowed membrane as microvilli laying flat on their sides, and re-attached apically. This suggests that the deepening tongue and groove pattern in the oldest fibres are a consequence of age, and perhaps have no role in accommodative shape changes.

Another specialisation visualised by S.E.M. is the scalloped borders seen in superficial cortical fibres of rodents (Rafferty, 1985) and in deeper cortical fibres of the rabbit (Willekens & Vrensen, 1981). Also folds or wrinkles are sometimes seen around the equator.

Lens fibres have a cytoskeleton. Microtubules increase in number as the new lens fibres elongate, and orientate along the axis of the fibre (Kuwabara, 1968). Their presence in the nucleus is controversial, and they may have a structural role. It has been suggested that microtubules give the lens fibres their visco-elastic properties (Burnside, 1975; Farnsworth et al., 1980a).

Cytoplasmic filaments are thought to be actin filaments (Rafferty, 1985; Rafferty and Goossens, 1978b). There may be differences between those of species with non-accommodating

spherical lenses and those with flattened accommodating lenses (Rafferty and Goossens, 1978b).

One aim of this study was to investigate the morphology of primate lens fibres, with a view to understanding intra-lenticular mechanisms of accommodation in man. Since this study began, scanning electron microscopy of normal human lens fibres has been reported (Jongebloed et al., 1987; Willekens and Vrensen, 1982). Kuszak et al. (1988) have looked at the morphology of the deepest fibres of the primate nucleus (including the cynomolgus monkey) describing the tongue and groove surface pattern as furrowed membrane domains overlain with microvilli. However there is still a need for a comprehensive study of the primate lens, especially the nucleus, since there is evidence (Brown, 1973a) in support of greater nuclear accommodative shape change.

A second, smaller aspect of this study, considers the lens capsule, and its relation to accommodative curvature changes. It became apparent during the study, that the lenses of man and monkey differ in some details. These differences may be of value, to understanding the lenticular reaction to accommodation, in both species.

1:2 LENS SHAPE CHANGES IN ACCOMMODATION

The human lens increases dioptric power in accommodation to allow focusing of nearer objects, by

steepening mostly its anterior surface, (Fincham, 1937; Brown, 1972b). The posterior surface was thought to change little, (Helmholtz, 1909; Fincham, 1925), but Brown (1973a) has shown that it has a small contribution, whilst Koretz and Handelsman (1985) suggest that in advancing presbyopia, it is the posterior surface that struggles on to produce small accommodative changes, after the anterior surface has ceased to respond.

The exact form of both anterior and posterior lenticular surfaces is still a source of controversy, though contrary to traditional wisdom (Donders, 1864; Priestly Smith, 1883), Brown (1974a) has shown that both surfaces slowly steepen with age after the initial flattening of infancy. Helmholtz reported an anterior parabolic shape, that steepened centrally on accommodation. Zeeman (1908) found a doubling of an image reflected from the peripheral (3.5 mm from optic axis) posterior lens surface in the living human eye, suggesting a peripheral flattening, or even a furrow. Von Pflugk (1906, 1935) recorded a peripheral flattening accompanying the central steepening. This form is sometimes referred to as the lenticonus, because of its similarity to the shape of the accommodating diving bird lens, achieved by the dissimilar mechanism of direct ciliary and iris pressure. Young (1801) then Tsherning (1904) found a reduction or even reversal of the spherical aberration (barrel to pincushion distortion) of the isolated human lens, when changing from its unaccommodated form to

accommodated shape. This also indicated that the lens steepens more centrally with relative peripheral flattening. Fincham confirmed this finding in primates, but not other mammals. Slit lamp studies of young human eyes (Fincham, 1937) indicated much individual variation, with some young unaccommodated anterior lenses approximating to a spherical form within the visible pupil area, whilst others deviating more from the spherical, showed steeper curvature centrally than peripherally, as was always the case in accommodation. Fincham called this form a conoid, (a conoid is a solid shape, formed by the revolution of a conic section about its axis.) He found the posterior form was never spherical, but was often close to parabolic.

Fisher (1969b) described the anterior form of the excised human lens in section, as elliptical, whilst Howcroft and Parker (1977) found hyperbolic more appropriate, agreeing with Fincham on a parabolic posterior surface.

Brown (1973a) in his important slit-lamp study of the lens, photographed the lens shapes in human subjects aged 11, 19, 29, 45 years, relaxed and in different accommodative states. He attempted to fit the nearest spherical curve for the central (diameter=1.6mm) and mid peripheral anterior (4-7.2mm) and posterior (3.2-6.4mm) lens curvatures. He found that whilst in the relaxed unaccommodated state, the anterior surface was close to spherical over the visible area, in most accommodated states, both central areas

steepened more than the peripheral, whilst in the three older subjects both peripheral curvatures actually flattened. This suggested that the 'conoid' form does not exist in children. Brown's pictures were reassessed by Koretz, Handelman and Brown (1984), who concluded that all the curves (including internal curves) could fit parabolas.

So, there is agreement only in so far as the lens surfaces are not usually spherical! This point, however was one of the objections in the acceptance of Helmholtz theory, since it has been argued (Tsherning, 1909; Von Pfluck, 1935; Coleman, 1970) that a conoidal (parabolic, elliptical etc.) lens shape could not occur from radial zonular tension alone.

1:3 CAPSULAR THEORY OF ACCOMMODATION

Salzmann (1912) measured the thickness of 17 human lens capsules ranging in age from 14 days to 71 years. He commented on the wide variation of thickness both among individual lenses and between lenses of different ages. The thinnest point of each lens capsule was always at the posterior pole (2-3.4 mm), with the anterior and equatorial capsule being thicker. The thickest parts of the capsule formed two zones concentric with the equator, one anterior about 3 mm from the anterior pole, one posterior more peripherally placed. The thickness at the anterior pole showed some increase with age whilst at the posterior pole there was little change. Salzmann commented that these

thickened zones, correspond to the areas of relative flattening reported anteriorly by Tsherning (1904) and posteriorly by Zeeman (1908) and Von Pflugk (1909), but speculated no further.

Helmholtz's theory considered the whole lens to be elastic, though he was aware of the elastic nature of the lens capsule, and had mentioned its possible role in supplying some of the elastic force to oppose the zonules, but it was Fincham who explored this point. He confirmed Salzmann's finding of peripheral thickened capsular zones, in human lenses of unknown age, noting that the anterior maximum occurred slightly closer (2mm) to the pole than Salzmann's finding of 3mm.

Fincham (1929) measured the capsular thickness of several mammals. In those believed incapable of accommodative lens shape changes, (reindeer, sheep, rabbit) he found a fairly consistent anterior capsular thickness whilst in the primates (monkeys, baboon, man) he found the peripheral thickened zones noted by Salzmann. He noted that the monkey (*cynomolgus*) lens flattened and lost its central conoidal form on decapsulation, whilst the more spherical (non-accommodating) sheep lens remained almost unchanged. He concluded that since the conical accommodated anterior lens form (demonstrated by the 'pincushion' distortion of the released lenses) only appears in lenses with a variable capsular thickness, that the elastic capsule has a role in differential lens shape moulding, in other words, the thickened peripheral capsular zones cause the relative ring

of flattening around the steeper central form in accommodation.

This idea of lens capsule deformation dependence on capsular thickness, was supported by O'Neill and Doyle (1968) in their "Thin Shell Deformation Analysis of the Human Lens," in which they calculated incremental pressure changes (3200N/M^2) and suspensory ligament tension changes (12.3 N/M) for changing from the fully accommodated to unaccommodated state. They used Helmholtz's (1866) data for accommodated and unaccommodated lens geometry, Fincham's (1937) measurements of capsule thickness, and McCulloch's (1954) data for suspensory ligament insertion position. The bulk modulus ($E=6 \times 10^6\text{ N/M}^2$) and Poisson's ratio ($\nu=0.5$) were determined experimentally for the anterior cat capsule.

Weale (1962) pointed out the lens substance was elastic not plastic as Fincham had concluded. This is demonstrated by the decapsulated lens returning to a flatter form, and its ability to recover from manual deformation (Fincham, 1929). He speculated that since the elastic forces of the lens substance and capsule are in opposition, perhaps presbyopia is in part due to a change of balance between these antagonistic forces, and a greater understanding of the lens elastic properties may help to solve the mystery of presbyopia.

This challenge was passed on to Fisher (1969a and b, 1971, 1972, 1976) who through a series of careful experiments, studied the elastic properties of the complete

human lens, it's capsule, and lens substance. He also looked at differential nuclear and cortical elastic properties, throughout the human life span.

Fisher (1969a) found the Young's modulus of elasticity of the capsule to change from 6×10^7 dyn/cm² in childhood to 3×10^7 at age 60 and decline to 1.5×10^7 dyn/cm² in extreme old age. Since the energy stored in the capsule, is increased as it thickens (up to age 60) and as the lens shape flattens (now known to be in early childhood only, Brown 1974a) so these may partly compensate for the weakening elastic properties, that contribute to presbyopia. Agreeing that the elastic capsule (Fisher, 1969b) plays an important role in moulding the lens in accommodation, (and therefore its decline to presbyopia) he could not agree with Fincham's notion of differential lens moulding, after finding that the force required to rupture the capsule and zonules (Fisher 1986) is lower than the force (calculated by O'Neill and Doyle, 1968) required to achieve a conoidal lens shape in accommodation. In other words the lens capsule and even the zonule would break before sufficient force could be applied to give a conoidal lens form!

More evidence against Fincham's notion of localised capsular lens moulding was supplied by Fisher and Pettet (1972), who in an attempt to avoid fixation artefacts, measured the thickness of unfixed fresh detached human lens capsules. They found the young capsules were thickest at the equator, and only in capsules over 40 years old, was the anterior periphery thickest, as Salzmann and Fincham had

found. They suggest that Fincham was misled by measurements from elderly lenses (they were of unknown age), and ignored Salzmann's similar findings of peripheral capsular thickening in young eyes. Fisher and Pettet proposed a new capsular theory, - the young released capsule, being thickest round the equator, behaves like an elastic band around the equator, forcing the enclosed lens to reduce in equatorial diameter, and bulge centrally. When the equatorially thickened band is unable to act, neutralised by zonular tension, the anterior capsule, the next thickest zone, flattens the anterior lens.

Koretz and Handelman (1982) are of the opinion that the capsule acts as a force distributor, ie the capsule redirects and spreads the zonular pull.

1:4 INTRA-LENTICULAR CHANGES IN ACCOMMODATION

Some of the first insight into internal lens changes in accommodation, came from Brown's (1973a) slit-lamp study, which looked at external and internal lens curvature changes in human eyes, with accommodation and age. The nucleus of the lens is in this case defined as that enclosed between the most internal zones of optical discontinuity (Neisel, 1982). The nucleus was observed to thicken axially in accommodation, providing virtually all the axial lenticular thickening, with the cortex changing far less , except to steepen around the steepened nucleus. However the relaxed lens nucleus remains almost constant in axial thickness

(Brown, 1974a) throughout life, despite growth, whilst the cortex thickens, suggesting perhaps some compression of the nucleus with age. Brown also used colour television density analysis, finding marked expansion of the areas of low density representing the nucleus in accommodation. This suggests that the light scattering properties of the lens as a whole reduces in accommodation, perhaps indicating a change in the distribution of lens fibres (Brown, 1973b). It was this point that prompted the discussion on internal lens changes in accommodation reported earlier.

Brown had observed the greatest tendency to lenticular central cone formation in accommodation, around the age of 30, and suggested this was caused by the steepened nucleus shaping the cortex. The younger lens (11 years) showed no tendency to cone formation - there was no flattening of the mid peripheral lens, because the young lens is nearly all nucleus, and gives a more even overall steepening. The capsule, visible in the photographs, showed only gradual thickening towards the periphery.

Fisher (1971) showed that Young's modulus of elasticity increases with age. The equatorial and polar elasticity are similar (isotropic) at the extremes of life, but increase at different rates, being most different around age 30. Fisher deduced that young's modulus of the nucleus remains fairly constant up to age 40, whilst there is a continuous rise in cortical elasticity with a slight decline after age 50. This indicates that the nucleus is softer and more easily

deformed than the cortex, during the accommodative years. Brown and Fisher's findings both support the idea of a more flexible nucleus, with an ever growing less flexible cortex contributing to the accommodative failure of presbyopia.

Koretz and Handelsman (1985, 1988a and with Brown 1984) also looked at internal lens dynamics in accommodation. Having found that the unaccommodated and accommodated arc lengths of any given layer of the lens (caught in cross section by the slit lamp), differ by less than 1%, they were able to investigate movement of any point on or in the lens during accommodative shape changes. They found that spacing changes between layers only occurred peripherally in the cortex, and centrally in the nucleus. Their preliminary calculations of volume changes (Koretz and Handelsman, 1985) in selected regions during accommodation suggested a mass redistribution within each layer defined between the internal and external curves. At the level of the individual lens fibres, this suggests a flow of cytoplasm from the equatorial regions into the fibre arms, causing a change in fibre shape and curvature. They go on to suggest that presbyopia is a geometrical problem, caused by increased growth of the lens.

1:5

EXTRA-LENTICULAR CONSIDERATIONS

1:5.1 The Vitreous

To leave the lens briefly, a point more peripheral but still relevant to this study, relates to the role, if any,

of the vitreous.

Except at the equator, the vitreous lies in contact with the posterior surface. This is the steeper of the two human lens surfaces, steepening only slightly in accommodation. Why the posterior lens curvature changes less is still a matter for speculation. During accommodation, the lens thickens axially, pushing the anterior pole anteriorly, whilst the posterior pole moves back less (Fincham, 1925; Brown, 1973a). This forward movement of the lens has been confirmed with ultrasound measurements (Coleman, 1970).

The vitreous is ascribed an important role in achieving the lens shape change of accommodation, by Tsherning and von Pflugk (1935), assuming hydraulic pressure to be responsible for formation of the lenticonus of accommodation. Coleman (1970, 1986) in his hydraulic suspension theory of accommodation, points out that the fibrous anterior vitreous is adherent to the lens, and together they may form a hydraulic diaphragm, separating anterior and posterior chambers. In support, Coleman points to the drop in accommodative amplitude with raised intra-ocular pressure (glaucoma).

A more passive supporting vitreous is the basis of other theories of accommodation. Fincham thought vitreous support the reason for the lesser movement of the posterior pole and smaller curvature change, whilst Preistly-Smith (1929) pointed to the observation that when the cornea (Fincham, 1929) was removed, zonular tension was maintained despite a fall in IOP; and suggested this was due to

attachment of the vitreous. Koretz and Handelsman (1984, 1985, 1988b) like Fincham, see the vitreous as a passive supporting force for the posterior lens.

That the vitreous is unimportant to accommodation, is a view held by Fisher (1982, 1983) who points to a case of monocular vitrectomy in a young man resulting in full accommodative amplitudes despite the missing vitreous.

1:5.2 The Zonular Fibres

It is generally agreed that the zonules allow the lens to take up its accommodated shape when they reduce tension, and impose a flattening on the anterior and posterior lens face when the ciliary muscle relaxes.

1:6. NON PRIMATE AND PRIMATE ACCOMMODATION

Accommodation is not a privilege of all species. Many of the species used to study lens structure have little or no accommodative facility, or accommodate by a different mechanism.

The chick, subject of many electron microscopy studies, is a bird, though capable of up to 20 D accommodation (Sivak et al., 1986) is thought to squeeze its soft lens into a lenticonus by direct pressure of the ciliary body and iris, and may even have some corneal accommodation. The frog is thought to move its lens towards the cornea, whilst the cat is thought to use its ciliary muscle to move its lens

forward (up to 11D). Rohen et al. (1989) have recently shown that the Raccoon has a similar mechanism to man, allowing up to 19 D accommodation - the largest amplitude identified as yet in a non-primate terrestrial mammal.

Mice and rats have rounder lenses, (Sivak, 1980) with no accommodative facility, though their stenopaic pupils allow some depth of focus. Sheep and calves also have rounder lenses and probably no accommodation. Squirrels have a flatter lens but accommodate only one or two diopters. Rabbits also have flatter lenses with up to four diopters.

Von Pflugk (1909) obtained flattening of the cynomolgus monkey lens with atropine, and marked steepening with eserine which was maintained after death and captured with his freezing technique. Tornqvist (1966) included cynomolgus and rhesus monkeys (both macaques) in his study of accommodative amplitudes, and has observed amplitudes up to 15 - 20 with pharmacological stimulation, (topical carbachol) and 10 - 12 D by nerve stimulation (1967) in the cynomolgus. He noted the maximum accommodation in two monkeys that looked older with worn teeth, was only a third of the younger animals, indicating some age related accommodative decline, as is found in the human. Chin, Ishikawa, Lapin, Davidowitz and Breinin (1968) recorded values as high as 29 diopters by stimulating the brainstem of cynomolgus monkeys. More recently a group of workers in America including Bito and Kaufmann (Bito et al., 1982, Kaufmann et al., 1982; Bito et al., 1987 etc.) have indicated the suitability of the Rhesus monkey (*Macaca*

mulatta), as a suitable model for the study of human accommodation and presbyopia.

Their studies (Bito et al., 1982) demonstrated a remarkably high accommodative amplitude, a mean of 34 diopters in animals up to 5 years old induced by topical cholinomimetics (pilocarpine, carbachol, and 2.5% phospholine iodide). The rhesus and human lens show the same growth pattern, with the polar axis of the monkey, continually thickening after the age of five. The rhesus also shows an age related decrease in pharmacologically induced accommodative amplitude (Kaufmann et al., 1982).

There are many similarities between the rhesus and human accommodative systems. The monkey lens also thickens axially in accommodation. The greatest amplitudes (over 40 diopters, Bito et al., 1982) are, as in the human, found in the juvenile. Duane (1912) in his study of human accommodative amplitudes, found that accommodative decline was slightly greater in adult life. The rhesus also shows more decline during the second trimester of its life span, from skeletal maturity between age 5 and 6, and menopause around age 25. There is however rather more variation (spread) in rhesus accommodative amplitudes with age, than in man, as shown in Duane's data. One monkey of 24 years old showed a pharmacologically induced amplitude of greater than 30 D, 'suggesting that presbyopia is not a totally predictable consequence of ageing in the rhesus.'

Brown's technique of Scheimpflug photography has been

scaled down for use with the rhesus, by Koretz et al (1987a, 1987b, 1988a), and was used with ultra-sound to investigate lens position (1987a) and both external (1987b) and internal (1988) lens shape changes with age and accommodation.

Both lens surfaces flatten and the polar thickness decreases in the first 5 or 6 years of life, with the anterior chamber depth deepening as the eye grows. Thereafter (once globe growth has ceased) lens growth continues, and the anterior chamber (as in the human) narrows. Lens axial thickness increases, and both surfaces steepen, though the anterior slightly less so. Unlike the human lens, the monkey lens exhibits only two zones of optical discontinuity. One lies anterior, and one posterior. They first become visible in iridectomized eyes around the age of 7. Their thickness and separation are independent of age.

Iridectomized monkeys were of particular value in this study. Like man, the rhesus lens thickens in accommodation, and the anterior pole moves forwards more than the posterior pole moves back. Unlike man, the posterior lens surface steepens as much or up to 20% more than the anterior surface, so that the posterior surface is always the steepest. The axial separation of the two zones of discontinuity increases with increased accommodation, with no thickness increase in the surrounding cortex. Like man (Brown, 1973a) this suggests that overall changes in shape and thickness with accommodation, primarily reflect changes in shape of the central region.

Scanning electron microscopy and light microscopy were used to examine intra-lenticular modifications in accommodation. The hypothesis of lens fibre form modification or lens fibre shearing faces was tested. Morphological correlates were sought in support of differential nuclear/cortical curvature changes. The capsular theory of accommodation is re-examined in the light of differences between man and monkey.

CHAPTER TWO

2.1

EXPERIMENTAL DESIGN

The last chapter poses many questions. How does the internal lens react to allow lens shape changes? What happens to the seemingly ordered array of lens fibres within the lens? The presence of junctional structures would seem to limit sliding, but could there be areas or special layers, (shearing faces) where sliding does occur? Or perhaps lens fibres change shape, redistributing their bulk, (along their great length) at the capsule's behest? And what of the capsule that transmits the accommodative force to the internal lens? If Fincham was right in his measurements of the anterior monkey lens capsule thickness, then a disparity occurs between the latter and Fisher's observations in man. Is there a species difference, and if there is, can this add to our understanding of primate accommodation?

There are three main studies within this work, aimed to address the above questions. The first is the examination of the morphology of lens fibres in the cynomolgus monkey lens. This, using SEM, aimed to explore the possibility of sliding between individual layers of lens fibres, and search for any evidence of restricted sliding limited to putative 'shearing planes', as a means to internal lens shape changes. The second study looks for signs of lens fibre shape changes, to test the second hypothesis for lens shape changes within the capsule. The last study looks again at the thickness of the

lens capsule in both man and monkey and questions aspects of the contemporary capsular theory of accommodation.

Crystalline lenses of cynomolgus monkeys (*Macaca fascicularis*), of both sexes and various ages, were used throughout this study. These monkeys were chosen because of the known pharmacological and anatomical similarities relating to accommodation with that of man, (page 35).

CHAPTER THREE

3 LENS FIBRE MORPHOLOGY IN THE CYNOMOLGUS MONKEY

Since the major bulk of the lens is composed of lens fibres with little intercellular space, the overall change in lens curvature (demanded during accommodation by structures external to the lens fibres) can only be exacted by some change at lens fibre level. Therefore, knowledge of individual lens fibre shape, size, surface structures, and interrelations with neighbouring fibres, is primary to any understanding of lens shape changes in accommodation.

Scanning electron microscopy, which allows an almost three dimensional view of surface structures, was chosen to explore the topography of lens fibres and, in particular the structures apparently joining lens fibres.

3.1 MATERIALS

Crystalline lenses for study of lens fibre morphology were obtained from three perfuse-fixed, young adult cynomolgus monkeys (MR37, M54, MR86). All these animals were used in other medical studies, but were selected so that previous procedures would not affect their accommodative system. (A fourth lens was examined (MR72) which was part of a failed attempt to induce accommodative spasm, see 4.2.). A summary of these and other animals used in this study, operative procedures and method of fixation can be found in Appendix A.

Fixation was carried out by perfusion (Appendix B), and material was stored at approximately 4 degrees C. in a solution of 3% glutaraldehyde and 2% paraformaldehyde prior to dissection.

3.2

METHODS

3:2.1 Preparation for Scanning Electron Microscopy

Lenses were dissected in a sodium cacodylate buffered sucrose solution under an operating microscope with illumination arranged through fibre optics from below. This increased visibility of the sutures. Though it is possible that sutures may have some role in shape changes of the lens, tissue was selected to avoid this complication. The lens (resting on its anterior surface) was bisected, then again cut radially to form a segment, like a wedge of dutch cheese. Further segments were prepared in the same way (Fig. 4:4 shows a similar dissection). Each segment was found to divide fairly easily with gentle pressure into five or six layers or arcs of tissue around the innermost nucleus, forming natural separation planes. Further divisions required substantially greater effort and were considered to be forced separation planes. The hypothesis that these natural separation planes may divide more easily due to a scarcity or absence of junctional structures, was tested when both natural and forced separation planes were examined and the density of junctional structures compared.

The division of the lens into cortex and nucleus is subject to variable definition. That the most superficial lens fibres are cortical and the deepest fibres are nuclear is clear: classification of the layers of fibres between these two extremes has been done in this case by using the the five or six layers into which lens segments easily separate. These have been termed cortex (layers f and e), intermediate (layers c and d) and nucleus (layers a and b). The superficial cortex is part of layer 'f' and the deepest nucleus is in layer 'a'.

The posterior and equatorial parts of each layer of tissue were retained for electron-microscopic examination. Only two anterior lens segments were examined, one from each of two lenses, (MR37 and MR72).

Tissue was next dehydrated through graded ethanol, then transferred still in absolute alcohol to the Samdri critical point drier. After critical point drying, tissue was mounted on brass specimen holders with the surface required uppermost, using double sided sticky tape. These were then coated with a thin layer of gold (10 - 20 nm) using an E.M.Scope splutter-coating unit. The specimens were then examined using a JOEL JEM 100B electron microscope at 40kV, spot size 3. Photographic records were made using a Polaroid camera attachment and a slow scan speed (60 seconds). Stereo paired photographs were obtained by taking a second photograph with the specimen stage rotated by 12 degrees.

Since magnification varies slightly with specimen height, (and is directly related to the current required to focus the beam), the exact magnification can be calculated from the current required to focus on each part of the specimen. Calibration specimens (diffraction grating replicas) of known size (2,100 lines per mm) were photographed at different heights to relate the focusing current to actual magnification. The maximum possible variation in magnification, due to specimen height changes, was found to be just under 7%. Calibration specimens were used to check for day to day variation in magnification. Magnifications of up to x10,000 were used.

3:2.2 Preparation for Light Microscopy.

Tissue samples from the same lenses were also examined using light microscopy. Larger samples were dissected, washed in distilled water and post fixed in osmium tetroxide for about one and a half hours. They were then dehydrated through graded ethanols, (using two changes of absolute ethanol) over a further one and half to two hours with constant agitation. After immersion in xylene for 20 minutes then a xylene/Araldite mixture for a further 20 minutes the tissue was agitated in Araldite for sixteen hours. It was then transferred into Araldite filled containers or gelatine capsules, and incubated at 55 degrees C for 48 hours.

Sections of Araldite embedded tissue were cut to be 0.5 - 1 um thick with a Reichart ultra microtome, and then

mounted on glass slides and left to dry. The Araldite was removed using the sodium methoxide technique (Mayer, Hampton and Rosario, 1961) and stained for five minutes in a mixture of toluidine blue and sodium bicarbonate solution (Trump et al., 1961). The sections were covered and left to dry slowly on a glass covered hot plate. Many other staining techniques were tried to provide better stain contrast, but finally Toluidine blue, with subsequent storage until differential fading occurred, was adopted routinely. Sections were examined under oil using a Zeiss light microscope. Measurements were made using a measuring eye piece.

3.3

OBSERVATIONS AND RESULTS

Lens fibres of the cynomolgus monkey, in common with other species, are very long and very thin. In cross section, the lens fibres are usually six sided, forming long flattened hexagonal fibres, with two long broad faces parallel to the lens surface, and the four short faces lateral to the broad faces.

Scanning electron microscopy allows an almost three dimensional topographical view of lens fibres and their processes. This therefore gives a better appreciation of the relationship between lens fibres than light microscopy alone.



Fig. 3.1 Fibres from the intermediate zone of the lens (layer 'd') as viewed with scanning electron microscopy. Lens fibres are very thin and ribbon-like. The broken fibre gives an impression of their thinness (arrow-head). x1580

3:3.1 Scanning Electron Microscopy of 'Natural' Fracture Faces

At low magnification lens fibres appeared thin and ribbon-like (Fig. 3.1). The hexagonal shape of the fibres was not always obvious, but occasionally detectable even in areas where fibres were densely coated in processes.

Lens tissue was dissected by gently tearing between layers of lens fibres along a curve roughly concentric with the outer lens shape. As the arrangement of lens fibres is basically hexagonal, the broad faces of the fibres should be exposed by this dissection. There are two possible presentations of lens fibres predicted, as illustrated in Fig. 3.2. The actual fibre aspect usually observed was that of the broad face and one short face, hence the surface of the exposed fibre layer revealed only one broad face and one thin short (apical) face of each fibre, arranged in a series of very shallow steps (Fig. 3.3 a and b). This has been confirmed from stereo photomicrographs in deeper lens fibres. Separation tended to occur between layers of lens fibres of similar depth with occasional steps up to a more superficial layer or down to the next deeper layer.

The lens fibres are so thin that the broad fibre face appears parallel to the observation plane although, as they are six sided, this face must actually be slightly tilted away or towards it. Only when there has been disturbance to this layer are other faces of a lens fibre seen.

Despite knowledge of the basic hexagonal arrangement

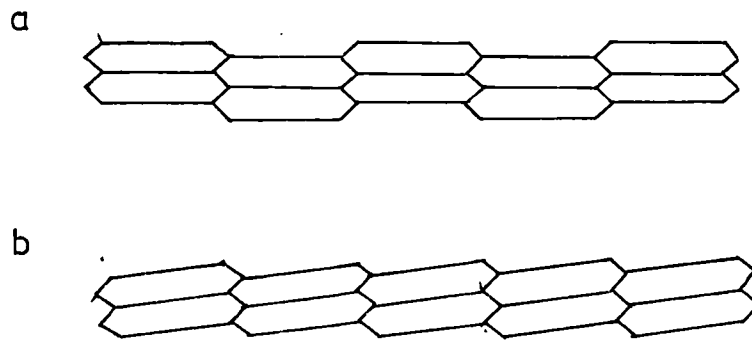
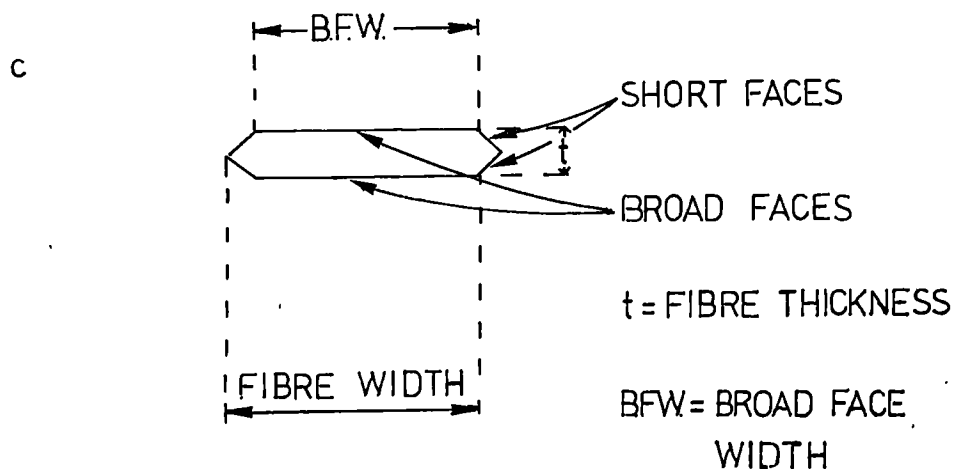


Fig. 3.2 Schematic drawing to show predicted layer patterns in a hexagonal cell system. The actual aspect usually presented by a natural fracture interface, is similar to b).



c) Diagram to define the terms used in describing lens fibre shape. The broad and short faces are indicated. 'Fibre width' is not used to describe the maximum width of the fibre, but that part of the fibre which is exposed by dissection. When fibre width is defined as indicated, the cross-sectional area of the fibre is width multiplied by the thickness ($W \times T$).

from light microscopy and S.E.M., the main impression (even with the assistance stereo-micrographs) is that most of the cortical lens fibres are exceptionally thin with the upper and lower broad faces joining together either directly, or by very short side faces. These short faces are in this case almost perpendicular to the broad faces. The fibres of the nucleus do have a more regular six sided appearance, although this too may be variable. Occasionally a fractured nuclear fibre appears to have only five sides in section whilst others, though still asymmetric, may have six (Fig. 3.4). This pattern of irregularity is also mirrored in the light micrographic sections (Section 3:3.4).

Processes lay along the angles formed by face junctions, (Fig. 3.3a and b) apparently linking neighbouring fibres and these are termed angle processes. In many areas of the lens, the broad fibre faces were either liberally or sparsely coated with other junctional processes and pits (Fig. 3.5). These and their pits, have been called ball and sockets, in keeping with the term used previously in the literature. The surface pattern of wrinkle-like folds seen on the nuclear fibres (Fig. 3.3) has been described as both "microplique" and "tongue and grooves" in other studies: but the latter title is used here.

Generally, raised areas and projections are seen brighter (more electrons collected), whilst depressions and holes are darker (fewer electrons). Interpretation of surface features is greatly aided by the addition of stereo

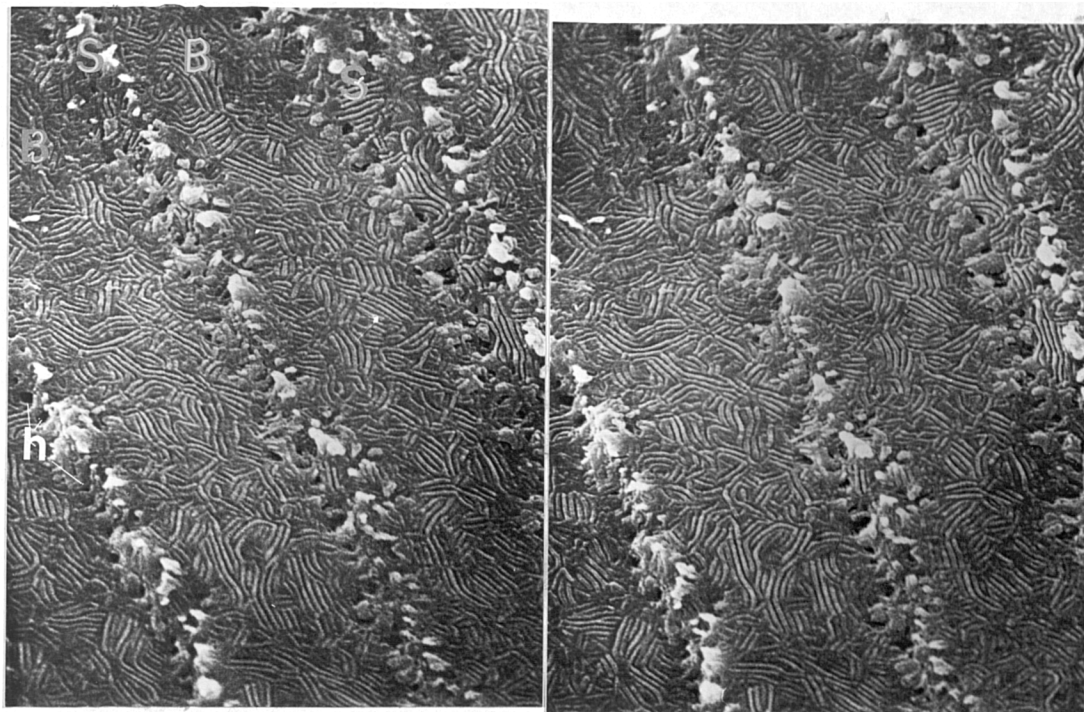


Fig. 3.3 Stereo pair showing only the left short face (S) and upper broad face (B) of nuclear lens fibres, -the other faces of each fibre are hidden by neighbouring fibres. Surfaces are covered in tongue and groove junctions. Angle processes lock together. Rows of holes (h) exist along the line of the angle processes, assumed from the removed overlying fibres. x3000

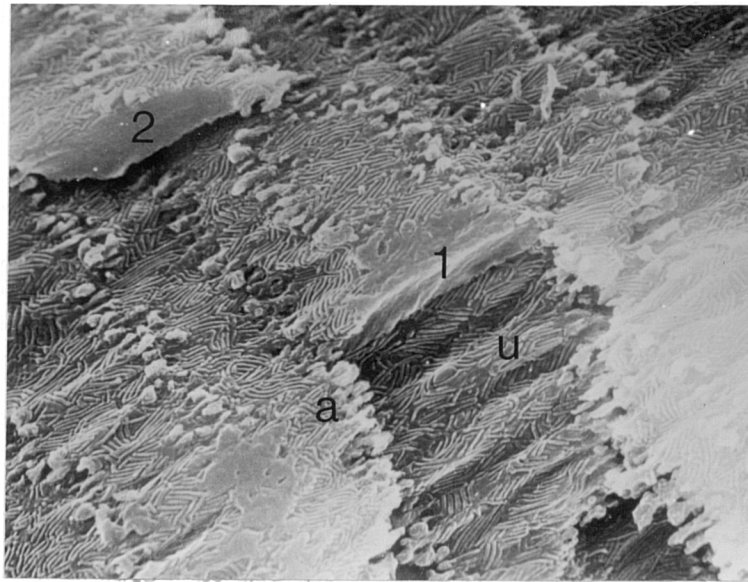


Fig. 3.4 Two fractured fibres from the equatorial nucleus, reveal their thickness. The fractured fibre (2) appears to have only four sides. Fibres display a marked transverse undulation (u) on their faces. Angle processes (a) and tongue and grooves are prominent. (ML73) x3010

photography.

Features of the Lens Fibre Interface

Ball and Sockets Ball and sockets junctions have only been observed on the broad faces of cortical and intermediate fibres. The processes of the ball and socket junctions varied in shape from thin and finger like to club shaped. They have slightly thickened ends in all but the more superficial fibres, but are not really ball ended. However it is convenient to refer to them as ball processes to distinguish them from processes not associated with ball and socket junctions.

They were $0.2 - 0.5\mu\text{m}$ in diameter, and up to $1.5\mu\text{m}$ in height. Small holes or sockets of similar incidence, occurred in association with the processes (Fig. 3.5).

Ball processes fit into the socket of the apposing lens fibre (Fig. 3.7) so joining two fibres together (Fig. 3.6). Rarely, when a fibre has pulled away from its underlying neighbour, a process can be seen to have displaced from a socket in the neighbouring fibre. Sometimes, ball processes appeared to have broken away at their necks and the ball head is seen within its socket (Fig. 3.7).

Processes of the ball and sockets were absent in the most superficial developing fibres. When first observed they were very short (less than $0.5\mu\text{m}$ high) with infrequent sockets. Just a layer or two deeper, these now abundant processes were longer, thicker and finger like, with equally

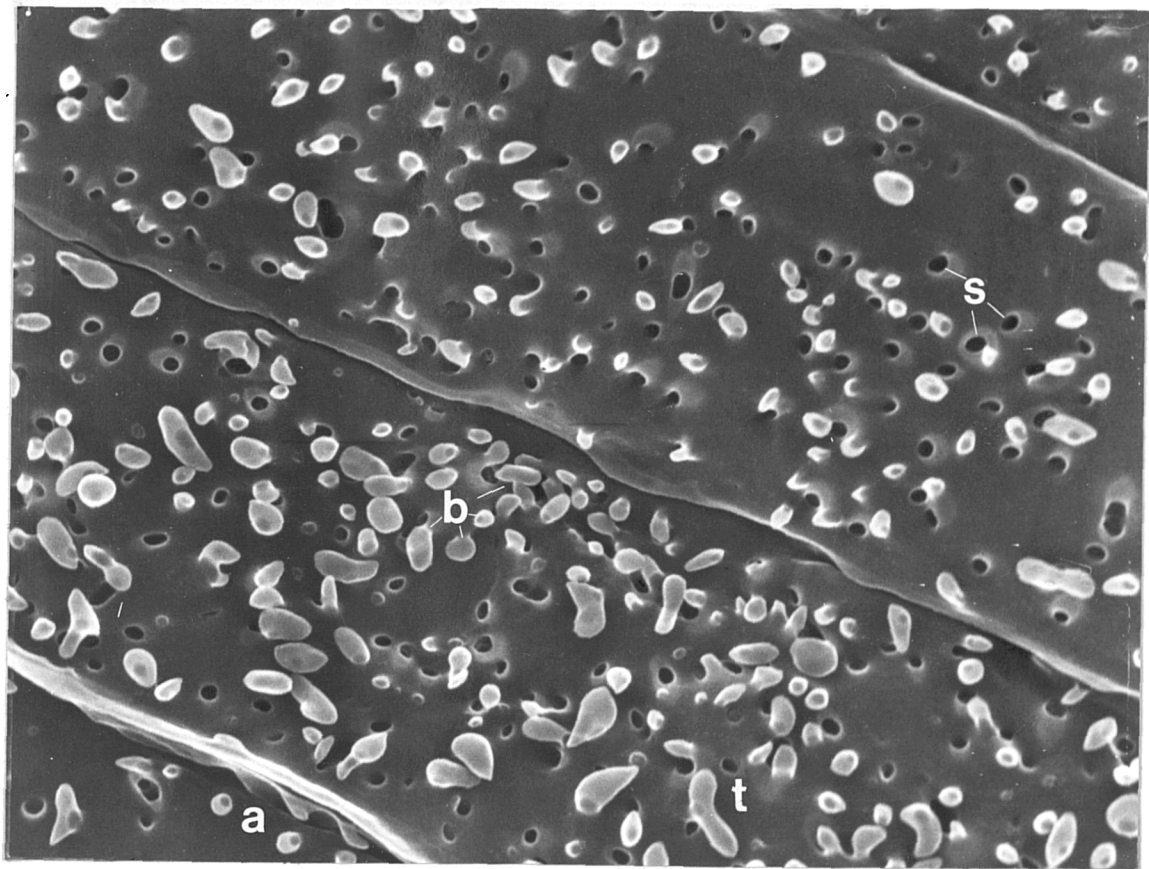


Fig. 3.5 Ball (b) and sockets (s) covering fibres from the anterior mid-cortex (level e). Ball processes vary in shape and size, and are occasionally paired (t). Angle processes (a) are infrequent. x7900

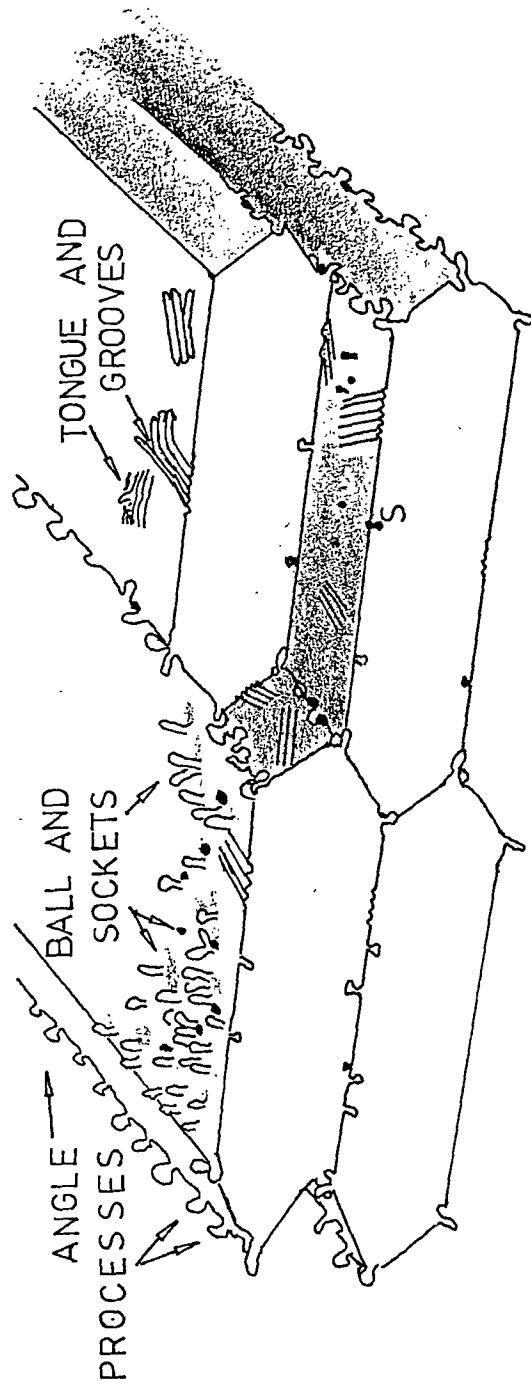


Fig. 3.6 Schematic representation of junctional structures.

Angle processes are found at fibre face junctions, ball and sockets (s) between the broad faces of two adjacent fibres. Tongue and grooves involve all six surfaces of fibres in the intermediate zone and nucleus.

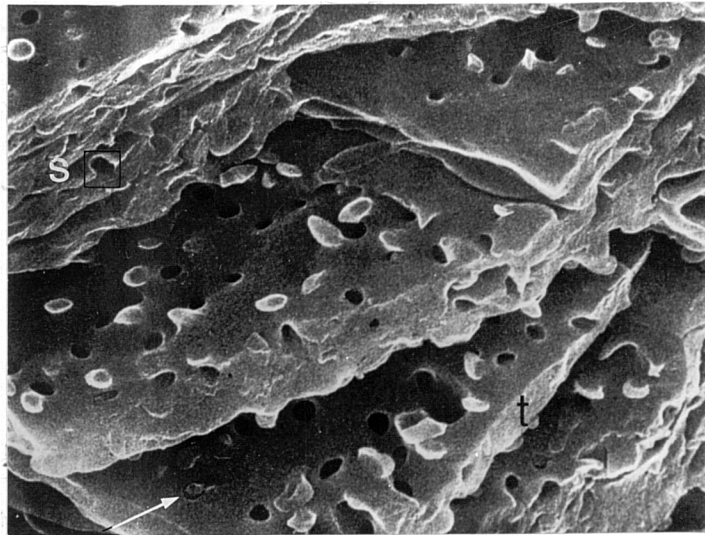


Fig. 3.7 Lens fibres from the superficial cortex (layer f) have been fractured, and their thinness (t) is demonstrated. Small ball processes and sockets cover the broad faces. A broken ball process still in its socket (fine white arrow) is seen. Some sockets (s) have been split open by the fracture. Note the absence of angle processes. x10,000

numerous sockets. Deeper still, the finger like processes broadened with slightly thicker ends and became club shaped. These ball and socket junctions, are most profuse in para-equatorial regions in the intermediate and outer cortex (layer e and inner layer f). The occurrence of ball and sockets diminish with depth, and are absent in the deepest nucleus. Fig. 3.8 shows the incidence of ball and socket junctions in the posterior portion of the (MR37) lens. The distribution within the anterior lens is broadly similar, but this was investigated in less detail in two lenses (MR37, MR86).

Angle Processes. A second type of process was observed, unrelated to sockets. These varied considerably in shape and size, from finger like to club or spade shaped, being thinner close to their origin, with swollen or flap like ends. They were found close to or at the junctions between faces and were intimately associated with similar angle processes from adjacent fibres. Angle processes (when small could look very similar to the processes of the ball and sockets, but were characterised not only by the lack of sockets, but their position along the fibre face junctions.

Angle processes varied in incidence in mature fibres from 30 to 130 processes per 100 μ m at each fibre face junction and in size from under 0.5 μ m in height and width up to 2 μ m. The separation between angle processes was usually small, - from 0.2 to 5 μ m.

The interlocking nature of these processes was observed

Frequency of Ball and Socket Joints

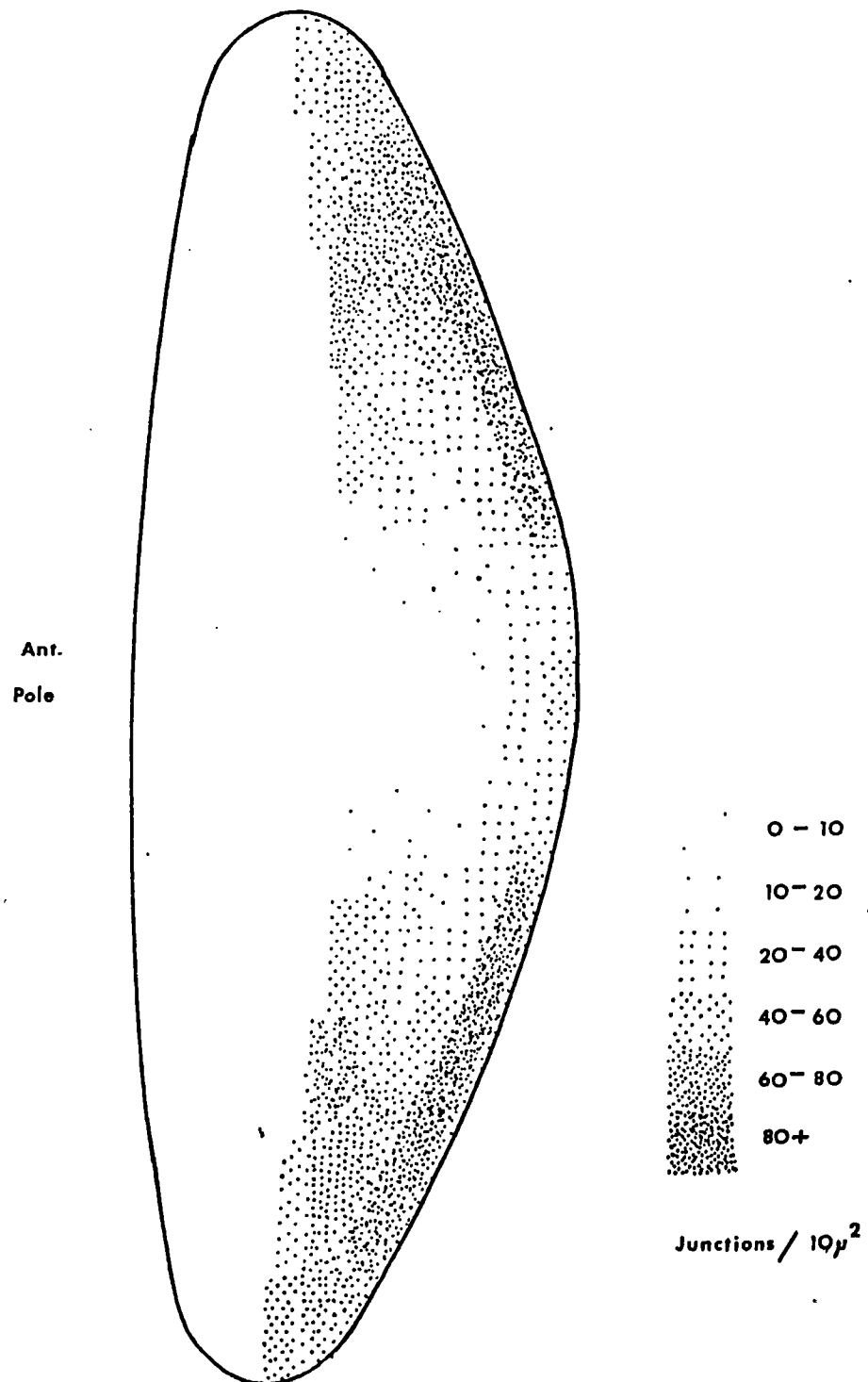


Fig. 3.8

Incidence of Ball and Sockets in the Posterior Lens (MR37)

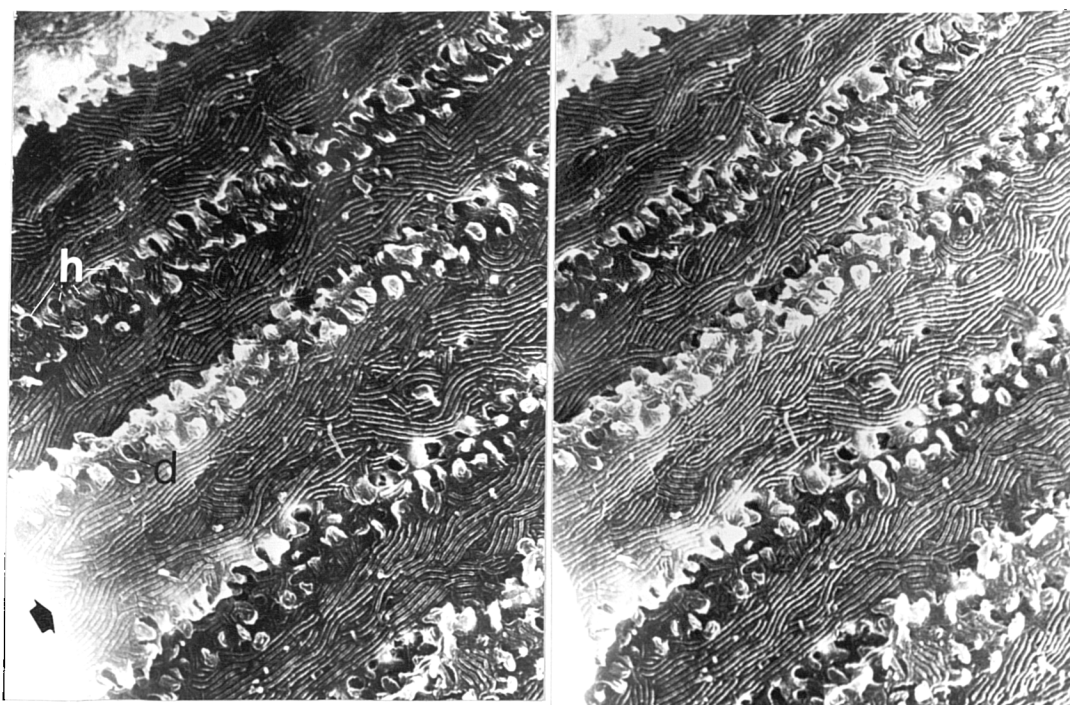
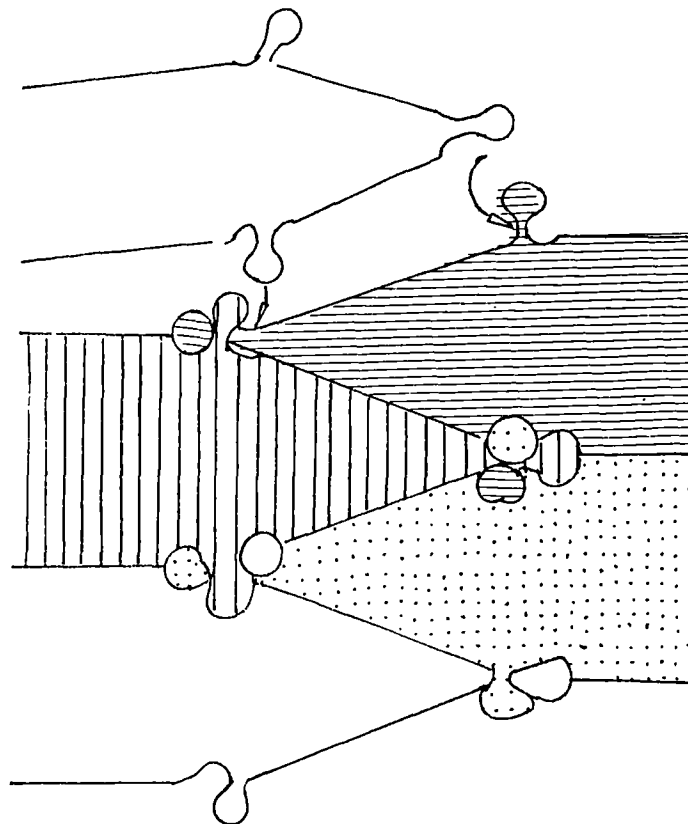


Fig. 3.9 Stereo pair of nuclear fibres close to the polar axis. The central fibre (arrow) has been detached at one end (arrow end), so that the junction of two short faces of this fibre is just visible. Angle processes are shaped like jigsaw pieces along face junctions. Socket-like depressions (d) are seen in the short fibre face. Rows of holes (h) are formed between angle processes, presumably to receive the angle processes of the missing layer of fibres. see text
x3000

when a nuclear fibre layer was disturbed by damage during dissection causing fibres to pull apart or break away (Fig. 3.9a and b). Processes from one fibre appeared to interlock with processes from both the adjacent fibres (Fig. 3.10). Thus each row of angle processes (in the deeper lens zones) link together three fibres, like a zip - but a zip with three rows of teeth. The usual picture observed when the upper fibre has been removed by dissection, (Fig. 3.9 Fig. 3.11) was of two rows of zip-like processes linked together, with a row of spaces formed between the necks of the club shaped processes. Presumably, since the spaces were smaller than the thickened ends of the processes (Fig. 3.11) but of similar diameter to the process stalks, the row of holes gave access to the processes belonging to the fibre removed from the surface at dissection.

Surface fibres (see Fig. 3.7, Fig. 3.17) have only the most rudimentary angle processes (less than $0.5\mu\text{m}$ long and in diameter) whilst in deeper regions the processes are longer (up to $2\mu\text{m}$), thicker and more frequent. Angle processes are most marked in regions close to the polar axis, especially close to fibre terminations at sutures where they may be lobed or branched or even form long irregular extensions. They are thickest, longest and widest in the nucleus.

Tongue and Grooves. Where ball and socket junctions became infrequent, a second surface feature was observed involving all six fibre surfaces. This took the form of small groups



INTERLOCKING ANGLE PROCESSES

Fig. 3.10 Diagram to show how the angle processes interlock in the intermediate lens and nucleus.

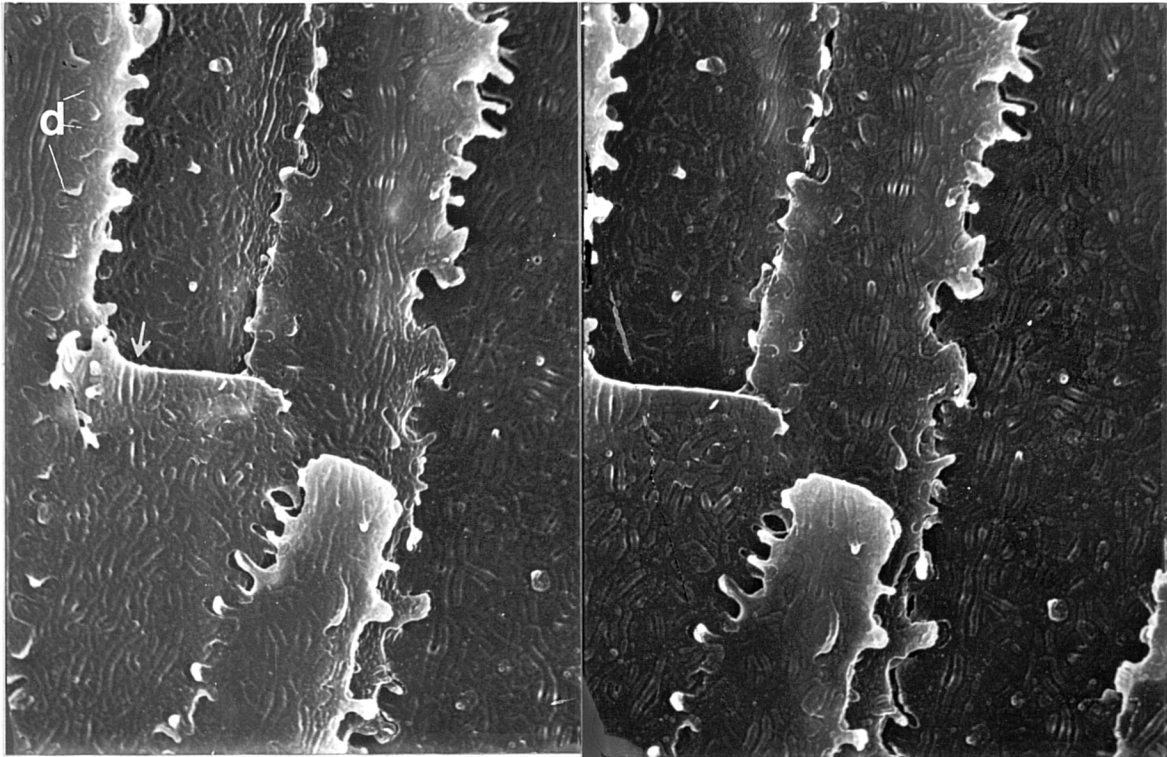


Fig. 3.11 Stereo pair to show shallow tongue and grooves on fibres from the intermediate zone of the lens. One group of tongue and grooves is transversely fractured, revealing shallow ridges and grooves in section (arrow). Angle processes are shown, and depressions (d) receiving them. (Close to polar axis) x5000

of short parallel alternate ridges and furrows, which have been called tongue and groove junctions.

This pattern was first encountered in the intermediate zone (layer d and deeper), where it looked much like the random creases of a smoothed out paper bag (Fig. 3.11a and b). In the deeper nucleus the depth or height of the ridges and furrows increased and occupied all surfaces, even occurring on some angle processes (see Fig. 3.12).

The tongue and grooves usually occurred in groups of three to five. They were orientated parallel to the fibre axis, transversely or obliquely. They varied in length from under $0.5\mu\text{m}$ to over $4\mu\text{m}$. Each ridge was about $0.1\text{--}0.13\mu\text{m}$ wide, with a separation between widest points of the ridges of under $0.1\mu\text{m}$. This suggests that the ridges, and presumably also the grooves, were slightly club shaped in cross section.

The ridges and furrows of the tongue and grooves appear to intermesh with the furrows and ridges of apposing fibres (Figs. 3.13, 3.25).

Close to the equator, shallow tongue and grooves formed groups about $0.5\mu\text{m}$ square often orientated diagonally across the fibre surface with a sharp change of axis in adjacent groups, suggesting a basket weave pattern. Away from the equator and in the deepest nuclear fibres, the tongue and grooves were deeper, groups were larger (up to 8 ridges), longer (up to $4\mu\text{m}$), and orientated closer to the long axis of the lens fibre. They were not always straight, and were



Fig. 3:12 High power micrograph of nuclear lens fibres, from the same area as fig. 3.9. Part of the short face of one fibre is shown centrally (between stars), above is the broad face of the same fibre. The angle processes of two adjacent fibres interlock with the central fibre. The row of 'sockets' along the fibre edge (large open arrow) are formed by angle processes from the two fibres illustrated; the holes are presumably from the processes of the removed lens fibre.

The tongue and grooves form a pattern of linear ridges and furrows on all faces, even affecting some angle processes (see left of open arrow tip). Some 'tongues' have broken away, (small arrows) and imitate finger processes. The two detached tongues indicated, are broken part way along their length, whilst others are damaged at one end. x10,000

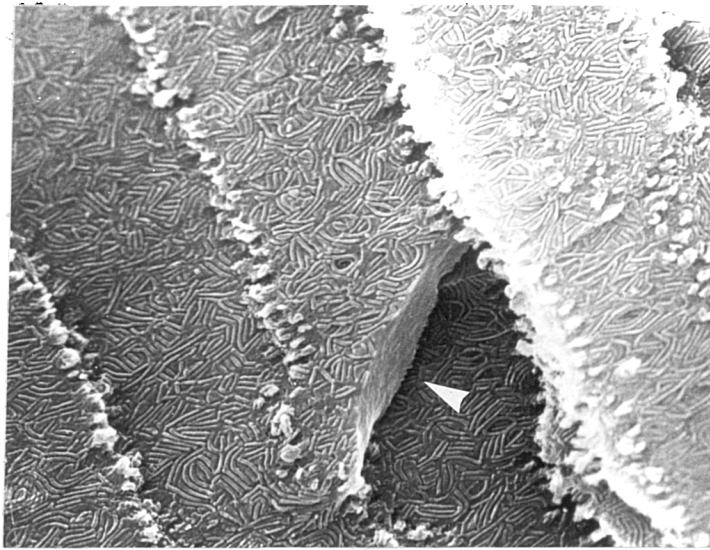


Fig. 3.13 Fibre thickness can be seen in the obliquely fractured nuclear fibre. Note the tongue and groove pattern. The fracture has exposed the profile of a tongue and groove patch (arrow head) on the hidden under-face A similar opposing tongue and groove are seen on the underlying fibre, suggestive of meshing of opposite faces. (Layer a) x3000

sometimes curved sharply in an 'L' shape at one end of the patch, or divided into a Y'shape. When the tongue and groove pattern is marked, the ridges had the appearance of being 'undercut', with a thinner attachment to the fibre face than the width of the groove. Rarely (Fig. 3 12), a ridge was partly broken away from the fibre face and raised, resembling a finger-like ball-process. This leaves what appears to be a (lighter coloured) narrow short linear ridge, as if the tongue had been torn from the fibre.

In areas where both ball and sockets and tongue and grooves are present, the face processes of the ball and sockets were thin and finger like.

Lens Fibre Width. Lens fibres in any one layer are usually widest as they cross the equator. Their width reduces to a minimum, about 0.3mm before terminating at a suture. Whilst fibre widths are fairly uniform across the equator in each specific layer, variability increases towards the axial zones.

Fibre Characteristics Under the Equator Transverse undulations of fibres (Fig. 3.4) were frequently observed, in fibres where they curved steeply beneath the equator. These occurred on both superior and inferior broad faces, in nucleus and especially cortex.

Although lens fibres showed width variation with depth, there was greater uniformity at the equator within each layer rather than in other locations.

LEVEL	EQUATORIAL	PARA-EQUATORIAL	INTERMEDIATE	PRE-AXIAL	AXIAL
'f' outer cortex	11.5		9 7	6	9
'e' mid cortex	13	12	9 8.5	6.5	10
'd' deep cortex	11	9	8 6.5	6	7.5
'a' deep nucleus	6	5.5	4.5 3.5	3	6

* To nearest 0.5µm. Mean of three counts, each recording number of adjacent fibres in 100µm

Table 3d Variation in Lens Fibre Width (microns), with depth and distance from equator. Mean of 30 - 60 fibres in each location, measured during S.E.M. from fibres which terminated close to the polar axis. (M37)



Fig. 3.14 A cortical posterior suture. Lens fibres broaden as they change direction and curve (arrow) into the suture line. (Layer e) x480

usually turn in to meet and terminate on opposing fibres along a suture line (Fig. 3.14). This change of direction means that the fibres meet at a less acute angle. Pre terminal lens fibre modifications were frequently seen before the path change. Angle processes thickened, sometimes branched, and even displayed small finger-like processes of their own, which appeared to insert into holes in other fibres (Fig. 3.16). Sometimes fibres appear to twist their main faces slightly into the suture, as if 'banking' into the curve, and the faces may show gentle transverse undulations similar to those of the equator (Fig. 3.15). Opposing fibres meet in flat very wide apparently overlapping spade shaped terminals. Occasionally a narrow arm-like fibre extension, covered in processes, (similar to that shown in Figure 3.16) was seen to embrace an adjacent fibre which appeared to terminate short of the suture line. This feature was more common in deeper nuclear areas.

Dissection damage to suture areas was common, which seems to indicate strong attachment between fibres in adjacent layers. There was a tendency for tissue to break apart along the posterior suture (Fig. 3.14), as if the attachment between opposite terminals in the same plane is vulnerable. Sutures are fascinating but not part of this work, and will not be described further.

Changes in Lens Fibre Form with Depth

In describing the changes in lens fibre form at each

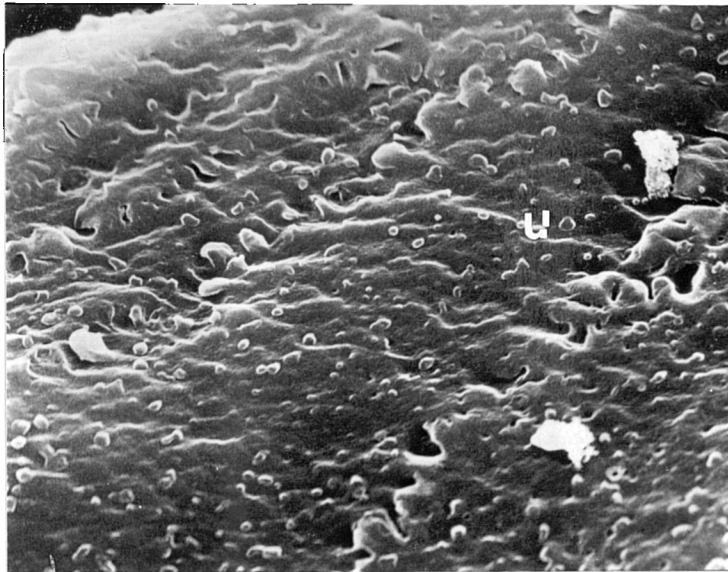


Fig. 3.15a Anterior polar cortical lens fibres close to a suture, show gentle transverse undulations (u), a common characteristic in lens fibres close to sutures. These fibres are fairly superficial, and have small under-developed ball processes and sockets. x3000

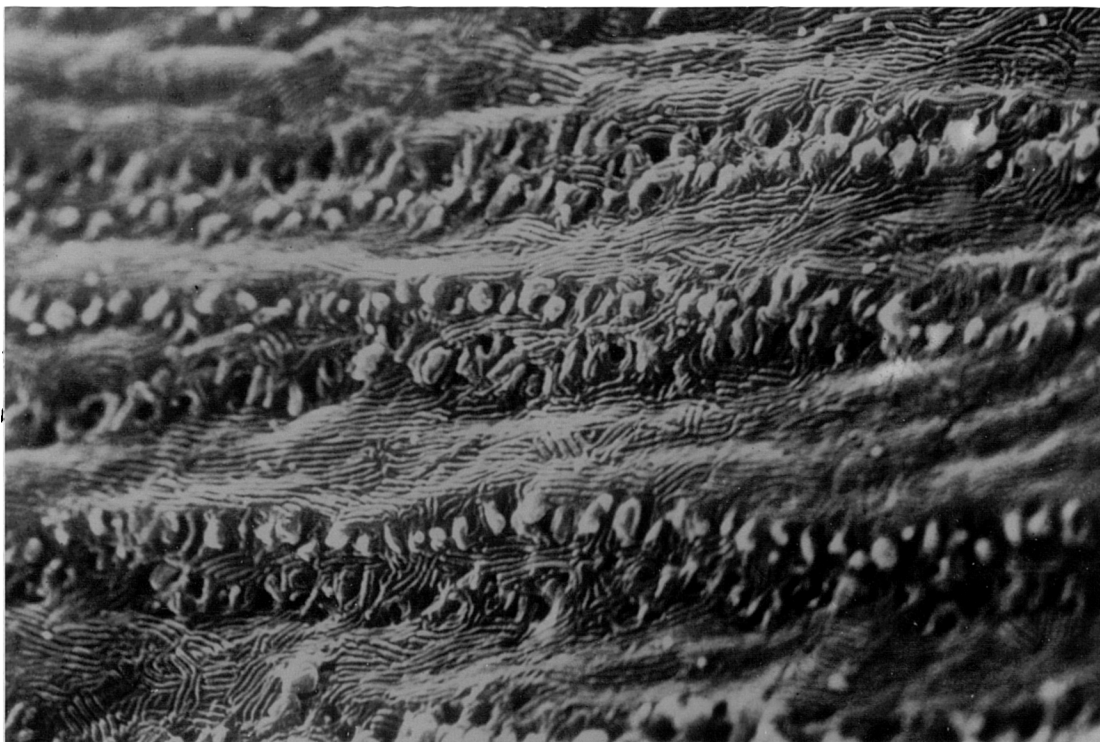


Fig. 3.15b Nuclear lens fibres close to a suture at the posterior pole. The surface of the fibres is slightly uneven. Note the abundant tongue and grooves. x4800

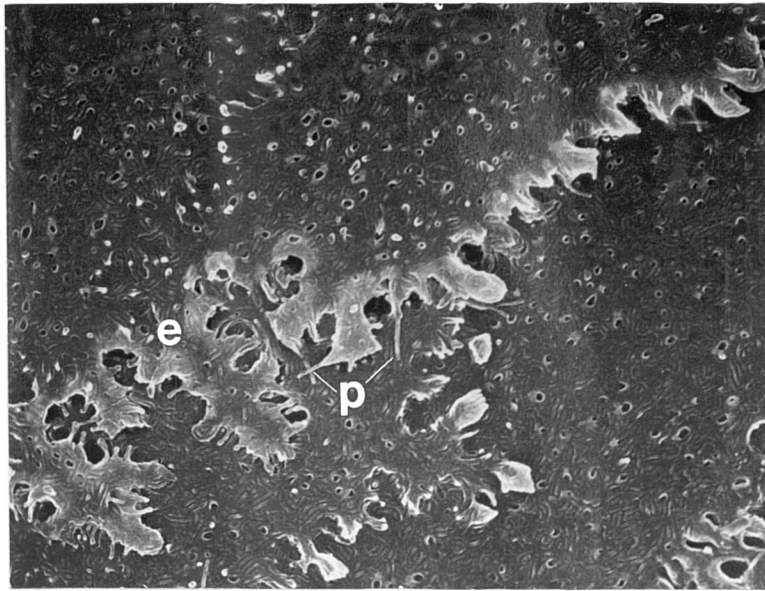


Fig. 3.16 Cortical fibres (level e), close a suture at the posterior pole. The fibre edges are irregular. Angle processes and fibre extensions (e) have tiny finger-like processes (p). x3070

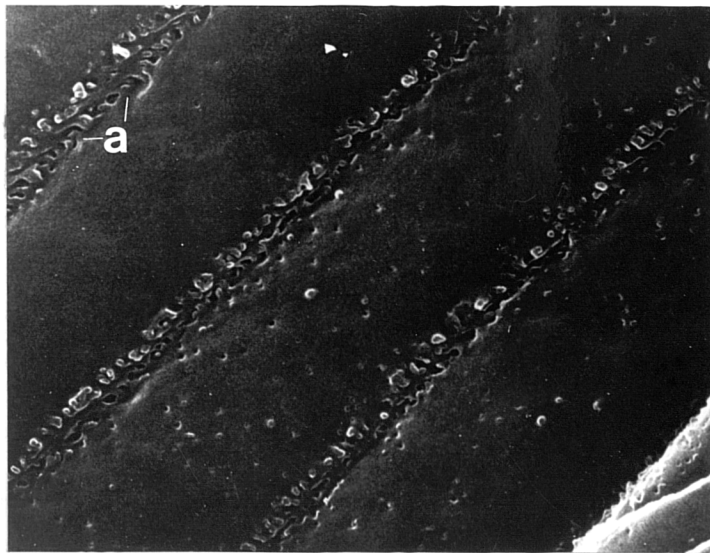


Fig. 3.17 x3000 Immature superficial lens fibres, (three cells below the capsule) have only a few short ball and sockets on the broad faces, but angle processes, although small are numerous. (Level f, close to polar axis) x3000

level of the lens, it is most convenient to start from the newest superficial fibres (layer f) found immediately beneath the lens epithelium and posterior capsule, progressing inwards to the deepest nuclear fibres (layer a). It is also convenient to start descriptions from the equatorial portion of the fibres and follow them along to their terminals. Specimens were selected that contained fibres that terminate close to antero posterior axis

Superficial Fibres (Layer f) Superficial fibres were thin with flat faces almost devoid of junctional structures (Fig. 3.17). Two or three fibres deeper, angle processes were first seen intermittently along the smooth broad fibre edges in the intermediate and axial zones away from the equator. In the same area, rudimentary ball processes were first observed. These were short and thin (0.2-0.5 μ m long, 0.2-0.3 μ m diameter), without the characteristic swollen end and not always accompanied by tiny sockets. A layer or so deeper, ball and sockets (now equally represented) were more prolific and thicker, if still rather short. Angle processes were still fairly rare, about 30 per 100 μ m length, but were longer (0.4-0.6 μ m) and seen to interlock. Figure. 3.18 illustrates the increase in processes with increasing depth below the surface.

Mid-Cortical Fibres (Layer e) Fibres in the equatorial zone (8-10 μ m across) had a few small processes and gently transverse undulations. Away from the equator, ball and

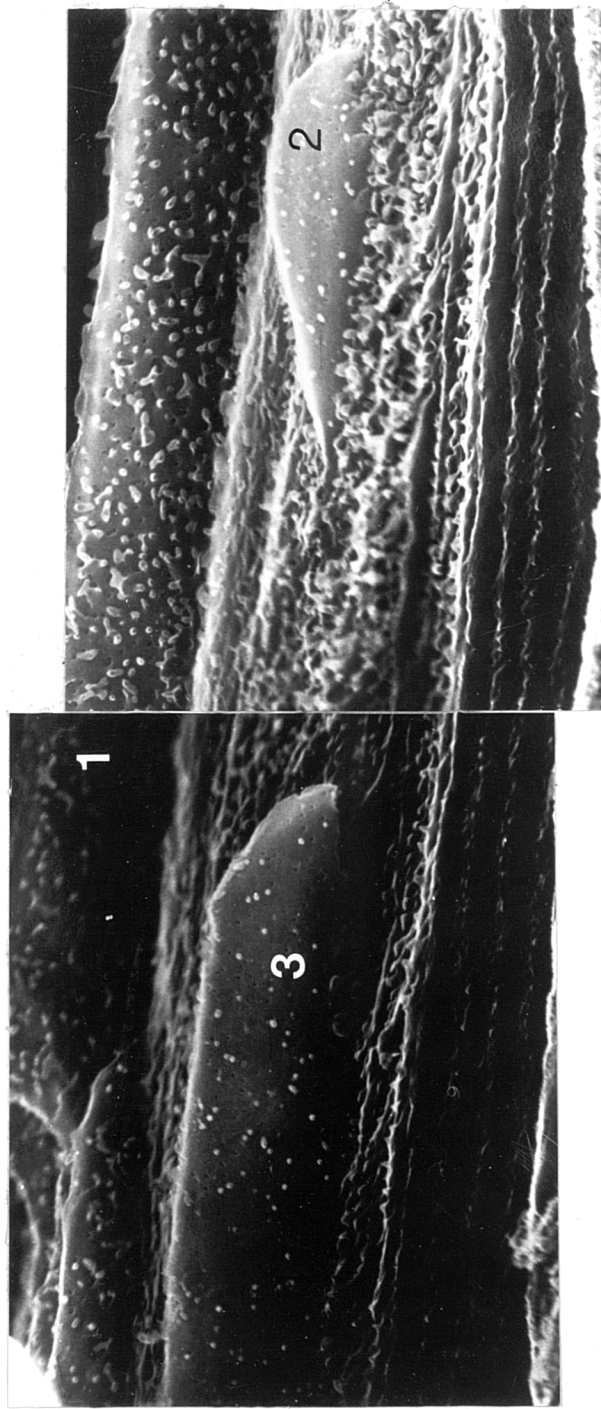


Fig. 3.18 The short faces of a group of fibres have been separated in a plain perpendicular to the surface, exposing a number of layers, from surface fibres (lower left) to mature cortical fibres. The viewing aspect is similar to looking down at a brick wall whilst standing on top of it. At the bottom of the 'wall' the broad face of a single cortical fibre (1) is seen, and some others are seen part way down (2 and 3), which were not removed properly when the tissue was torn apart. The incidence of ball and sockets and the size of angle processes is greater in deeper fibres. x3000

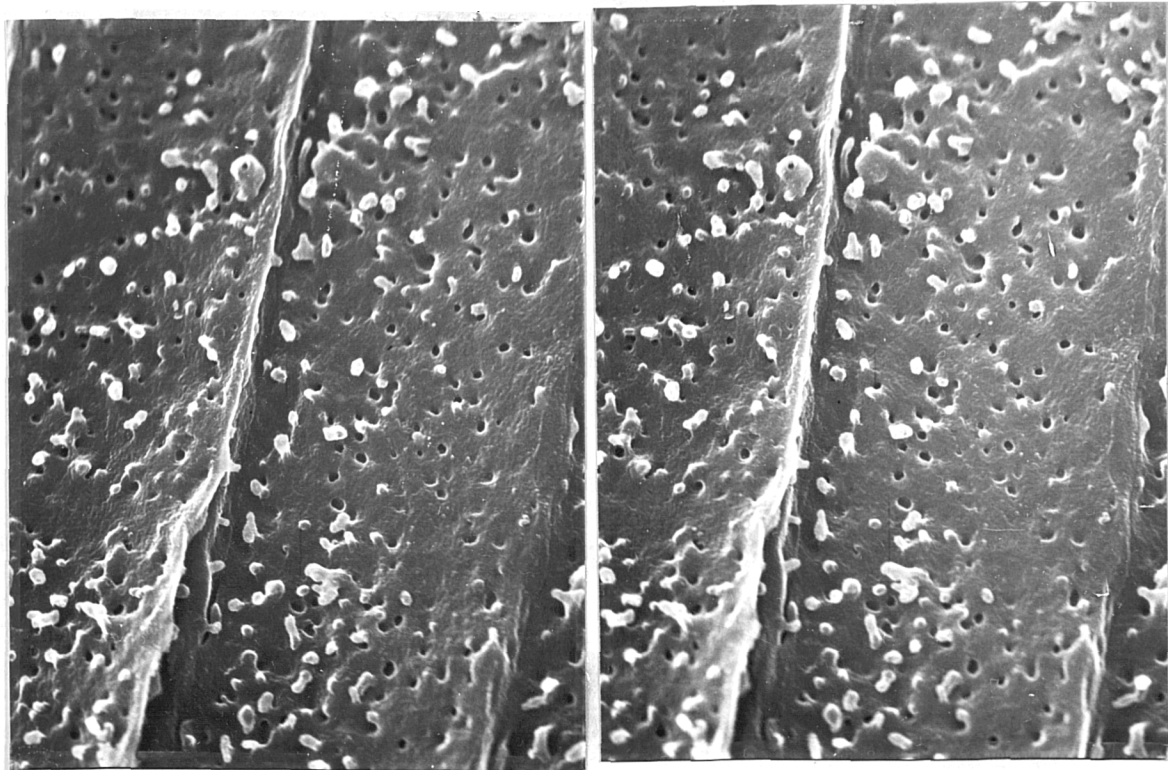


Fig. 3.19 Stereo pair. There is a moderate covering of ball and sockets, and the faintest trace of a tongue and groove pattern, on these fibres from the posterior deep cortex. The fibres are so thin that the short faces are not discernible. (Level d/e) x5000

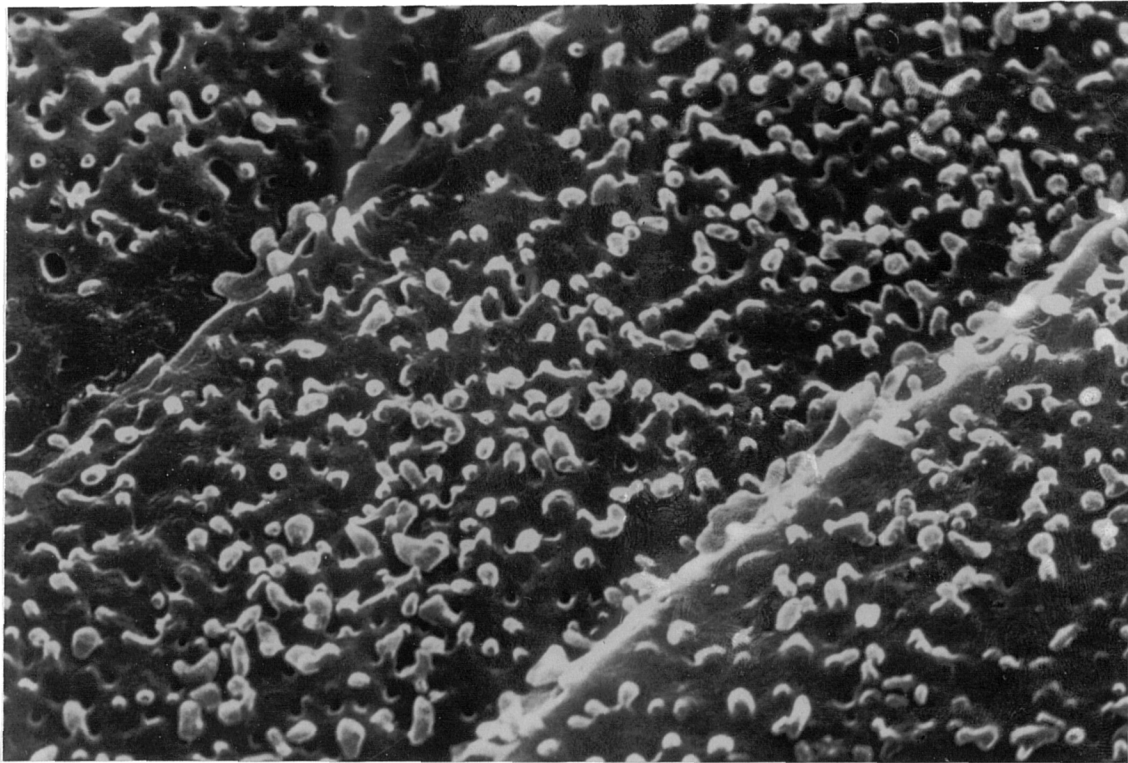


Fig. 3.20 Ball and sockets cover the broad faces of post-equatorial cortical fibres in great profusion. There are more than 120 processes per 10 square microns. Compare this picture to that of a light micrograph, Fig 3.27, from a similar area. (Posterior, level e/f) x4800

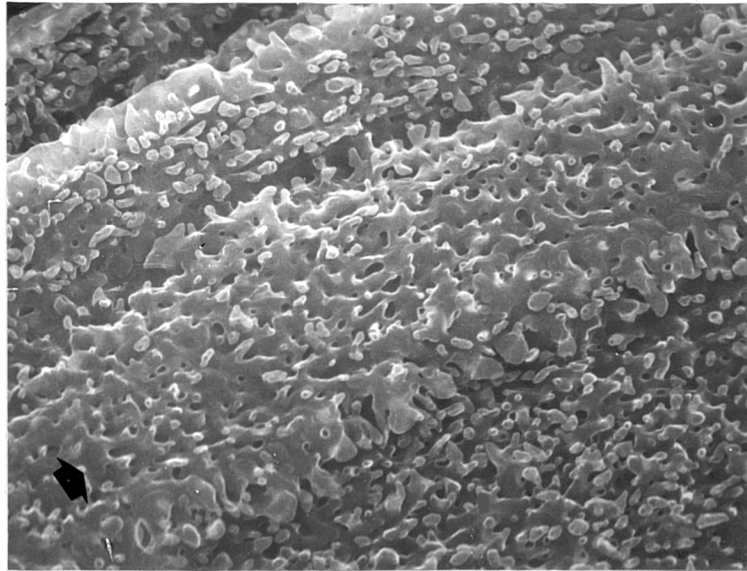


Fig. 3.21 Cortical lens fibres from a natural fracture face, close to the polar axis, level e/f. The fibre layer has separated along a different plane to that usually seen (see Fig. 3.2a), and the central fibre (arrow) is partly detached, from the rest of the layer. Flap-like angle processes are seen, which seem to extend from the short face junctions, which would normally be partly hidden. The broad face is covered in ball and sockets, some of which appear to have sustained damage, from either the electron beam or dissection.

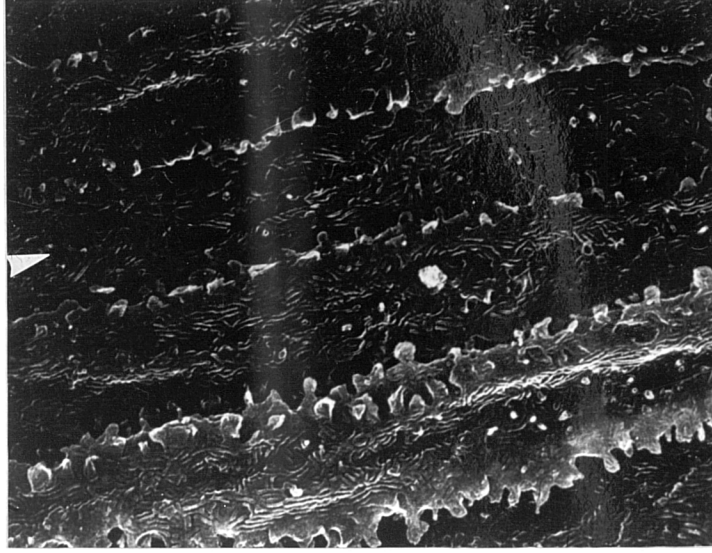
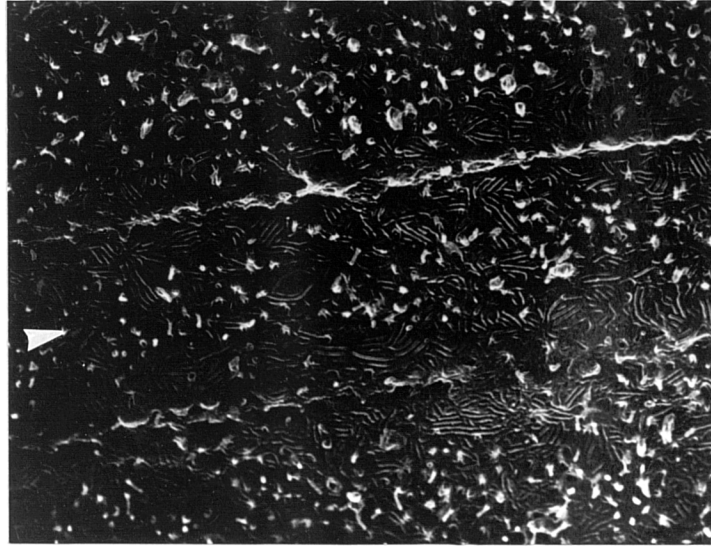
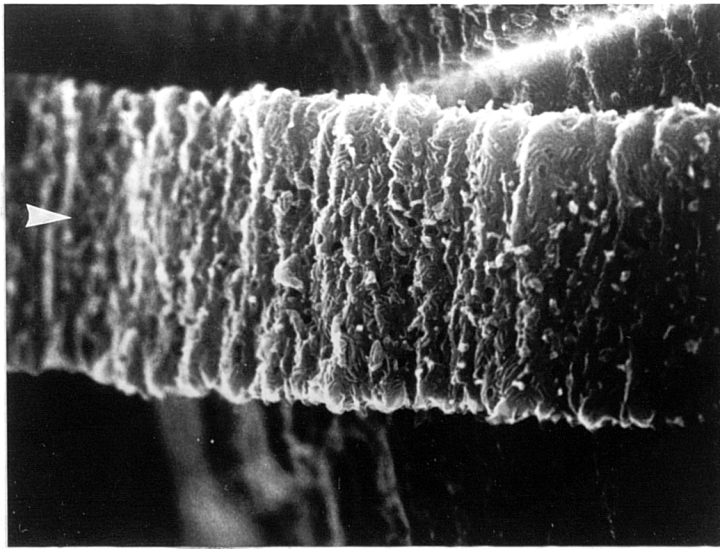
x3000

sockets (Fig. 3.19a and b) increased in density (up to 80 per 10 square μm) and size (0.3-0.5 μm diameter, up to 1 μm long) and became so profuse as to almost cover the fibre surface in a carpet of processes (Fig.3.20), thinning slightly close to the pole. Angle processes although sparse at the equator (Fig.3.20), progressively increased in size and incidence as the pole or axis was approached (Fig.3.21).

Intermediate (Layer c and d). Lens fibres of the intermediate lens between cortex and nucleus were slightly thicker than more superficial fibres. The change in the appearance of the lens fibre from equator to polar axis can be illustrated by a series of scanning electron micrographs, which follow a single fibre in layer 'd' along its posterior length.-

In the equatorial region (Fig.3.22a), the fibre is at its widest, with a moderate covering of small thin flap like ball projections (0.3 μm diameter, 0.3-0.6 μm long 50-80 per 10 μm square) and sockets. Thin (0.3 μm) flap-like angle processes are sparsely scattered along fairly smooth-edged fibres (20-30 per 100 μm edge). Where curvature is greatest, transverse undulations occur. Shallow tongue and grooves are faintly visible in a basket weave pattern.

Transverse undulations of the fibre surface disappeared as the curvature of the layer fattened out, and the fibre became slightly narrower. Ball and sockets were larger (1-1.5 μm in height) with narrower stalks and wider ball



a **b** **c**

FIG. 3. 22 A single lens fibre (arrow head), from the intermediate lens zone (level d) in three locations, along its length.

a) Equatorial!— The fibre is detached and shows transverse undulation.

b) Mid way between equator and pole.

c) Close to the polar axis!— Only the broad face of the fibre (arrow) is shown.

Compare the fibre width and orientation of tongue and grooves in the three locations.



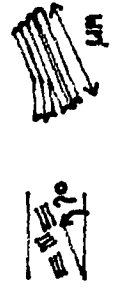
x 3000

endings, but of slightly reduced frequency. The tongue and grooves are clearer and the angle processes (50 - 60 per 100µm fibre length) both thicker and longer (0.3 - 0.7µm).

The width of the fibre is thinner in the intermediate zone between equator and axis (Fig.3.22b). Tongue and grooves are deeper, often in groups of up to five furrows and ridges and up to 1.5µm in length. Tongue and groove ridges tend to be orientated parallel to the long axis of the fibre. Angle processes are now about 0.2 - 0.3µm thick and between 0.4 - 1µm long, and become more prominent than previously. The frequency of ball and sockets reduces to 10-20 per square 10µm.

Close to the axis, but before terminating, the fibre width reduces further (Fig.3.22c). Ball and sockets are infrequent and angle processes up to 1.3µm in length. The fibre later showed some twisting (not illustrated) as it approached the suture and broadened. Closer to the suture, fibres overlapped each other.

Nucleus (Level a and b). Nuclear fibres are illustrated in section 3:3.1. Although they were narrower, nuclear fibres were thicker than those of the cortex. Ball and sockets, which covered the broad faces of fibres in cortical layers, reduced here in both size and especially frequency (0 -20 per square 10µm) in layer b and are absent in the deepest nucleus (layer a). Angle processes are thicker and longer and although their frequency is not much higher than

LEVEL	BALL AND SOCKETS 	ANGLE PROCESSES 	TONGUE AND GROOVES 
'f' outer cortex			
Equatorial	rare	rare	none present
Mid	0.2 - 0.3	0.3	0.4 μ m
Axial	0.2 - 0.3	0.6	0.6
'de' mid cortex			
Equatorial	0.3	0.3	0.3
Mid	0.3 - 0.5	0.5	0.5
Axial	0.3 +	0.5 - 0.8	1.5
'a' deep nucleus			
Equatorial	none present	0.5 - 0.8	0.8 - 1.5
Mid	none present	1.0	1.0
Axial	none present	1.0	1.0

≡ < Percentage of tongue and grooves orientated within 10° of the long axis of the lens fibres
>
more than 45°

TABLE 3a2 Variation in Size of Junctional Structures in the Lens (microns) (from H37)

in other sub-cortical layers, their increased size ensures that all face junctions in nuclear fibres are crowded with interlocking angle processes (80- 130 per 100 μm fibre length). Sometimes large irregular globular 'processes' are seen randomly distributed on the broad faces, especially in the deepest nucleus, similar in size and shape to deep angle processes.

Fibres of the deepest nucleus in layer a, (the oldest) are only about 5-6 microns wide as they cross the equator. The reduction in width away from the equator, seen in all other layers, occurs only to a limited extent here. Although tiny in width, they are well over a micron thick. Angle processes are thick and club shaped, and are especially prominent away from the equator, giving the nuclear fibres a characteristic irregular profile. Close to termination at a suture and often before the fibre changes direction, angle processes branch and become more complex. Ball and sockets are very rare or never occur but the tongue and groove pattern is marked.

3.3.2 Scanning Electron Microscopy of Forced Fracture

Faces

Lens fibres observed from forced separation planes have similar characteristics to those of natural separation planes from comparable locations (Fig. 3.23). Figure 3.24 shows fibres from a single forced interface between levels e and f.

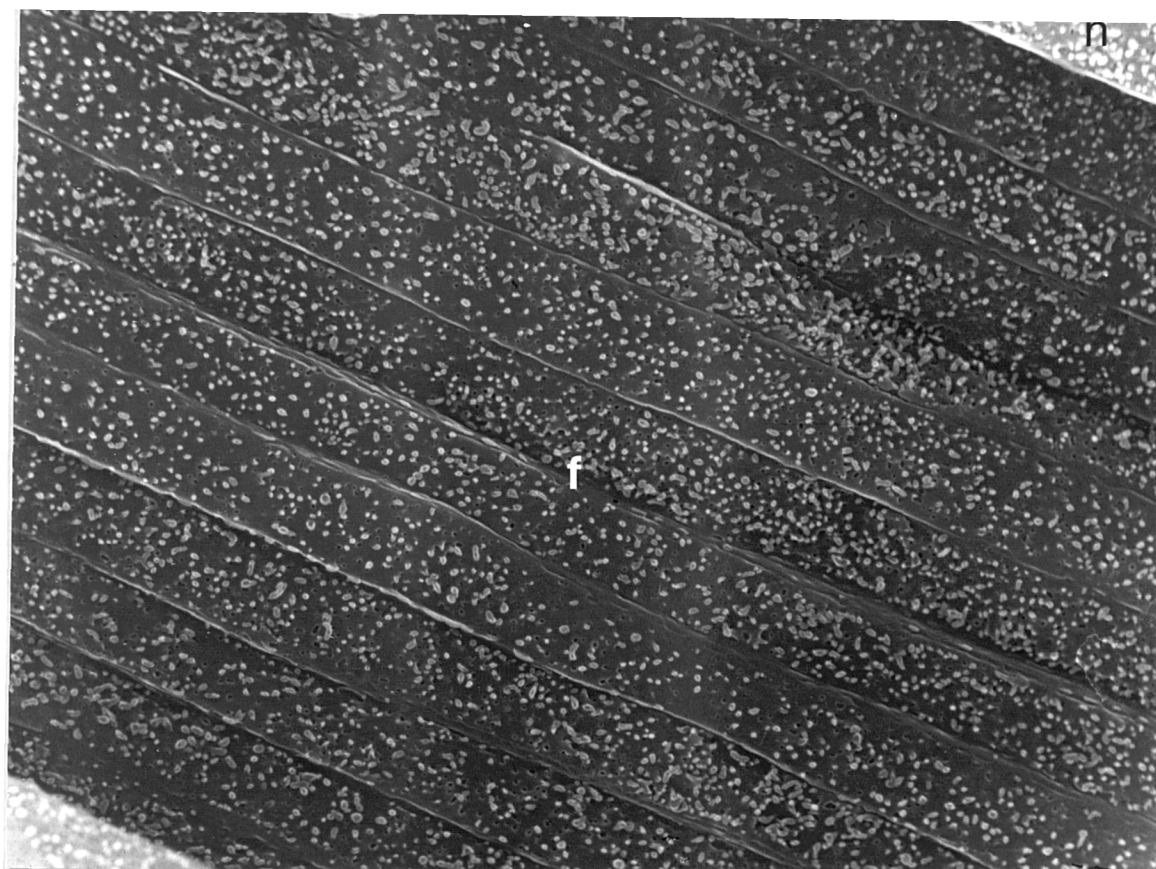
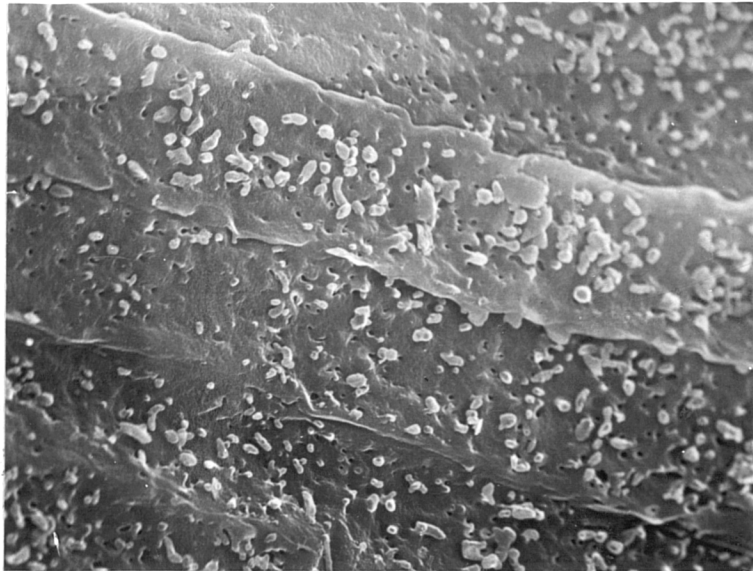


Fig. 3.23 Lens fibres from this forced fracture face (level e) are well covered in ball and sockets (f). The density of junctional structures was comparable with that of the natural fracture face fibres (n) from a slightly more superficial layer, shown in figure 3.5. x 1580

a)



b)

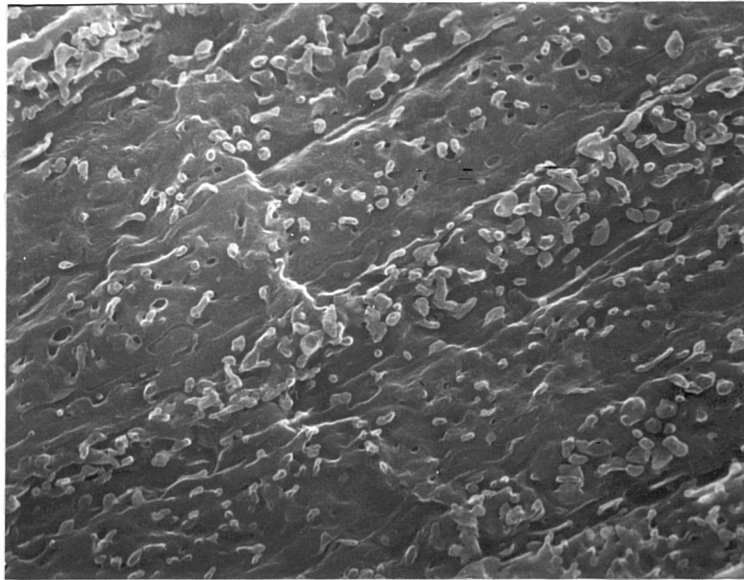


Fig 3.24 Cortical lens fibres of a single forced interface (level e), between equator and pole.

a) Fibres from the convex surface,

b) Fibres from a similar location of the concave surface.

Note the similarity in lens fibre shape and irregularity in distribution of finger-like ball processes. x3000

The variation in appearance from different locations between fibres from natural and forced separation planes, was similar to those found between two natural separation plane.

One consequence of using greater force to separate layers during dissection, not apparent in material subjected to gentler treatment was the greater damage present amongst the forced separated fibres. Some fibres had broken off and pulled away and fibres of several layers exposed. Such damage sometimes hindered assessment and photography of these layers.

3.3.3 Comparison of Natural and Forced Fracture Faces

Junctional structures occurred throughout the lens between both natural and forced separation faces. There was no evidence of junction-free faces.

The only area found to be consistently bare of putative junctional structures was the most superficial cortical layer of lens fibres. Sparse distribution of junctional structures was occasionally found over small areas of lens fibre layers, but these were usually surrounded by areas of normal profusion.

To illustrate the similarity between fibre surfaces from natural fracture surfaces and other layers, a detached fibre on a natural fracture face is shown in Figure 3:25. The density and size of junctional structures is similar in both the under-side (representing a forced fracture face)

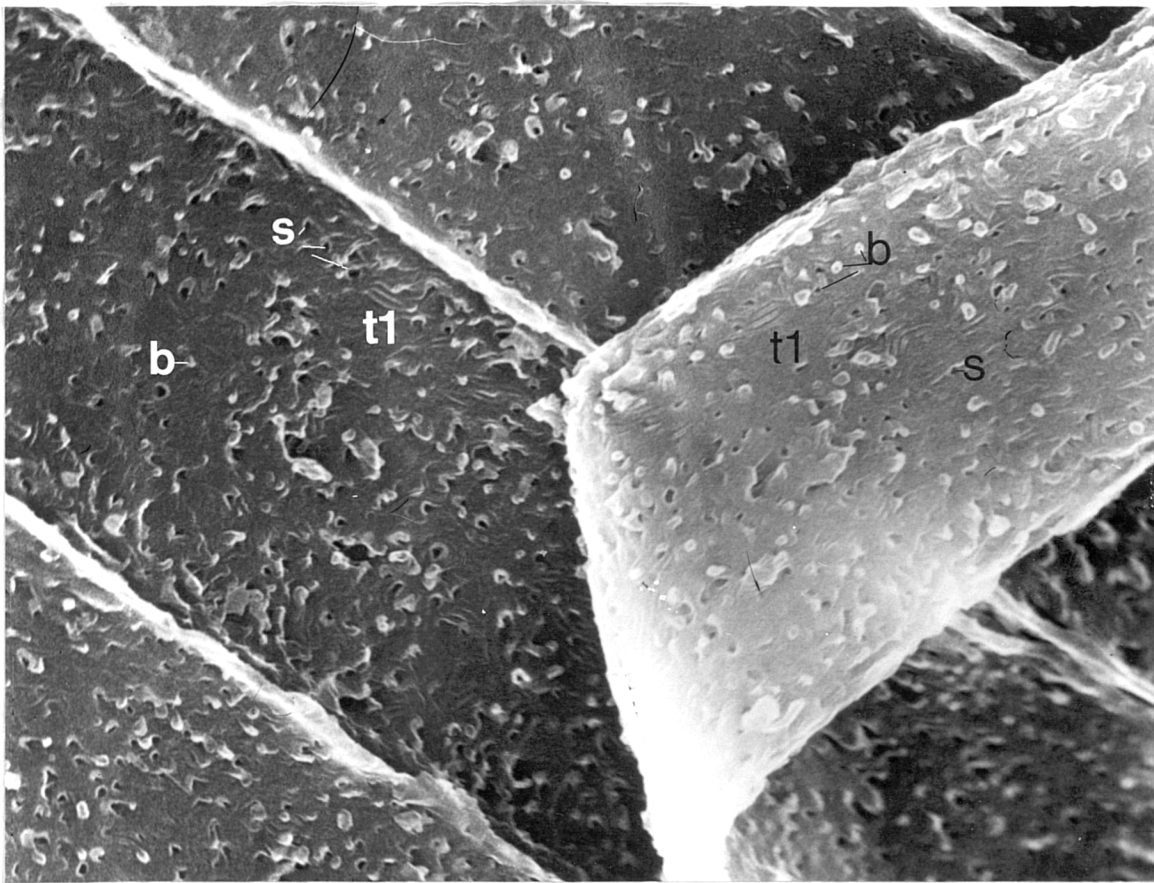


Fig. 3.25 Anterior intermediate lens fibres, of a natural fracture face. One fibre is detached and folded back, showing a similar density of junctional structures on both its upper and lower broad faces. Note the junctional structures on the underside of the reflected fibre (white t,b,s) and the exposed face of the underlying fibre (black t,s,b) appear to be a 'mirror image' of each other. (Level d) x4800

and undisturbed upper faces of the fibres of the natural fracture face. Mild surface damage, typical of a forced fracture face, is visible on the 'forced' exposed broad face of the underlying fibre.

3:3.4 Observations with Light Microscopy

Whilst resolution would limit the study of junctional structures, light microscopy (L.M.) of sections is better suited (than S.E.M.) to demonstrate the cross sectional shape of fibres. It was used to provide complementary information and to clarify points raised by S.E.M. Comparison of natural and forced fracture planes in an attempt to resolve the problem of putative shearing planes was not the intention and was not attempted with L.M.

Shape The classical flattened hexagonal pattern (Fig. 3.26) reported in other species was only seen clearly in fibres lying close to the equator or within the nucleus. In other regions, such as in deeper cortical areas close to the polar axis (Fig. 3.27), the pattern of lens fibres was less clear, and the flattened hexagonal fibre shape was rarely encountered. Lens fibres in this position, observed with light microscopy, can be so profusely decorated with membrane processes (ball and sockets and angle processes) that without S.E.M. the resulting tangle of membranes was difficult to interpret (Fig. 3.28).

Superficial cortical fibres stain differently to those

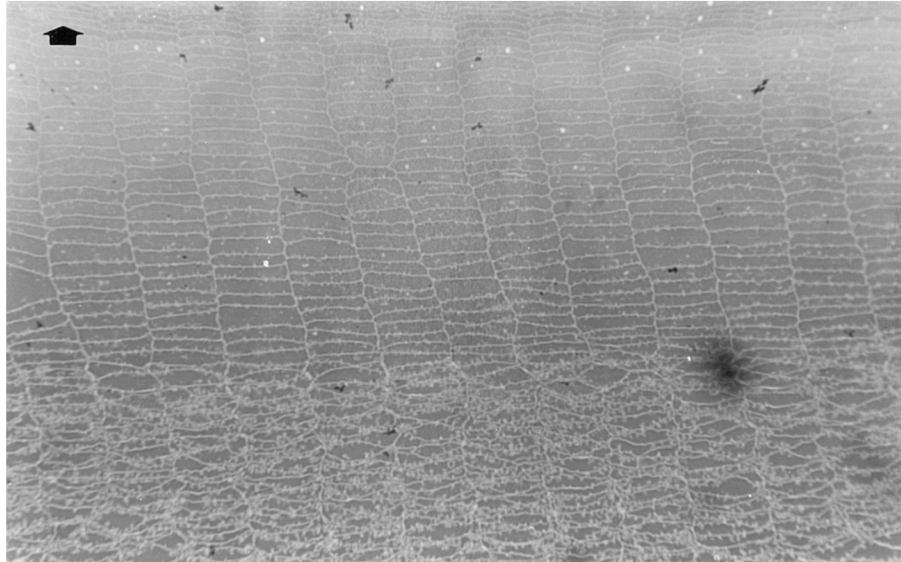


Fig. 3.26 Superficial lens fibre under the equator. Lens fibres in transverse section are basically six sided. The arrow indicates the direction of the surface.

This and all successive micrographs are of sectional material viewed with a light microscope. x730

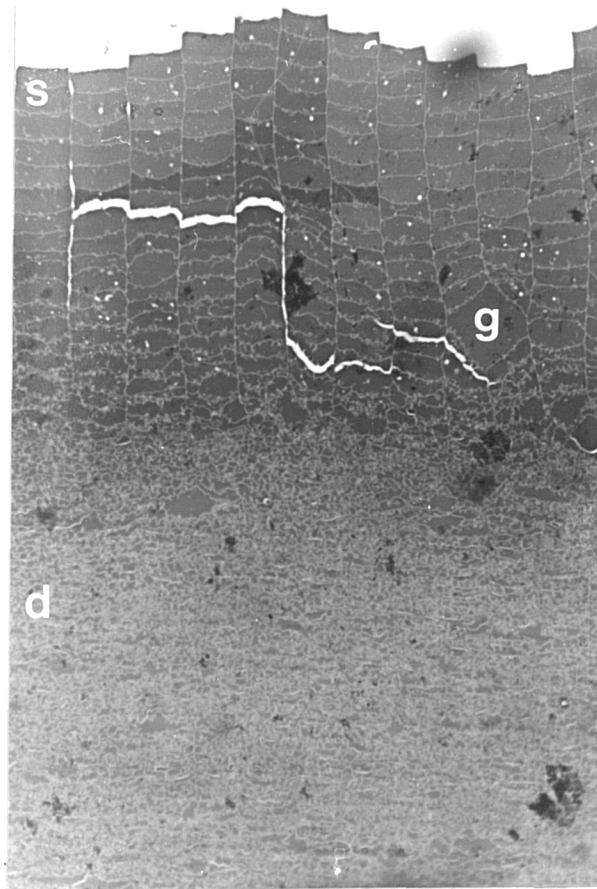


Fig 3.27 Cortical lens fibres between equator and pole. Superficial fibres (s) have a fairly regular pattern, but the deeper fibres (d) are very thin. Note the 'giant' fibre (g) occupying at least the space of four normal sized fibres. x730

in the rest of the lens. The cytoplasm of these fibres usually stained lighter than the deeper fibres with some variation from fibre to fibre and differential staining of the cell membrane (Fig. 3.26). They had six straight sides in transverse section and were arranged in a hexagonal pattern. Occasionally a larger 'giant' fibre was seen (as in other layers but since the 'giant' occupied the space expected of two or four fibres, the neat almost geometric pattern was only minimally disturbed (Fig. 3.27). Fibres at this level were from 1 μ m to 2 μ m thick.

Fibres gradually became more irregular with depth. They were thinner and interdigitation could be seen along their broad sides (Fig.3.29). Deeper still the hexagonal fibre shape was further distorted as the interdigitation increased both in frequency and prominence (Fig. 3.30). Irregularity was most marked in mid to deep cortical zones away from the equator such that the six sided nature of the fibres was obscured by marked interdigitation (Fig.3.28).

Interdigitation along the broad sides reduced in the deep intermediate zone and nucleus and the flattened hexagonal fibre shape was re-established (Fig.3.31). However the pattern of fibres was less regular than in the superficial cortex. In the deep nucleus of the lens (Fig. 3.32) fibres were smaller and less thin.

L.M. confirmed the findings from S.E.M. in that lens fibres are widest at the equator and also confirmed their extreme thinness. Lens fibres varied in thickness from about 0.5 μ m to almost 3 μ m and in each layer were generally

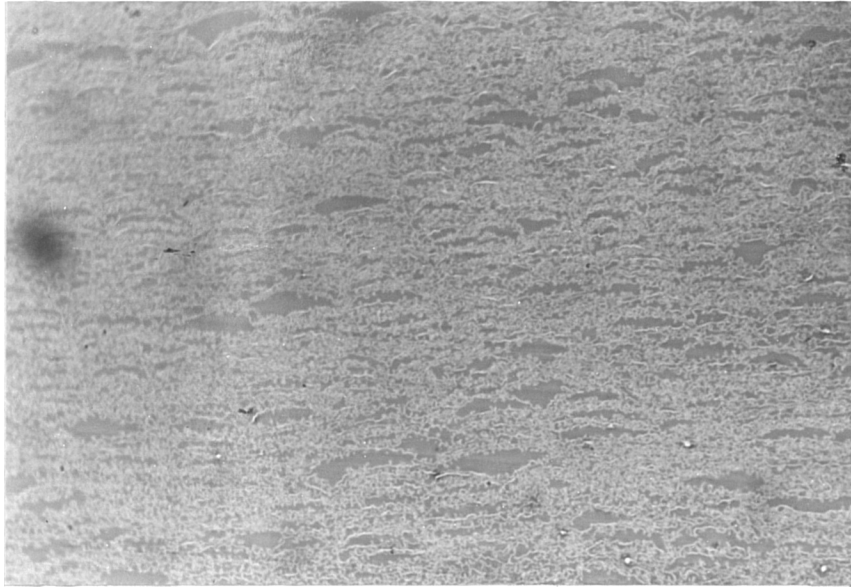


Fig 3.28 Interdigitation is profuse, in cortical fibres close to the polar axis. Fibres are thin and the hexagonal fibre shape almost completely hidden. x730

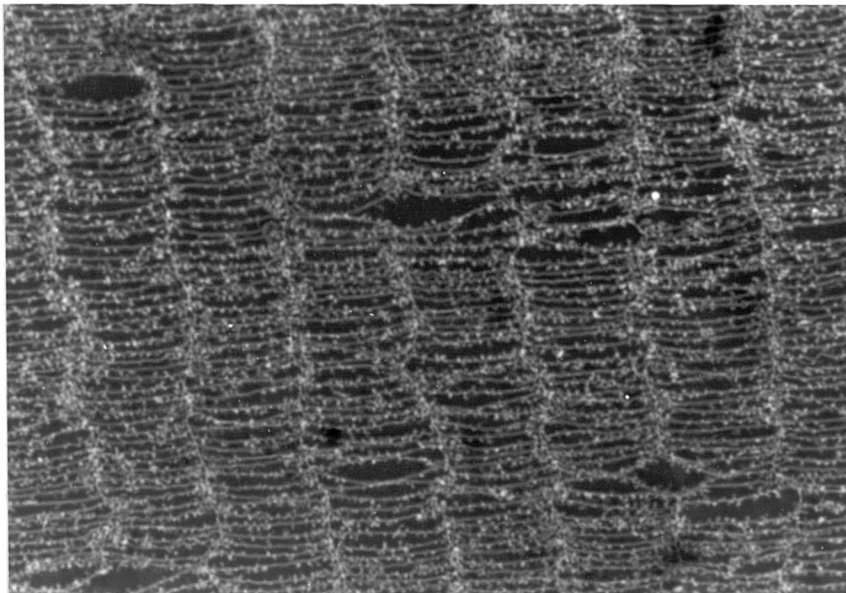


Fig 3.29 The flattened hexagonal fibre shape is apparent in these deep cortical/intermediate fibres from level d. x1030

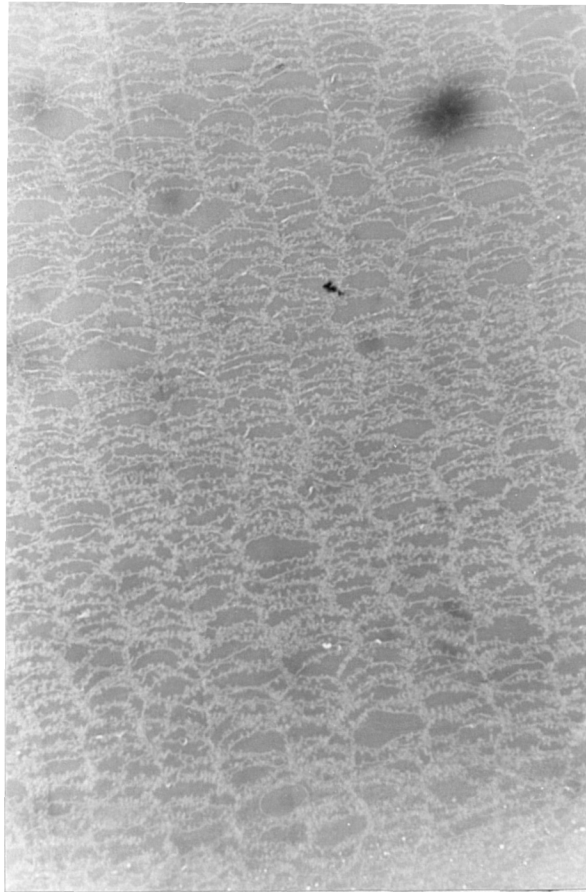
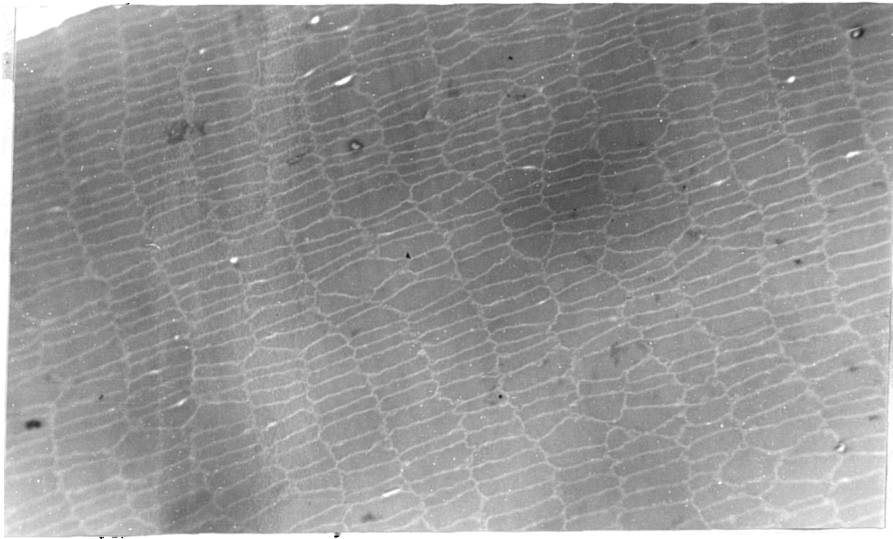


Fig 3.30 In cortical fibres (layer e/f) close to the equator, the flattened hexagonal shape is distorted by prominent interdigitation. The fibres are also slightly bowed or crescent shaped, with the convex curve facing the equator. Some of the fibres are cut slightly obliquely.

(MR78) x730

a)



b)



Fig 3.31 Interdigitation has diminished in fibres of the deep intermediate/nuclear lens (level b/c) and are roughly hexagonal in cross-section. x730

a) from under the equator

b) from close to the (posterior) polar axis

Lens fibres are wider and thicker near the equator.

thickest under the equator, being thinnest some distance from the polar axis. The thinnest fibres were the irregular fibres of the deep cortex and outer intermediate zone (equivalent to layer e and d) which varied from 0.5 - 1.2 μ m. The deepest nuclear fibres were between 1.7 and 2.5 μ m thick.

Interdigitation Interdigitation can be seen along the broad sides of lens fibres in both transverse and longitudinal section (Figs. 3.33, 3.34). These were seen as tiny club-shaped processes giving the fibre walls a very irregular appearance. Interdigitation was less clear along the short sides which in transverse section looked somewhat irregular. Only with S.E.M. was the interlocking nature of the angle processes demonstrated. The membranes in nuclear fibres appeared slightly wavy, as the tongue and groove pattern was too shallow to be observed with L.M.

The long flattened hexagonal fibre shape is still the underlying shape of lens fibres throughout most of the lens but in much of the lens this is modified and distorted by extreme thinness in cortical layers, the presence of junctional structures, and the changes characteristic of fibres near sutures.

3.4

DISCUSSION

There are other studies (Dickson and Crock, 1972; Hogan et al., 1971; Kuszak et al., 1988) that look at the

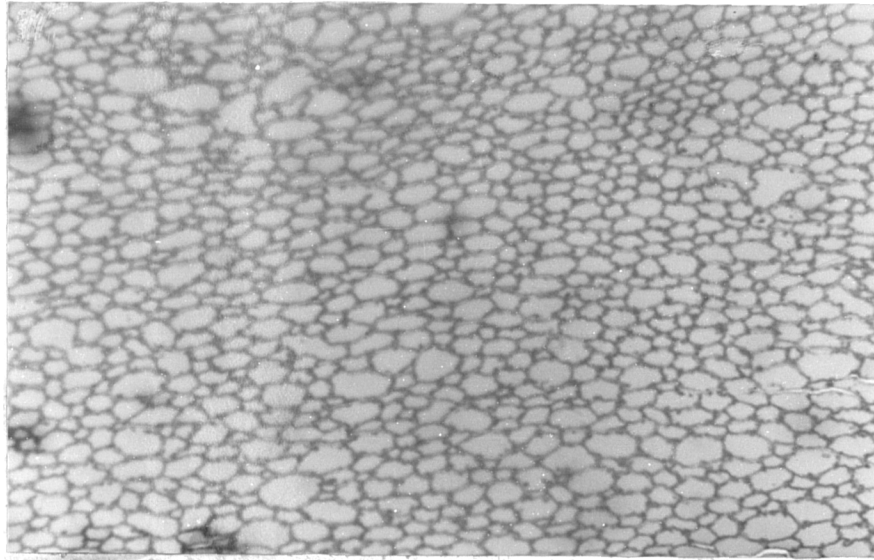


Fig 3.32 Lens fibres from the deep nucleus, close to the (posterior) polar^{axis}. Though narrow, the fibres are rounder than in the cortex, and are rather irregular in shape.

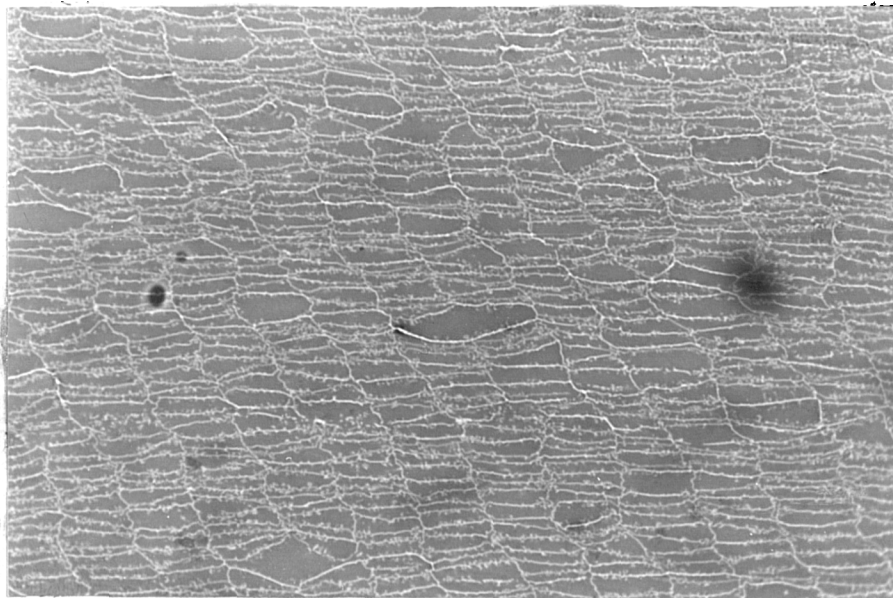


Fig. 3.33 Transverse section of deep cortical fibres under the equator. Club and ball shaped processes can be seen along the fibre borders. x730

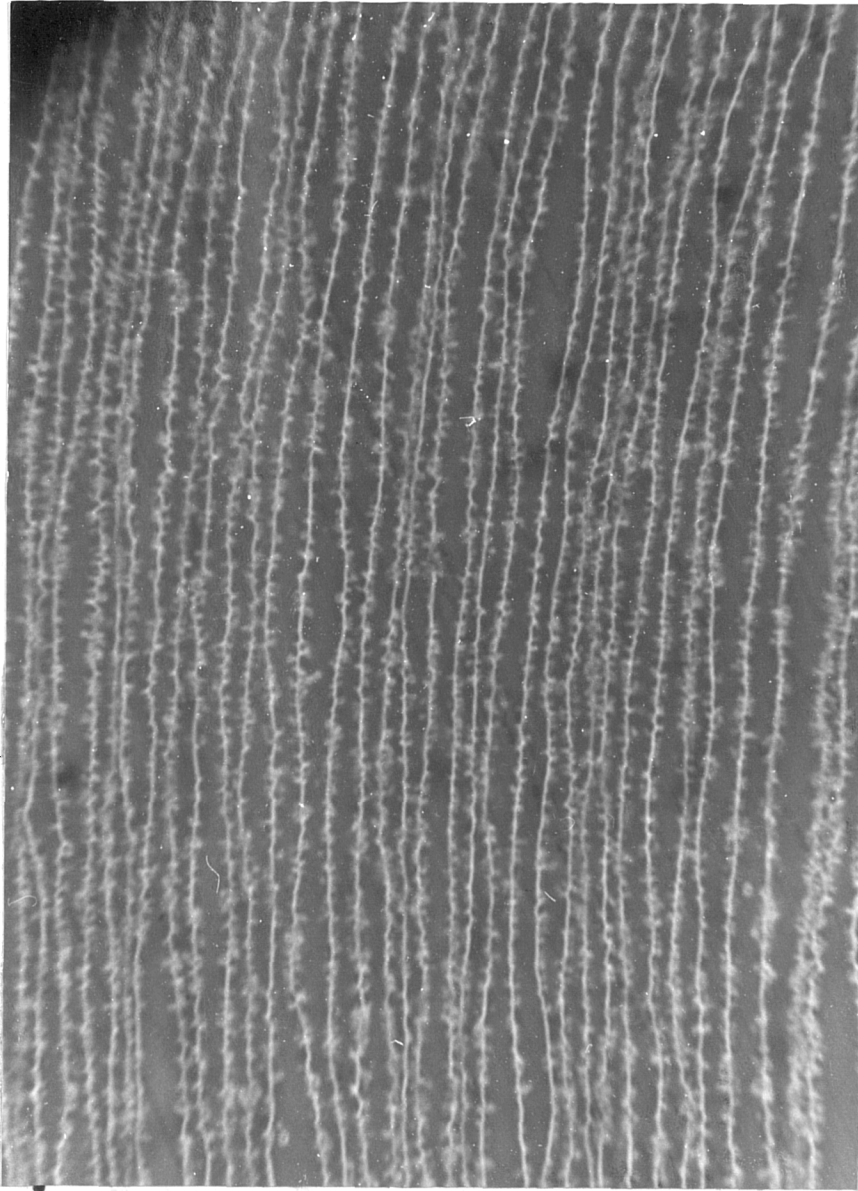


Fig 3.34 Fibre processes produce an irregular border, in this longitudinal section of cortical fibres. x1080

morphology and the three dimensional interlocking of lens fibres in primates, but this work had the specific aim of understanding the mechanism of internal lens shape change in accommodation.

Lens Fibre Shape

Lens fibres of the cynomolgus monkey observed here, do not all show the regular flattened hexagonal shape reported for many other species (Willekens and Vrensen, 1981; Kuszak et al., 1984; Maisel et al., 1981) but as Kuwabara (1975) also found, the actual shape of the lens fibre varies with location within the lens. This point is controversial since Jongebloed et al. (1987 human), Dickson and Crock (1972 monkey), Kuszak et al. (1988 monkey, baboon), have reported a more regular hexagonal pattern.

Kuwabara (1975) described the bow cells (immature lens fibres) as cylindrical in shape, the outer cortical fibres as flattened hexagonal cylinders, and the deeper cortical layers as band-like. The present results are in agreement apart from the shape of the superficial fibres, (equivalent to bow cells), which were similar in shape to the adjacent underlying fibres. However in the deeper nucleus, (not examined by Kuwabara) the fibres take on a slightly flattened hexagonal fibre shape again. In parts of the nucleus, the classical flattened hexagonal shape was seen, but at others, occasional four or five sided fibres or isolated fibres that suddenly double in width or thickness,

(as if to fill in for a damaged neighbour), were seen.

The flattened hexagonal cylinder, is the basic fibre shape, which is seen in the youngest fibres, but in much of the lens this is modified, and distorted, by extreme thinness (in the mid cortex layers f and e) by broad face and angle junctional structures, most marked near sutures.

The fibres of the mid-cortex show the greatest irregularity, whilst the deepest fibres of the nucleus and the most superficial cortical fibres, are more regular in shape. Although fixation problems could be the cause of fibre irregularity, in this case since the outermost and innermost layers do not show the irregularity, fixation artefacts are an unlikely cause.

n. n. lines give rise to + artefact to birefringence, cytoskeletal elements to + (aligned along long axis of fibres) in areas where membranes small + dist + + (Bettelheim) - see The Dark as lens (Mandel 98-)
← see theory of transparency

Lens fibres are usually wide as they cross from anterior to posterior, their width gently reducing to almost half towards the axis, which has been described as the spindle-shape (Hogan et al., 1971). Then they rapidly widen as the suture is approached. The actual width of terminating fibres is variable and was not measured here, but appeared to be similar to the equatorial width. This is similar to the width changes observed in the living human surface lens fibres (anterior), reported by Brown, Bron and Sparrow (1987). Cortical lens fibres, were of similar order of width (4-14µm) to those found in the human (Salzmann, 1912 8-12µm Kendall, 1982, 5-12µm).

causing of from birefringence - known of fibre system by (-) with (+) intrinsic birefringence (due to molecular orientation of cytoskeleton)

Junctional Structures

Until now little distinction has been made in the primate lens literature (Cohen, 1965; Wanko and Gavin 1959 Hogan et al. 1971) between the processes which occur on lens fibre faces and those found along the angles formed by the joining of faces. In this study two types of finger-like processes were identified; the face processes with their true sockets (ball and sockets), and the processes found along the angles, which had no discrete sockets. The angle processes, appeared to interlock in pairs or threes, knitting together like a three dimensional zip, (made of three sets of teeth), joining three different fibres. Interlocking of angle processes became more complex with increasing depth in the lens. In the equatorial cortex, angle processes are thin and flap-like, and received by shallow depressions in neighbouring fibres. In some parts of the nucleus, much longer angle processes, appeared to interlock, like a three-way dovetail joint. Angle processes were accommodated between depressions in the faces of lens fibres. After the removal of a lens fibre layer by dissection, rows of 'holes' were observed, formed between angle processes and depressions in the lens fibre faces, presumably to receive the angle processes of the absent layer. Although these spaces were socket-like, they were different from the true sockets seen on the broad faces of lens fibres, and the description used in the past of the angle processes as 'ball and sockets' (Hogan et al 1971,

Dickson and Lock 1972), is misleading.

Willekens and Vrensen (1981), and Carhart (1981), demonstrated a similar system of 'interdigitating protrusions' in the rabbit. Jongebloed et al. (1987), as part of a study of human cataract, looked specifically at the junction of the short faces of cortical lens fibres with S.E.M., and noted the similarity of the angle processes to a (normal two way) 'zipper system'. They commented only on the angle processes, and incidentally, noted the loss of these structures in cataract.

In the chick, two types of interlocking processes have been described along the fibre edges (Kuszak, Alcala and Maisel, 1980). Where the short sides meet, ball processes extend and fit into sockets (formed between broad faces), and along the meeting of short and wide faces, flap-like processes fit into opposing 'imprints'.

In the rabbit Willekens and Vrensen (1981) described imprints, left when an interdigitating protrusion (angle process) is pulled away (freeze fracture), which they argue suggests the presence of gap junctions. Depressions (rather than imprints) from angle processes that have been removed by dissection, have been observed for the first time in the monkey, in this study.

Angle processes in the monkey have a lower incidence (30-130 per 100µm fibre length) than in the rabbit (130-260 per 100µm Willekens and Vrensen, 1981) but are rather larger.

Because of their ubiquity, prominence, packing and involvement of three fibres, the angle processes impress as the most effective fibre locking devices observed in this study.

True 'ball and socket' junctional structures were only observed between the broad faces of lens fibres. Interdigitating processes between lens fibres, have been reported in the literature, since they were described by Wanko and Gavin (1959) and Cohen (1965), although Hogan et al. (1971) were probably the first to name them 'ball and sockets'. Both Hogan et al. (1971) and Dickson and Crock (1972), used the term to describe face and angle processes, a point challenged, on the basis of their differing appearance, location and distribution.

Ball and sockets have been described in several other species (Leeson 1971; Kuszak et al., 1980; Willekens and Vrensen, 1981; Kuszak and Rae, 1982) but they are dissimilar from those of the monkey, and man (Kuwabara, 1975) in their profusion. The appearance of ball projections in some parts of the monkey fibres, bears more resemblance to the sea of microvilli found on the corneal surface than to the often single row of centrally aligned ball and sockets described in rodents! The chick, with its powerful accommodating lens, (by marked anterior lenticonus), presents a different picture, of tiny villi-like ball and sockets found only in the posterior cortex, on the inner of the two wide faces.

No evidence was found of a greater profusion of ball and sockets in the anterior lens, as reported in some studies.

Ball projections were up to $1.5\mu\text{m}$ in length, and between $0.2 - 0.5\mu\text{m}$ in diameter, which is a little smaller than Kuwabara's (1975) found in man using T.E.M. They were most profuse, in the outer to mid-cortex, (except the first 15 fibres below the capsule), in the area of lens directly beneath the suspensory zonules. Willekens and Vrensen (1981) have observed a similar distribution of ball and sockets in the outer cortex of the rabbit. It is arguable that the ball and sockets provide extra binding strength, in an area perhaps most exposed to torsional forces.

Willekens and Vrensen (1981) observed transverse fibre undulation in equatorial fibres in the rabbit and make the point that these folds or undulations could unfold, to allow lengthening of fibres across the equator in accommodation, with the extra dense covering of ball and sockets to prevent sliding. They postulated that change in lens fibre length, is an important factor in accommodation. Transverse fibre undulations were observed in equatorial fibres of the monkey in the present study.

Tongue and groove junctions, were found only in deeper lens fibres. The pattern of ridges and grooves, increase in height and length with increasing lens depth, a point also noted by Kuwabara (1975), who described the groups of ridges

as forming a 'waffle pattern'. Near the equatorial bend, the ridges tend to orientate diagonally across the long axis of the fibre, but away from the equator, their orientation changes, such that in axial zones the majority of ridges fall along the long axis of the fibre. T.E.M. studies (Dickson and Crock, 1975; Kuwabara 1975) have demonstrated additional fusional membrane modification (gap junctions).

The tongue and grooves vary in length (0.5-4 μ m), height (up to 0.2 μ m) and number in a group; only 2 or 3 shallow ridges present where they were first seen, compared with 4-8 deep ridges where the pattern was most marked. In the deep nucleus, the tongue and grooves were longer than described before this study began (Kuwabara, 1975; Sakuragawa et al., 1975), a point also noted by Kuszak and colleagues (1988), who together with the present study have examined lens fibres from the deepest nucleus.

Kuszak et al., (1988) noted a tendency for ridges to pull away, and resemble thin finger-like processes, and used stereo imaging to assist in interpretation.

They interpreted the tongue and grooves to be microvilli, lying along furrowed grooves, on their sides and reattached at their tips. Detachment of the microvilli tips from their reattachment sites, was artifactual, and revealed the underlying furrowed domains.

Observation of tongue and grooves in their shallower state, puts doubt on this theory. It is hard to imagine microvilli developing from the shallow linear ridges of the

deep cortex (Fig. 3.11). The tongue and groove pattern changes progressively with depth, rising higher from the surrounding surface, more like wrinkles than processes. If they are microvilli, how do they develop, from the soft shallow folds seen in the deep cortex? The tongue and groove pattern has also been noted on the surface of angle processes, a feature consistent with a junctional role. The apparent intermeshing of tongue and grooves of apposing fibres, observed in this and earlier studies (Dickson and Crock, 1975; Kuwabara, 1975), is also more consistent with a junctional function, than a sign of membrane senescence (Kuszak et al., 1988). Transmission electron microscopy of nuclear lens fibres might elucidate this problem.

Dickson and Crock noted that in their preparations, damage to ball and socket structures was more common than to tongue and grooves, suggesting the former is firmer junctional structure. They wondered if tongue and grooves help reduce 'lateral' (presumably transverse) sliding. With the findings here of a change in orientation from equator to axis, an extension of this line of thought is that the basket like surface pattern of the equator may reduce sliding along the fibre, the parallel tongue and groove pattern of the axis, prevent sliding across the fibre.

Intra-lenticular Mechanism of Accommodation

The distribution of processes varies throughout the lens, but putative junctional structures of one sort or

another, are found in all parts of the mature lens, such that gross sliding between lens fibres is not tenable.

The search for shearing planes revealed occasional fibre faces with reduced density of junctional structures, but these occurred in both natural and forced separation planes. For a shearing face to function all the fibres in the face would need to be junction free. Therefore the notion of sliding between putative shearing faces is not supported.

The only faces consistently devoid of junctional structures were those of the most superficial, elongating immature lens fibres, - a feature also noted by Willekens and Vrensen (1981) in the rabbit, which they suggested was consistent with their need to slowly elongate and slide into their new position.

In addition to the numerous interlocking junctional structures throughout the lens, junctional membrane modifications (gap junctions), have been demonstrated (Kuwabara, 1975; Dickson and Crock, 1972). Though not studied here, they have been observed both associated with and separate from junctional structures and would presumably add to the adherence of fibres, restricting sliding still further. One alternative to sliding, is that lens fibres change shape (Gullstrand, 1924; Kuwabara, 1975; Koretz and Handelman, 1985), perhaps by redistribution of cytoplasm along the length of individual lens fibre. The great length

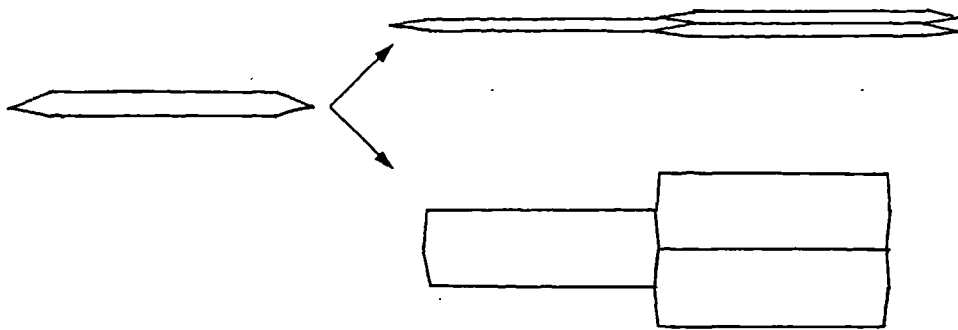
of the fibres spanning from anterior to posterior sutures, may facilitate redistribution of cytoplasm (Philipson, 1975) along the length of the fibre to the axial zones in accommodation, and back towards the equator when accommodative power is relaxed.

According to Kuwabara (1975) the lens appears to change shape mainly by changing intracellular fibre shape in the superficial zones, and "perhaps also a little sliding", a point which is not in agreement with the present findings. The small tightly packed fibres of the nucleus appeared too solid to Kuwabara to allow movement.

The superficial immature developing lens fibres (bow cells) may have some role to play in accommodative shape changes, but since they form only a relatively small proportion of the lens, only some modification of the mature full length fibres (or their arrangement) could achieve the axial thickening required in accommodation.

Brown (1973a) has shown that the nucleus of the human lens thickens axially in accommodation to a greater extent than the cortex. If all lens fibres were equally capable of changing shape by cytoplasmic flow, at the dictate of the capsule, the force would affect the cortical fibres and exact a shape change in them before being transmitted to the deeper nuclear fibres. The implication of Brown's findings however, suggests that it is the nucleus not the cortex where such redistribution takes place (Brown, 1973b). The concept of selective nuclear thickening demands that the

a)



b)

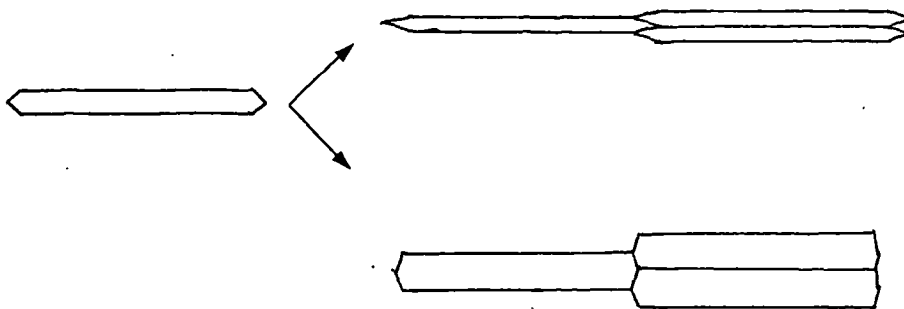


Fig. 3.35 Diagram to explain the effect of the 'short face' dimensions on the potential for variation in cross-sectional area. The broad face is drawn the same width in both (a) and (b), but the dimension of the short faces in (b) is half that of (a).

zonular and capsular forces, acting through the cortical layers, trigger a local nuclear mechanism. Do any of the observations already made give any clues as to how such a mechanism could operate? Consideration of the effect of fibre shape on redistribution of cytoplasm may provide an answer.

Fibres were thinnest in the deep cortex and intermediate lens zones. Deep nuclear fibres were the narrowest fibres of the lens but were amongst the thickest.

The facility for transverse fibre shape change is dependent on the length of the short sides. A hexagon can be very thin, with its short sides meeting at very acute angles, or almost rectangular, with the junction of short sides nearly in alignment (Fig. 3.35). The potential range of incremental cross sectional area variation is proportional to the length of the 'short' sides. If this holds true, nuclear fibres with their greater thickness, have more potential to expand or contract, than the thin band-like fibres of the cortex.

The presence of junctional structures throughout the lens is inconsistent with relative movement of lens fibres (sliding) to achieve the overall lens shape changes of accommodation, but not inconsistent with the notion of intracellular redistribution of cytoplasm.

The prominent angle processes in the nucleus could perhaps allow tiny adjustments between fibres to accommodate changes in internal fibre shape, in the same way that wire

mesh can be distorted, and maintain a regular pattern.

CHAPTER FOUR

4 EVIDENCE FOR CYTOPLASMIC FLOW IN THE ACCOMMODATED LENS

The previous chapter leaves unanswered the question of implementation of lens shape changes in accommodation by the lens fibres, and pointed to a need to compare lens fibre shape and form in differing states of external curvature.

4:1 INTRODUCTION: HYPOTHESIS OF CYTOPLASMIC FLOW

The circumference of the accommodated lens is smaller than that of the unaccommodated form and its anterior posterior axial thickness greater. Since sliding cannot occur, the number of fibres crossing the equator in any one layer must remain unchanged so the reduction in lens circumference must be effected by a reduction in the individual width of the lens fibres. As the aperture or diameter of the lens also reduces in accommodation, thinning would also be required of the equatorial portion of the lens fibres. This suggests the need for a loss of both fibre thickness and width, or local volume, in those portions of the fibres under the lens equator. Since the lens thickens axially in accommodation, thickening of the axial portions of the lens fibres can be predicted. Since the total volume of each fibre is unlikely to alter, redistribution of individual fibre contents is postulated. A requirement of this theory is a redistribution of volume along the lens fibre. If this theory holds it is possible to predict that

the 'spindle'* shape of lens fibres, noted in the last chapter, should become less marked in accommodation.

Lens fibres inevitably experience a change in curvature as a result of accommodative lens shape changes, however, the phrase "lens fibre shape change" will be used not to indicate these curvature changes, but localised volume changes along the lens fibre.

4:2 MATERIALS TO TEST THE HYPOTHESIS OF CYTOPLASMIC FLOW

In order to test the hypothesis of lens fibre shape changes as a mechanism for overall lens shape change, measurements of lens fibres from lenses in different curvature states were required. Experiments were undertaken to produce lenses fixed in differing curvature states.

4:2.1 Induction of Accommodative Spasm

Drugs capable of inducing ciliary spasm (and miosis) in man have been used to produce a similar reaction in the monkey.

* The fibres cannot really be spindle-shaped, since fibres increase in size at their terminals. The term 'spindle-shaped' refers to their tendency to be widest and thickest at the equator and taper anteriorly and posteriorly, with distance along their length from the equator.

Tornqvist (1966) used topical carbachol (a direct acting parasympathomimetic) in the cynomolgus monkey, and von Pflugk (1909) had used the anticholinesterase drug eserine (physostigmine), to induce an accommodative lens shape change. This change was maintained after enucleation and rapid freezing.

Previous experience with phospholine iodide (ecothiopate iodide) indicated that this anticholinesterase drug used topically has a miotic and cyclospasmic effect in the rhesus and cynomolgus monkey (Ruskell 1981, personal communication). However unlike man, in which phospholine iodide has a long lasting (irreversible) action, in the monkey the miotic and cyclospasmic effect wore off after only a day or two, and further applications had reduced affect. Phospholine iodide is used ophthalmologically in man because of its powerful and lasting action, and is occasionally used in children (who have maximal human accommodative facility) in the treatment of accommodative esotropia. Phospholine iodide was therefore chosen for its known cyclospasmic action.

A first attempt (M72) to induce and maintain accommodative spasm through fixation, using 0.25% phospholine iodide topically 24 hours and one hour prior to fixation, failed and produced little shape change.

Fortunately the next attempt to maintain an accommodative shape change through fixation was more successful.

An adult female cynomolgus, weighing 4.8Kg, was found to be almost retinoscopically emmetropic whilst sedated with Vetalar (R&L RX +0.25DS). After sedation, 0.2ml 1/4% phospholine iodide was injected subconjunctivally and drops of the same strength instilled into the right conjunctival sac. Three and a half hours later, after sedation, the right (treated) pupil was only one mm in diameter, the left (untreated) still 4.5mm, and retinoscopy indicated a refractive difference of around 6 diopters. After fixation by perfusion (Appen. B), the right pupil remained tiny, and subsequent careful removal of both lenses from the orbits revealed the treated right lens to be steeper on both surfaces than the untreated left (Fig. 4:1). Thus some induced curvature change was maintained through fixation. The posterior surface showed some peripheral flattening close to the equator, such that the central posterior steepening appears conical.

Lens	diameter	axial thickness	post*radius	ant*radius.	
ML73	8.3 x 8.45	2.68	4.78 ²⁰⁹	(26.81)	37.3
MR73	7.85 x 8.25	3.05	4.39 ²²⁷ (9' 3" 86)	21.43	46.2 (25°)

* post = posterior, ant = anterior

Table 4:1 Lens dimensions from M73 in mm

Topical phospholine iodide was also given monocularly, to other monkeys prior to perfusion, with variable results. In one monkey (M91) 2.5% phospholine iodide applied topically, the treated right pupil remained small after perfusion but the right lens was badly distorted; this pair

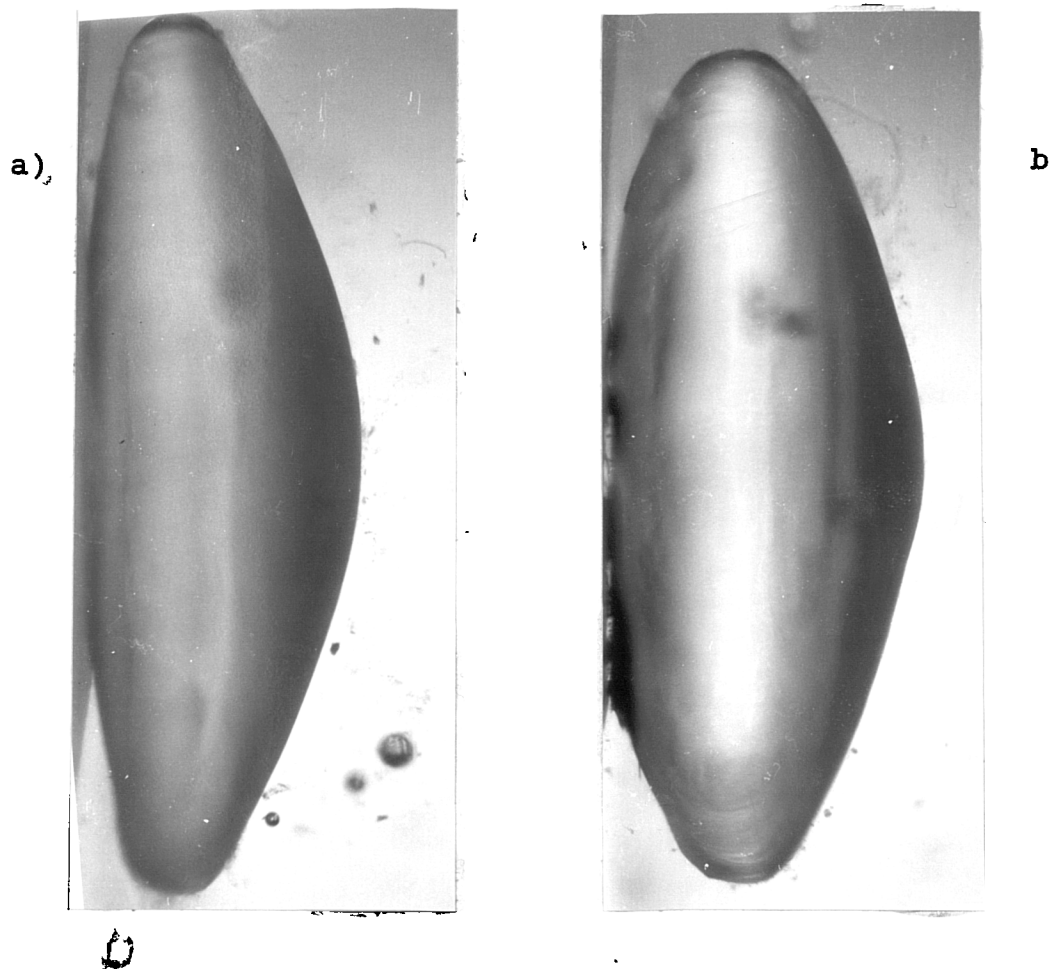


Fig. 4:1 a) Profile of the control lens (ML73). The anterior surface is on the left, the steeper posterior surface on the right. x13.5

b Profile of the lens from the phospholine iodide treated eye (MR73), similarly orientated. Both anterior and posterior surface of the treated lens are steeper than those of the control. x13.5

was not used in the study.

It is interesting to note that within months of the experimental use of phospholine iodide, its cyclospasmic effect in the rhesus monkey was confirmed by Bito et al. (1982) and Kaufmann et al. (1982). They used most of the standard parasympathomimetic and anticholinesterase drugs used in ophthalmological practice (including 2.5% phospholine iodide) producing marked accommodation in the rhesus monkey.

4:2.2 Unocular Lens Dislocation.

Attempts to maintain drug induced accommodative spasm through fixation had little success, so an alternative method of producing an accommodated-like shape change was sought. When the zonules supporting the crystalline lens are cut, the lens assumes a steeper rounded form, similar to its maximally accommodated shape.

Dislocation of the right lens by surgically severing the zonules was performed on a young adult male cynomolgus monkey (3.4kg) under general anaesthesia with Nembutal, immediately prior to perfusion (Appendix B).

There was a marked difference in external curvature between the resulting pair of lenses (Fig. 4:2). The dislocated lens was distorted, so pieces of tissue used in this study were selected to avoid the most distorted areas of this lens.

Part of the control lens was damaged on removal from

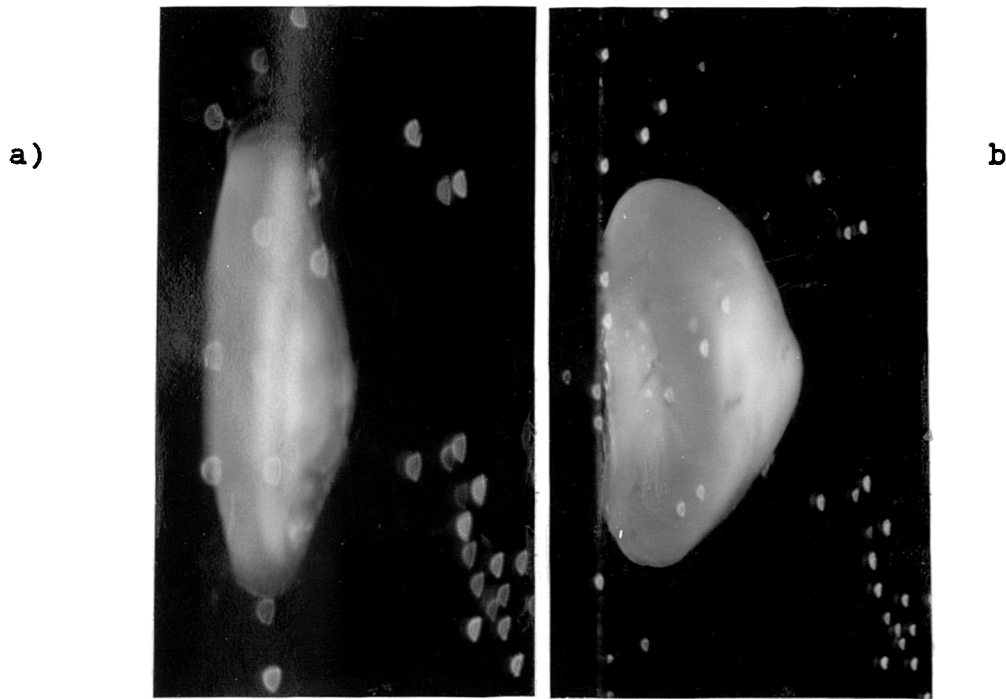


Fig. 4.2 a) Profile of the control lens ML78. The anterior surface is on the left, the posterior on the right. This lens was damaged after fixation, and part has been cut away. x8

b) Profile of the dislocated lens, MR78, similarly orientated. It is distorted, due probably to a fixation artefact, but the posterior surface is much steeper than that of the control. The axial thickness is greater, and the equatorial diameter reduced. x8

the globe. Only the unaffected half was retained for use in this study.

Lens	Frontal diameter	axial thickness.
ML78	8.08	2.4
MR78	6.55	3.37

Table 4:2 Dimension of lenses from M78 in mm

The anterior and posterior curvatures were not calculated in view of distortion to the right and damage to the left lens.

The anterior surfaces of all four lenses showed an artifactual central dimple. Since the artefact was small, the decision was made to proceed, restricting examination to posterior lens tissue.

4:3 METHODS TO TEST FOR CYTOPLASMIC FLOW

The hypothesis of cytoplasmic flow predicts local volume changes along the lens fibre. In accommodation, the equatorial circumference reduces so a reduction in width of fibres in the equatorial plane is predicted. ←

The width of equatorial surface lens fibres can be compared in control and simulated accommodated conditions to test the prediction made. Lens fibre width was measured during examination with scanning electron microscopy using techniques used previously, as well as by light microscopy. However, to test the notion that movement of lens fibre

cytoplasm is part of the mechanism for overall lens shape changes in accommodation, knowledge of lens fibre width alone is inadequate: the thickness must also be measured and a procedure permitting measurement of both is required for this purpose.

Preparation of lens fibre cross sections for light microscopy at known points along the lens fibre (equatorial-polar arc) was the method chosen to test for local lens fibre volume changes in accommodation. Earlier work (section 3:3.1) had shown that lens fibres vary in thickness from nearly $3\mu\text{m}$ to under $0.5\mu\text{m}$, pointing to potential difficulties with the limitations of resolution available using a light microscope.

4:3.1 Width Measurement of Surface Lens Fibres

Surface lens fibres can be observed and measured directly using a dissecting or light microscope. These are seen most clearly in whole specimens after removal of capsule and epithelium. The fixed lens, immersed in dissecting fluid, was supported in such a way that the surface to be measured was perpendicular to the viewing axis of the microscope. Small translucent plastic or glass rings of different diameters and tilt angles, were cut from tubing and weighted. This assisted in positioning and immobilisation of the lens for each measurement.

The mean width of lens fibres crossing the geometric equator was assessed in both the dislocated and control pair

m78 using a Zeiss microscope fitted with a measuring eye piece. Surface lens fibre width between the equator and posterior pole was also measured, taking all measurements midway between sutures.

4:3.2 Lens Fibre Morphology and Width Measurements Using Scanning Electron Microscopy.

Scanning electron microscopy was used to compare lens fibre morphology from control and treated lenses.

Questions raised from the previous chapter related to:-
(i) the transverse undulations observed in lens fibres under the equator; and (ii) the height of tongue and groove junctions. Could the transverse undulations be smoothed out in accommodation as claimed by Willekens and Vrensen (1981) to allow lengthening of fibres under the equator? Could the tongue and groove pattern deepen to assist in fibre width or length reduction, or the folds expand and flatten to allow an increase in volume? These questions warranted a comparison of lens fibre morphology from lenses of differing curvature states.

Fibre morphology was examined throughout one segment from each lens. Also, the width and appearance of lens fibres at the suture free equator was compared in additional tissue from the same pair of lenses.

Segments from each of the phospholine iodide treated (MR73) and fellow control (ML73) lenses were dissected out and divided into layers as in the previous chapter (section

3.2). Whilst the posterior portions of some segments from both lenses were preserved for examination, others were prepared to allow examination of the equatorial portions only.

Tissue was dehydrated, dried at the critical point and sputter coated, (see chapter 3:2), and a code assigned to each piece by an independent person. The original code and therefore the origin and position of the lens pieces were unknown to the writer. The equatorial tissue arcs were mounted (convex outer surface up) so that the area of sharpest curvature (under the equator) was parallel to the observation plane.

As lens fibres are basically six sided, two or three uppermost sides can be observed with this technique, - only one broad face and some of one or both short faces of each fibre are exposed to view. Commonly the broad face is clearly seen as well as one short face, the other short face being covered by the neighbouring fibre. The broad face width is easily measured but of more interest is the surface width occupied by each lens fibre, here called the lens fibre width (usually the width of a broad face plus one short face, see Fig 3:2). All measurements were made with the exposed tissue normal to the electron beam. Average posterior lens fibre width and individual broad face width were recorded at regular intervals along the surfaces exposed by dissection. Measurements of individual broad face widths were recorded at approximately x3000 and mean fibre

width assessed at x1000.

Photographic records aided in the analysis of other features. Transverse fibre undulations were graded on a simple subjective scale (0=no undulation, 1=just detectable, 2=moderate, 3=marked undulation). The orientation of tongue and grooves was assessed from photographs. Measurement of tongue and groove height from stereo photographs was found to be unreliable and not pursued.

4:3.3 Preparation of Sections to Test for Local Volume Changes.

Lens fibres are formed in layers or sheets so that each fibre runs its course within that layer or sheet (Fig 4.3). Looking at an individual lens fibre, its path is straight (perpendicular to the equatorial plane) across the equator and follows the curve of the layer it sits on. It then proceeds radially towards the pole, curving away from the radial line to terminate at a suture. To cut the fibre in cross section at points along its length would require cutting perpendicular to the surface of the layer and at right angles to the radial line the fibre follows (Fig. 4:3). It follows that although obtaining accurate cross sections of a small segment of a layer of fibres is possible near the equator, it is more difficult once lens fibres curve to meet a suture. Lens fibres change shape and become more complex when approaching a suture prior to termination. The presence of sutures could complicate an attempt to

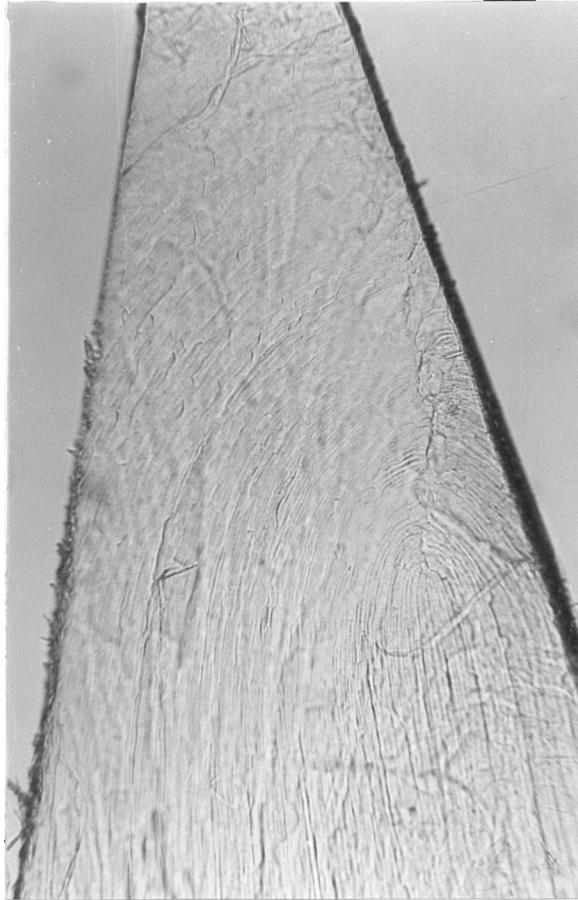


Fig. 4.3 A segment of lens tissue from the outer cortex, to show the problem caused by lens fibres curving in to meet the sutures, when attempting to cut lens fibres transversely. A suture is pictured on one side of the segment,- the path of lens fibres change to curve in to meet the suture.

isolate the effect of accommodative shape change on lens fibre shape.

The first experimental approach was to ignore the sutures using tissue from M78 (Fig. 4.4), with the most marked shape difference. The simplest suture pattern is the 'Y' suture found deep in the nucleus, with progressive complexity of the suture pattern in the more external layers. The more peripheral suture pattern, based as it is on the three pointed 'Y' shape, also has an approximate three way similarity. So a whole third of each lens was dissected and each divided into layers (Fig. 4:4). The cortical layers (surface and outer) 'f' and 'e' and nucleus 'b' were selected, and each layer divided into six narrow segments of tissue ready for embedding in Araldite and cutting. Transverse sections were cut at four equally spaced intervals (along the equatorial-polar arc), normal to the arc surface. Sections were stained with toluidine blue and lens fibre density counted from coded photographs as described below.

The intention was to pool the data from each of the six segments, (from each layer at each position) which would have included obliquely sectioned fibres turning into sutures. (Fig. 4.3 is one of these pieces of tissue and shows that transverse sections of the segment layer would cut fibres at differing angles of obliquity.) However those sections taken close to fibre terminations could not be counted because of the complexity of the lens fibres at this

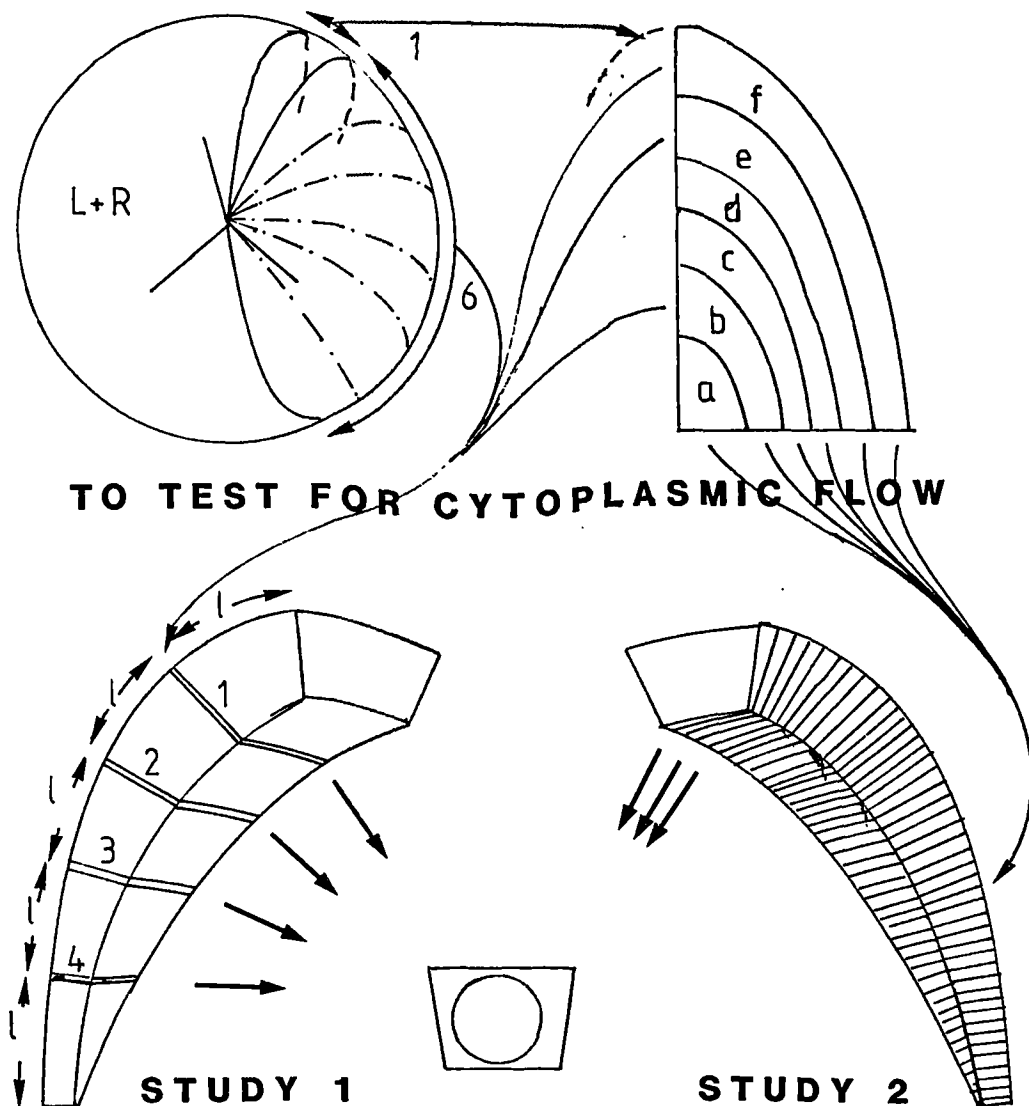


Fig. 4.4 Diagram to illustrate design of experiments to test for cytoplasmic flow. In the second study, a single posterior segment from each lens (control and dislocated M78, and control and drug treated M73) was divided into layers, and sectioned at 50 -100µm intervals. The fibre density or mean cross-sectional area was assessed. The first study, was abandoned.

point. It was difficult to distinguish between small lens fibres and the large processes found at sutures have been described in the previous chapter (section 3:3.1). A further problem was the irregular profile of the subsurface cortical/intermediate lens fibres (layers 'd' and 'e') which also made counting fibre density almost impossible. Without density counts from each of the six pieces of tissue for each layer, further study was impossible.

In a second study, also using tissue from the pair showing greatest curvature difference (control/dislocated M78), an attempt was made to avoid sutures by dissecting small segments of lens tissue, one from each layer ('a,b,c,d,e, and f') with lens fibres terminating axially from both the dislocated (MR78) and control (ML78) lenses. It was hoped that this would provide measurable material except close to the polar axis. The intention was to section the tissue at frequent intervals to provide a more comprehensive insight into any lens fibre shape changes. The position of sutures and the lens fibre pattern was recorded for each piece of tissue to assist with orientation for cutting transverse sections. After embedding in Araldite, each piece of tissue (which could not be coded due to the need for accurate orientation) was orientated to allow the cutting of lens fibres in cross section from posterior pole through to the equator at 50 - 100 μ m intervals.

One segment from each lens (MR78b/c and ML78b) was sectioned from near the equatorial plane to the polar axis

with linear separation intervals of 50 - 100 μm , calculating the actual curved arc position from photographs of the internal lens shape. Subsequently, the micrometer advance fitted on the microtome was used with frequent re-orientation to follow the external arc of the tissue and to measure the position along the outermost arc of tissue. The tissue was also re-orientated at each cutting interval to allow for the segment curvature.

Small segments of each lens from M73 (R=phospholine iodide treated) were treated in the same way, but divided into thicker layers (a/b, c/d, e/f) to speed up the procedure. Because of greater steepness of curvature in the deepest piece of tissue from each lens, these nuclear arcs (MR73a/b, ML73a/b) were orientated to obtain cross sections in level 'b' only.

Sections were stained as before with Toluidine blue, covered and left to dry on a hot plate in the light. Poor or uneven staining contrast was a constant problem which was not reliably solved! Although some sections remained uncountable, the use of filters and image enhancement assisted in data collection from many slides.

4:3.4 Methods for Counting Lens Fibre Density, and Lens Fibre Mean Cross-Sectional Area.

Lens Fibre Density

Sections were photographed using a Balzar (B40 557 7 or

B40593 7) interference filter to enhance contrast at a standard magnification using oil immersion. Prints were enlarged and printed at x1480 to facilitate counting. Each photograph was cross coded (so that counting could be performed without knowledge of tissue origin) and fibre densities counted using a fixed frame technique. The fixed frame used was a circle equivalent to $2500\mu\text{m}^2$. (The density of the two pieces of tissue analysed first, MR78b/c and ML78b, were measured using a square fixed frame also of $2500\mu\text{m}^2$, placed randomly on the photograph.) Each density count included all complete fibres within the frame plus all incomplete fibres touched or cut by the frame which were counted as half. A circular frame was used to avoid the bias a square frame may give when counting what is often a regular array of hexagonal shaped fibres. Each count was repeated four times after small movement of the frame, and the results averaged.

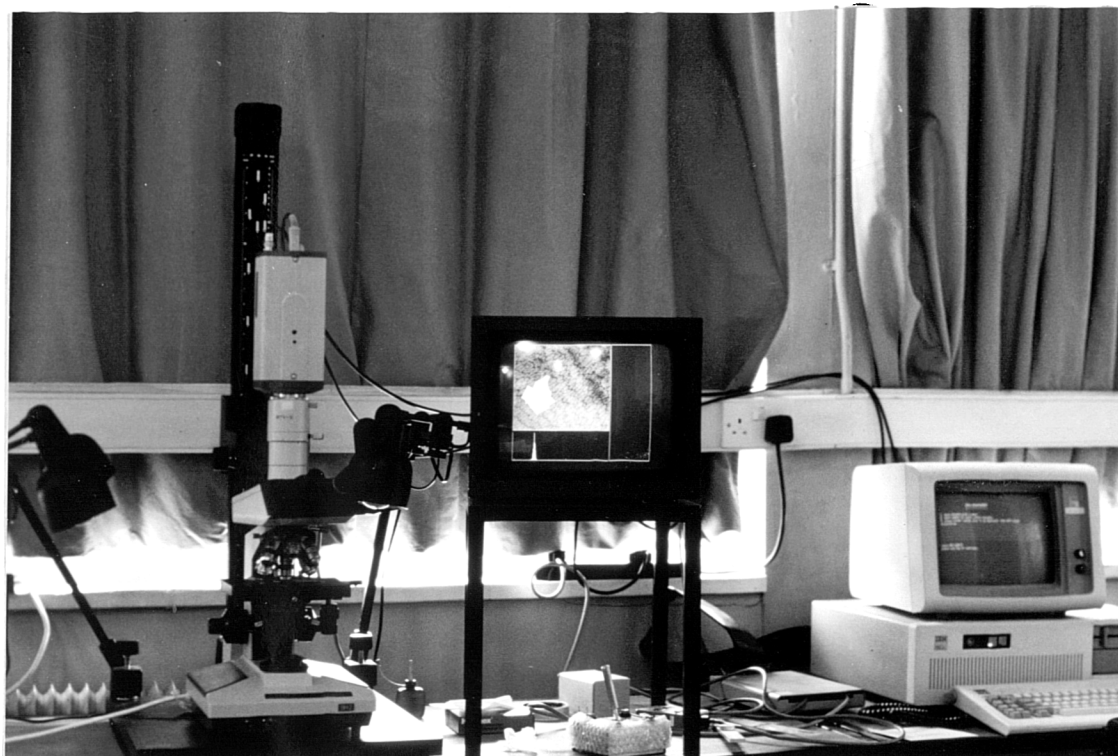
Lens Fibre Mean Cross Sectional Area

A second method of counting was developed to help solve the two problems of poor contrast and the large numbers of photographs required.

A newly acquired Olympus microscope, designed to link up with a closed circuit television (CCT) camera (Fig. 4:5), allowed the incorporation of image processing using a pluto frame grabber, an IBM AT PC, and specially written software (Appendix C). Image processing provided artificially

CCT Camera

Enhanced image on display



Microscope

Joy-stick control

Computer

Fig. 4.5 The equipment used to count lens fibre mean cross sectional area. Transverse sections are viewed through a light microscope, linked via a C.C.T. camera and frame grabber, to a computer equipped with image analysis software.

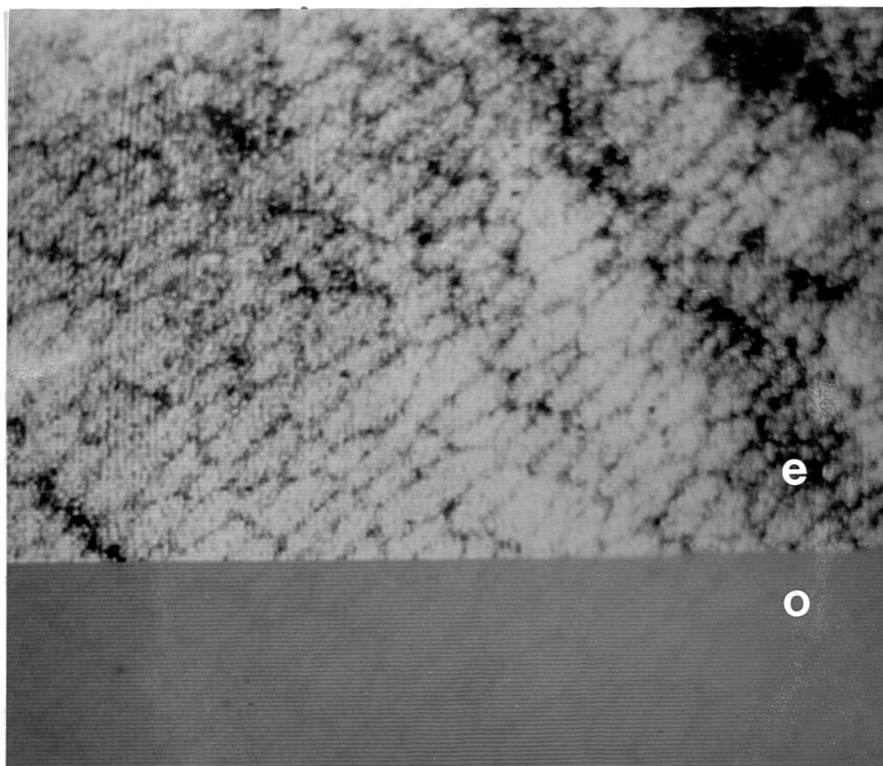


Fig. 4.6a

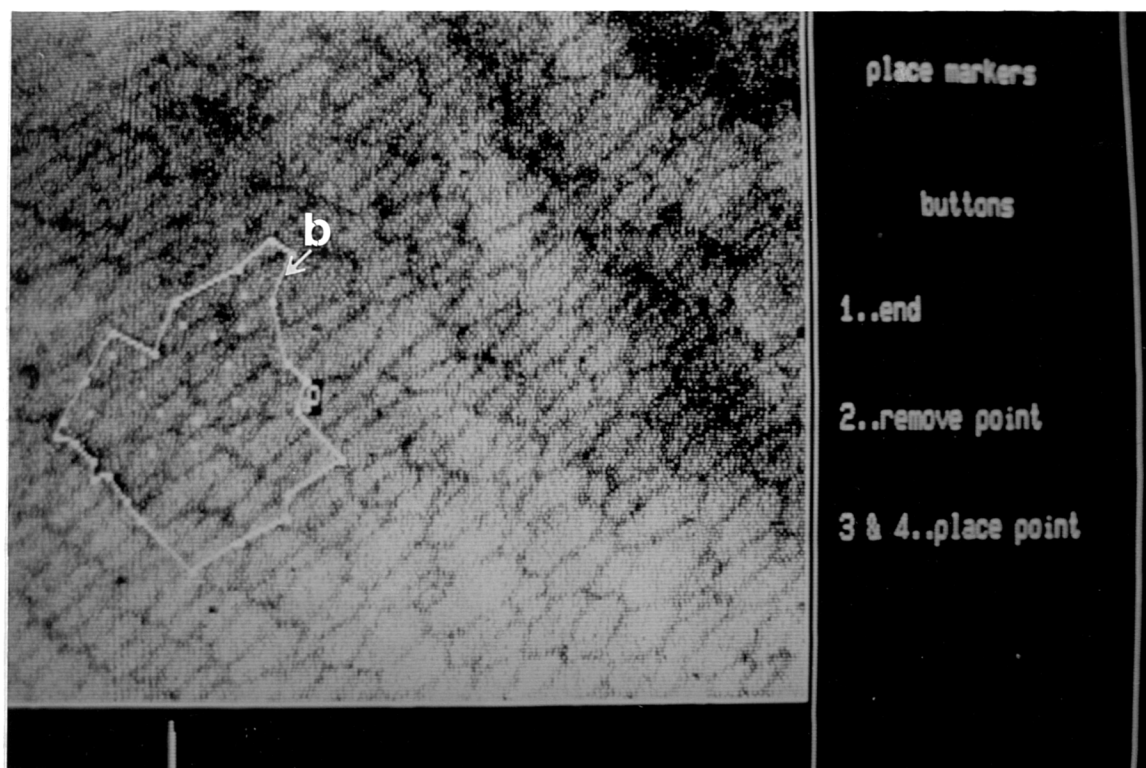


Fig. 4.6b)

See legends on following page.

Fig. 4.6a Shows the image on the display unit, whilst image processing was in use to enhance (e) the contrast of a section with poor stain contrast (o).

Fig. 4.6b The programme allowed the drawing of a border (b) around a group of fibres, and the number of lens fibres (seen in cross-section) within the area, assessed. A larger area of the screen was used than illustrated in this picture.

improved contrast in sections that were previously too poorly stained to assess with the earlier method (Fig. 4.6). Attempts to achieve automated computer counting were not successful due to uneven staining, confusion caused by ball and socket processes, and other difficulties of pattern recognition.

The program allowed drawing of a border around a group of lens fibres to be measured, (and further borders around unclear or damaged areas within the original area, to be omitted). Each lens fibre within the bordered area was marked using a specially made analogue joystick control (to ascertain the total), then the enclosed area computed, and divided by the number of fibres marked to calculate the mean cross sectional area of fibres in the group (Fig 4:6a and b).

Calibration of the screen (to allow the computer to convert the number of pixels within the counted area to square microns) was achieved using a grid placed in the eye piece and a stage micrometer (rotated to check each meridian). This was checked and reset at each session. As some distortion around the edge of the screen occurred, the same part of the screen was used for each count. In common with the earlier density method, this gave only an average count with no information of fibre size variation. Counts were made at x40x5 and using oil immersion at x60x5 and x100x5, (with an additional screen magnification in each case of x4.25), depending on the thickness of the lens

fibres to be counted.

Control and treated material were counted using the same magnification and similar area size. Even with the help of image processing, some sections (mostly from the cortex) presented real difficulties in assessment since even at the highest magnification, individual lens fibres were poorly defined and only small areas of fibres could be counted.

4:4

RESULTS

4:4.1 Comparison of Lens Fibre Morphology in Control and Phospholine Iodide Treated Lenses using S.E.M..

Lens fibre width, the shape and size of junctional structures, and the presence of fibre cross folds and undulations were investigated in the search for clues to the mechanism for intra-lenticular accommodative shape changes. Of particular interest were the cross folds and undulations of lens fibres around the equator. It had been suggested (Willekens and Vrensen, 1972) that these may allow lengthening of lens fibres in accommodation. Undulation had also been noted in axial zones. Tongue and grooves had been shown to vary both in orientation and height with location: could these perhaps vary with lens shape changes?

Four pairs of lens segments (each subdivided into 5 or 6 levels) of equatorial tissue were examined. Two sets could not be used to measure width, due to problems with calibration.

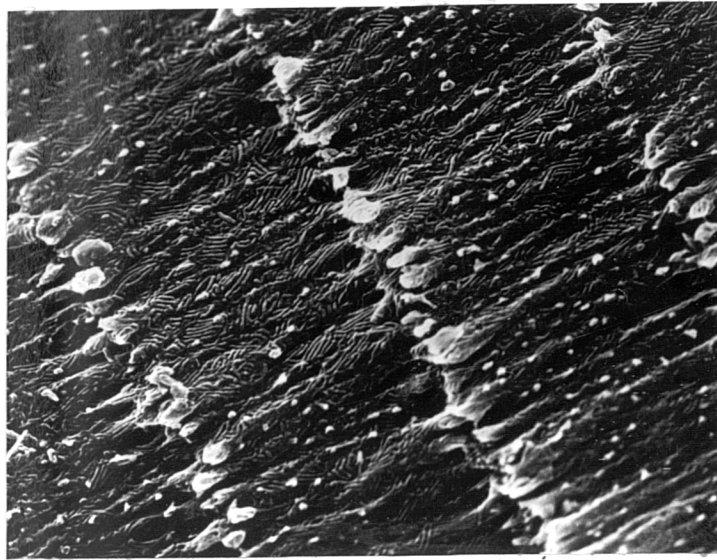
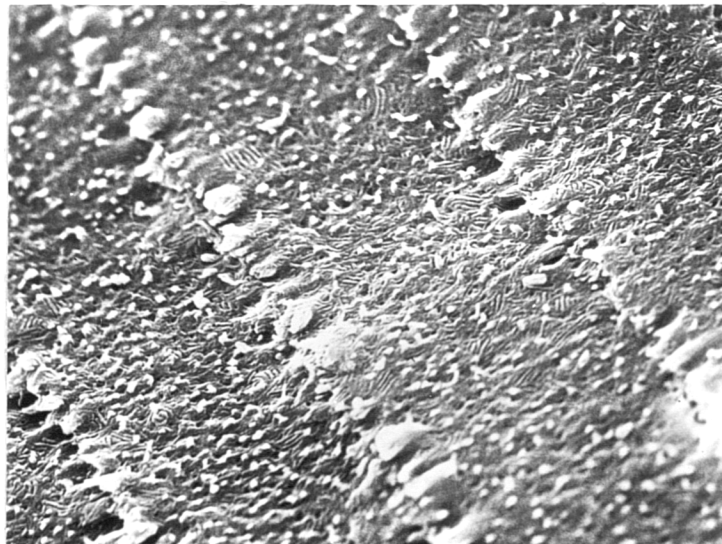


Fig. 4:7 a) Scanning electron micrograph of equatorial fibres from intermediate depth (level c) of the control lens ML78. Undulation across the fibres is marked. x3000



b) Fibres from a similar location to that of (a) from the dislocated lens (MR78). Transverse undulations are less marked. The increased frequency of ball and sockets suggests that these fibres are marginally more superficial than those shown above. x3000

Equatorial Transverse Undulation. Because measurement of cross fold height was unsuccessful using S.E.M., a simple subjective grading system was used to assess the degree of transverse undulation in equatorial fibres from photographs of the coded tissue pieces. Each coded picture was given a grade from 0 (no undulation) to 4 (very marked undulation). These were also given to naive observer to grade in the same way, to reduce possible bias.

On this basis, a reduction in equatorial fibre undulation was noted (Fig. 4.7) in the tissue from the phospholine-iodide treated lens, especially in the cortex. This awaits development of a better assessment method.

Ball and Socket Junctions. The frequency of ball and sockets was similar in the drug treated and control lenses, and similar to that indicated in Figure 3.8.

Tongue and Grooves. Tongue and groove orientation was assessed both at time of examination (subjectively) and more accurately from photographs, on both the equatorial tissue and the posterior arcs. Subjective assessment of the height of tongue and grooves at the equator indicated a slight reduction in the treated ('accommodated') lens. Small differences in orientation were found between the control and treated material in either case (Fig. 4:8).

Lens Fibre Width. Cortical fibre broad face width (as defined in Fig. 3.2) at the equator, was smaller in the drug

Fig. 4:8 (Following page)

The proportion of tongue and groove groups on the broad faces of nuclear fibres, orientated within 45 degrees of the longitudinal fibre axis, from the nucleus of control (green) and phospholine iodide treated lenses (red).

NUCLEUS: TONGUE AND GROOVE ORIENTATION

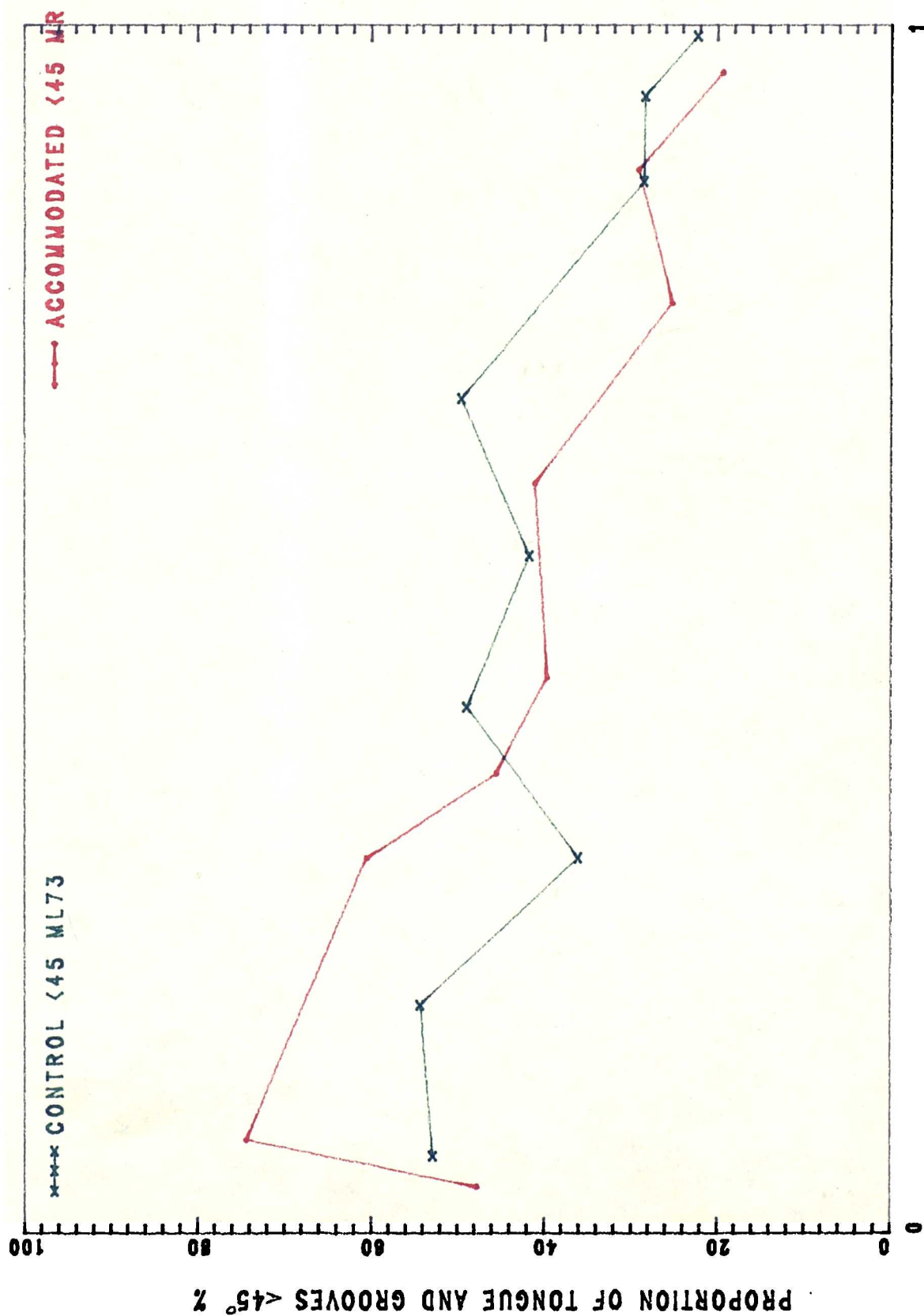


Fig. 4.8

Fig. 4:9 (following page)

Variation in broad face width of equatorial lens fibres observed with S.E.M. with lens depth. Data from the control (unaccommodated) lens is presented in green, and from the treated (accommodated) lens in red. Mean broad face width of equatorial lens fibres, is plotted against proportional distance between the outermost equatorial layer and the centre of the nucleus.

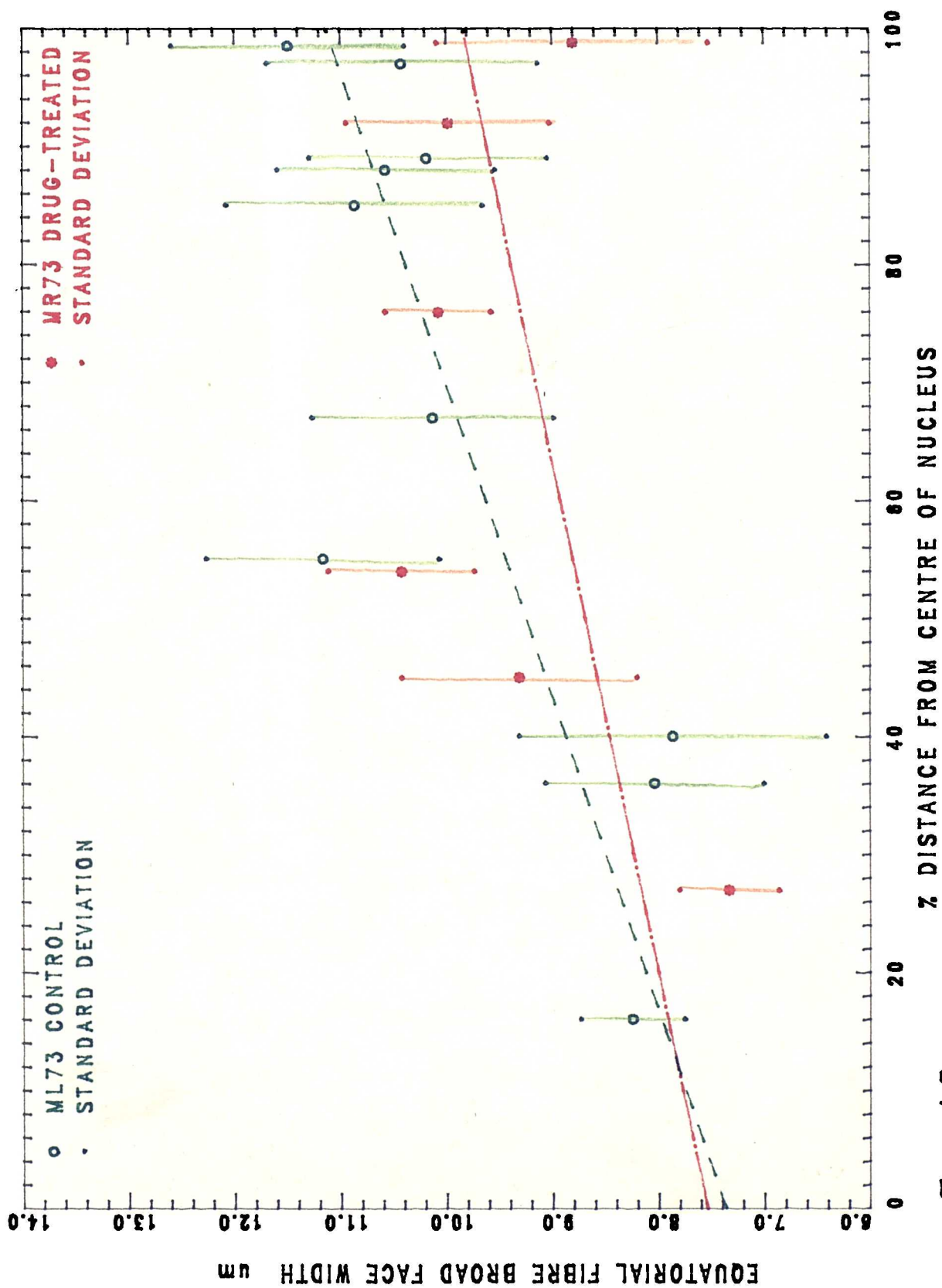


Fig. 4.9

treated (MR73) lens, than in the control lens (Fig. 4.9). At intermediate depth, lens fibres of the treated ('accommodated') lens were similar in broad face width to those of the control (unaccommodated) lens, when compared to their absolute depth from the centre of the nucleus. Lens fibre width and broad face width reduces with depth in both control and treated lenses.

Although similar trends to those of Figure 4.9, were seen with a second batch of control and treated tissue, measurements collected on different days, did not compare well. This may have been due to difficulties with measurement of lens depth, or problems of erratic drying and shrinkage. In Figure 4.9 simple proportional scaling of lens depth was used, which may be subject to error, since it cannot be assumed that all levels of the lens change shape in precisely similar proportions.

Since variability was large and reliability of measurements, questionable, results of fibre width and broad face width using S.E.M., were of limited utility.

4:4.2 Measurement of Surface Lens Fibre Width, of Dislocated (MR78) and Control Lenses (ML78), Before Dissection, Using a Light Microscope.

Mean lens fibre width, was measured for surface fibres, around the equator and compared with the change in total equatorial lens circumference (Tab. 4:3).

Since the equatorial circumference of the dislocated

LENS	W*	N*
MR78 Control	16.26um	167
ML78 Dislocated	13.71um	194

The ratio of the circumferences $C(t)/C(c) = 20.58/25.39$
(predicted ratio of lens fibre widths) = 0.81

The ratio of mean fibre widths $W(t)/W(c) = 13.71/16.26$
= 0.84

$$\begin{aligned} \{ C(t) &= 2\pi r = 2 \times 3.14 \times 3.275 = 20.58 \} \\ \{ C(c) &= 2\pi r = 2 \times 3.14 \times 4.04 = 25.39 \} \end{aligned}$$

* KEY

W = mean equatorial surface fibre width in microns

N = number of fibres counted

C = lens circumference

c = control (ML78)

t = treated (MR78)

r = half lens equatorial diameter

π = pie

Table 4:3 Control and Dislocated Surface Equatorial Fibre Width Compared with Circumference.

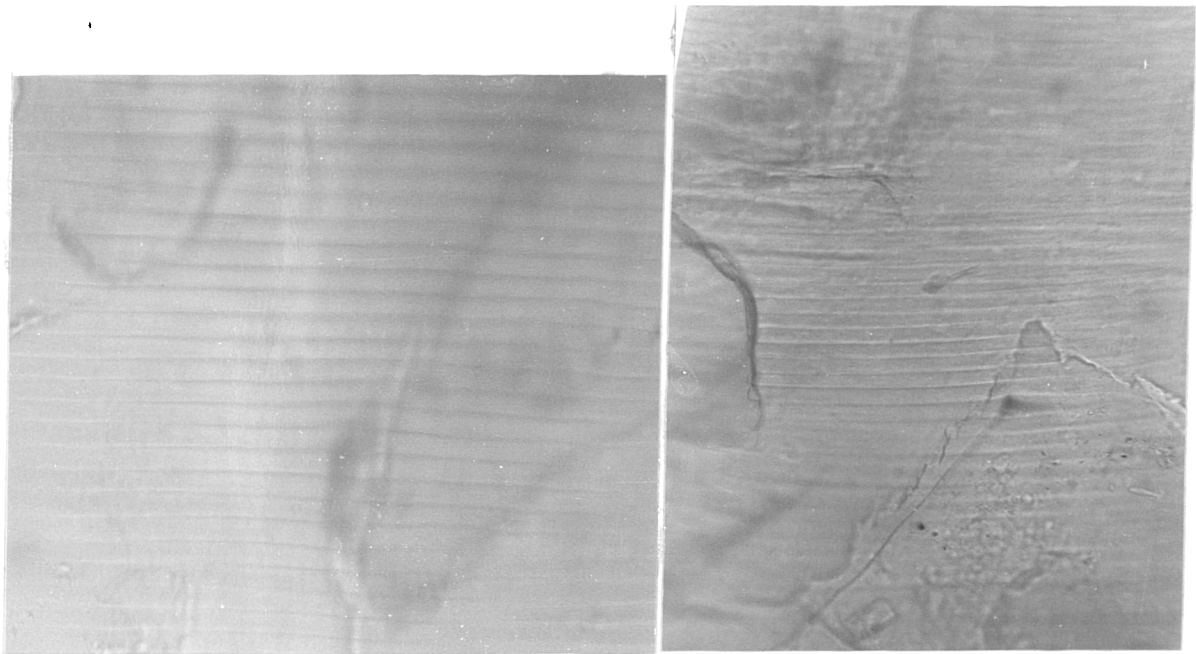
lens was smaller (0.81) than that of the control lens, it was predicted that the width of equatorial lens fibres just beneath the capsule would be similarly reduced in the dislocated lens. The mean measured width of the surface lens fibres of the dislocated lens was smaller (0.84) than that of comparable fibres of the control lens.

The width of the equatorial fibres from the dislocated lens (MR78 simulating the accommodated shape) was smaller than that of the control lens (ML78 Fig. 4.10).

Measurements of surface lens fibre width at intervals along the curved surface from posterior pole to equator, was attempted. The linear distances between each assessment point (50 - 100um apart) were measured with the surface tangential to the observation plane, such that each linear division, was a chord of the arc between equator and posterior pole. The distance from the equator, recorded for each point is the sum of these chords, and not an accurate measurement of arc length.

The lens fibre width (Fig. 4:11) in the control lens, reduced from the equator to the last point measured, close to the polar axis. The fibre widths of the dislocated lens, were narrower at the equator than in the control lens, and initially in progressing along the posterior surface, fibre width reduced, but subsequently showed little difference.

The results from these two preliminary studies, encouraged a more extensive study, specific to test this hypothesis of cytoplasmic flow.



a

b

Fig. 4:10 a) Surface lens fibres at the equator from the control lens ML78. The lens, with only capsule and epithelium removed, was supported in dissecting fluid, beneath a light microscope, with part of the equator parallel to the observation plain.

b) Surface lens fibres at the equator of the dislocated lens MR78, photographed at the same magnification and under the same conditions as a. The lens fibres of the dislocated lens are narrower in this location, than those of the control.

Fig. 4.11 (Following page)

Width of surface lens fibres, measured using a light microscope. The width of fibres at the equator is plotted at 0 on the abscissa, and at the posterior pole at 100. Mean width was corrected as far as possible for curvature. (M78)

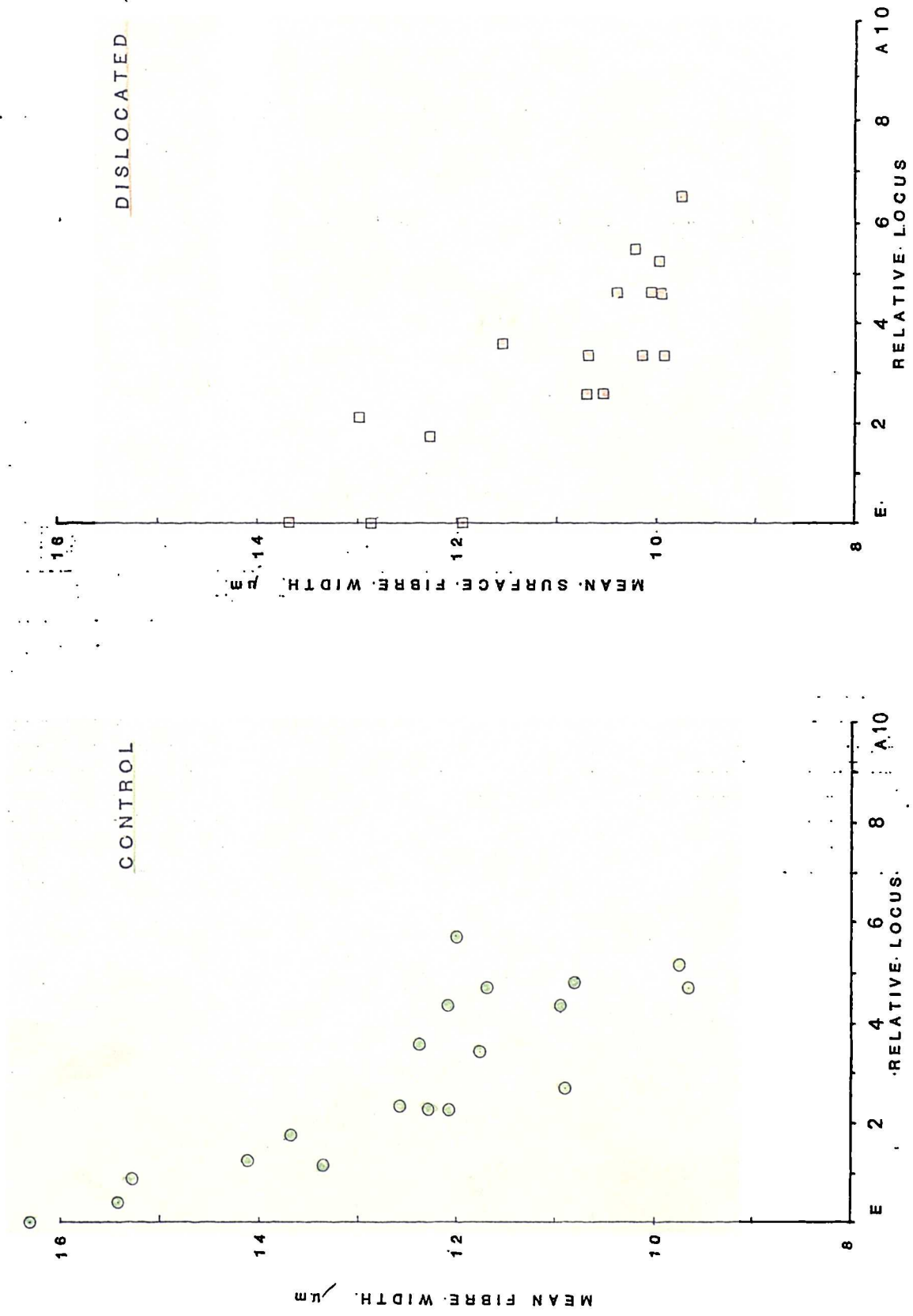


Fig.4.11

If cytoplasmic flow is part of the mechanism for accommodative lens shape change, certain predictions can be made and the results compared.

In accommodation the local volume of lens fibres should reduce at the equator, but increase at their distal (polar) ends (see 4.1, page 73). Because the fibre cross sectional area is smaller, the density of lens fibres should increase at the equator, and conversely reduce near the polar axis, when the fibre cross sectional area increases in accommodation. Exactly what may happen to the local volume of the lens fibre mid way between polar axis and equator, is difficult to predict, and may differ with depth within the lens (Koretz et al., 1985).

It was predicted that any local volume changes would be smaller in the paired lenses showing the smaller shape change.

**Local Fibre Volume in the Dislocated/Control Lens Pair,
(M78).**

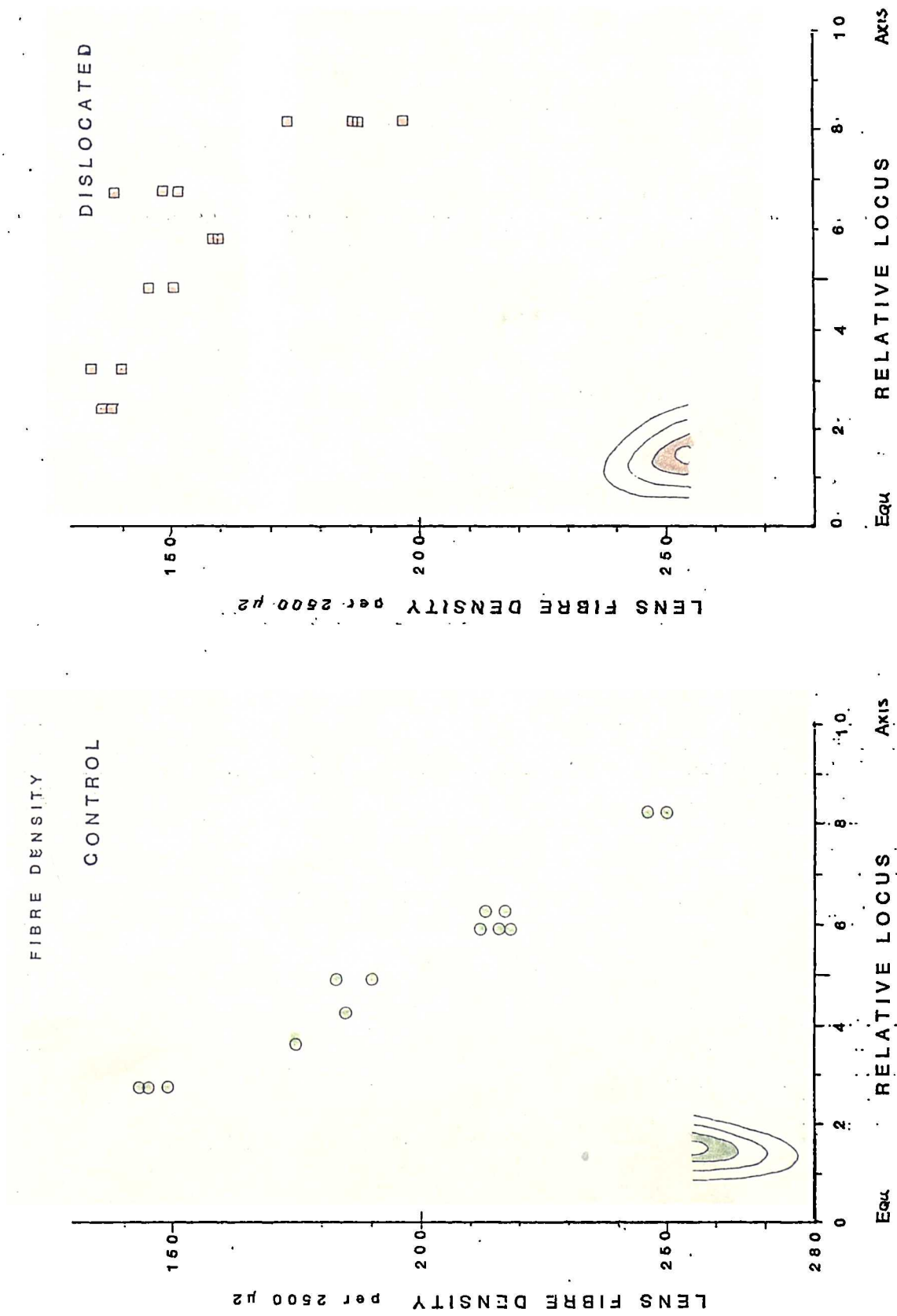
In a preliminary study, a piece of tissue (from outer nuclear layers of similar depth) from each lens, was compared in advance of the remaining tissue layers from both lenses (Fig. 4:12).

The density of lens fibres in the control lens (layer bc) was low near the equator, (the fibres were large) but

Fig. 4:12 (Following Page)

Fibre density in the outer nucleus of control and dislocated lenses. Fibre density is plotted against proportional distance along the arc joining the polar axis and the equator. The equator is at 0, the polar axis at 10, on the abscissa. Fibre density is plotted inversely (ordinate) so that areas of fibre of small cross sectional area, appear low on the graph.

The gradient of the data points from the dislocated lens is flatter than the control lens gradient, indicating a smaller range of cross sectional area along the length of lens fibres in the dislocated lens.



FIBRE DENSITY

Fig. 4.12

increased almost linearly towards the polar axis (the fibres got smaller). The density of fibres from the dislocated lens (layer b) was also lowest (the fibres were largest) near the equator, but there was a slower increase in fibre density away from the equator (the plot is flatter). Although the density of fibres from control and dislocated lens pieces, is similar post-equatorially, there is a suggestion (from extrapolation because the data plot gradient is flatter for the dislocated lens), that if measurements had been made closer to the equator, those of the dislocated would be higher (or the fibre cross-sectional area smaller) than those of the control. Close to the polar axis, as predicted the opposite occurs, and the fibre density of the control lens is higher than that of the dislocated lens.

Fibre thickness was also measured and compared in these two pieces of nuclear tissue (control layer b, dislocated layer bc, Fig 4.13). Fibres of the control lens were thickest close to the equator, thinning away from the equator. Fibres of the dislocated lens showed only small changes in thickness along their length. Whilst fibre thickness was greatest in fibres close to the equator in the control material, the thickest part of the fibres from the dislocated lens, was about half way along the equatorial polar arc. The fact that the thickness of the control fibres is greater throughout their length, perhaps reflects the slight inequality in depth of the control and dislocated tissue pieces, and the increase in thickness with depth

Fig. 4.13 (Following page)

Thickness of fibres from the same level as Figure 4.12, plotted against position along the arc between polar axis and equator.

LENS FIBRE THICKNESS μm OUTER NUCLEUS

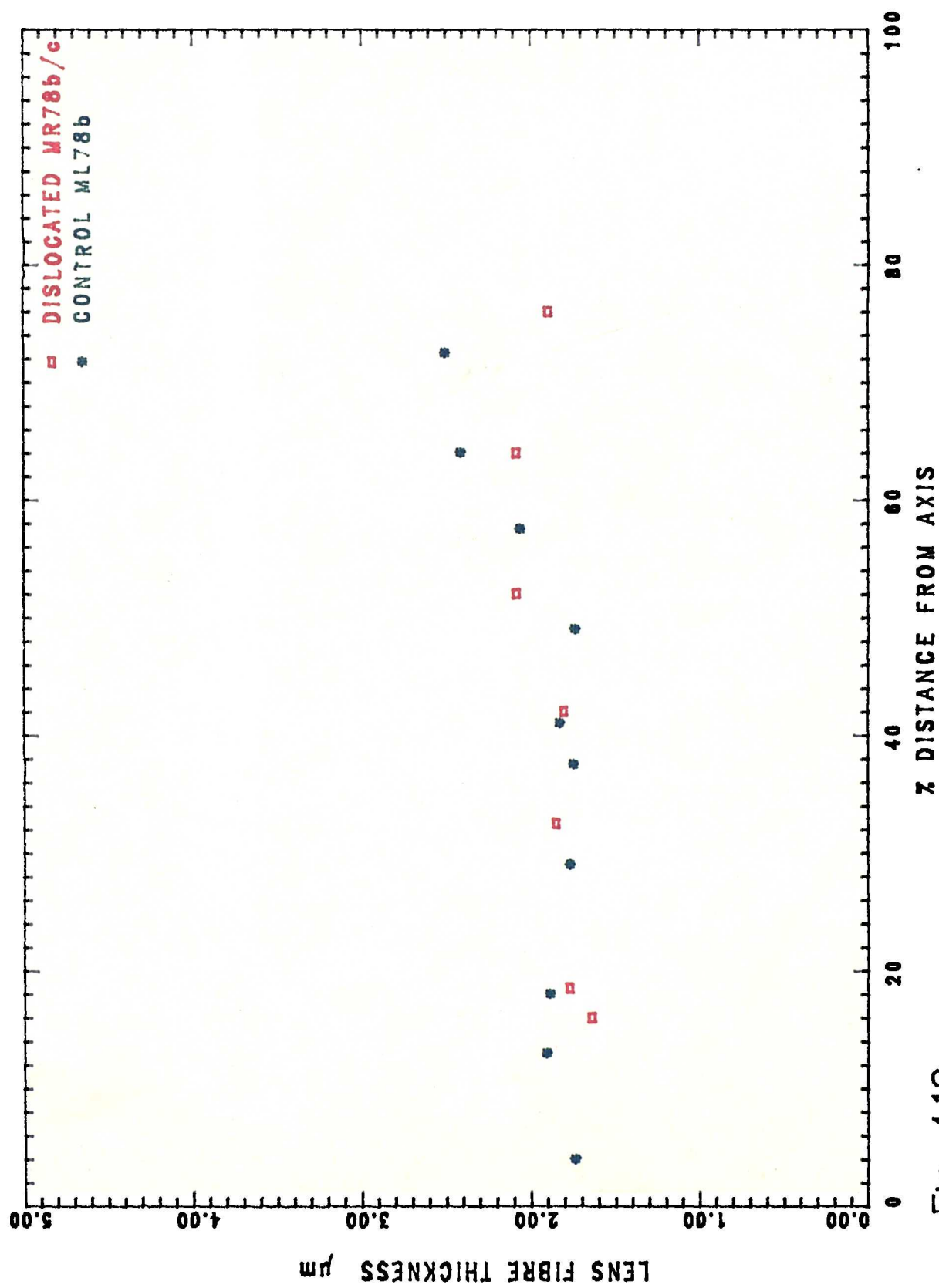


Fig. 4.13

reported earlier.

After the first trial, certain modifications were made to allow preparation of sections closer to the equator, and improve the accuracy with which the tissue arc length could be measured (4:3.3).

The curving of fibres away from near radial orientation to join sutures, was a problem (see Fig 4.3). Where ever possible tissue was orientated to obtain true cross sections in at least one part of each section. However this was rarely possible close to the polar axis (due to the proximity of sutures), and is one of the reasons for inadequate data in these areas. The curving of fibres away from a radial orientation, was more of a problem in cortical tissue, and curiously, especially in the control cortical tissue; Unfortunately all fibres in sections within a third the distance from polar axis showed obliquity, in level e/f of the control tissue.

Results of fibre cross sectional area and fibre density are represented graphically for all the remaining tissue layers in Figures 4:14 and 4:15.

In the control lens, lens fibre cross-sectional area at each level was greatest at the equator, and reduced away from the equator. This reduction in fibre cross-sectional area away from the equator was most marked close to the equator (the gradient of the plots Fig. 4:14 was steepest) but changed less close to the polar axis (the plots flatten out).

Cross-sectional areas of fibres from the dislocated lens

Key to following pages

Fig. 4.14

Mean cross sectional area of fibres from the control lens at different depths, plotted from the polar axis to the equator. The posterior pole is represented at 0 and the equator at 100, on the proportionally scaled abscissa. The absolute length of the outermost cortical tissue arc layer e/f was 3.2mm, and the innermost arc layer a 1.32mm.

ML78 Control

Fig. 4.15 Mean cross sectional area of fibres of the dislocated lens at different depths plotted from the polar axis to the equator. The outermost arc 'f' measured 3.9mm, whilst the innermost nuclear arc 'a' was 1.7mm in curved length. Tissue of comparative depth in Figure 4.14, is represented by the same colours.

MR78 Dislocated.

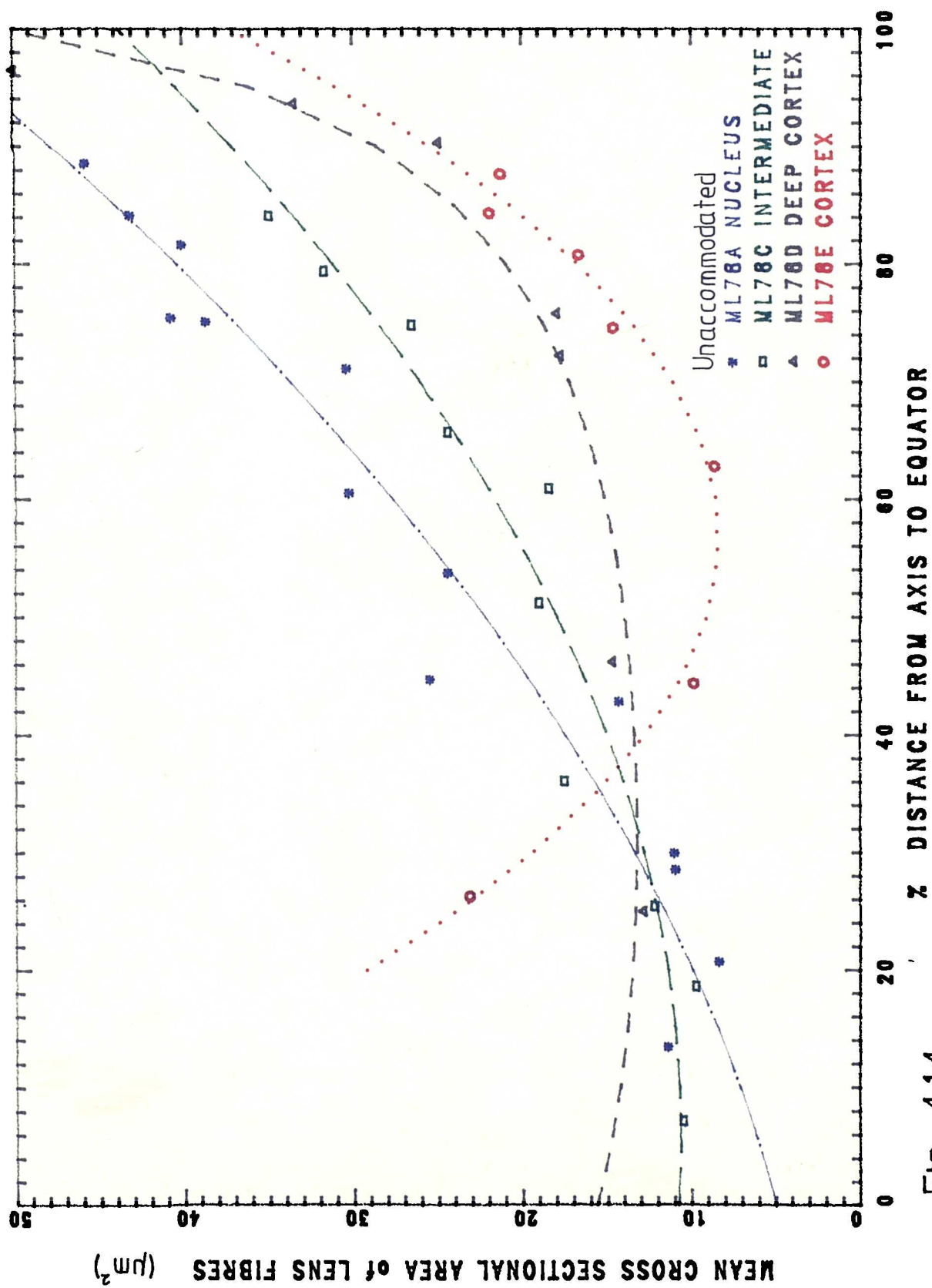


Fig. 4.14

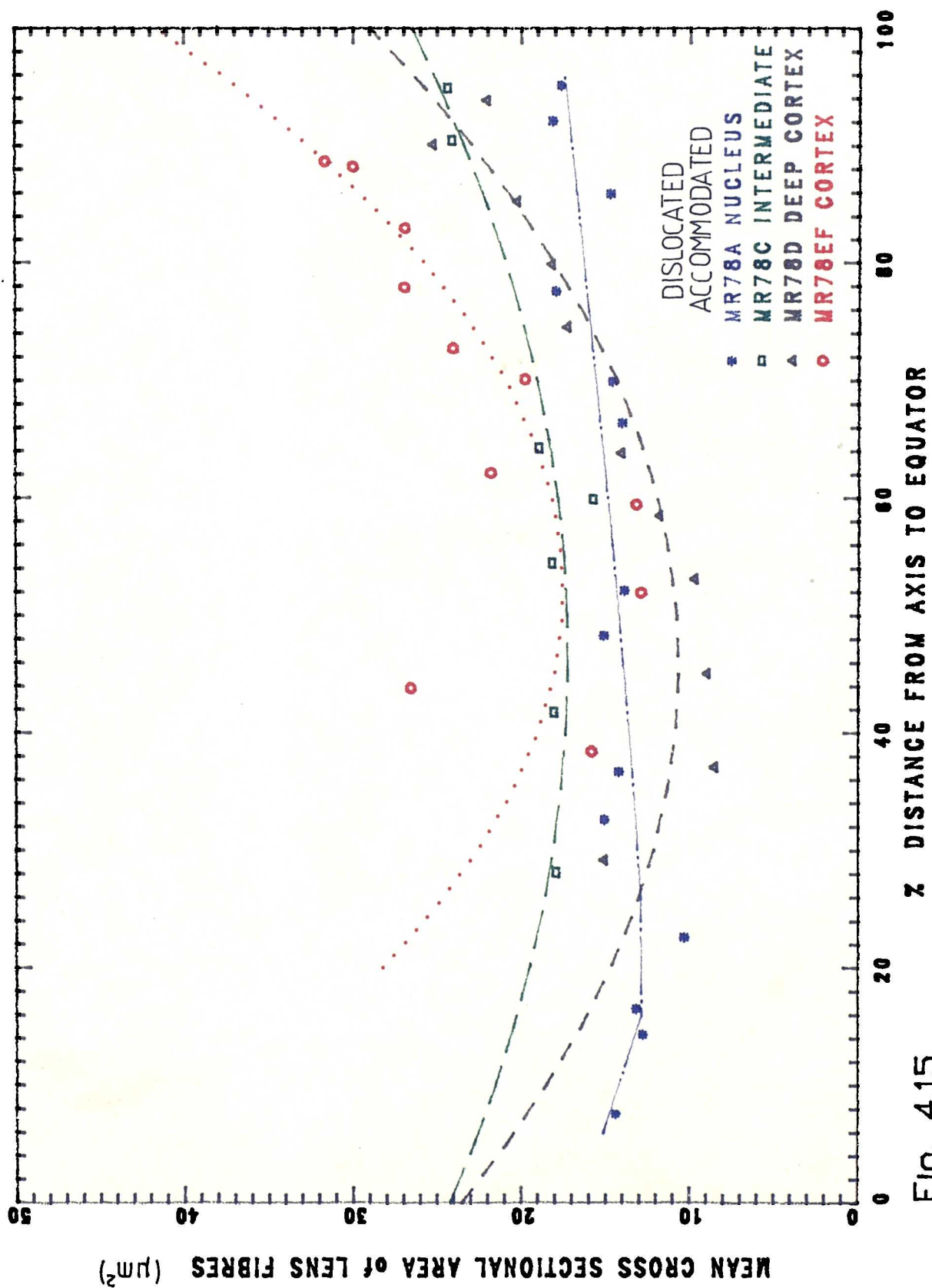


Fig. 4.15

Fig. 4:16 (Following page)

Change in fibre cross sectional area from polar axis to equator, in the nuclei of the control and dislocated lenses. The cross sectional area of fibres at the equator (right on the abscissa) in the control lens (green) is large (high on the ordinate).

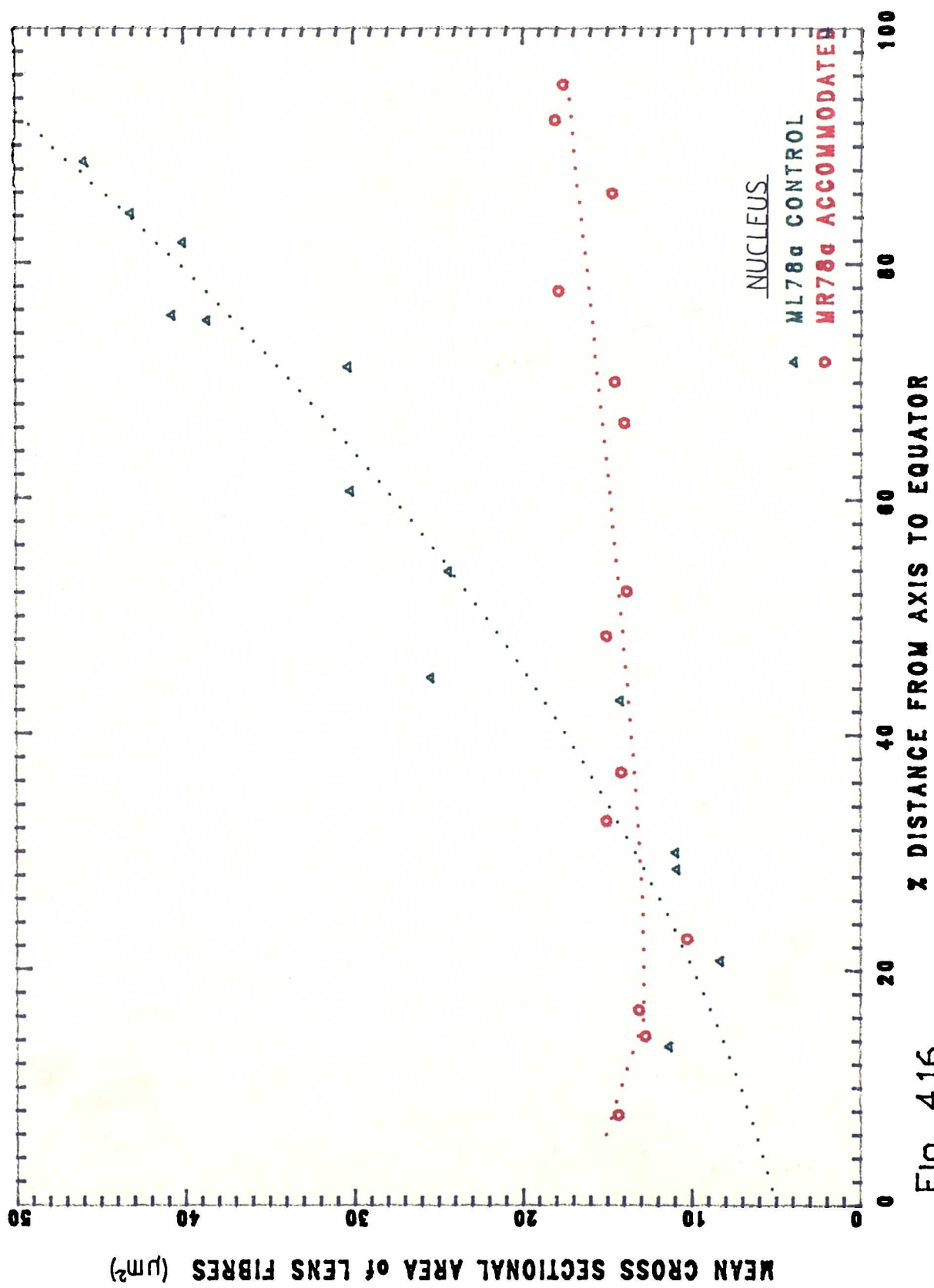


Fig. 4.16

(Fig. 4.15) were also greatest at the equator, and showed a small decrease in fibre cross-sectional area initially when progressing along the fibre length from the equator, but subsequently showed either no change (nucleus and intermediate levels) or a slight increase (cortex).

Cross sectional area of lens fibres at the equator was smaller in the dislocated lens, at all levels except the outer cortical layer (f).

The reduction in fibre cross sectional area with distance away from the equatorial zone, was less marked (flatter on the graph) in fibres of the dislocated lens. There is only a small decrease in fibre cross sectional area from equator to polar axis, in fibres of the deepest nuclear layer (Fig. 4:16).

Whilst the cross sectional area of the fibres continues to slowly decrease as the polar axis is approached in the control material, (the results suggest the fibres were spindle-shaped in long section) in the dislocated material either no decrease or a small increase in the fibre cross sectional area occurred close to the polar axis.

The outer cortical layers of both lenses (control level e/f and dislocated level f) show a different pattern. As the level markers indicate, the two pieces of tissue are not directly comparable. The outer cortical dislocated tissue piece (MR78f) contained superficial lens fibres, including the lens capsule, whilst the cortical tissue segment from the control lens (ML78e/f), did not include the most

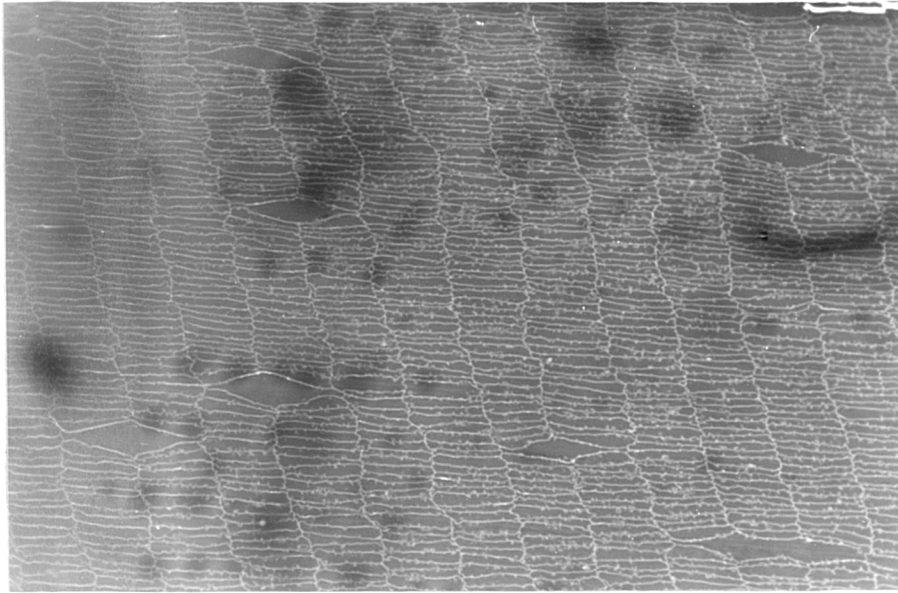
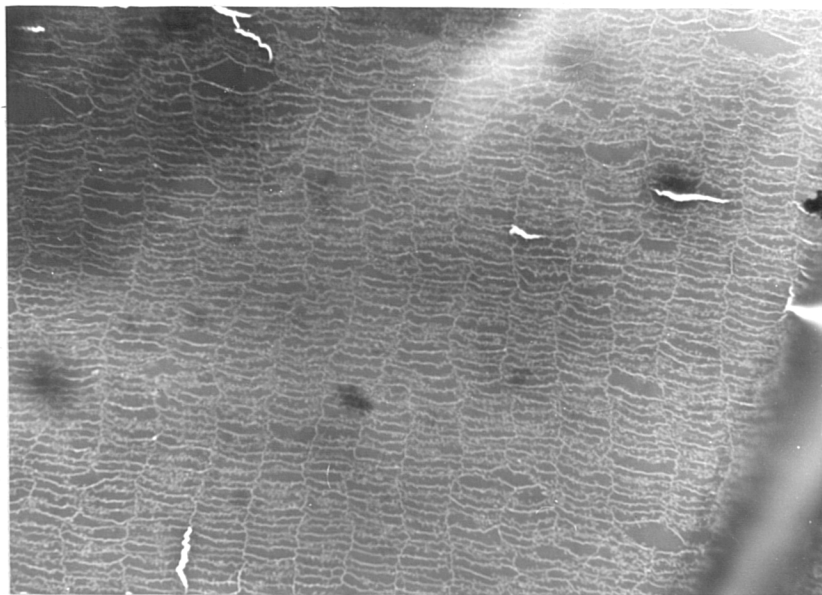


Fig. 4.17 a) Transverse section of deep cortical lens fibres, close to the equator, from the control lens ML78.
x650



b) Deep cortical lens fibres, close to the equator, from the dislocated lens, MR78. Compare their shape and size with (a) showing fibres from a comparable location in the control lens. x650

superficial fibres or capsule, (the piece ML78f was very thin and unfortunately lost during drying through alcohol) but did include fibres of the mid-cortex (level 'e'). As already mentioned orientation for true transverse sections, was not possible for the axial portion of the control piece (ML78e/f). There was large variability in the cross sectional area at each point and along the length of the dislocated lens piece (MR78f), and the correlation of the plotted points, to the 'best fit' curve (a parabola) was a very low 0.56, indicating a large spread in the measurements, (for ML78e/f also fitted to a parabola it was 0.928,). There was quite a difference in thickness between the superficial lens fibres and those found a little deeper, which would also prevent direct comparison between mean fibre cross-sectional area, in the two tissue pieces.

Generally the cross sectional area of fibres throughout the dislocated lens, varied less along their length (the plots are flatter), than that of the 'unnaccommodated' control.

Local Fibre Volume in the Phospholine Iodide-Treated/ Control Pair of Lenses.

Longer strips of anterior equatorial tissue were left on the tissue segments prepared from this pair of lenses (M73), to allow sectioning closer to the equatorial plain. Results are presented in Figures. 4:18 -4:20.

Lens fibres of the control lens (fellow of the drug

Key to following pages

Fig. 4:18 Mean cross sectional area of lens fibres at different depths from the control lens ML73, plotted from polar axis to equator. The posterior pole is represented at '0' on the abscissa, the equator at '100'. Control ML73

Fig. 4:19 Mean cross sectional area of fibres at different depths from the phospholine iodide treated lens MR73, plotted from polar axis to equator.

Drug-treated MR73

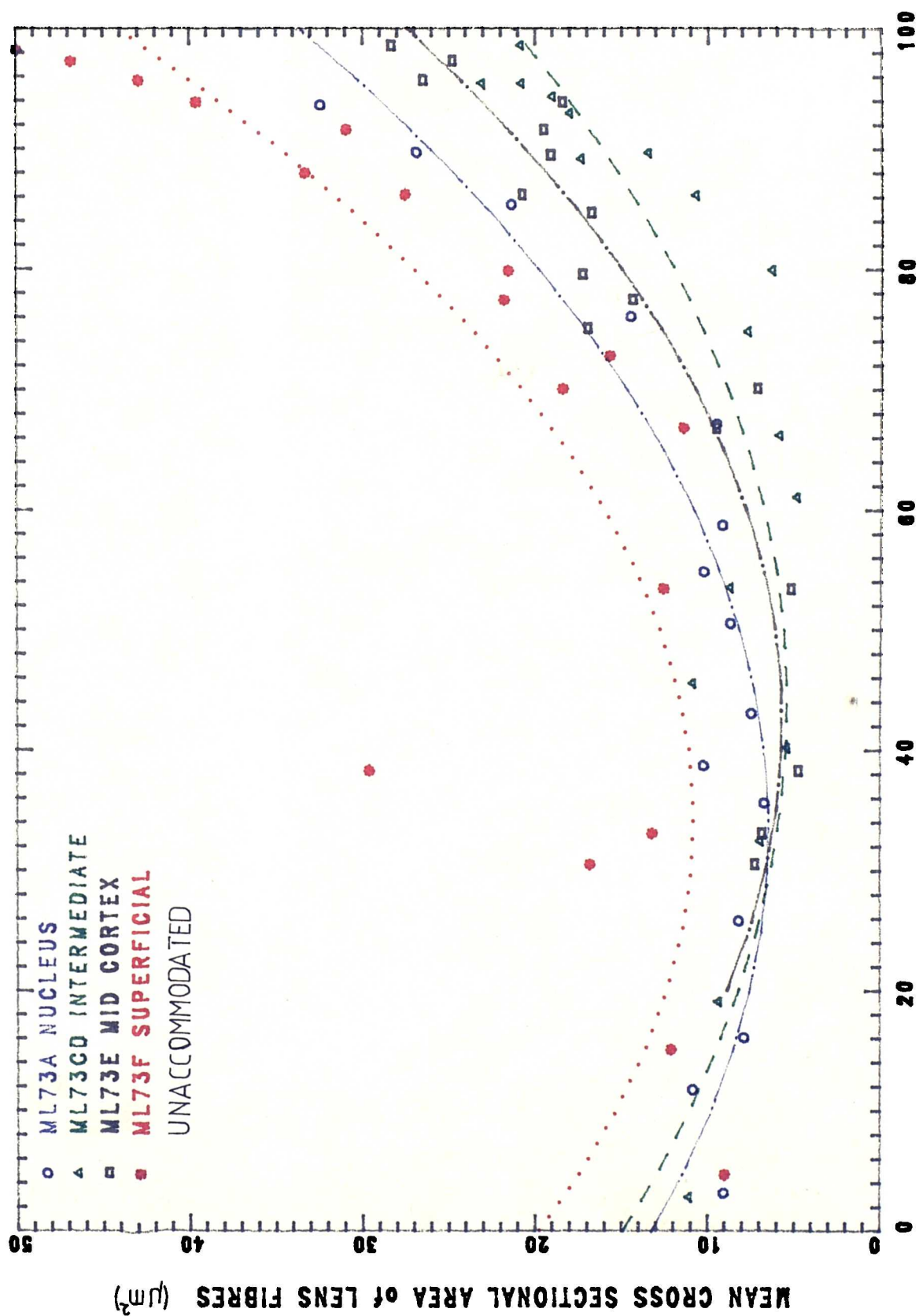


Fig. 4.18

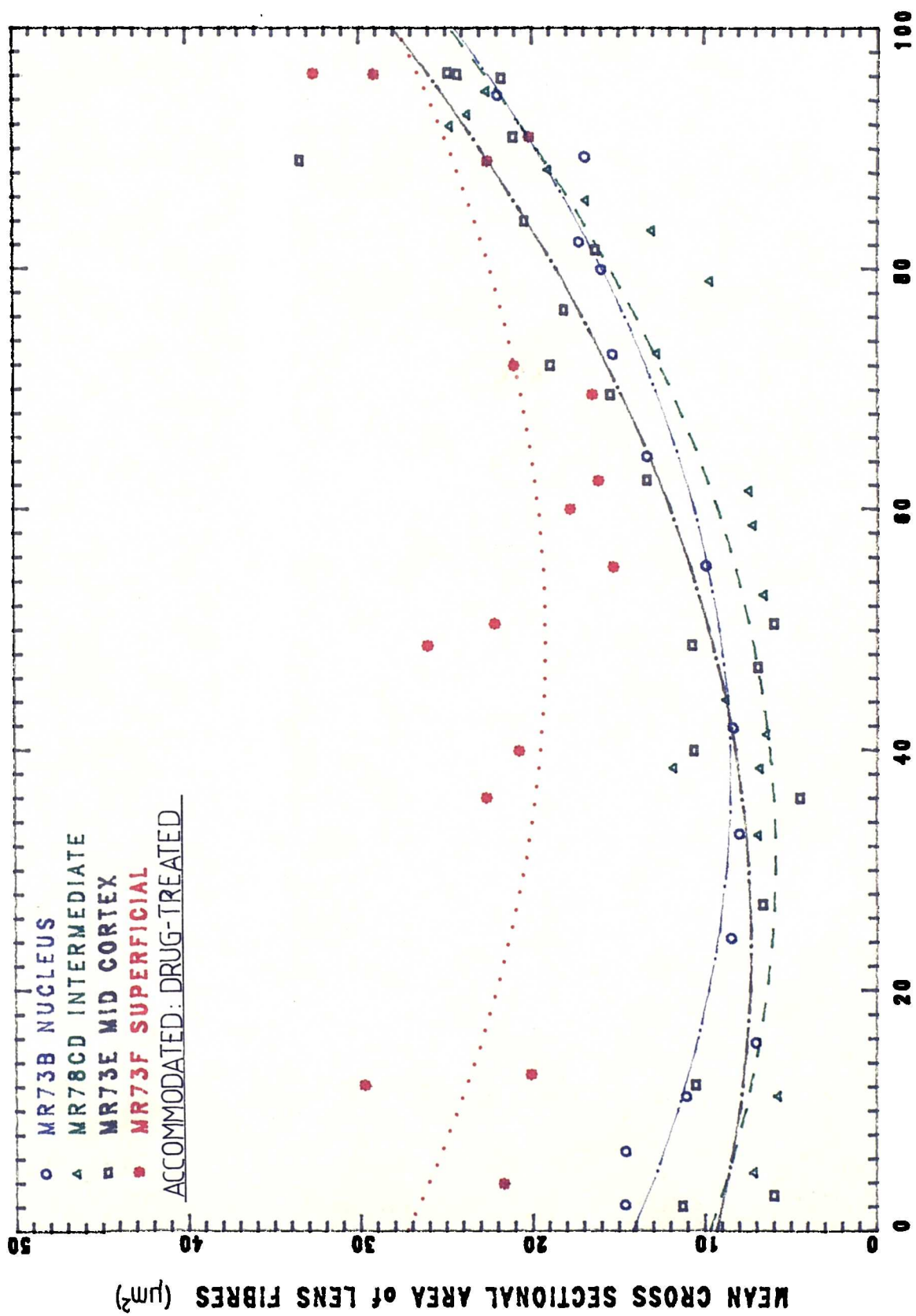


Fig.4.19

Fig. 4:20 (Following page)

Comparison of fibre cross sectional area in
nuclear fibres of the control and treated lenses,
ML73 (plotted in green) and MR73 (plotted in red).

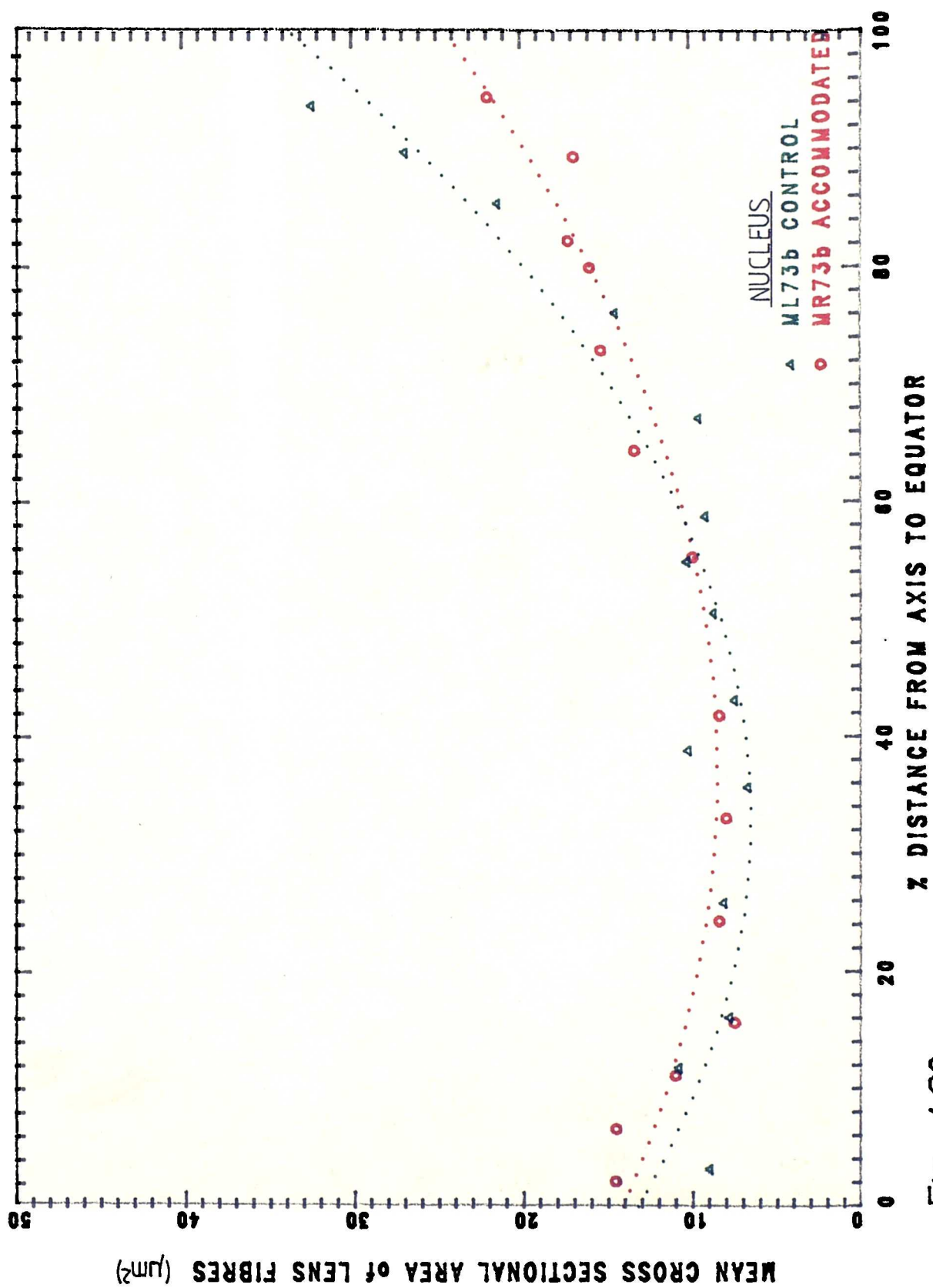


Fig. 4.20

Fig. 4:21 (Following page)

Comparison of fibre cross-sectional area of cortical lens fibres in control and drug-treated lenses, ML73 (green) and MR73 (red).

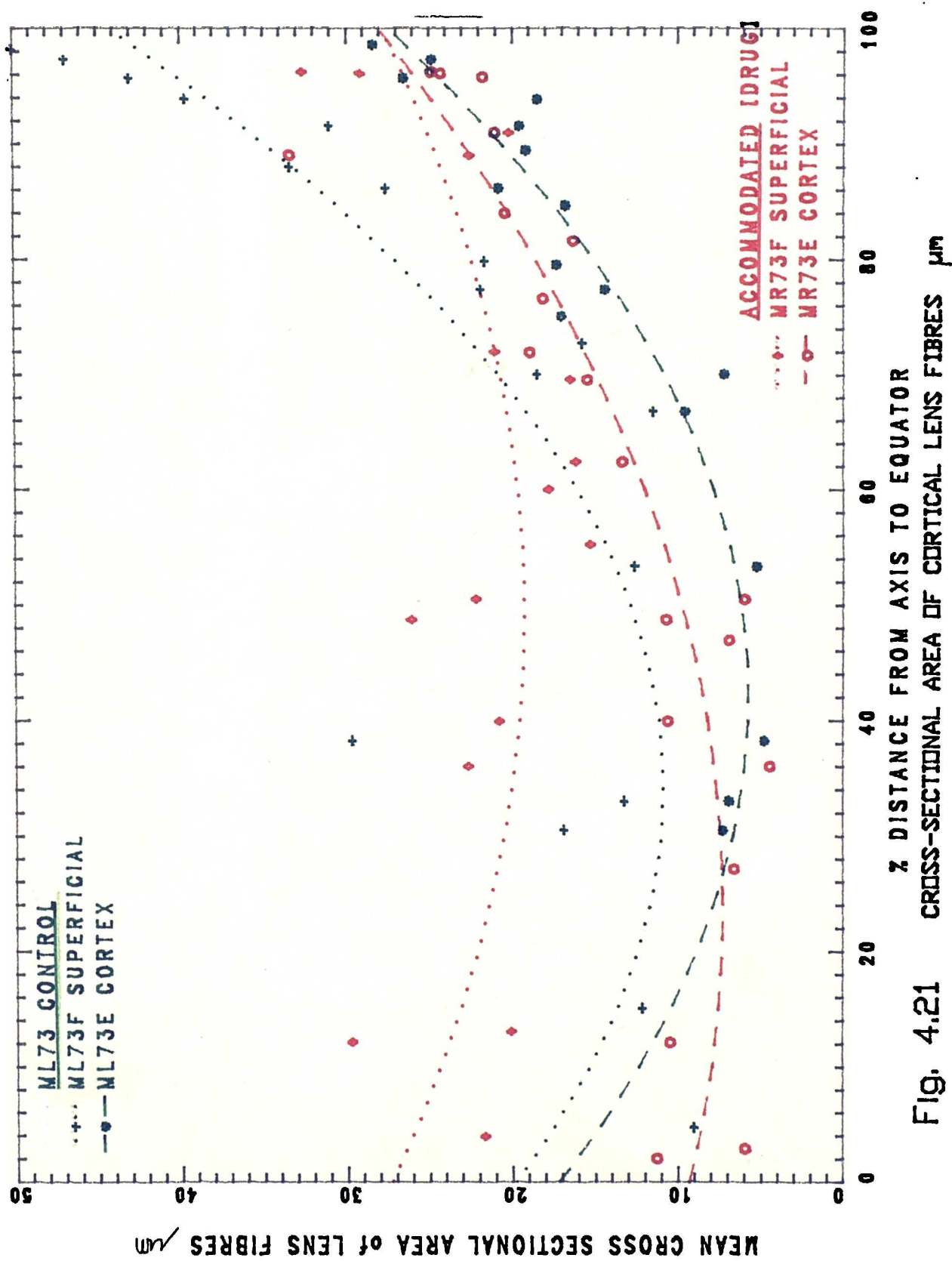


Fig. 4.21 CROSS-SECTIONAL AREA OF CORTICAL LENS FIBRES μm

treated eye) showed greatest cross-sectional area at the equator, followed by marked decrease in regions close to the equator and a smaller reduction followed by an small increase with distance from the equator (Fig. 4:18).

Lens fibres of the drug treated lens were also of greatest cross-sectional area at the equator, and showed an initial decrease close to the equator and a small increase in size close to the polar axis (Fig. 4:19).

There is less difference in the local cross sectional areas between the control and treated lenses of this pair (M73), than in the previous pair (M78).

Lens fibres of the equatorial nucleus were of slightly greater cross-sectional area in the control lens (Fig. 4:20) than in the drug-treated lens. The nuclear lens fibres of the drug treated lens showed less reduction in cross-sectional area with distance from the equator, than the control nuclear fibres.

There is very considerable variation in the mean cross sectional area results for the piece of superficial tissue, from the drug-treated eye, with poor correlation to any standard curve. The subsurface fibres of the treated lens, in the central zone, (mid way between pole and equator), were larger in cross section than their most superficial neighbours, giving a wide spread of results. This was not the case close to the equator, nor was there such difference between superficial and subsurface lens fibre thickness, in fibres of the control lens. The difference in cross

sectional size of control and treated superficial tissue, at the equator was consistent and not subject to the problems reported for the mid-zone.

4:4

DISCUSSION

The notion of cytoplasmic flow is not new. Gullstrand (1924) suggested that "in accordance with the histological structure of the lens (the intracapsular mechanism of accommodation) demands an axipetal movement of the portions of the substance of the lens that are nearest to the points of attachment of the zonule". Cytoplasmic flow has been discussed and suggested as a mechanism in recent years (Koretz, Handelsman and Brown, 1984 and Koretz and Handelsman, 1985). Observation with the slit-lamp microscope of the change in thickness of layers of the lens separated by zones of optical discontinuity, as a result of accommodation, suggested a mass redistribution within each layer (Koretz et al., 1985). At a fibre level, this was consistent with cytoplasmic flow from the equatorial portion into the posterior and anterior portions of the fibre.

Certain predictions would have to be fulfilled, if the hypothesis of cytoplasmic flow were to hold true. These were that in accommodation: a) the local volume of (at least some) fibres at the equator would reduce with commensurate changes in width and thickness; and b) the local volume of fibres away from the equator would increase.

results agree but
as not reported
why the matter
than at flow
only occurs close to
equator in order
to only continuity in
modern

Lens Fibre Width

The width of surface lens fibres (M78 measured using L.M.) and cortical lens fibres (M73 measured using S.E.M.) crossing the equatorial plane, was less in the two 'accommodated' lenses (the drug treated and dislocated lenses were in a simulated accommodated state) than in the controls. This conforms to the predictions above.

Although in line with the predictions for cytoplasmic flow, surface lens fibres are the youngest and are not necessarily representative of the remaining fibres in the lens. However the width of equatorial fibres at all depths were smaller in the accommodated (drug treated) lens than in the control, when measured with S.E.M.

The widths of the equatorial fibres and of their broad faces was lower in the cortex of the accommodated (drug-treated) lens than the control. In intermediate depth lens fibres, the same widths were comparable to those of the control when measured relative to their actual distance from the centre of the nucleus to those of the control. In other words, the fibre width reduction is consistent with the reduction in circumference of each layer, (at least in the intermediate zone of the lens) in accommodation.

Some of this fibre width reduction appears to be achieved by the equatorial fibres displaying mild transverse bending, so that the lens fibres appeared slightly crescent or 'banana' shaped in cross-section. This was more marked in cross-sectional material of the accommodated (dislocated and drug-treated) lenses than in the controls.

The only other significant difference in the appearance of lens fibres fixed in the two different shape states, was the apparent reduction in the prominence of transverse undulation. It is possible that these undulations could be wrinkling caused by shrinkage in fixation and the apparent reduction in their prominence due to the flatter equatorial curve in the treated lens. However, Willekens and Vrensen (1981) had predicted a reduction in the equatorial fibre transverse undulations in accommodation. Their suggestion was that lens fibres could lengthen around the equator and the undulations which they called 'folds' could unfold to aid this. This supposed lengthening at the equator would be accompanied presumably by a similar local length reduction elsewhere as lens fibres are unlikely to increase in total length (Koretz et al., 1985).

Tongue and grooves were examined to explore the idea (Willekens and Vrensen, 1981) that they may unfold to assist with local length or volume changes. Height of tongue and grooves could not be measured accurately, so orientation was measured as an indirect means of assessing changes in tongue and groove height. If tongue and grooves could unfold, then the proportion of tongue and grooves of a particular orientation would reduce. In accommodation, cytoplasmic flow from the equator would reduce fibre bulk locally and the slackened membrane may be taken up as deepened or increased numbers of tongue and grooves (along the fibre axis), and visa-versa at the polar axis. It was expected that any

increase in equatorial tongue and grooves at the equator would be orientated parallel to, rather than across, the long axis of the fibre. There was a small difference in orientation of tongue and grooves between the nuclei of the drug treated and control lenses, but it was not as predicted. The significance of the apparent difference between the two lenses is not yet understood.

Changes in Local Volume of Lens Fibres in Accommodation.

A dislocated lens is arguably in the steepest curvature state achievable and the dislocated lens in this study shows much steeper curvature than the fellow control lens. The phospholine iodide treated lens had a much smaller difference in curvature from the fellow control lens, and it was expected that any local ^{fibre} volume change would be correspondingly smaller.

Comparison of the results of density and cross sectional area along the lens fibre for the accommodated (dislocated) and fellow control lenses indicate the predicted reduction in volume of lens fibres at the equator at all but the most superficial level (f). Control lens fibres show a reduction in fibre volume with distance from the equator, for more than half the distance to the lens axis (Fig. 4.14): the fibres (away from sutures) are slightly spindle shaped in long-section (Hogan et al., 1971). In the fibres of the dislocated lens, the local volume (cross sectional area) at the equator (right of the graph Fig. 4:15) is smaller, and there is a smaller reduction in volume with distance from

the equator (the graph is flatter) as compared with the control lens. Extrapolation of the plots on the graphs suggests a small increase in fibre volume (an upturn in the graph Fig. 4.15) as the polar axis is approached in the accommodated (dislocated) lens. All these findings are in line with the predictions that in accommodation, the local volume of lens fibres would reduce at the equator and increase close to the polar axis.

These results appear to support the concept of cytoplasmic flow. Graphical representation of the findings, shown by comparison of the gradients of control and dislocated lens plots, are clearly most different at nuclear level (Fig. 4.16), indicating greatest cytoplasmic flow in the deeper fibres.

As expected, there is less difference in the local fibre cross sectional areas between the phospholine iodide treated eye and its control.

Comparison of the data from the phospholine iodide treated and control lenses offers less convincing evidence of cytoplasmic flow. Only in the nucleus (level 'ab' Fig. 4.20) and the superficial cortex (level 'f' Fig. 4.21) do the predictions possibly hold true. In accordance with the predictions of cytoplasmic flow, the cross-sectional area of fibres in the nuclear equatorial zone was smaller in the accommodated (drug-treated) lens than the control. This was also true of fibres in the most superficial layer (f) at the

equator. However at the next deeper level (level e) curiously the opposite trend to that predicted ^{was} is shown. The fibres of the control lens were similar in cross sectional area to those of the drug treated lens at the equator itself, but were smaller in the control lens post-equatorially! So fibres in the deeper cortical layer of the 'accommodated' lens appear to contradict the prediction, and counteract at least some of the changes achieved by the superficial cortex. Unfortunately the most superficial cortex of the control lens twined with the dislocated lens was lost, and a direct comparison of the most superficial cortex cannot be made in this pair.

The smaller accommodative shape difference between the drug treated and control lenses appears to have initiated cytoplasmic flow in the superficial cortex (youngest fibres) and nucleus (oldest fibres) only. The larger shape difference between the dislocated and fellow control lens, appears to have produced cytoplasmic flow at every level, but to the greatest degree in the deeper (nuclear) layers.

It was anticipated that the plots for the two control lenses would be similar. However the cross sectional area of the intermediate and nuclear fibres in the equatorial plane of the 'dislocated' control* lens is greater than that of the drug-treated control* lens, whilst they were similar only close to the polar axis. The gradients of the graphs

* meaning the unaccommodated control lens, from the fellow eye of that which was dislocated or drug-treated.

are also different, the plots of the former being a little flatter, suggesting that the difference in cross sectional area between the two control lenses is slightly greater para equatorially.

Fixation of lens tissue is subject to a variety of problems but the result was unlikely to be artifactual, as the two lenses had been prepared in exactly the same manner and the difference found is presumably ~~due~~ attributable to ← natural variation and perhaps age difference. The exact ages of the monkeys were unknown (although it was likely to be between the ages of three and eight), but the monkey in which the lens had been dislocated was probably the younger. It was a male weighing 3.4Kg, the other animal was a female weighing 4.8Kg, with a larger control lens.

Comparison of the 'maximally' accommodated (dislocated) lens with its fellow control lens, suggests that in the accommodated state the 'spindle' shape of fibres normally seen in the unaccommodated state (widest and thickest at the equator) is all but lost, and the fibres become more cylindrical in ⁽¹⁵⁾ shape, with less variation in cross sectional area along their length. This was most marked in the nucleus. Disaccommodation perhaps involves the lens fibres returning to their spindle shape. A comparable difference was found in the accommodated lens of the second pair (drug-treated and control) at superficial cortical (f) and nuclear levels (ab), but the difference was smaller and was not found at other levels. The disparity between the two results

may be due to the smaller curvature difference between accommodated and control lenses in the second animal.

In both lenses there is greater evidence for cytoplasmic flow in the deepest lens fibres. Therefore the accommodative force expressed by the capsule, must be transmitted to the deep nucleus through a layer (d and e) of fibres which themselves show little cytoplasmic flow, perhaps because they have a greater resistance to cytoplasmic flow. This same layer corresponds to the area hardest to count due to the extreme thinness of the lens fibres and profuse interdigitation.

The simplest analogy of cytoplasmic flow is movement of a fluid through a smooth-walled pipe. Laws of fluid mechanics suggest that a pipe of circular cross section gives less resistance to flow than a flatter or irregular shaped pipe with a greater ratio of internal surface area to volume. It follows that a thin flat fibre may present more resistance to internal movement of cytoplasm than a thicker fibre with the same cross sectional area. If the internal surface area of this irregular fibre-like pipe is increased by the addition of protrusions into the lumen, resistance to fluid flow is increased. The photographs of mid and deep cortex show that the ball and sockets protrude into and complicate the internal shape of the lens fibre (Fig. 4.17). It is suggested that this type of cortical fibre would present more resistance to cytoplasmic flow than the fibres of the deep nucleus (no ball and sockets) and superficial

cortex which present a less irregular internal fibre surface.

Brown (1973a) and Koretz et al. (1988a) have shown that the nucleus shows greater axial thickening than the cortex. Since the nucleus is more remote from the capsule which effects the shape change, the opposite might be expected if the visco-elastic properties throughout the lens were similar. However it is known that this is not the case and the elastic properties of the nucleus and cortex do differ (Viggiano, 1966; Fisher, 1971). It is suggested that the structure of the mature cortical lens fibres is consistent with this greater nuclear shape change. This area of thin heavily interdigitating firmly-attached lens fibres, whilst resisting cytoplasmic flow itself, could transmit the accommodative force to the more obliging fibres of the deep nucleus.

There are fewer lens fibres in any one fibre layer in the nucleus than the cortex, therefore cytoplasmic flow could be expected to be greater in the nucleus, to achieve a similar overall effect (Koretz and Handelman, 1985). Since there is no evidence of cytoplasmic flow in the intermediate and deep cortex in the lens of the second animal (drug-treated), these results are consistent with Brown's finding of greater nuclear action in accommodation. The results of the dislocated/control pair, would require further mathematical analysis, to clarify this point.

The problem of cytoplasmic flow is more complex than

simple fluid flow through a pipe. It must take into account that transparency depends on the maintenance of an ordered system, with correct distribution of the crystallins within the cytoplasm (Koretz et al., 1984). The optical density or refractive index of each part of the lens, is dependent on the concentration of crystallins, and it is even possible that redistribution of fibre contents may entail indecial variation. In addition the fibre has an internal skeleton. The microtubules have been implicated in giving the fibres their visco-elastic properties (Farnsworth et al., 1980a) and it has been reported that the internal pattern of cytoplasmic filaments is lattice-like only in species capable of lenticular deformation (Rafferty and Goossens, 1978). Although the exact function and distribution of the elements of the cytoskeleton is not fully understood, there is some evidence of differing distribution from nucleus and cortex, (Kuwabara, 1968; Rafferty and Goossens, 1978; Bradley et al., 1979; Farnsworth et al., 1980a; Rafferty, 1985). The role of the cytoskeleton may be central to cytoplasmic flow and accommodative shape changes.

To return to the experimental results from the two monkeys, it is possible that the smaller variation in cross-sectional area of the fibres of the control (drug-treated) lens were age related - perhaps a sign of very early pre-presbyopic failure. Perhaps inability of lens fibres to return to their 'spindle' shape in disaccommodation (drug-treated control) contributes to presbyopia! In the

continually growing lens, perhaps the new mature cortical fibres are of the thin profusely interdigitated, highly resistant to cytoplasmic flow type, thus producing a greater proportion of the lens unable to change shape as age progresses.

In reality although these results appear to support the hypothesis of cytoplasmic flow, the method used has limitations. The thickness of lens fibres relative to the resolving power of the light microscope prevented the measurement of individual lens fibres, so that only mean values were obtained with no indication of variety. This prevented the use of standard statistical tests to assess significance. Only a small part (less than 1/10) of each of the two pairs of lenses were used to test the hypothesis. A major problem with the method is that it is very time consuming.

It is hoped that this work will inspire future study to further test the hypothesis of cytoplasmic flow, using a wider variety of sample tissues. This could then provide a sound statistical basis on which to judge the hypothesis.

CHAPTER FIVE

5

LENS CAPSULE THICKNESS AND LENS SHAPE

Fincham's (1929) study of the monkey anterior lens capsule, found an annular zone of thickened capsule concentric with the equator and relative thinning of the capsule at the anterior pole and the equator. He likened this pattern in the monkey to that found previously in human lens capsules (Salzmann, 1912; Fincham, 1925).

Much later, Fisher and Pettet (1972) found a different pattern in young human lens capsules where there was maximum thickening at the equator and assumed Fincham had been misled by perhaps looking at material from presbyopic subjects. This threw doubt on Fincham's findings in the monkey, were they similarly questionable?

Observation on the phospholine iodide treated lens (Fig. 4:1) showed the same kind of 'conical' lens shape noted by Fincham, but it occurred on the posterior rather than the anterior surface. This unexpected result poses two questions. Is the greatest monkey lens capsule thickness coincident with the apparent base of the cone shape? If so, does Fincham's concept of differential lens moulding by the elastic capsule apply?

Sections of monkey lens, initially prepared to look at lens fibres, seemed to show an area of marked capsular thickening in the posterior periphery, in a similar position

to the observed area of relative curvature flattening (Fig. 4:1). This same observation was made by Salzmann on the human lens eighty years ago. This initiated a series of experiments to look not only at cynomolgus lens capsule thickness, both *in situ* and removed from the lens, but also to look at curvature and to re-examine human lens capsule thickness.

5:1

MATERIALS

Lens capsule thickness was investigated in juvenile and adult monkeys. Two methods of fixation were used, perfusion (Appendix B), and immersion up to seven hours after death, in the same buffered mixture of 3% glutaraldehyde /2% paraformaldehyde (Appendix B). The lens from one perfused fixed rhesus (*Macaca mulatta*) monkey was also included in this study. Material was stored in the fixative at 4 degrees C.

Some human lenses were also used in the study of the lens capsule, fixed by immersion in the same buffered fixative, up to forty eight hours after removal or death. These ranged in age from twelve to seventy two years.

5:2.1 Measurement of Monkey Lens Capsule Thickness :Perfuse-fixed Material

Undamaged crystalline lenses from nine adolescent and adult monkeys (eight cynomolgus and one rhesus, aged between 2 and 8 years old) were cut into two slightly unequal halves. They were embedded in Araldite and whole sections (3/4-2 μ m thick) prepared (using either a Cambridge Huxley or Reichart ultramicrotome) to show the capsule at both anterior and posterior poles. Sections were then stained with toluidine blue, either by the usual method (3:2) or by floating the Araldite section on a warmed stain bath, washing and then mounting on a glass slide without removing the Araldite.

The thickness of the capsule at points around the lens was assessed using a measuring eye piece.

In addition to the eleven control perfuse-fixed lenses, the thickness of the posterior capsule of both MR78 (the dislocated lens) and MR73 (the phospholine iodide treated lens) were measured. These were taken from the interrupted serial sections prepared to measure lens fibre cross-sectional area. The tissue had been orientated with the later in mind and the capsule may have been cut slightly obliquely at the points of greatest curvature. Unfortunately, not all of the capsule of the control lenses, ML78 and ML73, were present on these slides for direct

comparison. M78 and M73 were both perfused fixed animals and, with the above reservation, may be compared with the lens capsules from untreated perfuse-fixed eyes.

5:2.2 Measurement of Human Lens Capsule Thickness

To compare the variation in the cynomolgus monkey lens capsule with that of man, it seemed prudent not to rely on existing data, but to use broadly similar methods to those described for the monkey, to briefly investigate lens capsule thickness in man. Three methods of preparation were used.

a) Thickness of Capsules in Whole Lenses

Human eyes were obtained after removal of corneas for transplantation. These were fixed by immersion in the same buffered glutaraldehyde/ paraformaldehyde mixture used formerly (Appendix B,). One eye was from a child aged 12 and another from a presbyopic subject aged 54/55. A third eye from a subject in their mid thirties was immersed complete in fixative, nearly thirty six hours after death, without removal of the cornea.

These were sectioned, stained and measured in the same way as the monkey material.

b) Thickness of Detached Human Lens Capsule

Further single human lenses were obtained from post mortem and donor eyes, up to 48 hours after death, from

subjects aged 24, 44, 61, 66, 67, and 70.

As Fisher and Pettet's (1972) measurements were done on unfixed human lens capsules (free from tensions exerted by the lens fibres and the zonules), this part of the study also examined the thickness of unstressed capsules. However, unlike Fisher and Pettet, the samples were fixed after release. The areas of greatest interest in this study (because of the differences in Fisher and Pettet's and Fincham /Salzmann's findings) were the equator and the zones on either side of it, so particular care was taken in preparation to avoid damage to these areas.

These eyes were immersed in saline, after removal of the corneal discs for transplantation and the posterior poles for other research, before immediate transport to our laboratory for dissection.

Each lens was carefully removed from the ciliary body by severing the supporting zonules. In order to avoid damage to the capsule, no attempt was made to fully remove or dissolve the zonules. The capsule was removed from the underlying lens fibres by carefully cutting in a diagonal curve from the posterior post-equatorial zone across the equator to the anterior pre-equatorial zone, leaving at least half the equator undamaged. The lens capsule which then curled out with little encouragement, could be peeled back from the lens fibres (as if removing a pillowcase). Care was taken to avoid touching the uncut half of the

capsule equator. The lens epithelium and sometimes a few lens fibres were left attached to the capsule. The presence of the epithelium and especially the newest (differentiating) lens fibres were helpful in orientation.

The removed capsule was then immersed in similar fixative to that used for whole lenses. The capsule is an elastic membrane and may change according to the pressures exerted on it, such as the capillary attraction of a cover slip, or when cut. It is likely that fixation destroys the capsule's elastic properties. Usually the removed in-side-out lens capsule bag, curled up, rather like a scroll.

The curled capsules were embedded in Araldite, and sectioned across the roll endeavouring to cut through the undamaged equator and the rest of the capsule transversely. Sections were stained as above and the capsule thickness measured using a measuring eyepiece. It was assumed that the thinnest part of the posterior capsule occurred at or near the posterior pole, since this was the case in the whole lens sections.

A few capsules from older subjects unfortunately split across the previously undamaged area of equatorial capsule during dehydration or embedding. Only those with sufficient area of undamaged equatorial capsule in each case were included in this study.

c) Thickness of Anterior Human Lens Capsules, from Intracapsular Extractions.

Discs of anterior human lens capsules were obtained

after intracapsular extraction (for cataract removal), and immersed immediately in fixative. This gave the advantage of immediate fixation but only gave information on the variation between mature subjects, of the central anterior capsule thickness. Material was from subjects with abnormal lenses, suffering cataracts, aged 54 to 72.

5:2.3 Experiments to Investigate the Effects of
Decapsulation on Lens Shape and Capsule Thickness.

The eyes of five cynomolgus monkeys, aged between 3 months and twelve years, were removed immediately after death. They had all received an overdose of Vetalar. These eyes were stored in saline for two or three hours during transport to the laboratory.

Each eye, still in saline, was dissected to remove the crystalline lens undamaged. Each lens was photographed in a small square sided glass tank filled with saline. A surface silvered mirror was placed beneath a dissecting microscope at an angle of 45 degrees, adjacent to the tank, to obtain a silhouette profile of the isolated lens. The lens was supported on a flat glass platform, almost in contact with the inside of the tank wall through which the lens was photographed. Resting on the flat platform, caused some flattening of the basal surface. The lens was therefore turned over to rest on its other face and re-photographed to obtain an adequate profile of each surface. All five pairs of lenses were photographed in this way.

One of each pair of lenses was then put in buffered fixative, (the right lenses of the four youngest subjects, the left of the twelve year old). The lens from each fellow eye was then decapsulated in the same way as the human lenses earlier, taking care to avoid damage to the underlying lens fibres. The removed capsules were also placed in fixative. Each decapsulated lens substance was photographed to allow comparison of the lens shapes with and without the capsule.

A saline bath was used, because it was feared that an oil bath (as Fincham had used) though supporting the lens better, may dehydrate or otherwise affect the capsule. A curved support (as used by Fisher) was also considered but rejected as it would also affect the shape of the lens unless it matched perfectly each time.

All material was fixed by immersion and stored in 3% gluteraldehyde/ 2% paraformaldehyde within seven hours of death.

a) Measurement of Lens Capsule Thickness.

After fixation the five whole lenses were bisected (marginally to one side of both poles) and the slightly larger half embedded in Araldite, in the same way as earlier material. Meridional sections were prepared from each lens, to allow thickness measurement of the capsule and epithelium, around each lens.

Freed lens capsules, were embedded complete, the older

ones rolling up in a similar way to the human lens capsules. These were serially sectioned in a manner to include a transversely cut capsule through the undamaged equator and both poles. It was rare for the capsule to be curled in such a way that both poles were cut simultaneously, so information from several sections was amalgamated.

A measuring eye piece was used as before to assess lens capsule thickness. Epithelial attachment and termination assisted in determining orientation. The equator could be located approximately, on the detached capsule of each pair, by counting the number of epithelial cells lying posterior to the geometrical equator in the whole lens sections. The maximal and minimal anterior and posterior capsule thickness were then compared in each pair.

Assessment of the separation of maxima and minima, was achieved by digitising scale drawings. Digitising was achieved using an Epsom plotter (Hi-80) and Amstrad 1640 computer. The pen housing was replaced with a transparent sheet engraved with 'cross hair', which could be held close to the drawing, to minimise parallax errors. The plotter was then used (with specially written software, Appendix C) in reverse of its normal function, to digitise points on the drawings. The scale drawings were made from sections, using a Camera Lucida attachment to the microscope and capsule thickness was assessed using a measuring eyepiece and recorded at intervals along the drawing. A graph plotting program (Share Ware, 'Dataplot') was used to plot capsule length against thickness. Approximate capsule length, and

separation between specific points such as maxima and minima, pole and equator could then be read directly off the graph (Figs. 5.4-5.8).

This method of length measurement (from scale drawings), results in an accurate representation of capsule thickness, so that comparisons between adjacent maximum and minima may be made. However this does not give an accurate representation of capsule thickness at a given point on the capsule.

b) Lens Shape

Prints of the lens profiles were digitised for computer aided analysis of curvature using an Epsom plotter (Hi-80). The plotter was used (with specially written software, Appendix C) in a similar manner to that described above, to digitise points on the lens outlines and about 100 data points were stored for each profile. Analysis of curves was performed using a commercially available programme (Shareware, CurveFitting, by T.S.Cox, Append. C) which optimises the best fit through the points with 25 known lines and curves, such as hyperbolas, parabolas and more complex statistical curves. Best fit spherical curves were fitted by overlying a transparent sheet marked with concentric curves, and simply assessing subjectively the curve of best fit.

5:3.1 Monkey Lens Capsule Thickness

a) Capsule Thickness in Perfuse-Fixed Monkey Lenses

The results are summarised in Table 5:1. The exact age of most of the animals was not known, so the information has been listed in order of their weight. In the cynomolgus monkey the capsules were thinnest at the posterior pole in each case (under $2\mu\text{m}$) and thickest ($13\text{--}38\mu\text{m}$) in the posterior mid-periphery, towards the equator rather than the posterior pole. This area of maximal capsular thickness was found in each monkey, posterior (further away from the equator) to the zonular attachments and posterior to the end of the epithelial mono-layer. Looking at the lens in a frontal plane, the thickened zone occurred at about $1\text{--}1.3\text{mm}$ from the equator, or $1.5\text{--}1.8\text{mm}$ around the curved arc from the equator.

The thickness of the equatorial capsule varied between $4\text{--}8\mu\text{m}$ and was the next thinnest zone. A point of minimum thickness was seen in each lens between the geometric equator and the area of maximum thickening in the posterior periphery. Immediately posterior to the end of the epithelium, this minima was usually only slightly thinner than at the equator itself. Thus the greatest variation of capsular thickness was seen in the posterior capsule.

The anterior capsule was thinnest close to the equator, in a mirror image of the slight thinning that occurred in

CAPSULE THICKNESS μm

CODE	SEX	WT/KG	ANTERIOR		EQUATOR	POSTERIOR	
			POLE	MAX		MAX	POLE
<u>CYNOMOLGUS MONKEY</u>					<u>UNACCOMMODATED</u>		
MR85)	F	2	9.5	14.6	4	25.5	1.8
ML85)			--(17)	17	3.6	38	1.8
MR86)	F		9.5	15	6.5	21	1.9
ML86)			9.5	17.5	6.5	20.5	1.7
ML77)	F	3	11.5	16	8	23	1.3
MR80)	F	3.3	5.5	12	5.5	13 (3.5)	--
ML80)			7.5	11	5	21	1
MR90)	F	3.4	6	15.5	5	21	1.8
ML90)			8.5	15.5	5	21.5	1.9
					<u>ACCOMMODATED</u>		
MR78	M	3.4	DISLOCATED		8.5	38 (5)--	
MR73	F	4.8	PHOSPHOLINE IODIDE		12.5	34	1.5
<u>RHESUS MONKEY</u>							
MR54)			16	20.5	8	36	(3)
ML54)			--	(11)--	5	--(12)	1.9

KEY -- Not available

() Capsule thickness, at some intermediate point, when thickness at pole/maximum/minimum unavailable.

Max Maximum thickness of capsule, between polar axis and equator

TABLE 5:1 MONKEY CAPSULE THICKNESS

the posterior capsule (1-2 μ m thinner than the equator itself). It was thickest (11-18 μ m) in a zone almost midway between equator and pole, closer to the polar axis (anterior) than the zonular attachments and the transitional epithelium. It was slightly closer to the equator than the pole, but closer to the pole than the equivalent maximal thickening on the posterior surface. The anterior capsule thinned slightly at the anterior pole (5-12 μ m). The variation in capsular thickness was less in the anterior, than in the posterior capsule.

The capsule of the rhesus monkey displayed a similar pattern of thickness variation to that of the cynomolgus, but was slightly thicker, except at the posterior pole.

Variation in thickness is illustrated in Figure 5.1. It should be pointed out that the cynomolgus capsule thickness illustrated is for ML85, which showed less variation in anterior capsular thickness than all the other lenses, perhaps because the section did not pass through the polar axis.

b) Capsule Thickness in Lenses Fixed in Accommodated States.

The thickness of the posterior capsule from the phospholine iodide treated lens (MR73) and the dislocated lens (MR78) (used in the previous chapter) are summarised in Table 5:1 (follows page 118) and displayed graphically in Figure 5.2. The thickness at the posterior pole is similar in the phospholine iodide treated lens (unfortunately the polar capsule was lost in the dislocated lens) to that of

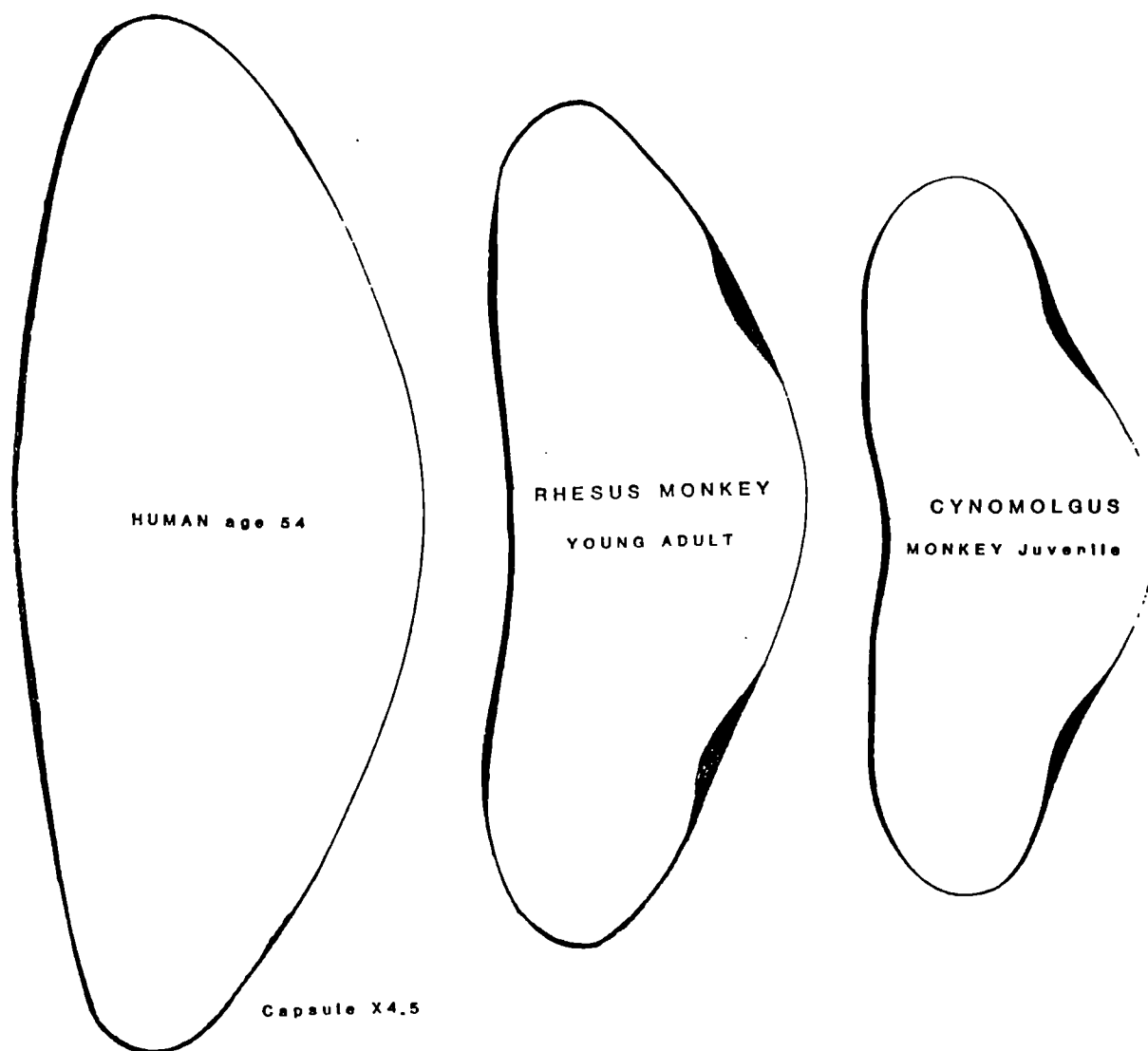


Fig. 5:1 Scale drawing to show the variation in the thickness of the lens capsule in fixed primates. The thickness of the capsule is exaggerated by x4.5 greater than the size of the lens profiles.

Fig.5:2 Thickness of the capsule from the lens of a perfused fixed young adult cynomolgus monkey of 7/8 years of age (ML90), plotted against distance from anterior to posterior pole.

Fig.5:3 Thickness of the lens capsule in cynomolgus monkey lenses fixed in an 'accommodated' state. The lens from one eye was treated with phospholine iodide prior to perfusion (MR73), whilst the other lens was dislocated prior to perfusion, to obtain a lens shape similar to a highly accommodated state.

MONKEY CAPSULE THICKNESS :WHOLE FIXED

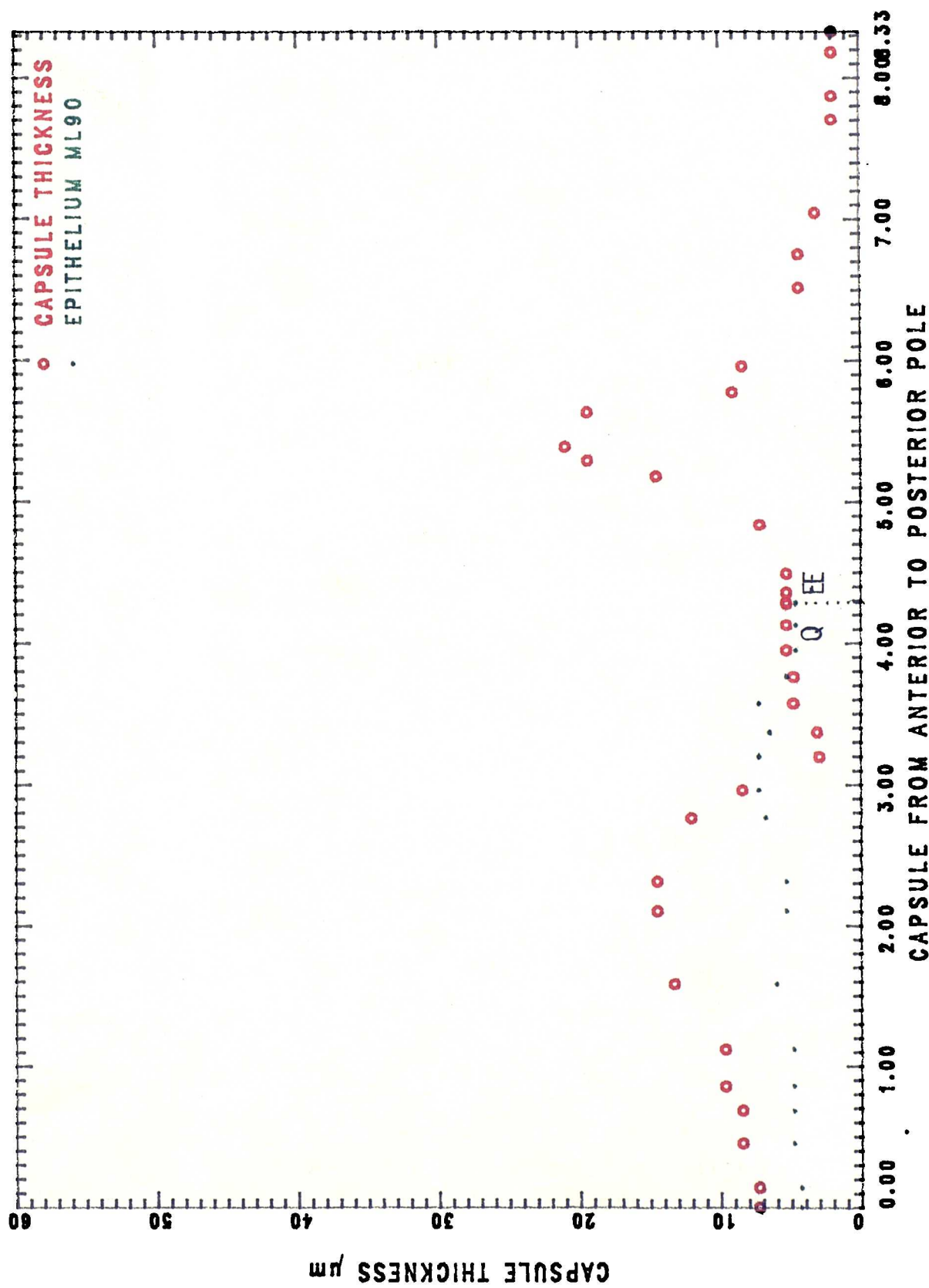


Fig. 5.2 Variation in Monkey Capsule Thickness :- Perfuse-Fixed

MONKEY CAPSULE THICKNESS: ACCOMMODATED

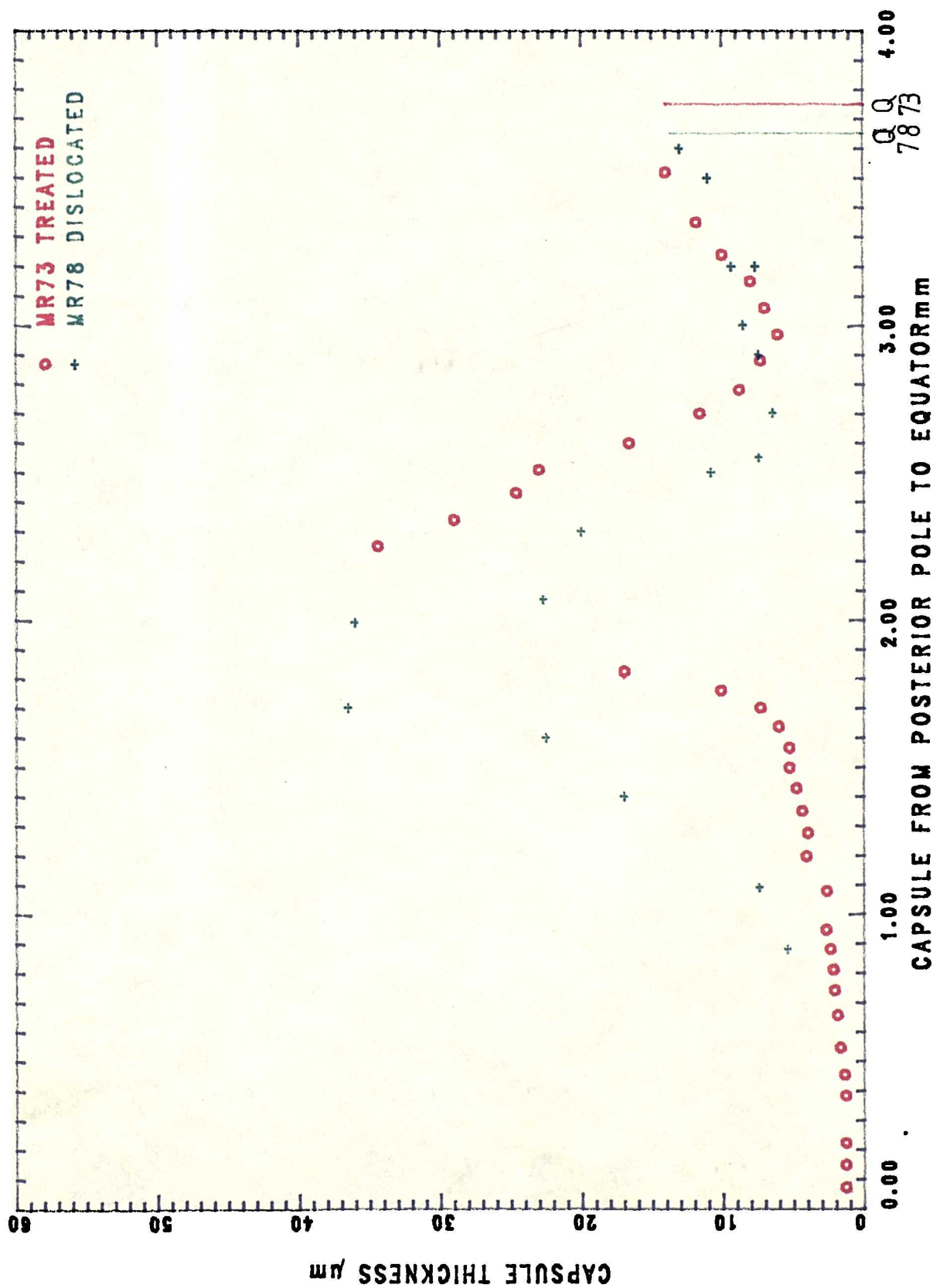


Fig. 5.3 Monkey capsule Thickness Variation - Accommodated

the untreated lenses. However, the area of maximum thickness in the posterior mid-periphery (1.5-2mm around the curved surface from the equator) is thicker in both these 'accommodated' lenses than in the untreated lenses.

c) Thickness of Dislocated and Detached Capsules in the Monkey

Pairs of unfixed lenses were obtained from cynomolgus monkeys aged 3 months, 11 months, 12 months, 10.5 years and 12 years old.

One lens of each pair was fixed whole, whereas the capsule of the fellow eye was removed from the lens prior to fixation. The thickness of both capsules were then compared. The capsule in the whole lens would have been subject to stress from the lens substance only, when it was fixed. The detached capsule would have been in a relaxed untensioned state. Both were inevitably subject to artefacts due to fixation and embedding procedures.

Variation in capsule thickness in these ten monkey eyes are summarised in Table 5:2 (next page). Thickness is plotted against capsule length for each pair of lenses in Figures 5:4.- 5:8. Posterior and equatorial capsule thickness in the detached state was slightly greater than 'whole' state. The thickest (34-64 μ m) part of the capsule in each case was part way along the posterior surface, closer to the equator than the posterior pole. There was a ring of lesser capsular thickening in the anterior periphery,

CODE	AGE	SEX	WT	ANTERIOR			EQUATOR	POSTERIOR		
				POLE	AMAX	AMIN	EQU	PMIN	PMAX	POLE
MP08	W 3m	M	0.84	6.5	12	6	3.1	3.1	38	1.7
MP08	D			7.5	12.5	6	5	4.5	64	3
MP17	W 11m	F	1.7	?	22	3	3.1	2.5	39	2
MP17	D			9	21	5	5	4.5	49	2.6
MP14	W 1y	M	1.4	5	12	2.4	3.2	3.4	35	1.9
MP14	D			6	12	3.6	4	4	50	2.4
MP76	W 10y	M	7.6	10.5	21	5	9	6	31	1.6
MP76	D			9	20	5	11.5	9	35	2
MP53	W 12y	M	5.3	9	20	5	9	7.7	39	2.5
MP53	D			9.6	20	6	12	12	43	2

KEY

W = CAPSULE ON WHOLE LENS

D = DETACHED CAPSULE

m = MONTHS

y = YEARS

M = MALE

F = FEMALE

TABLE 5:2 CAPSULE THICKNESS: DISLOCATED AND DETACHED

Figures 5:4- 5:8

Thickness of the lens capsule against distance from anterior (AP) to posterior pole (PP), in paired lenses fixed in two different states:

(a) thickness of the undamaged capsule still attached to the underlying lens substance, but removed from the eye.

(b) thickness of the detached (unstretched) capsule.

The position of the equator (Q), and end of the epithelial layer (EE) are indicated.

Fig. 5:4 Age three months.

Fig. 5:5 Age eleven months.

Fig. 5:6 Age one year.

Fig. 5:7 Age ten and a half years.

Fig. 5:8 Age twelve years.

CAPSULE THICKNESS μm AGE 3 MONTHS

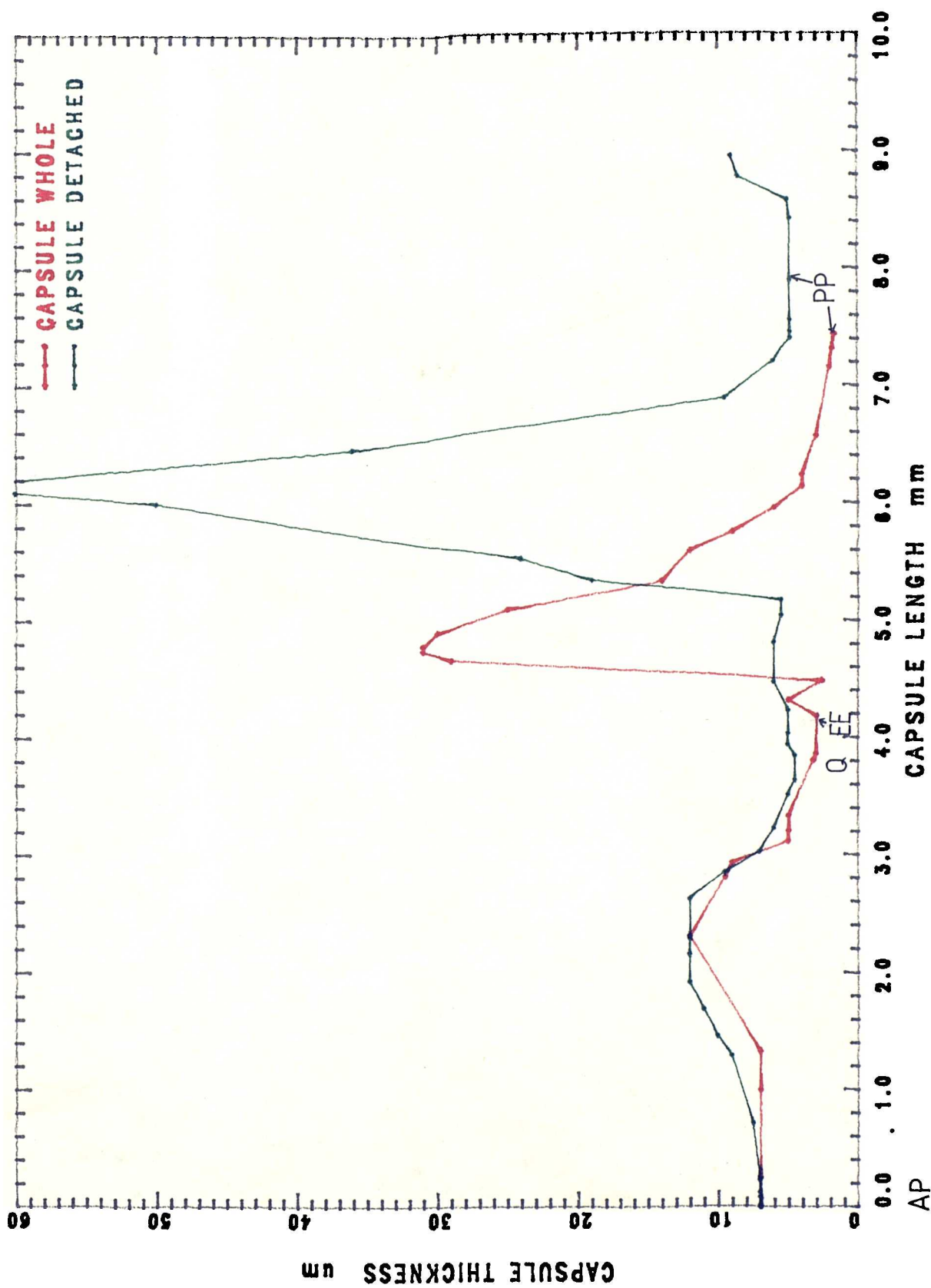


Fig. 5.4 Variation in Capsule Thickness in Monkey age 3 months

CAPSULE THICKNESS μm AGE 11 MONTHS

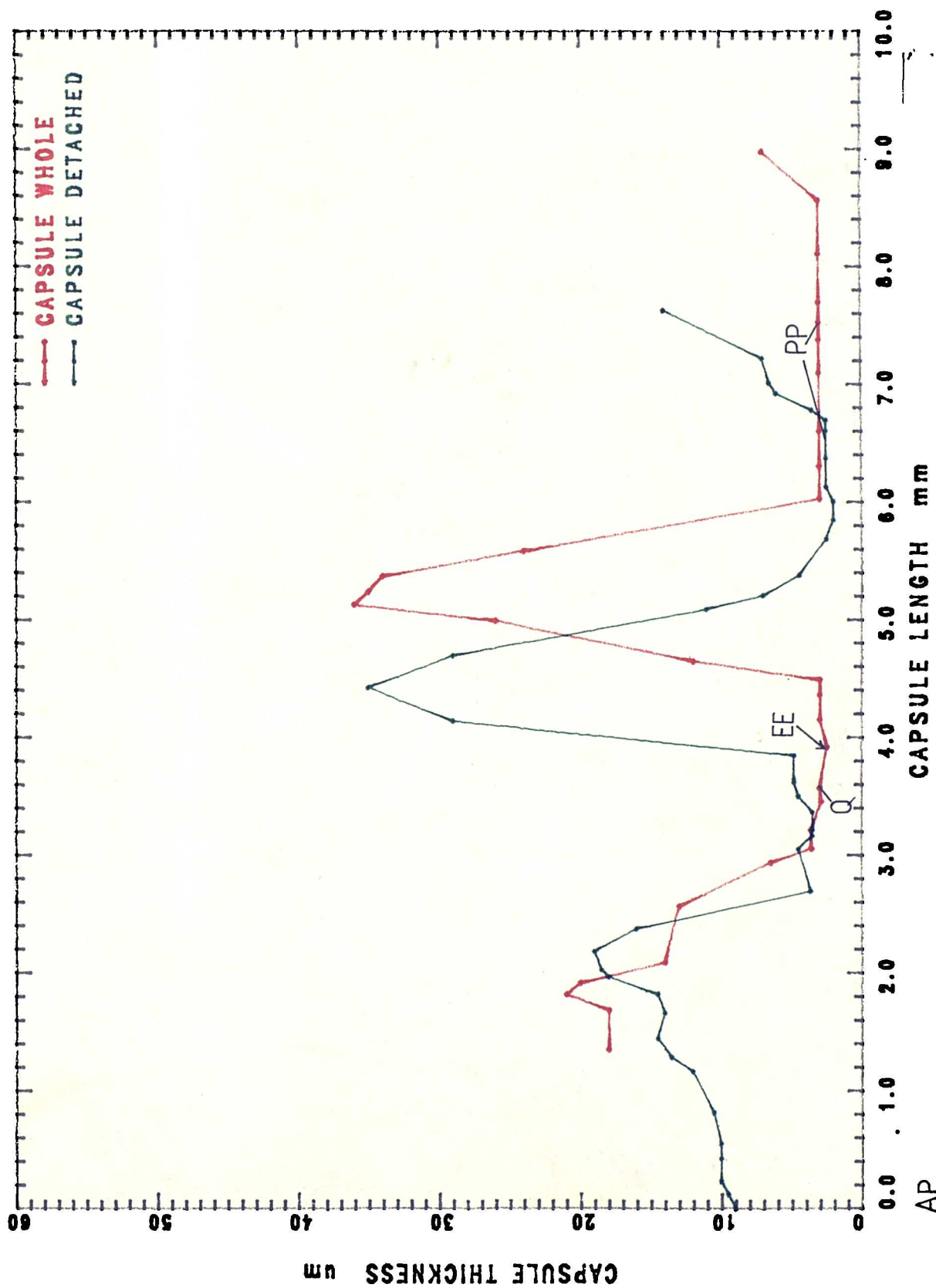
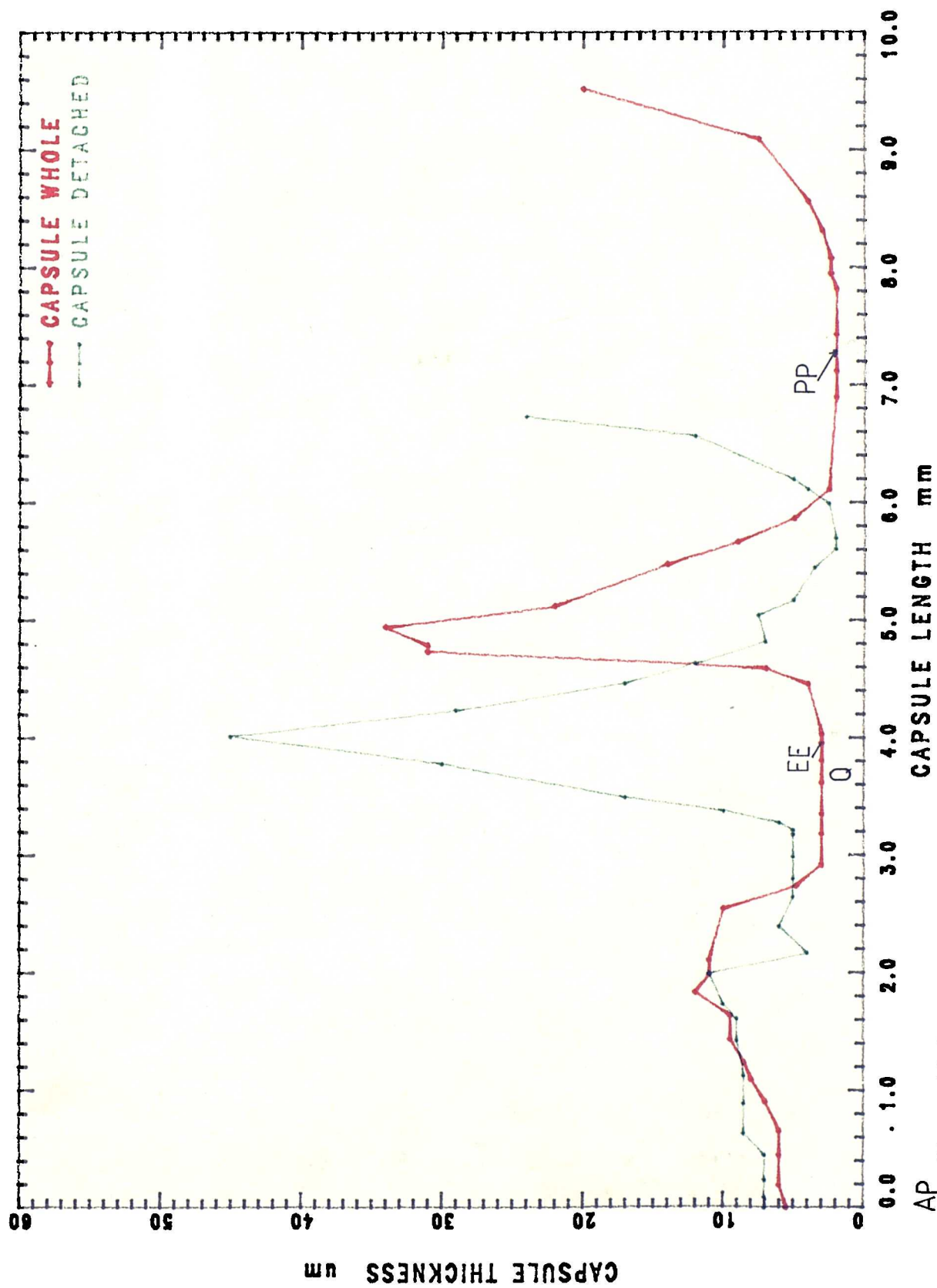


Fig. 5.5 Variation in Capsule Thickness in Monkey age 11 months

AP

CAPSULE THICKNESS μm AGE ONE YEAR



Monkey age 12 months

Variation in Capsule Thickness

Fig. 5.6

AP

CAPSULE THICKNESS μm AGE TEN YEARS

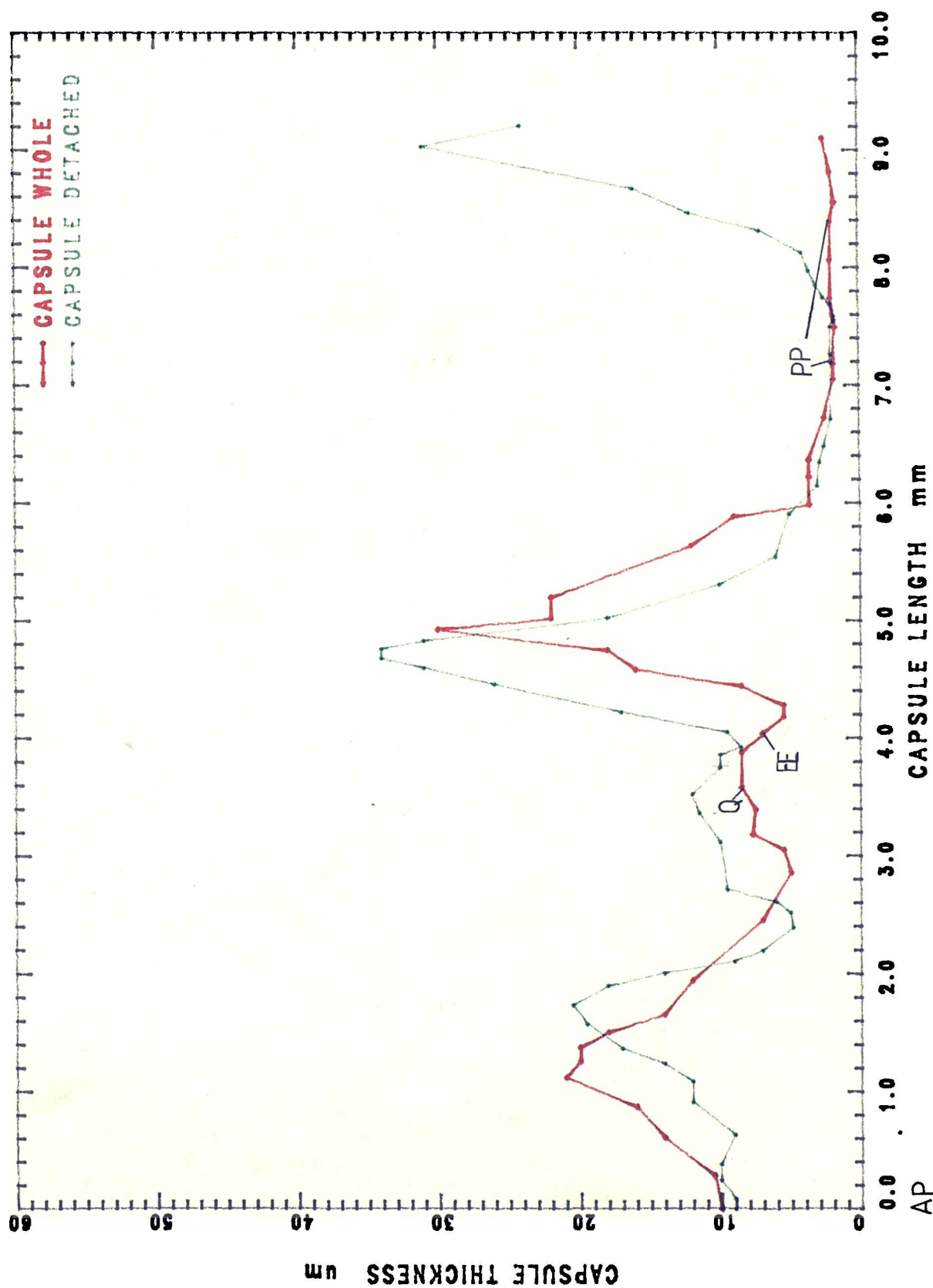


Fig. 5.7 Variation in Capsule Thickness in Monkey age 10 years

CAPSULE THICKNESS μm AGE TWELVE YEARS

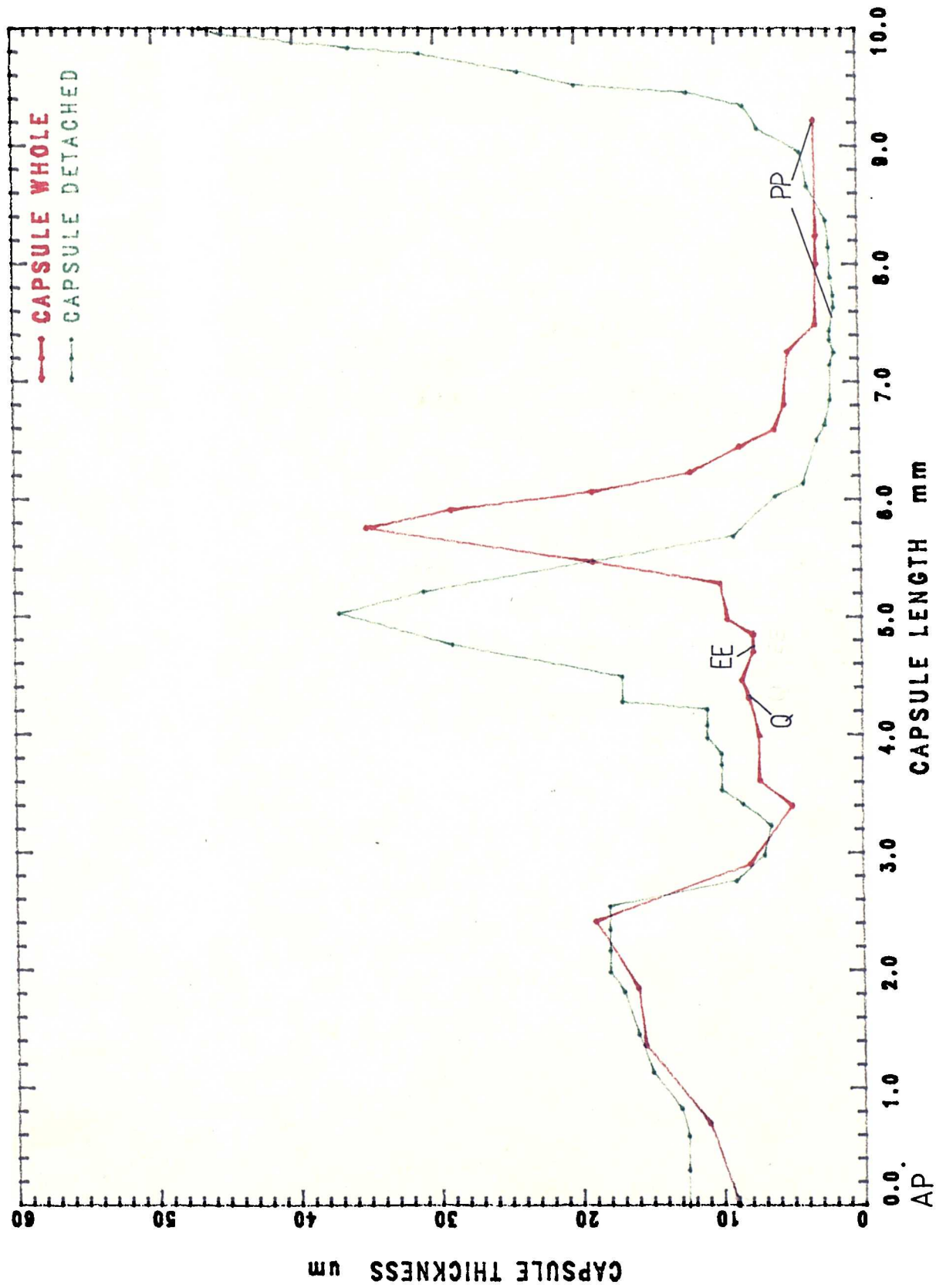


Fig. 5.8 Variation in Capsule Thickness in Monkey age 12 years

further from the equator than that of the posterior. The posterior polar capsule was always the thinnest (1.5-2.5 μ m) portion of the capsule, although the capsule at the equator was almost as thin (3-5 μ m) in the younger animals and was always thinner than that at the anterior pole.

There was a small increase in capsular thickness in older as compared with the younger animals, at the anterior pole and the equator whilst the posterior polar capsule is of similar thickness in each animal. Changes in capsular thickness variation with age are blurred by the variation between individuals. In the detached state the posterior peripheral capsular ring was actually thinner in the older animals, although there was little age related difference in the thickness of this zone when fixed surrounding the lens. The capsules of the older animals were longer.

Figures 5:9 - 5.11 illustrate the variation in capsular thickness.

5:3.2 Human Lens Capsule Thickness

a) Lenses Fixed In Situ

Only three lenses fixed in situ were examined, one from a twelve year old child, another from an adult (age estimated at 35 years) and the last from a fifty-four year old presbyopic subject. Capsule thickness is summarised in Table 5.3, and represented in a scale drawing in Figure 5:12. In the child, the thickest area of the capsule formed

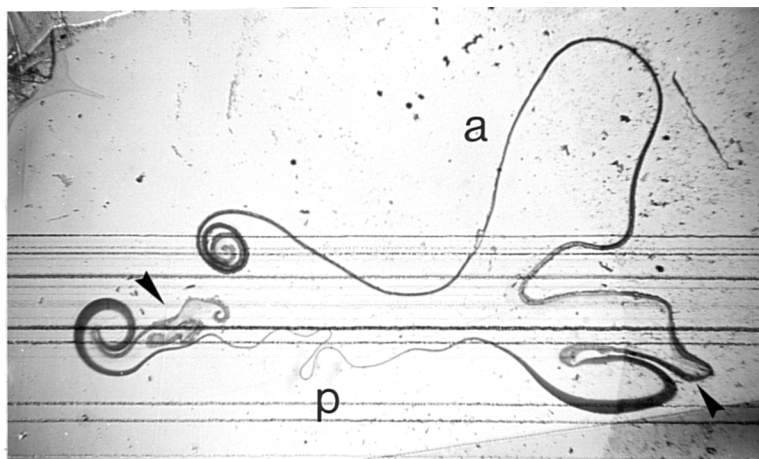


Fig. 5:9a

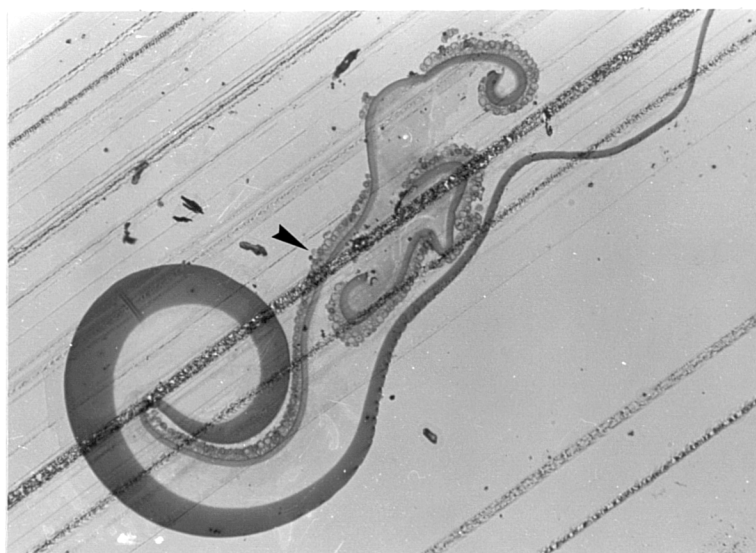


Fig. 5:9b

See legend on following page.

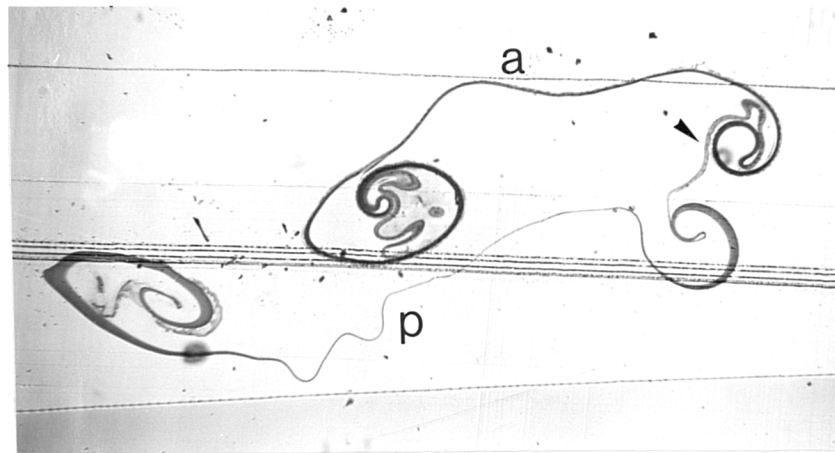
Fig. 5:9 Micrograph of the detached capsule from the lens of the 3 month old monkey. The capsule curled up like a badly rolled scroll after removal from the lens, and was subsequently transversely sectioned.

a) As the capsule rolled up slightly obliquely this section cuts through the anterior pole (A), but not through the posterior pole. Much of the epithelium is still attached to the anterior and equatorial capsule. Unfortunately the undamaged equatorial capsule (right side of section) was slightly folded at this point, and is not cut transversely.

x26

b) Small part of the equatorial and post-equatorial capsule. The capsule is thin at the equator (arrow head), but thickens dramatically away from the end of the epithelial layer. x104

a)



b)



c)

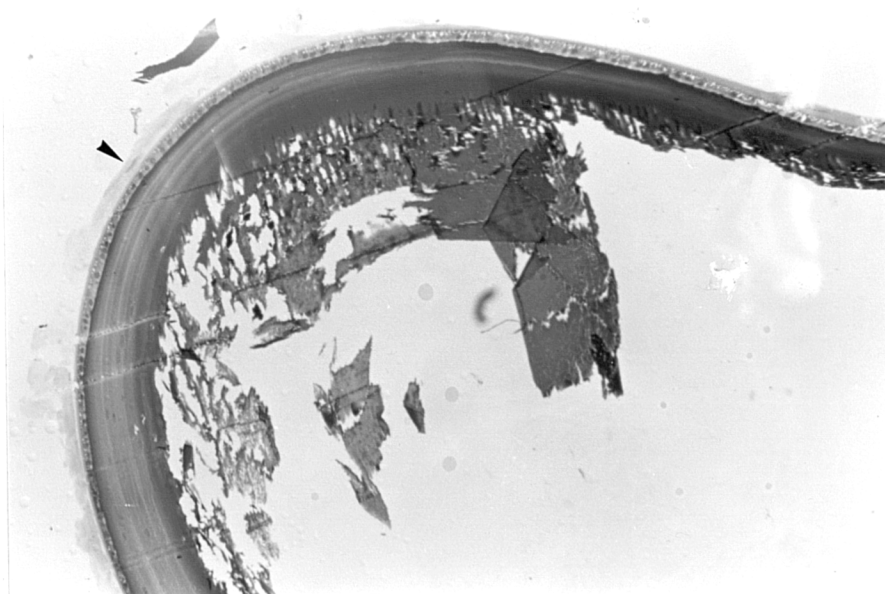


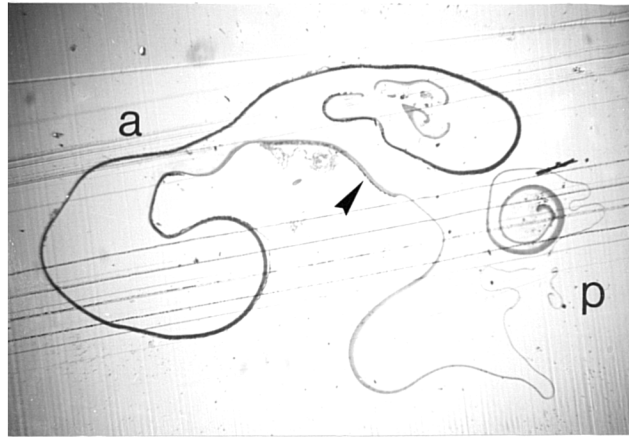
Fig. 5:10 See legend on following page.

Fig. 5:10 a) The detached capsule from the eleven month old monkey, was very thin at the equator (arrow head) and at the posterior pole (p). The thickest part of the capsule is just below the equator in this picture, and a similarly thickened zone is seen, (cut obliquely) on the other side of the posterior pole, on the left of the picture, with a few lens fibres attached. This section does not exactly cut through the anterior pole. Epithelial cells lie along the anterior (a) capsule. x26

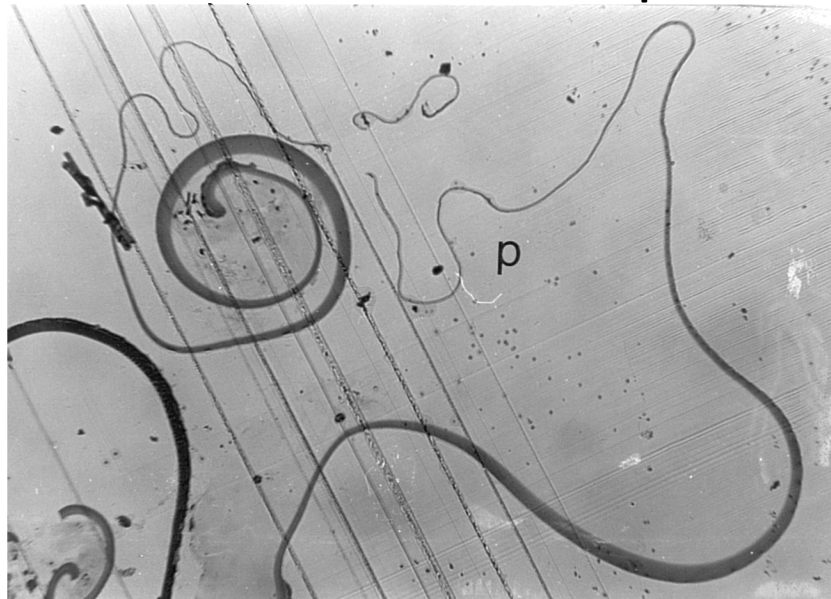
b) The equatorial and para- equatorial capsule of the same lens. The thinnest part of the capsule shown in this picture is at the equator (arrow head). There is a mildly thickened zone anterior (left) and a markedly thickened zone posterior (right) of the equator. x 104

c) The undamaged capsule of the fellow eye was also very thin at the equator (arrow head). A thickened zone can just be seen anterior (right) of the equator. This lens was a rather distorted shape after fixation. x104

a)



b)



c)



Fig. 5:11 See legends on following page.

Fig 5:11 a) The detached capsule of the ten year old although thinnest at the posterior pole (p), is very thin at the equator (arrow). x26

b) the posterior capsule has both the thickest zone (either side of (p) and the thinnest at the posterior pole (p). A small part of the deeper staining pre-equatorial anterior capsule is shown with thin epithelial cells attached. x 71

c) The undamaged attached capsule of the fellow eye, is very thin at the equator. x71

two rings concentric to the equator, one in the anterior and one in the posterior periphery; the posterior ring lay closer to the equator than that of the anterior. Looking at the lens in the frontal plane, the centre of the posterior thickened band is 0.87mm from the equator, and 3.83mm from the posterior pole, whilst the anterior thickened band is 1.8mm from the equator (2.9mm from the anterior pole).

The lens from the 35 year old eye demonstrated a similar pattern of thickening, but the posterior ring (3.8mm from the posterior pole) was slightly thicker (22 μ m) than the anterior thickened band (19.5 μ m, 2.8mm from the anterior pole). Except at the posterior pole, the capsule of this lens was slightly thicker than that of the younger one.

The lens from the eldest eye, had a thicker anterior capsule, than the younger lenses. The anterior ring of thickening was wider but a similar distance from the anterior pole (2.9 mm, measured in the frontal plane) - slightly further (2.2mm) from the equator than in the younger lenses. The posterior capsule had no discrete peripheral band of thickening, but thinned progressively from the post-equatorial zone to the posterior pole.

b) Thickness of Human Capsules Fixed After Removal from Lens

The thickness variation of eight detached human capsules were measured: one from a twenty-four year old; one from a forty-four year old, and the others (including two anterior

capsules from cataract extractions) from presbyopic subjects, aged 54-72, (Tab. 5:3). The pattern of capsule thickness was similar to that of the whole fixed lenses. The thinnest part of the capsule was always at the posterior pole, the thickest in a band in the anterior and / or posterior periphery. In the twenty-four year old lens, the anterior band was of similar thickness to the posterior, in the forty-four year old the posterior was slightly thicker than the anterior and in older lenses there was only an area of anterior thickening. The anterior polar capsules of the lenses in the seventh decade of life, were thicker than those of the younger lenses. In all the lenses, young and old, the equatorial capsule was the second thinnest zone.

The presence of epithelium and newly formed lens fibres was helpful in estimating the position of the geometrical equator. The variation in posterior capsule thickness can be seen clearly from sections (Fig. 5.13). One problem encountered with the older capsules was a tendency for the posterior and equatorial capsule to delaminate (Fig. 5:14) This was particularly true of material that was fixed more than 48 hours after death; this material was not included in the study.

5:3.3 Lens Shape: With and Without the Capsule.

All five unfixed monkey lenses flattened when the capsule was removed. The shapes of the anterior and

AGE	CODE	SEX	FIX	ANTERIOR		EQUATOR	POSTERIOR	
				POLE	AMAX		PMAX	POLE
12	HW22	F	W*	7	13.5	7.5	13.5	2.2
#35	HW21	?	W	12	19.5	16	22	3
54	HDAN		W*	15.5	24	11	11	3
24	HB4	M	DC	10.5	23.5	16	23.5	2.4
44	HB5	M	DC	12.5	19.5	14	23	2.7
61	HB3	M	DC	16	19.5	5	?6	2
66	HB8	M	DC	17	25	16	?	
67	HB1/2	M	DC	14	19.5	7-14		2
70	HB7	F	DC			7-14	14	2.6
54	KM10		DCX	15	(23)	-		
72	KM11		DCX	8	16	-		

KEY

M = MALE

F = FEMALE

STATE CAPSULE FIXED IN

W = WHOLE EYE FIXED (*AFTER CORNEA REMOVED)

DC = CAPSULE DETACHED BEFORE FIXATION

DCX= ANTERIOR CENTRAL CAPSULE REMOVED AND FIXED (CATERACT
EXTRACTION)

EXACT AGE NOT RECORDED

TABLE 5:3 HUMAN LENS CAPSULE THICKNESS

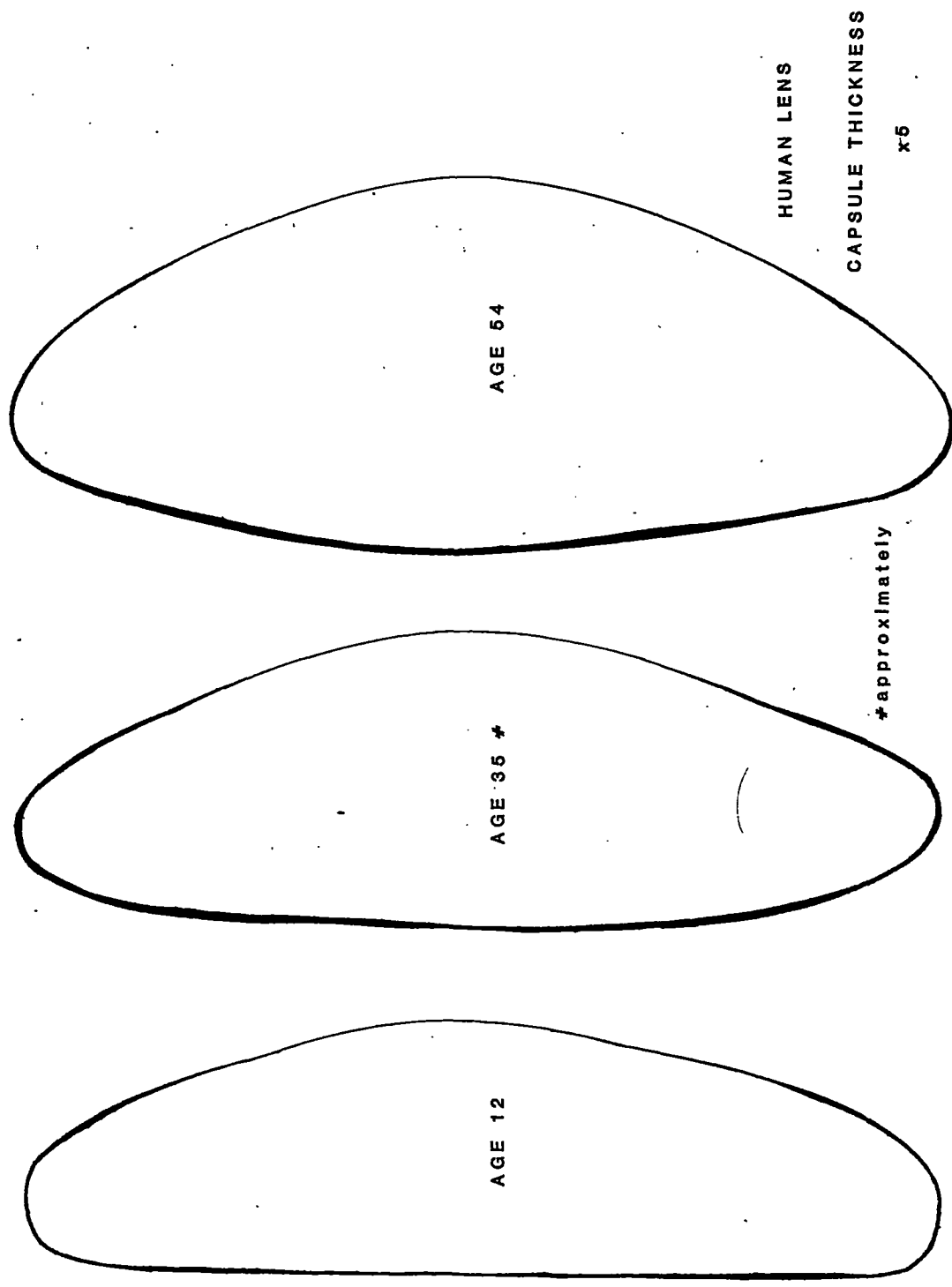


Fig. 5.12 Human Capsular Thickness See legend next page

Fig. 5:12 Scale drawing of capsular thickness (exaggerated x5) of three fixed human lenses, from twelve to fifty four years of age. The anterior lens surface is on the left in each case, the posterior to the right. All the capsules are thinnest at the posterior pole. The youngest lens (which was distorted) has two thickened bands on either side of the thin equatorial capsule, - the anterior band is closer to the polar axis than the posterior thickened band. The equatorial and anterior capsule is thicker in both the older lenses. The post-equatorial capsule, thickened in the younger lenses, is thinner in the fifty-four year old lens.

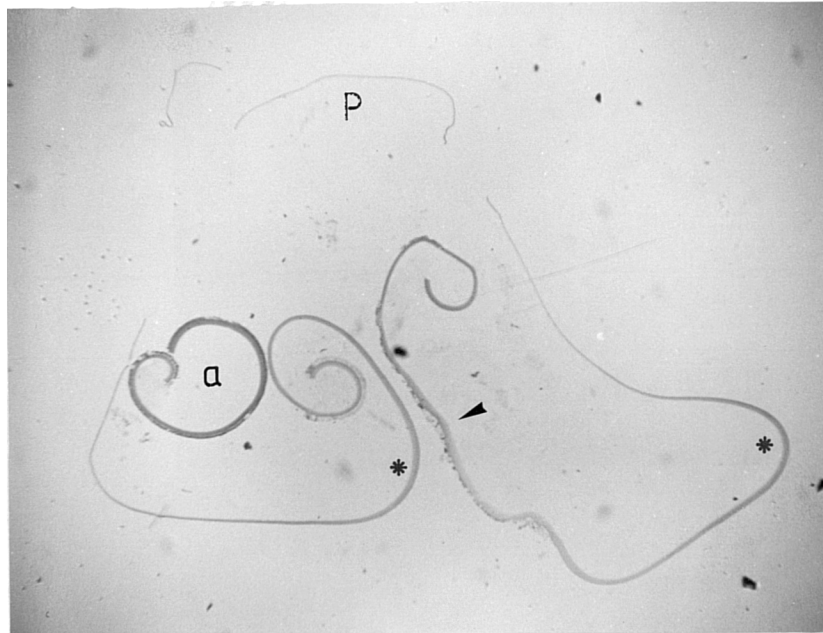


Fig. 5:13 This capsule was fixed after removal from the lens of a twenty four year old man. The posterior and equatorial capsule, pictured here, show a large variation in thickness. The thinnest part of the capsule is at the posterior pole (p), the thickest post (*) and pre-equatorially (not shown). The equatorial capsule (slightly oblique in this picture, arrow) is thinner than most of the anterior capsule (a). x 32

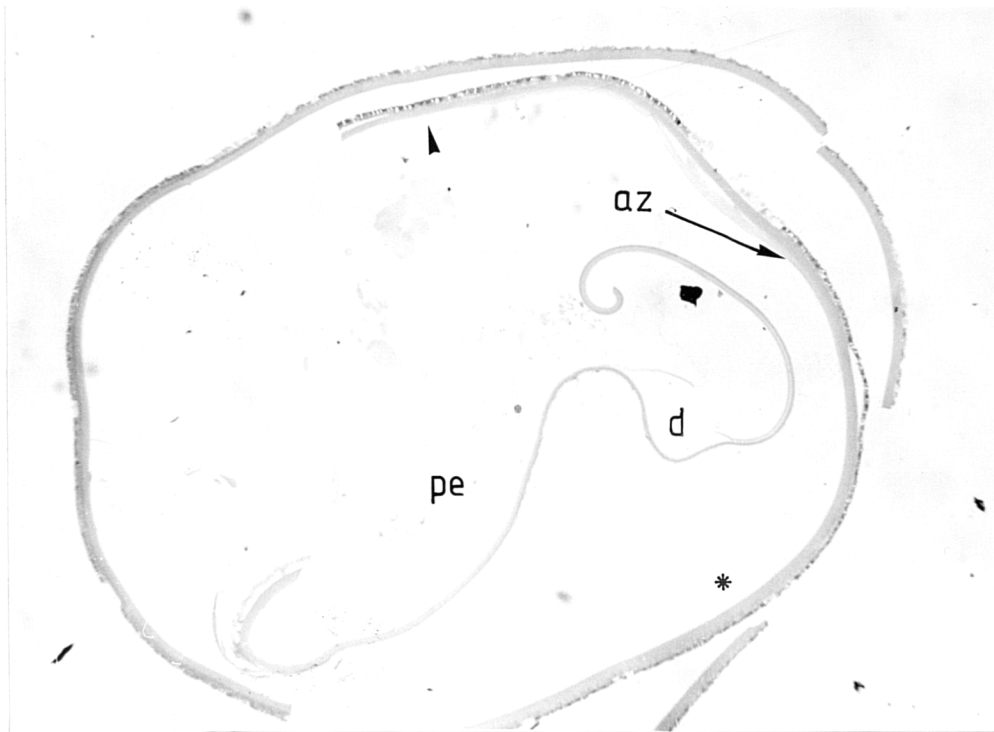


Fig. 5:14 Anterior and post-equatorial capsule (with epithelium) from a sixty-seven year old man, after removal from the lens. The post-equatorial capsule (pe) shows some delamination (d). The capsule is thickest (*) just anterior to the attachments of the anterior zonules (az). x88

posterior surfaces of the lenses both with and without their capsules were analysed (Fig. 5.15 - 5.24). This was in an attempt to isolate the effect of the capsule on the shape of the lens substance. In this unnatural situation, the lens was not subject to the normal effects of zonular tension, or either vitreous or aqueous pressure, but unfortunately the effects of gravity would still have been present, due to the lower specific gravity of the saline over the lenses.

The lens surface profiles were observed to be parabolic whether or not the capsule was in place. Except for the posterior profiles of the three month old and twelve year old before the capsule was removed, all lens profiles showed a correlation (r^2) to a parabola ($Y=A+BX+CX^2$) better than 0.97 for the central area of each surface (Figs. 5.20-5.24, Tab. 5.4 and Tab. 5.6). The central diameter chosen was 6mm in the younger lenses, and 7mm in the two older lenses, representing at least 85% of each curve, after which the correlation to a parabola dropped rapidly, due to the steepening in curvature around the equator. The region of capsular thickening (peaking at 2-2.5 mm from poles in frontal plane) was within the 6/7mm diameter for each lens.

The lens profiles were also matched to spherical curves over a small area where this gave an acceptable subjective fit (Tab. 5.5), so that curvatures could be compared.

The youngest lens was the steepest and smallest, both with and without the capsule. Unlike the older lenses this lens flattened centrally (Fig 5.20) and may have fitted an

Figures 5:15- 5:19

Profiles of unfixed lenses from five monkeys, photographed with the capsule (+C) and decapsulated (-C). The anterior surface is on the left and the posterior surface on the right in each picture. The photographed profiles are displayed in the order given below.

- a) Capsulated lens, the anterior surface was uppermost when this photograph was made, (ignore the flattened posterior profile).
- b) Capsulated lens, to show the posterior profile.
- c) Decapsulated lens, to show the anterior profile.
- d) Decapsulated lens, to show the posterior profile.

x12.1

Fig 5:15 Profiles of the left lens of the three month old cynomolgus monkey.

Fig. 5:16 Profiles of the left lens of the eleven month old monkey.

Fig. 5:17 Profile of the left lens of the twelve month old monkey.

Fig. 5:18 Profile of the left lens of a ten year old monkey.

Fig. 5:19 Profile of the right lens of a twelve year old monkey.

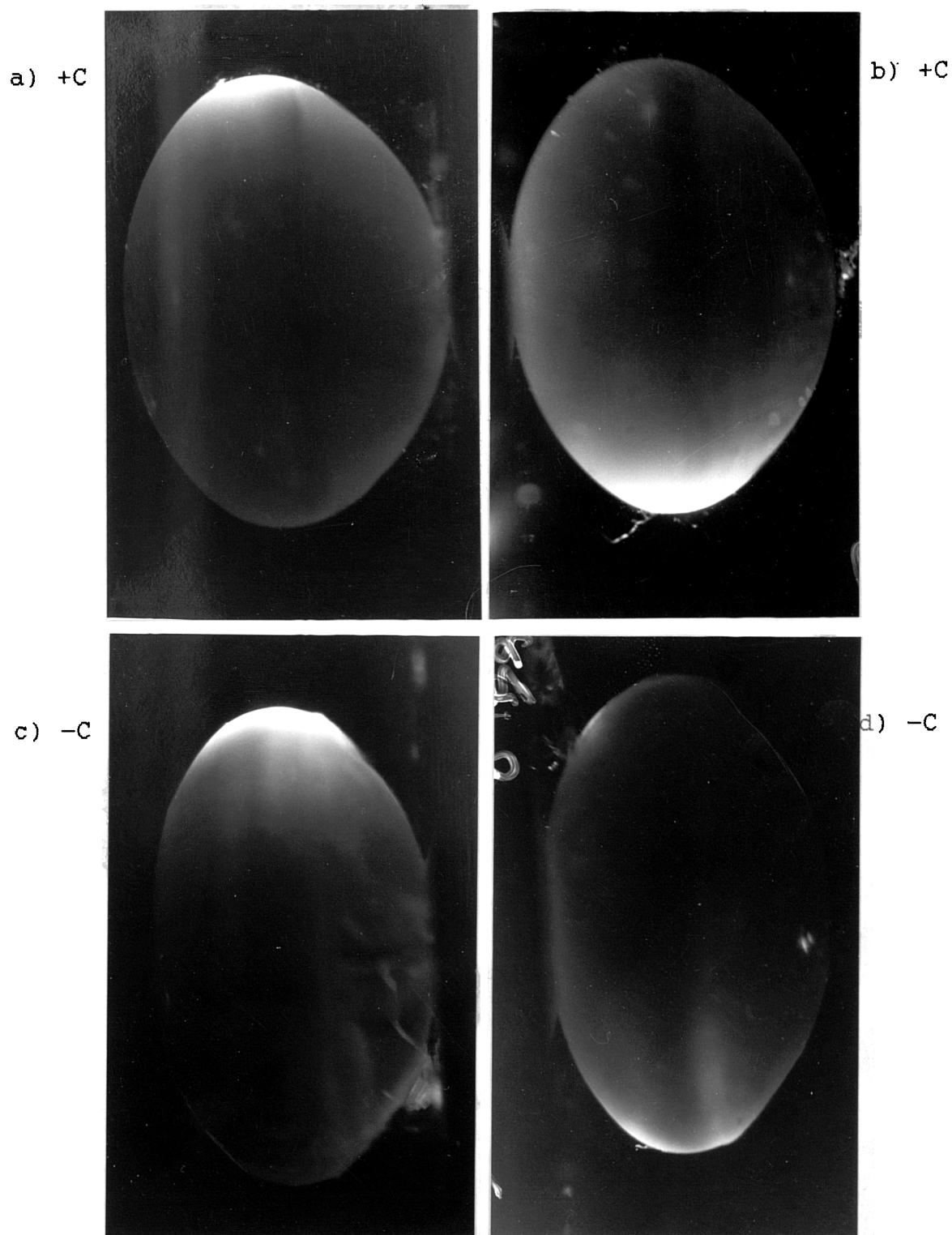


Fig. 5:15 Profile of left lens of 3 month old monkey.
See legend on previous page.

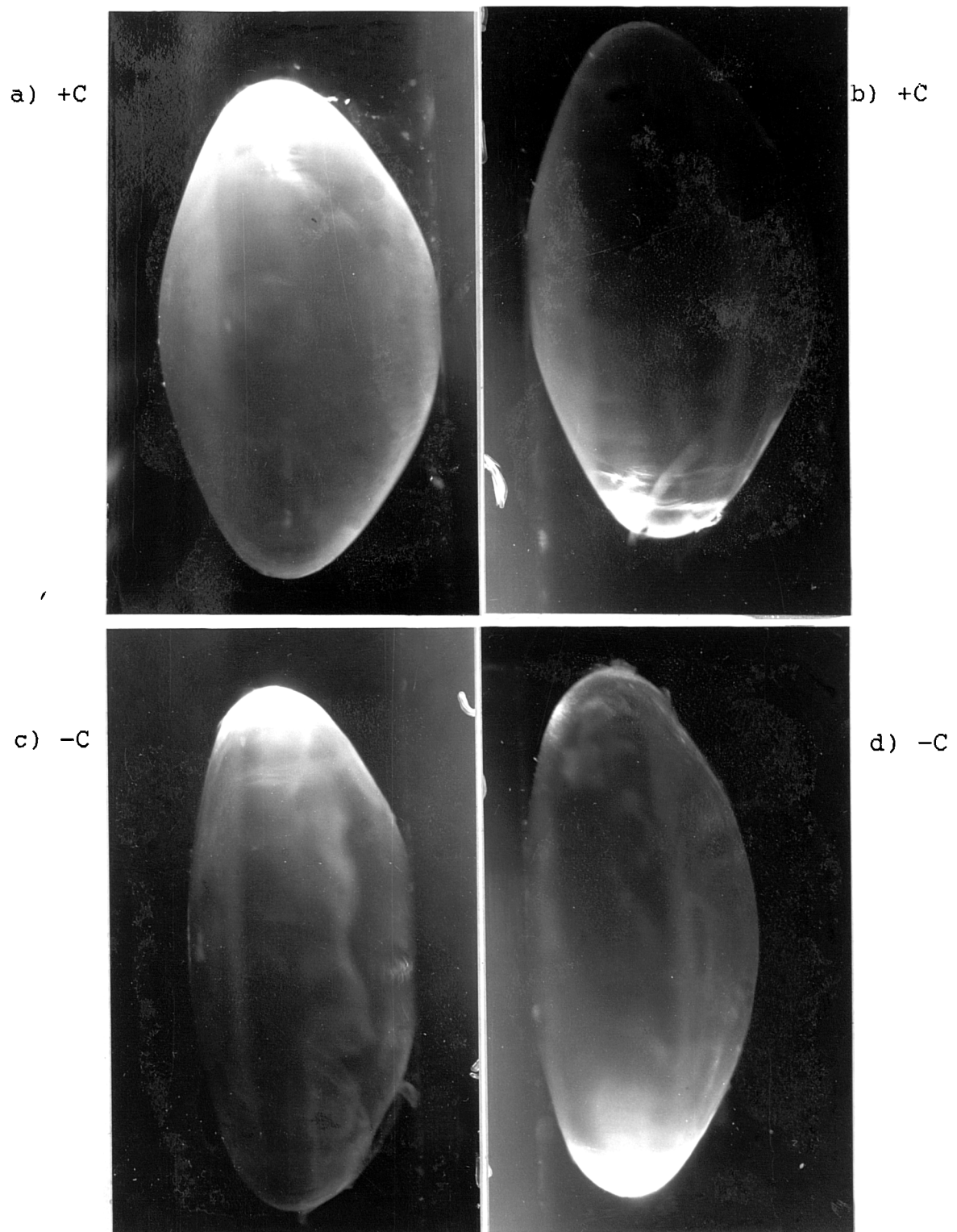


Fig. 5:16 Profile of left lens of 11 month old monkey.
See legend on page preceding Figure 5:15

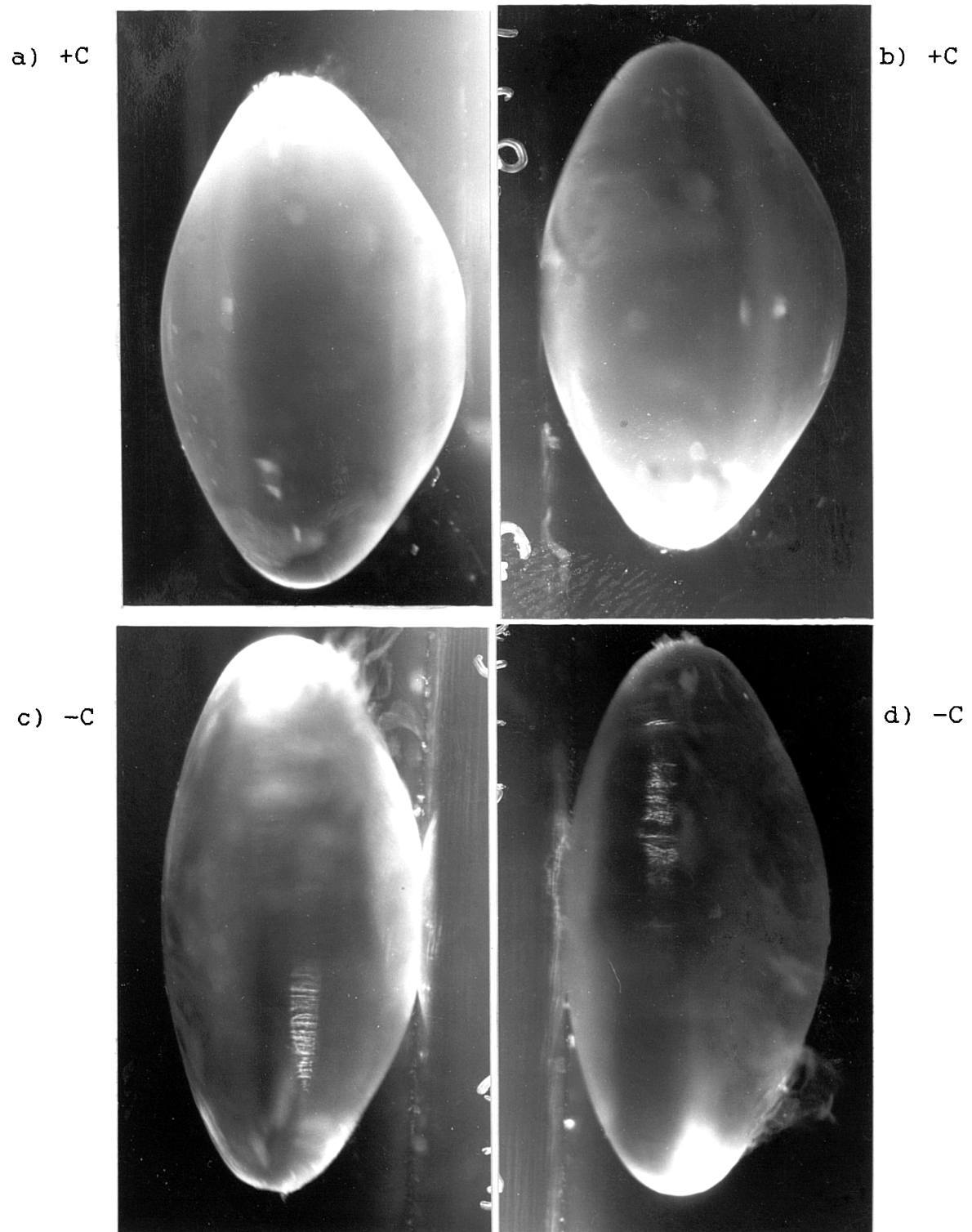


Fig. 5:17 Profile of left lens of 12 month old monkey.
See legend on page preceding Figure 5:15

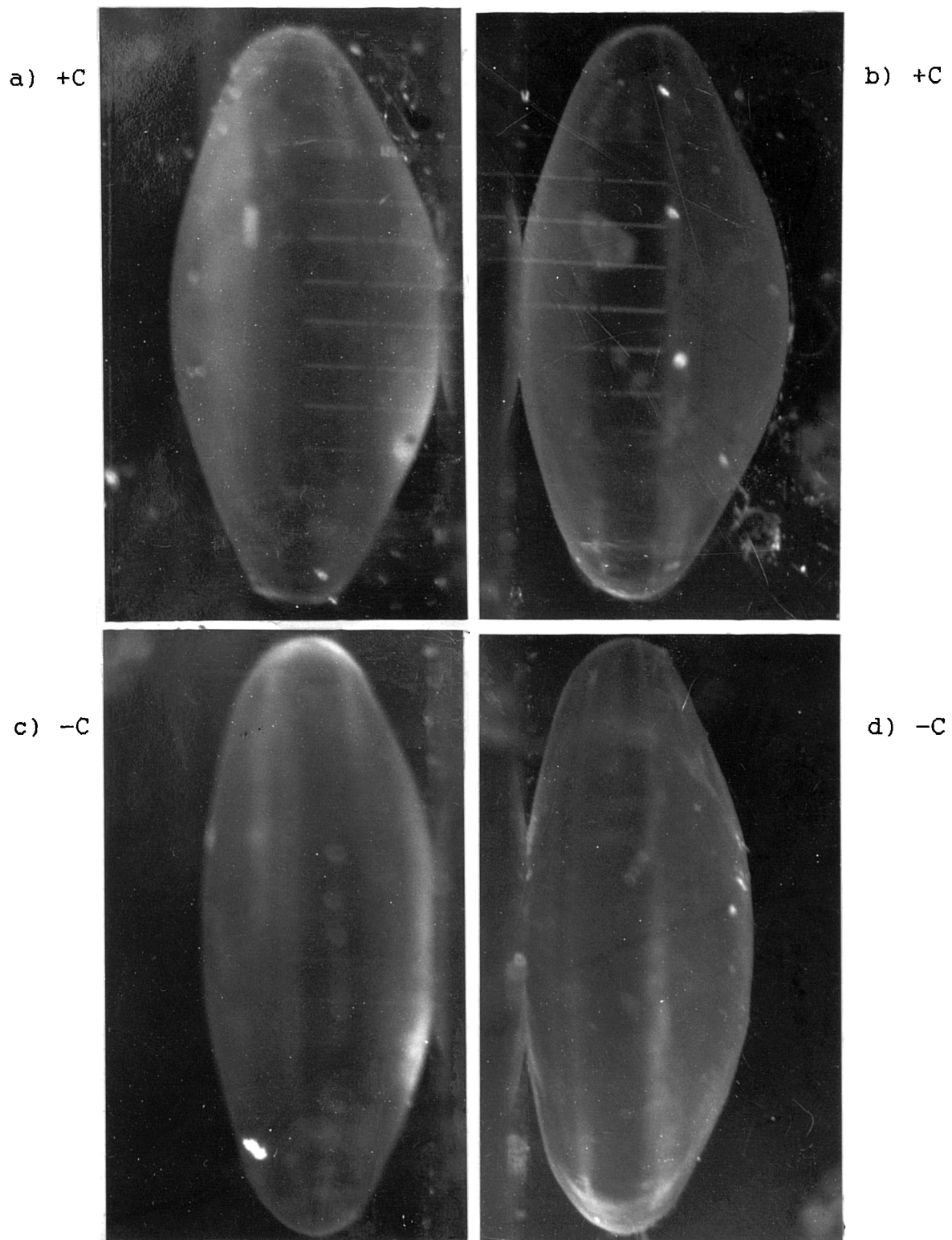
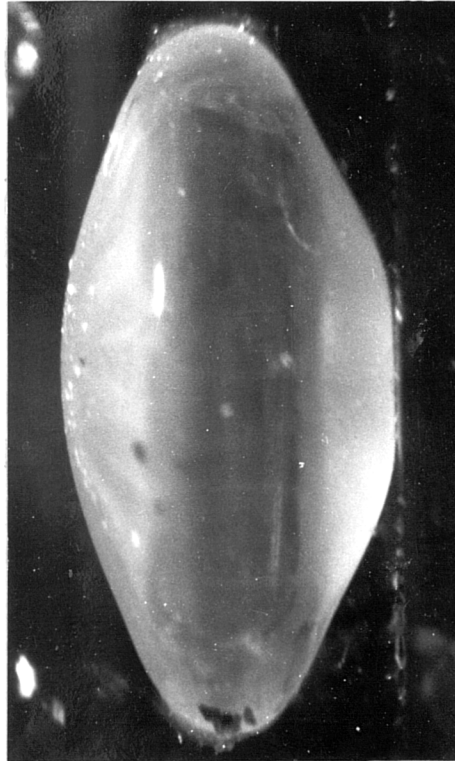


Fig. 5:18 Profile of left lens of 10 year old monkey.
See legend preceding Figure 5:15

a) +C



b) +C



c) -C



Fig. 5:19 Profile of right lens of 12 year old monkey.
See legend preceding Figure 5:15

Figures 5:20 - 5:24

Plotted profiles of the five monkey lenses, with the capsule (red) and without (blue), to show the correlation of the best fitting parabola. The anterior profile (A) is above the abscissa, the posterior (P) mostly below it. The correlation to a parabola was high for a diameter of up to 6mm in the three youngest lenses (Figs. 5:20 -22), and up to 7mm in the older lenses (Fig. 5:23-24)

Fig. 5:20 Profiles of the left lens of the 3 month old monkey, both with and without the capsule.

Fig. 5:21 Profiles of the left lens of the eleven month old monkey, both with and without the capsule.

Fig. 5:22 Profiles of the left lens of the one year old monkey, before and after decapsulation.

Fig. 5:23 Profiles of the left lens of the ten year old monkey, before and after decapsulation.

Fig. 5:24 Profiles of the right lens of the twelve year old monkey, before and after decapsulation.

LENS SHAPE AGE 3 MONTHS [LEFT]

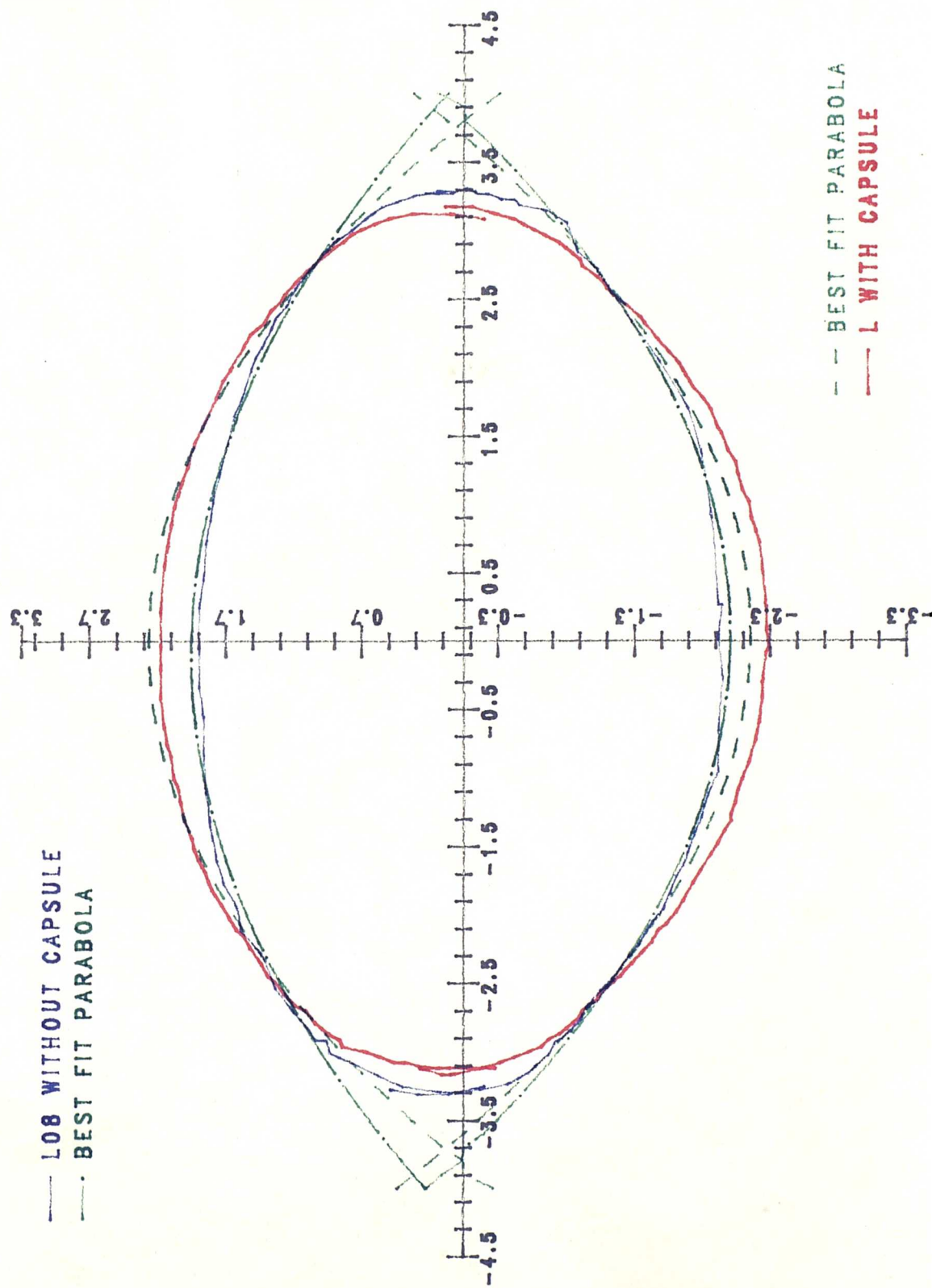


Fig. 5.20 Lens Profile Before and After Decapsulation

LENS SHAPE AGE 11 MONTHS [LEFT]

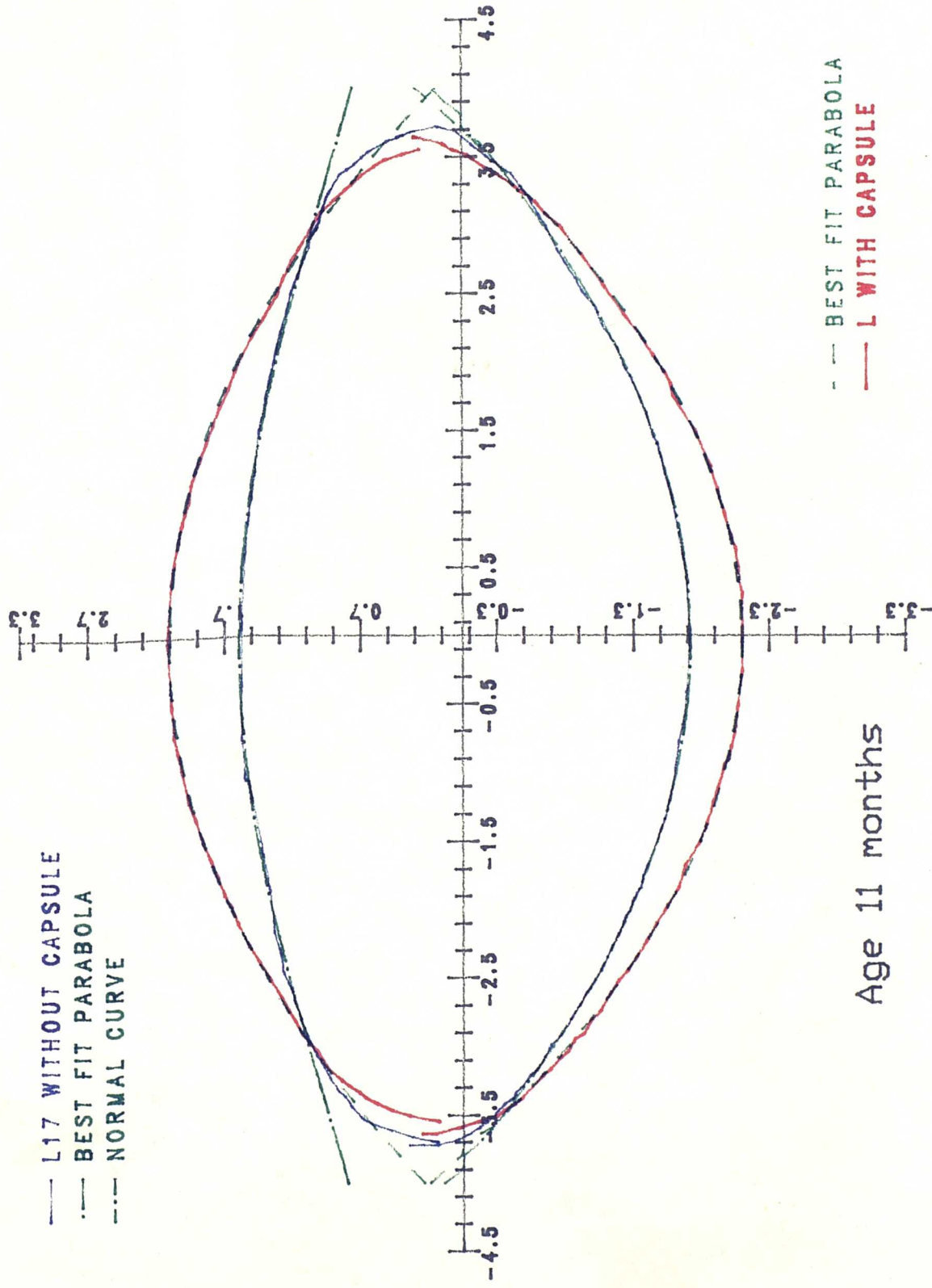


Fig. 5.21 Lens Profile Before and After Decapsulation

LENS SHAPE AGE 1 YEAR [LEFT]

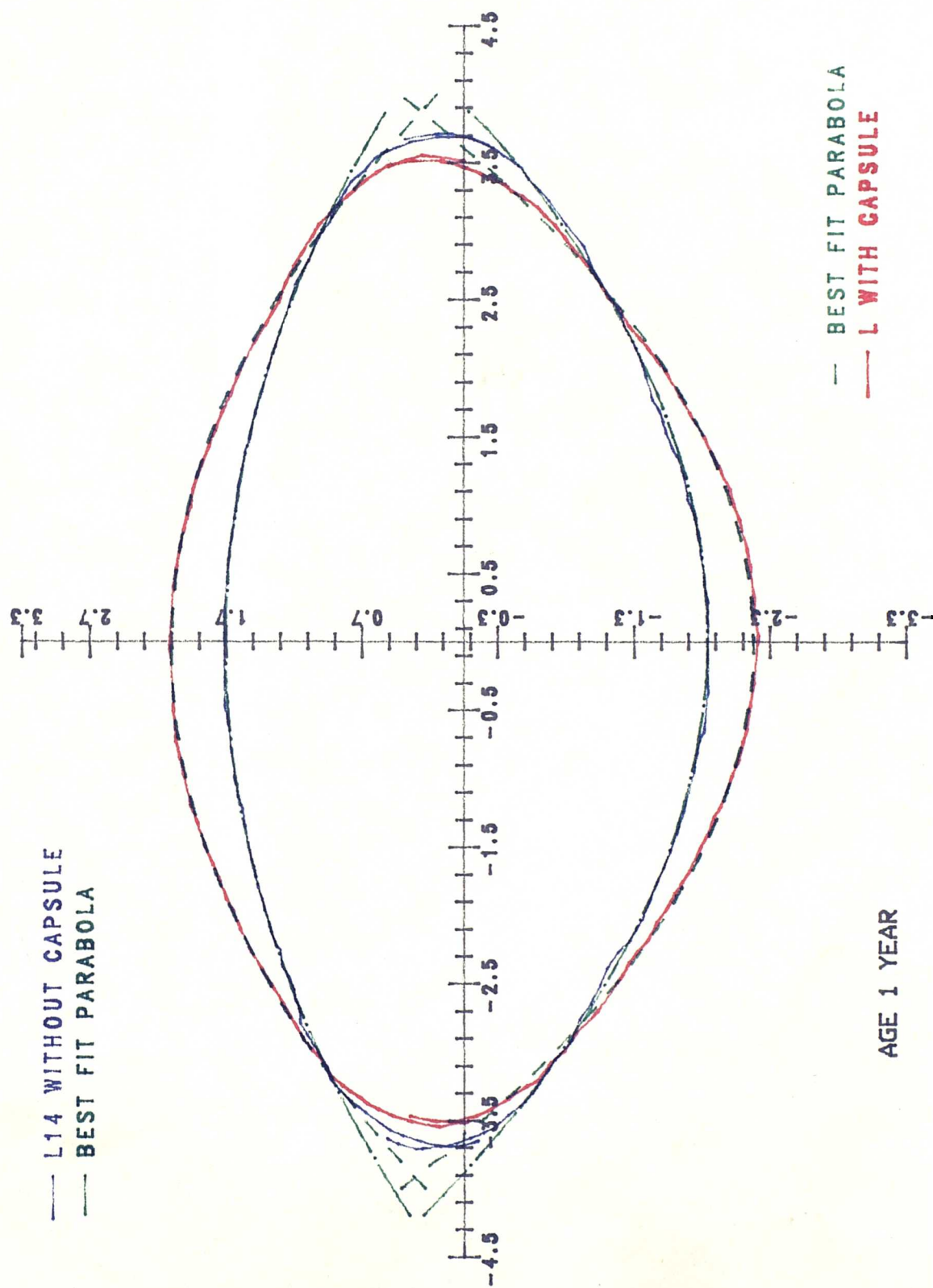


Fig. 5.22 Lens Profile Before and After Decapsulation

LENS SHAPE AGE 10 YEARS [LEFT]

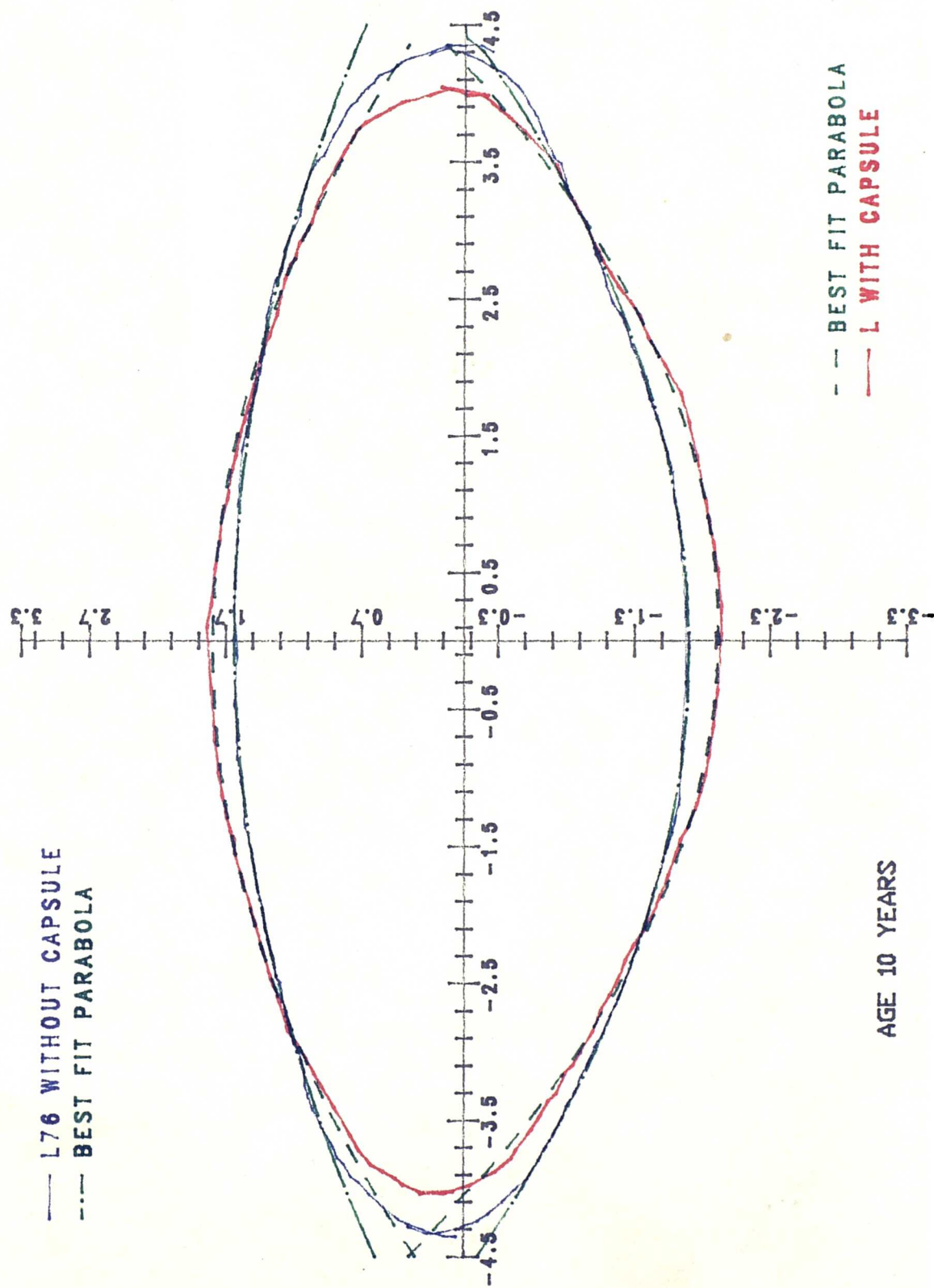


Fig. 5.23 Lens Profile Before and After Decapsulation

LENS SHAPE AGE 12 YEARS [RIGHT]

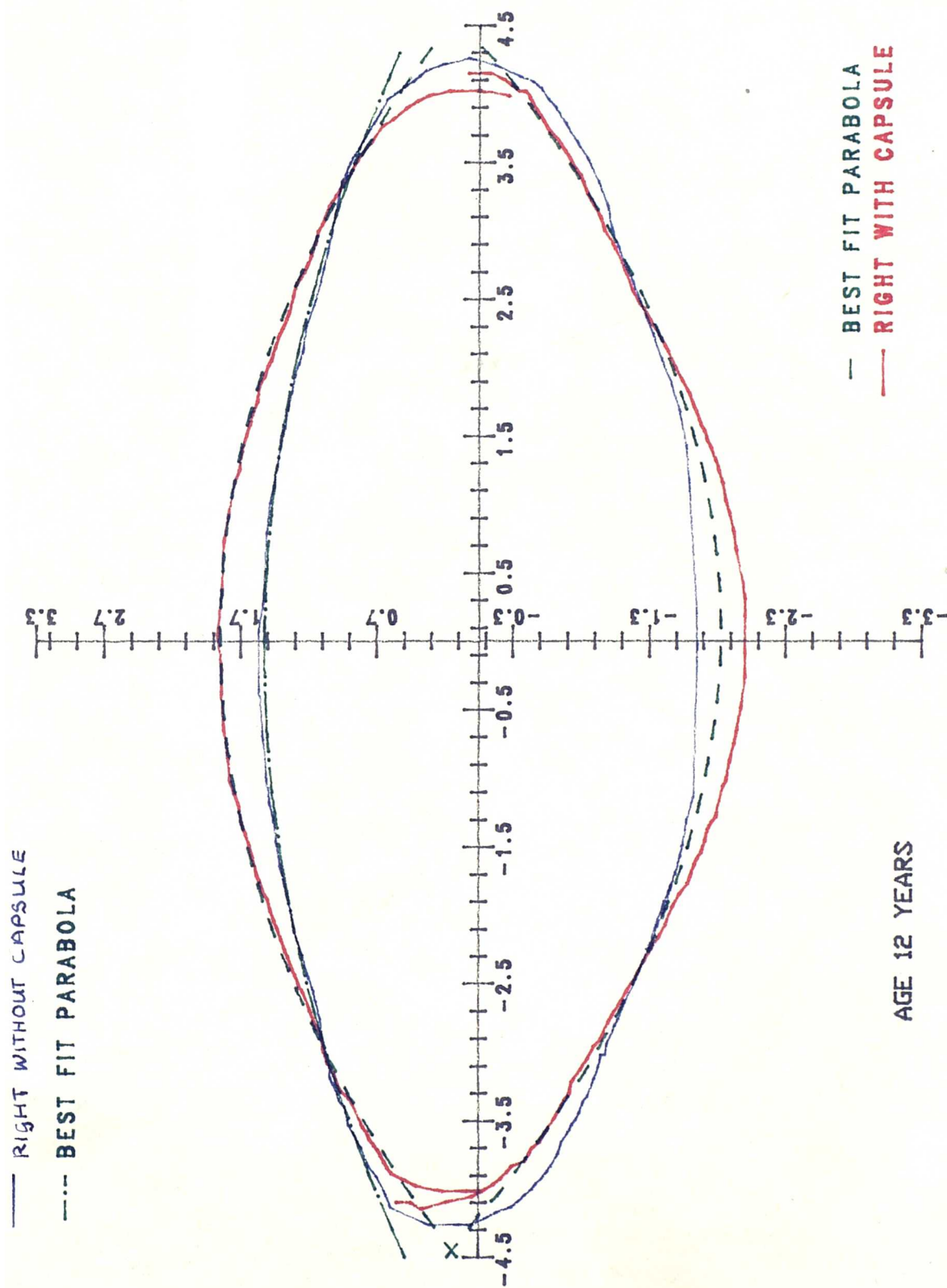


Fig. 5.24 Lens Profile Before and After Decapsulation

CODE	AGE	KG	STATE	SURFACE	CORRELATION PARABOLA	BEST FIT CURVE. CORRELATION
MPL08	3/12	0.84	+C	POST	*0.4753	CAUCHY 0.78953
				ANT	*0.9857	PARABOLA
MPL08			-C	POST	*0.9872	PARABOLA
				ANT	*0.9707	PARABOLA
MPL17	11/12	1.7	+C	POST	*0.9989	PARABOLA
				ANT	*0.9976	PARABOLA
			-C	POST	*0.9990	PARABOLA
				ANT	*0.9903	PARABOLA
MPL14	1	1.4	+C	POST	*0.9971	PARABOLA
				ANT	*0.9977	PARABOLA
			-C	POST	*0.9936	PARABOLA
				ANT	*0.99753	PARABOLA
MPL76	10	7.6	+C	POST	#0.9971	PARABOLA
				ANT	#0.9977	PARABOLA
			-C	POST	#0.9962	PARABOLA
				ANT	#0.9948	PARABOLA
MPR53	12	5.3	+C	POST	#0.41163	CAUCHY 0.8765
				ANT	#0.9738	NORMAL 0.9891
			-C	POST		
				ANT	#0.9869	NORMAL 0.9945

*correlation for central 6mm only

#correlation for central 7mm only

TABLE 5.4 DISLOCATED LENS SHAPE WITH CAPSULE AND AFTER
DECAPSULATION

FOR NEAREST SPHERICAL CURVE, SEE OVERLEAF

MONKEY	AGE years	STATE	CENTRAL RADIUS mm	FIT DIAMETER mm
ML08	3/12	+C P	3.33	5.2 S
		A	4.04	4.67 S
		-C P	(5.1)POOR	[3mm] S
		A	5.55	4.2 S
ML17	11/12	+C P	3.55	3.8 F
		A	4.22	5.1 F
		-C P	4.66	4.7 F
		A	8.88	5.8 S
ML14	1	+c P	3.11	3.8 F
		A	4.22	4 F
		-C P	4.66	4.7 F
		A	6.66	6.2 S
ML76	10	+C P	4.44	4.7 F
		A	6.66	4.9 -
		-C P	6.66	5.8 F
		A	9.33	5.4 S
MR53	12	+C P	4	4 F
		A	5.55	4.22 F
		-C P	aprox 6	
		A	8.9	5.33 -

KEY P = POSTERIOR SURFACE [CENTRAL]
A = ANTERIOR SURFACE [CENTRAL]

F = SURFACE FLATTENS AFTER DIAMETER IN COLUMN 6
S = SURFACE STEEPENS AFTER DIAMETER IN COLUMN 6

+C = SHAPE WITH CAPSULE -C = SHAPE AFTER DECAPSULATION

TABLE 5:5 LENS SHAPES WITH AND WITHOUT CAPSULE
(BEST FIT SPHERE)

AGE	SURFACE	A	B	C	R
3/12	P +C	(2.1042	0.0142	0.1584	0.4745)
	A +C	2.3143	0.0058	0.1597	0.9857
	P -C	1.9557	0.0097	0.1365	0.9864
	A -C	2.0011	0.0204	0.1129	0.9786
11/12	P +C	2.0494	0.0136	0.1464	0.9989
	A +C	2.1508	0.0125	0.1195	0.9976
	P -C	1.6708	0.0106	0.1155	0.999
	A -C				
12/12	P +C	2.1275	0.0024	0.1626	0.9971
	A +C	2.1508	0.0125	0.1195	0.9976
	P -C	1.7904	0.0061	0.1169	0.9936
	A -C	1.7555	0.0043	0.0779	0.9975
10yr	P +C	1.8663	0.0139	0.1087	0.9942
	A +C	1.8458	0.0049	0.0748	0.9946
	P -C	1.6474	0.0114	0.0789	0.9962
	A -C	1.6876	0.0089	0.0495	0.9946
12yr	P +C	(1.7737	0.0155	0.0957	0.4116
	A +C	1.8978	0.0081	0.0840	0.9738
	P -C	(Not Analysed)			
	A -C	1.572	0.050	0.0523	0.9869

KEY

P = POSTERIOR

+C = WITH CAPSULE

A = ANTERIOR

-C = DECAPSULATED

R = CORRELATION TO A PARABOLA $Y=A+BX+CX^2$

Table 5:6

EQUATIONS OF BEST FIT PARABOLA TO CENTRAL LENS SURFACES

ellipse better than the curves available in the computer programme.

The lens shapes of the 11 and 12 month old monkeys were similar, each giving a correlation to a parabola of >0.99 . On decapsulation, both lenses flattened centrally and the posterior surface steepened slightly peripherally (Fig 5.21 and 5.22).

The two older lenses also showed similarities in their profiles to each other. Unfortunately one of the photographs was not available (12 year old, posterior surface decapsulated) and so cannot be accurately compared. The ten year old lens (in common with the 11 and 12 month old lenses) showed central flattening and posterior peripheral steepening after decapsulation.

The anterior periphery flattened slightly on decapsulation in the eleven month old and ten year old lenses and remained similar in the others.

All capsulated lenses showed significant distortion after immersion in fixative (Figs. 5.25 & 26), and was most marked in the youngest lens. Because of the distortion, fixation induced shrinkage was not readily assessed, but the maximum overall reduction in diameter of the lenses was under 3%. The fixed nucleus of the youngest (3 months old) lens took on a very unnatural dumb-bell shape, with both anterior and mild posterior central dimples (Fig. 5.25)! The distortion shown by the older lenses after fixation was similar, although worse, to the distortion seen in the dislocated lens MR78 used in the last chapter. It can only



Fig. 5:25 Profile of the capsulated right lens of the 3 month old monkey after fixation was very distorted.

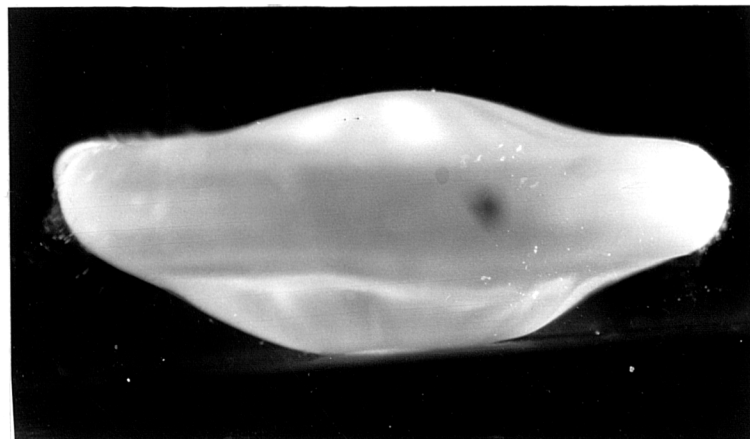


Fig. 5:26 The profile of the capsulated lens from the right eye of the eleven month old monkey was also distorted. Compare this with the profile of the unfixed left lens shown in Fig. 5:16

be concluded that the fixative used caused distortion and was worst in the lenses not supported by the zonules.

5.4

DISCUSSION

Capsule Thickness in the monkey

Little was known of the variation in capsular thickness in the monkey lens before this study began. Fincham (1929) measured the thickness of the anterior capsule in several primates of unrecorded age and found a zone of thickening in the anterior mid periphery. This was similar to that reported here in the cynomolgus monkey. He related this to the conoidal form of the accommodated lens in primates, suggesting that the mid-peripheral anterior flattening in the accommodated form was a result of the thickened capsule in that location.

A similar thickened ring of anterior capsule was present in all but one of the twenty one monkey lenses investigated in the present study, and a posterior ring of even greater thickening in each lens. The posterior thickened ring was closer to the equator and between 50 and 150% thicker than that of the anterior ring. Fincham's method did not allow him to measure the thickness of the posterior capsule.

Capsules were examined fixed both in situ with the tension imposed by the enclosed lens substance and isolated, - without any intended tension, allowing them to attain an

unstretched state. The anterior capsule showed little difference in thickness between the two states. Both the equatorial (including the para-equatorial posterior and anterior points of minimal thickness) and the peripheral posterior capsule was thinner in the in situ state than when isolated, suggestive of tension-induced stretching in these locations.

The central posterior capsule was the thinnest zone (2 μ m) in all 23 lenses. The second thinnest zone was at the equator, except in the two oldest monkeys once the capsule was detached. The thickest capsular zone was in the posterior periphery (20 - 64 μ m depending on state and age) in every lens.

The equatorial and para-equatorial capsule, including the posterior thickened zone, thickened after detachment from the lens. These regions were also slightly thicker in the accommodated state compared with the unaccommodated perfuse-fixed lenses. Although no comment can be made on changes in anterior capsule thickness in accommodation, perhaps this indicates some local para-equatorial capsular moulding.

The posterior capsule, was of comparable thickness in all animals, whilst the anterior and equatorial capsule showed an age related thickening.

Capsule Thickness in Man

Eleven single human capsules in differing states were

sectioned and the thickness measured. Only three were from subjects under forty. This is a very small sample, in view of the variation between individuals of similar age reported by Salzmann (1912).

In common with earlier studies (Salzmann, 1912; Fincham, 1925; Fisher and Pettet, 1972; Seland, 1974), the central posterior capsule was the thinnest zone (2-3^{mm}). Contrary to Fisher and Pettet's (1972) findings in unfixed human capsules, the equator was not the thickest zone in any of the lenses examined. Findings were similar to those of Salzmann (1912) and Fincham (1937), who reported two thickened annular zones concentric to the equator, one on each surface. This was so in the four youngest lenses (aged 12 - 44, the posterior ring was marginally thicker in two of the lenses and equal to the anterior in the other two), but only the anterior thickened ring was found in the older capsules. These thickened rings lay on the axial side of the zonular insertions, the posterior ring was closer to the equator than the anterior, a point also in agreement with Salzmann. Fisher and Pettet (1972) found no evidence of peripheral thickening in pre-presbyopic lenses. <

All the human eyes received were single eyes, not pairs, so it was not possible to compare the thickness variation of the capsule in the detached and in situ state in one individual. Consequently, the effects of detachment on capsule thickness are difficult to isolate from the normal variation between individuals.

Experiments were designed to investigate capsular thickness variation in differing states. This was to explore the possible causes of the discrepancy between the classical findings (Salzmann, 1912; Fincham, 1929), and those of Fisher and Pettet (1972). There are two main differences in technique used to measure capsular thickness. Fisher and Pettet, in an attempt to avoid fixation artefacts, examined fresh unfixed detached capsules. Earlier workers would almost certainly have used some fixative (although details are not given) before sectioning their lenses. Unlike their predecessors, Fisher and Pettet removed the capsules from the lens. Although it cannot be ruled out, it seems unlikely that fixation could cause localised thinning of the capsule at the equator and thickening close to it. The notion that the difference in findings was due to detachment of the capsule was unsupported by the findings here, and has important implications on the current capsular theory of accommodation (Fisher, 1988).

The sample of young human lenses here is too small, - to discount Fisher and Pettet's findings completely. Only two detached capsules (of 24 and 44) were examined from subjects of an age usually able to accommodate, and one of these barely so. It is, however, possible that their findings were subject to error: to remove the elastic capsule from the lens they cut around the equator, - the very region where their results differ from classical studies. It is possible that the cut edge curled up slightly, or perhaps the results were affected by capillary attraction.

Whatever the reason for the discrepancy, Fisher and Pettet discarded Fincham's theory of capsular moulding and substituted a modified theory, of equatorial circumferential force, which is now in question in the light of the early and present findings.

Comparison between Capsule Thickness in Man and Monkey

In both monkey and man the thinnest part of the capsule was at the posterior pole. In neither, was the equator the thickest zone. Thickened annular zones were found in both the human lenses under fifty years of age, and the monkey lenses (all of pre-presbyopic age). However the posterior ring showed greater thickening in the monkey, and was slightly closer (relatively) to the polar axis than in man.

Fisher and Pettet (1972) and Salzmann (1912) reported an increase in anterior capsular thickening with age in man. From the small sample of monkeys of known age, this appeared to be also true in the monkey, although there is evidence for capsular growth in all areas overlying the epithelium. It is possible that the apparent reduction in the thickness of the monkey posterior mid-peripheral thickened ring in the unstretched state, is a consequence of increasing posterior capsular length, with age, in an area with no epithelium to maintain capsular growth.

Though the number of human capsules examined in the detached state was too small to challenge Fisher and Pettet's (1972) data effectively, the absence of equatorial

thickening in the in situ human capsules and those of the monkey, adds weight to the observed lack of equatorial thickening in the few human lenses examined. Although there are known differences in some details of accommodation between the two species (Kaufmann et al., 1982; Bito et al., 1982; Koretz et al., 1988a), radical differences in the mechanism would be surprising.

Lens Shape in the Monkey

With the capsule in place, both surfaces (of the four older lenses) showed the classical conoidal form: - steep centrally, with relative peripheral flattening, followed by steeper curvature around the equator.

On decapsulation, both anterior and posterior profiles flattened centrally. A parabolic form was identified in both states.

The shape changes of the posterior and anterior mid-peripheral surfaces was of greatest interest due to putative local capsular moulding (Fincham, 1937). The posterior mid peripheral surface was slightly steeper after decapsulation in all but the youngest lens (which showed less mid peripheral flattening in the capsulated state). The anterior mid-peripheral surface showed no consistent change.

The shape change, to greater central steepening with greater peripheral flattening in the accommodated state, has been observed in man on the anterior lens surface (Tscherning, 1909; Fincham, 1937; Brown, 1973a). This centrally steepened/peripherally flattened accommodated

shape change will be referred to as a 'lenticonus'.

A parabaloid is steepest centrally, and progressively flattens peripherally. A lens where both surfaces are parabolic (around the polar axis), except close to the equator could fit the description of a lenticonus form, except that whilst the central curve steepens with accommodation, the mid-peripheral curve flattens. It is possible for a lens displaying a "lenticonus" in the accommodated state, to have a lens profile still showing a high correlation to a parabola. This was demonstrated in the profile of the 29 year old human lens, photographed by Brown (1973a) which displayed an accommodative lenticonus as defined above, but still showed a high correlation to a parabola (Koretz et al., 1984).

If the two lens states investigated here (capsulated and decapsulated) are compared to the accommodated and unaccommodated states, it can be seen that all the lenses (other than the 3 month old) display a posterior lenticonus, that is,- there was actual steepening of the peripheral region of the profiles after removal of the capsule.

The question arises as to whether the ring of marked posterior capsular thickening, described earlier, could be related to the formation of the posterior lenticonus.

Lens shape was compared (5:3.1c) in two different states,- capsulated and decapsulated, neither of which occurs naturally. The first state was used in an attempt to

isolate the affect of the intact elastic capsule on the shape of the lens substance. The second, recorded the shape of the decapsulated lens fibre substance, in the absence of all normal external forces acting upon it.


The youngest pair of lenses investigated (age 3 months) showed no lenticonus, in the capsulated state, but showed a posterior ring of very marked capsular thickening. This finding would seem to invalidate the notion (Fincham, 1937) that the capsule provides localised moulding of the lens shape dependent on its thickness. However, the thickness of this capsular ring changes less after removal from the lens, in the older animals, suggestive perhaps of a change in the elastic interaction between capsule and lens substance. So whilst the thickened capsular ring of the three month old does not cause a local flattening in the youngest lens, it cannot be completely ruled out that it may perhaps contribute to the lenticonus in older monkeys. A mathematical analysis of the elastic interaction of capsule and lens substance is beyond the scope of this study.

Fisher and Pettet (1972) rejected Fincham's (1937) notion of local capsular moulding because they failed to find annuli of capsular thickening on either side of the equator.

Brown (1973a) suggested that the lenticonus observed in the adult human accommodated lens was due to the unthickened cortex moulding around the axially thickened nucleus. Koretz et al. (1988a) reported a similar greater nuclear action in

the Rhesus monkey. The lenticonus observed in the capsulated state (this study), may also be caused by greater nuclear than cortical axial thickening.

In the decapsulated state, the lens surfaces are flatter centrally, and there is less evidence of a lenticonus. If the nucleus was capable of expressing an independently steeper shape, it does not do so in the absence of the capsule, suggesting that the nucleus steepens as a result of capsular persuasion rather than capsular release.

According to the findings on capsular thickness reported here, Fincham's (1929, 1937) hypothesis of differential capsular moulding appears to have been rejected by Fisher and Pettet (1972) for an invalid reason, raising again the possibility that the bands of capsular thickening reported in the posterior periphery in the cynomolgus monkey, may influence the formation of the accommodative lenticonus. Since almost perfect parabolic profiles ^{was} observed in both  attached and detached states, the true lenticonus was small. The absence of a lenticonus shape in the youngest capsulated lens exhibiting the greatest difference in posterior capsular thickness, together with Fisher's (1969b) calculation that the capsule was too weak to exert the force required to induce a conoidal shape in the human lens, suggest that the lenticonus has some other explanation.

The hypothesis that the capsule acts like an elastic circumferential girdle around the lens equator (Fisher and Pettet, 1972) is now clearly called into question, since the

capsule is thin in this location in the cynomolgus monkey.

There is little doubt that the elastic capsule provides the force to reshape the elastic lens substance in accommodation. It is not yet clear if the thickened annular bands may, by local capsular moulding, contribute to the lenticonus form of accommodation.

CHAPTER SIX

DISCUSSION AND CONCLUSIONS

The present investigation of lens fibres, profiles and the capsule, was undertaken in an attempt to increase understanding of the lenticular mechanism for accommodative shape change.

Difference in whole lens shapes in fresh capsulated and decapsulated lenses leaves little doubt that the elastic lens capsule is responsible for initiating shape changes. It therefore has the role of redirecting the force from the ciliary muscle and the zonules to the lens (Helmholtz, 1909; Fincham, 1937; Fisher and Pettet, 1972; Coleman, 1986; Koretz and Handelman, 1988).

The manner in which the capsule redirects the zonular force and how the lens reacts to this force at fibre level is the subject of discussion.

Evidence presented here rejects the notion of sliding between lens fibres, but supports the hypothesis of cytoplasmic flow proposed by Gullstrand (1909).

Having found the thickest part of the young human capsule to be around the equator (perhaps erroneously) Fisher and Pettet (1972) rejected Fincham's (1937) capsular theory of accommodation and suggested a hypothesis of circumferential capsular pressure. These authors are alone in finding the maximum thickness of the capsule at the

equator and their results are rejected here in favour of the earlier data of Salzmann (1912) and Fincham (1937).

Fisher and Pettet's measurements had the virtue of being obtained from unfixed material but their method suffers from poor visibility of the capsule, necessitating indirect thickness measurements. Fixation was used in this as in the other studies predating Fisher and Pettet's work, with the precaution of fixing *in situ* (in accommodated and unaccommodated lenses) and after removal from the lens. In each case the results were comparable, reducing the validity of the criticism that fixation produces significant artefacts.

Fincham's (1925) findings, and the results reported here, are similar to those of Salzmann (1912) - in neither monkey nor human lenses was the thickest part of the capsule at the equator, so there is little evidence to support the Fisher and Pettet hypothesis of circumferential capsular pressure when the zonule is released.

Fincham (1937) found the thickest part of the capsule located anterior and posterior to the equator, where surface flattening occurs in accommodation. He therefore attributed the conoidal profile of the lens in accommodation to local capsular moulding. Fincham's notion was rejected by Fisher (1969b) who calculated that the force required to tear the human capsule was less than that required to achieve a conically deformed lens shape as determined theoretically by O'Neill and Doyle (1968). Since the capsule breaking force

was less than the minimum moulding force, the conoidal shape could not be a consequence of local capsular moulding. The writer is not in a position to criticise their data but the fact that greatest capsular thickness, close to the area of flattening is confirmed, reopens the discussion.

Fincham found greatest peripheral flattening in accommodation and thickest capsule on the front surface of the lens in man. In monkey these parameters again coincide but at the posterior surface, although the anterior surface demonstrates a similar coincidence (second thickest capsule zone with anterior flattening). However the lack of a lenticonus in the youngest monkey examined in this study, with marked post-equatorial thickened capsular ring, is inconsistent with Fincham's notion of local capsular moulding.

Brown (1973a) discovered that in human accommodation, the nucleus thickens axially more than the cortex, and attributed the conoidal lens shape (or lenticonus) to the cortex moulding around the bulging nucleus. This pattern of greater nuclear axial thickening was also observed in the monkey (Koretz et al., 1988b).

The elastic properties of the human lens substance changes with age (Fisher, 1971, 1988). In the very young (and the old presbyopic lens), the elastic properties of the lens nucleus and cortex are similar. However in the cortex, the Young's Modulus increases during the accommodative years (Fisher, 1971), whilst in the nucleus changes occur only after the fourth decade of life. This is not only consistent

with Brown's finding of greater nuclear axial thickening in accommodation, but with Brown's finding that the 'lenticonus' was most marked around the age of thirty when the elastic properties of the nucleus and cortex are least similar.

There is support here also (chapter 4) for the notion of greater nuclear 'shape' change in accommodation. There is more evidence of cytoplasmic flow in the nucleus than in the intermediate and cortical zones based on the use of drug treated and dislocated lenses to simulate the accommodated state. The shape of the thicker nuclear lens fibres appears to be more suitable to allow fluid flow within the fibres than the thin fibres of the cortex, with their irregular cell borders and almost non-existent short faces. Cortical fibres have a liberal covering of interdigitating ball and sockets which give the cell membranes such an irregular appearance. These ball and sockets are most prolific in fibres beneath the zonules and are also roughly coincident with the flattened zone and the thickened capsule (Fig 3:8). If ball and sockets frustrate cytoplasmic flow, their presence may also be related to the conoidal profile.

Nuclear fibres are thicker and held together by interlocking angle processes along the junction of their six faces. Such a system could hold the pattern of lens fibres firmly together, preventing relative sliding of lens fibres, but allowing sufficient flexibility for fibre shape changes.

As a result of this investigation, it would appear that the force from the elastic capsule dictates changes in lens shape. Results favour the conclusion that cytoplasmic flow (not sliding) is the mechanism by which the lens fibres react to the demands of the capsule. This is greatest in the deeper fibres of the lens nucleus, and limited in the intermediate and cortical fibres. This differential facility for cytoplasmic flow may be a factor in selective nuclear axial thickening in accommodation. Cytoplasmic flow is presumably a passive reaction to the capsular force.

The results of the present study, offer some tentative answers to aspects of the original question -"what is the intra-lenticular mechanism of accommodation". It provides further comment of matters of disagreement and offers a concept of differential fibre responses to capsular shaping.

The hypothesis of differential cytoplasmic flow in nuclear and cortical fibres, requires further attention, coupled with comparison of their organelle content.

Further work could address the problem of presbyopia. Is presbyopia in part, a consequence of reduced facility for cortical cytoplasmic flow? A comparison of factors reported here, together with details of cytoplasmic content in young and presbyopic lenses would be of interest.

APPENDICES

	Page
Appendix A	143
Details of material used in this study	
Appendix B	146
Fixation method	
Appendix C	147
Software used in this study	
Appendix D	148
Data: Lens fibre density/cross-sectional area	

APPENDIX A

DETAILS OF MATERIALS USED IN THIS STUDY

Key to Abbreviations

M	Monkey	C	Capsule study
H	Human	B,W, and K	are laboratory codes
R	Right		
L	Left		
m	Male	c	Cynomolgus
f	Female	r	Rhesus
p	fixed by perfusion		
i	fixed by immersion		
w	whole eye fixed (after cornea removed) lens in situ		
d	capsule fixed after removal from the lens		
age	approximate age in years if known		
TF	length of time elapsed after death to fixation (hrs)		
CoD	cause of death		
RTA	road traffic accident		
CVA	cerebral vascular accident		
MI	miocardial infarction		
CA	carcinoma		
LVF	left vetricular failure		

Monkey material

Reference	weight/age Kg yrs	procedures/drugs	fix	lens form
MR37 cm	3.5		p	normal
M 54 rm	5.35		p	normal
M 72 cf	3.9	R1/4% Phospholine iodide	p	R failed L normal
MR73 cf	4.8	R1/4% Phospholine iodide	p	R steep L normal
MR74 cf	3.55	R1/4% Phospholine iodide	p	R failed L normal
MR77 cf	3	R1/4% Phospholine iodide	p	R failed L normal
MR78 cm	3.4	R lens dislocated	p	R steep L normal
MR80 cf	3.3		p	R normal L normal
MR85 cf	1.98 2/3		p	
MR86 cf			p	R normal
MR90 cf	3.4 7/8	R1/4 Phospholine iodide	p	R?failed L normal
MR91 cf	2.64 4	1/4% Phospholine iodide	p	Rsteeper L normal
MCR1 cm	7.62 10	none	i	R whole L decap
MCR2 cm	5.34 12	none	i	R decap L whole
MCR3 cm	0.84 3/12	none	i	R whole L decap
MCR4 cm	1.4 1yr	none	i	R whole L decap
MCR5 cf	1.7 11/12	none	i	R whole L decap

Human Tissue

Code	Age	CofD	ToF	Treatment of tissue and	fix
HW22 f	12	RTA	24-	donor eye fixed. Lens sectioned	iw
HW21	3?	RTA	36	perforated eye fixed " "	iw
HD 1	55/56	?	?	Donor eye fixed	iw
HB4 m	24	RTA	?24	Ant & equ capsule removed, fixed	id
HB5 f	44	CVA	28	Capsule detached and fixed	id
HB9 m	58	MI	48-	Capsule detached and fixed	id
HB3 m	61	CA	48-	damaged capsule, whole fixed	i?
HB6 f	62	CA	45	Capsule detached and fixed	id
HB8 f	66	LVF	48-	Ant capsule detached, fixed	id
HB1 f	67	MI	46	Capsule removed and fixed	id
HB2 "		"		" " " " "	
HB7 f	70	MI	26	Lens damaged.	i?d

APPENDIX B

FIXATION

Fixation was carried out by perfusion. Vetalar (Ketamine hydrochloride 10-12mg/Kg body weight) injected into the gluteous maximus muscle, served as a premedication. General anaesthesia was induced with either 50mg/Kg Nembutal or Sagital (pentobarbitone sodium) administered intraperitoneally. The anticoagulant, heparin sodium (0.4ml) was introduced directly into the left ventricle, and the external jugular vein, cut. Warmed 1% sodium nitrate in saline was pumped into the ventricle (exsanguination) followed immediately by a solution of 3% gluteraldehyde and 2% paraformaldehyde, buffered with sodium cacodylate. Material was stored in the fixative at 4 C.

APPENDIX C

SOFTWARE USED IN THIS STUDY

a) 'Cell Eye'

written by Mr.D De Cunha, of the Applied vision research unit, Department of Optometry and Visual Science.

This is a programme written in 'C', for use with an IBM. A.T. personal computer, 'Pluto' frame grabber and monochrome CCT camera. The program allows counting of cells, and incorporates some image processing.

b) 'Digitise'

written by Mr. G.P.Stafford .

This programme was written in Basic a, for use with an Amstrad 1614 personal computer, and Epsom Hi-80 plotter fitted with an HP-GL emulation R.O.M. The pen housing was replaced with a transparent sheet engraved with a cross hair.

The program was used to digitise the lens profiles from photographs, and to compute the length of curled up lens capsules, from scale drawings. Details of capsule thickness could be stored against accumulated length.

c) Shareware 'Curvefitting' written by T.S.Cox.

This program is designed for use on any IBM. compatible machine. Available from Shareware Marketing, 87 High St., Tonbridge. Kent. TN9 1RX.

APPENDIX D

DATA: LENS FIBRE DENSITY/CROSS-SECTIONAL AREA

Key d distance along tissue arc from polar axis (μm)
 d% percentage distance along arc from polar axis
 n number of fibres counted
 t/area = total area of count (μm^2)
 x-area = fibre cross-sectional area (μm^2)
 mean density is per $2500\mu\text{m}^2$

ML78 Unaccommodated lens, from fellow eye of dislocated lens

CODE	SLIDE	d	%d	n	t/area	mean x-area
ML78a total length 1320 μm	2	178	13.5	55	628	11.38
	4	378	28.6	220	2405	10.93
	5	393	30	74	820	11.09
	6	567	42.9	164	2342	14.28
	6a	592	44.8	49	1248	25.48
	7a	710	53.8	153	3736	24.4
	8a	800	60.6	109	3294	30.22
	10	940	71.2	78	2368	30.36
	12	992	75.2	43	1665	38.71
	12a	1012	75.5	67	2732	40.77
	13a	1078	81.7	50	2006	40.12
	14	1112	84.2	50	2160	43.21
	15	1170	88.6	43	1972	45.85

ML78 (cont.)

CODE	SLIDE	d	%d	n	t/area	mean xarea/density
ML78c	1		7.2	238.5	2500	10.48
total arc length	6		18.6	1287.5	12500	9.71
2800µm	9		25.45	823	10000	12.15
	12		36.1	572	10000	17.5
	15		51.2	790	15000	19
	17		60.9	352	5000	18.4
	18		65.72	102.5	2500	24.4
	19		70.27	921	20000	21.7
	20		74.82	1484	40000	26.95
	21		79.36	709	22500	31.7
	22		84.14	143	5000	34.97
ML78d	3	750	25	280	3606.8	12.88
total arc length	9	1387	46.2	28	411	14.71
3000µm	16	2167	72.2	99	1762.7	17.8
	17	2273	75.8	31	558	18
	21	2708	90.3	70	1746.8	24.95
	22	2808	93.6	76	2546.3	33.50
	23	2900	96.6	44	2239.2	50.89
ML78e/f	5	725	22.6	108	2500	23.15
total arc length	6	840	26.3	10	231	23.17
3200µm	11	1340	41.9	15	231	15.4
	13	1420	44.4	71	699	9.86
	18	2010	66.4	294	2483.3	8.45
	21	2355	74.6	308	4453.3	14.65

CODE	SLIDE	d	%d	n	t/area	mean xarea/density
ML78e/f cont						
	23	2585	80.8	296	4943.8	16.70
	24	2700	84.4	136	2975.2	21.94
	25	2805	87.7	149	3172	21.29
MR78 Dislocated lens						
MR78a						
	2	130	7.67	263	3781	14.38
total arc						
length	4	244	14.4	194	2477	12.77
1700μm	5	286	16.6	286	3761	13.15
	8	386	22.7	179	1846	10.31
	10	557	32.7	156	2347	15.05
	12	627	36.8	290	4117.8	14.2
	15	720	42.4	169	2605.9	15.42
	18	822	48.4	289	4357.6	15.08
	19	892	52.5	525	7294	13.89
	22	1130	66.5	318	445.4	14.00
	24	1224	70	180	2620	14.56
	26	1321	77.7	264	4728	17.9
	28	1475	86	139	2044	14.7
	29	1568	92.2	105	1906.6	18.12
	30	1619	95.2	33	581.5	17.62
	31	1656	97.4	48	972	20.25
MR78d						
	16		28.2	112	2007.8	17.93
total arc						
length	13		41.82	114	2054.3	18.02
	10		54.46	337	6114	18.14
2600μm						
	9		59.95	443	6970.6	15.74
	8		64.32	181	3424.2	18.92

CODE	SLIDE	d	%d	n	t/area	mean xarea/density
MR78d cont	2		90.5	148	3568.7	24.11
	1		94.9	310	7557.7	24.38
MR78e	30		29.2	71	1075	15.14
total arc length 2800 μ m	27		37.1	64	549	8.58
	24		45.1	136	1226.9	9.02
	21		53.1	166	1451.6	9.74
	19		58.5	229	2719	11.87
	17		63.84	118	1667.6	14.13
	13		74.56	519	8789.3	16.94
	12		77.24	101	1635.2	16.19
	11		79.9	556	10137.2	18.23
	10		82.6	394	7714.5	19.58
	9		85.27	735	14905.8	20.28
	7		90.1	202	5106.6	25.28
	5		93.84	91	2009.3	22.08
MR78f	13		38.49	14	222	15.86
	15		43.86	40	1075.2	26.59
	18		52	59	763.8	12.95
	21		59.5	51	673.9	13.21
	22		62.2	52	1134.1	21.81
	25		70.16	533	10000	19.79 133
	26		72.76	208	5000	24.04
	28		77.95	169	4554.6	26.95
	30		83.04	160	4307.2	26.92
	32		88.24	166	5000	30.03 83
	33		88.71	164	5225.7	31.01

CODE	SLIDE	d	%d	n	t/area	mean xarea/density
ML73 Unaccommodated lens (Fellow eye was phospholine iodide treated)						
ML73a/b	1	72	3.2	22	181	9.05
	3	270	11.78	335	3446.5	10.85
	7	588	25.87	1039	8490.5	8.23
	9	803	35.64	327	2419.8	7.4
	10		38.76	392	4014.1	10.24
	11		43.11	213	1588.6	7.46
	13		50.53	49	424.3	8.66
	14		54.89	378	3870.2	10.24
	15		58.76	497	4542.2	9.14
	17		67.2	292	2772.8	9.5
	19		76.09	407	5877	14.44
	22		85.42	299	6392.2	21.38
	23		89.78	339	9108.7	26.87
	24		93.69	446	14453.8	32.41
ML73c/d total arc length 3600μm	2	102	2.8	11	122.5	11.13
	8	685	19.03	20	187.6	9.38
	13	1167	32.44	114	790.9	6.94
	16	1147	40.22	121	657.5	5.44
	18		45.55	68	742.24	10.92
	21	1925	53.47	203	1771.3	8.73
	24	2197	61.11	287	1401.52	4.88
	26	2385	66.25	231	1362.1	5.9
	28	2693	74.81	260	2016.28	7.74

CODE	SLIDE	d	%d	n	t/area	mean xarea/density
ML73c/d	30	2878	79.92	274	1742.63	6.36
	33	3125	86.11	266	2862.76	10.76
	35		89.17	301	5231.42	17.38
	36		89.64	316	4268.18	13.5
	39		93	379	6839.7	18.05
	40		94.31	345	6574.86	19.06
	41middle c		95.42	142	3290.7	23.17
	outer (d)			193	4019.6	20.83
	43 outer d		98.06	280	5845.36	20.88
ML73e	13	1175	30.52	29	209.96	7.24
	14	1273	33.04	29	198.68	6.85
	16	1473	38.26	54	255.84	4.74
	22	2055	53.38	29	150.48	5.19
	25	2342	66.83	83	788.17	9.5
	29	2710	70.10	387	2761.9	7.14
	31	2892	75.12	100	1697	16.97
	32	2983	77.45	158	226.86	14.34
	33	3075	79.82	150	2589	17.26
	35	3260	84.68	39	652.9	16.74
	36		86.18	113	2344.8	20.75
	38	3445	89.48	100	1910	19.1
	39		91.6	120	2340	19.5
	40		93.9	149	2746	18.43
	41		95.71	228	6038.64	26.49
	42		97.32	148	3666.8	24.78
	43		98.62	185	5243.3	28.34

CODE	SLIDE	d	%d	n	t/area mean	xarea/density
ML73f	3	178	4.68	5	45	9.01
	7	578	15.06	26	315.6	12.14
	13		30.52	11	185.6	16.87
	14		33.06	30	396.3	13.21
	16		38.26	103	3052.92	29.64
	22		53.38	9	113.2	12.58
	25		66.83	26	297.44	11.44
	29		70.1	200	3684	18.42
	30		72.78	179	2810.3	15.7
	32		77.45	116	2532.3	21.83
	33		79.87	69	1489.7	21.59
	36		86.18	65	1791.4	27.56
	37		88	48	1601.3	33.36
	39		91.6	53	1640.9	30.96
	40		93.9	43	1704.1	39.63
	41		95.71	44	1891.1	42.98
	42		97.32	56	2630.9	46.85
	43		98.62	51	2622.4	51.42
MR73 (Phospholine iodide treated) lens						
MR73a/b	1		2.14	80	1167.6	14.6
total arc length 2200μm	2		6.59	288	4193	14.56
	3		11.14	422	4655.6	11.03
	4		15.68	607	4574.5	7.54
	6		24.32	363	3061.2	8.43
	8		33.04	493	3935.4	7.98

CODE	SLIDE	d	%d	n	t/area	mean xarea
MR73a/b	10		41.82	269	2248.8	8.36
	13		55.32	195	1926.6	9.88
	15		64.41	260	3458	13.3
	17		72.95	339	5168.1	15.25
	19		80	306	4868.9	15.91
	20		82.27	391	6733.5	17.22
	22		89.41	113	1907.4	16.88
	24		94.41	367	8064.1	21.97
MR73c/d	2	160	4.8	44		7.2
total arc length	4	370	11.2	124	2163.72	5.77
	7	685	20.7	5		13.4
3200μm	11	1085	32.9	48	332.5	6.92
	13	1270	38.4 c d	73 79	865.1 541.6	11.85 6.85
	14	1368	41.27c	42	270.9	6.45
	15	1455	44.09c	40	352.4	8.81
	18	1745	52.88c	42	277.6	6.61
	20	1935	58.64	168	1213.4	7.22
	21	2030	61.52	188	1402.3	7.46
	25	2417	72.94	415	5296.3	12.76
	27	2605	78.94	326	3165.5	9.7
	29	2745	83.18c d	324 126	4633 1245	14.30 9.88
	30		85.76d	65	1096.3	16.87
	31	2913	88.24c d	54 335	1186 6228.4	21.96 18.59
	33	3030	91.8 d	351	8687.7	24.75

CODE	SLIDE	d	%d	n	t/area	mean xarea
	34	3068	92.8 d	368	8734.7	23.73
	35	3125	94.7 d	226	5119.3	22.65
MR73e	1	73	2	11	124.2	11.29
total arc	2		3.9	13	77.6	5.97
length	6		12.1	81	847.1	10.49
3550µm	13		27.1	90	400.4	4.45
	19		39.9	16	170	10.62
	24		48.7	10	107	10.7
	25		50.5	13	77.61	5.97
	31		62.4	56	745.9	13.32
	33		69.6	322	4967.9	15.43
	34		72	248	4687.2	18.9
	36		76.6	260	4708.6	18.11
	38		81.6	293	4771.62	16.29
	39		84	422	8610.9	20.4
	41		89	320	7164.8	22.39
	42		91	298	6270.4	21.04
	44		95.8	236	5133.8	21.75
	45		96.1	562	13646.1	24.28
	46		96.2	125	3105	24.84
MR73f	2		3.9	12	260.4	21.7
total arc	6		12.1	9	267.8	29.76
length	13		27.1	12	241	20.1
3550µm	17		36	20	453.2	22.66
	19		39.9	46	955.9	20.78
	24		48.7	13	339.04	26.08

CODE	SLIDE	d	%d	n	t/area	mean xarea
MR73f cont.	25		50.5	30	665.4	22.18
	27		55.2	90	1377	15.3
	29		60	194	3438.5	17.72
	31		62.4	284	4586.6	16.15
	33		69.6	189	3116.4	16.49
	34		72	77	1619.3	21.03
	41		89	103	2324.7	22.57
	42		91	60	131.4	20.19
	45		96.1	184	5361.8	29.14
	46		96.2	67	2187.55	32.65

REFERENCES

- Benedetti E.L., Dunia I. & Bloemendal H. (1974)
" Development of junctions during differentiation of lens fibres ."
Proc. Nat. Acad. Sci. U.S.A. 71, 12 5073 - 5077
- Benedetti E.L., Dunia I., Bentzel C.J., Vermorken A.J.M., Kibbelaar M. & Bloemendal H. (1976)
" A portrait of plasma membrane specialisations in the eye lens epithelium and fibres."
Biochim. Biophys Acta 457, 353 - 384
- Benedetti E.L., Dunia I., Ramaekers F.C.S. & Kibbelaar M.A. (1981)
" Lenticular plasma membranes and cytoskeleton. "
in " Molecular and Cellular Biology of the Eye Lens."
Ed. Bloemendal H., Pub: J Wiley and Sons. New York.
- Bito L.Z., DeRousseau C.J., Kaufman P.L., & Bito J.W. (1982)
" Age dependent loss of accommodative amplitudes in rhesus monkeys : an animal model for presbyopia."
Invest. Ophthalmol. & Vis. Sci. 23, 23 - 31.
- Bito L.Z., Kaufman P.J., DeRousseau C.J. and Koretz J. (1987)
" Presbyopia: An animal model and experimental approaches for the study of the mechanism of accommodation and ocular ageing."
Eye 1, 222 - 230
- Bradley R.H., Ireland M.E. & Maisel H. (1979)
" Age changes in the skeleton of the human lens. "
Acta. Ophthalmologica 57, 461 - 469
- Brown N.A.P. (1972a)
" An advanced slit-image camera. "
Brit. J. Ophthalmol. 56, 624 - 631
- Brown N.A.P. (1972b)
"Quantitative slit - image photography of the lens."
Trans. Ophthalmol. Soc. U.K. 92, 303 - 317
- Brown N.A.P. (1973a)
" The change in shape of the internal form of the lens of the eye on accommodation."
Exp. Eye Res. 15, 441 - 460.
- Brown N.A.P. (1973b)
in " The Human Lens in Relation to Cataract" Ciba Foundation Symposium, Pub:-Elsevier, New York pgs 65 - 78
- Brown N.A.P. (1974a)
" The change in lens curvature with age. "
Exp. Eye Res. 19, 175 - 183.

- Brown N.A.P. (1974b)
 " The shape of the lens equator. "
 Exp. Eye. Res. 19, 571 - 576.
- Brown N.A.P., Bron A.J., Sparrow J.M., (1987)
 " An estimate of the size and shape of the human lens
 fibre in vivo. "
 Brit. J. Ophthalmol. 71, 916 - 922.
- Burnside B. (1975)
 " The form and arrangement of microtubules: An historical
 primarily morphological revue "
 Ann. N.Y. Acad. Sci. 253, 14 - 26
- Carhart M.W.C. (1981)
 " Scanning electron microscopy of the crystalline lens "
 (Final year Project), The City University, London.
- Chin N.B., Ishikawa S., Lapin H., Davidowitz J., & Breinin
 G.M. (1968)
 " Accommodation in monkeys induced by midbrain
 stimulation."
 Invest Ophthalmol. 7, 386 - 396
- Cohen A.I. (1965)
 " The electron-microscopy of the normal human lens. "
 Invest. Ophthalmol. 4, 433 - 446
- Coleman D.J. (1970)
 " Unified model for accommodative mechanism "
 Amer. J. Ophthalmol. 69, 6 1063 - 1079
- Coleman D.J. (1986)
 " On the hydraulic suspension theory of accommodation "
 Trans. Amer. Ophthalmol. Soc. 84, 846 - 868
- Costello M.J., McIntosh T.J. & Robertson J.D. (1961)
 " Square-array fiber cell membranes in the mammalian lens"
 Proc. 42nd Ann Meeting Electron Microscopy Soc. Am.
 ed. Bailey G.W., publ: San Francisco Press Inc. U.S.A.
- Dickson D.M., & Crock G.W. (1972)
 " The interlocking patterns on primate lens fibres. "
 Inv. Ophthalmol. 11, 809 - 815
- Dickson D.M., & Crock G.W. (1975)
 " Fine structure of primate lens fibres." in Bellows J.G.
 " Cataract and Abnormalities of the Lens " Pub: Grune and
 Stratton, New York. pgs 49 - 59.
- Donders F.L. (1864)
 " On the anomalies of accommodation and refraction of the
 eye " New Sydeham Soc., London. Cited by Fincham 1937.

- Duane A. (1912)
 " Normal values of accommodation at all ages "
 J. Am. Med. Assoc. 59, 1010 - 1013
- Duke Elder (1958)
 " The Eye in Evolution " in vol. 1 " Systems of Ophthalmology " Pub: Henry Kimpton, London. Pgs 640 - 654.
- Farnsworth P.N., Mauriello J.A., Burke-Gadomski P., Kulyk T. & Cinotti A.A. (1976a)
 " Surface ultrastructure of the human lens capsule and zonular attachments. "
 Invest Ophthalmol. 15, 1 36 - 39.
- Farnsworth P.N., Burke-Gadomski P., Kulyk T., Mauriello J.A. & Cinotti A.A. (1976b)
 " Surface ultrastructure of the epithelial cells of the mature human lens. "
 Exp. Eye Res. 22, 615 - 624
- Farnsworth P.N., Shyne S.E., Burke P.A. and Fasano A.V. (1980a)
 " Cellular maturation of human lens fibres "
 in "Red Blood Cells and Lens Metabolism" Srivastava (ed) Elsevier N.Holland.
- Farnsworth P.N., Shyne S.E., Caputo S.J., Fosano A.U. and Spector A. (1980b)
 " Microtubules: A major cytoskeletal component of the human lens. "
 Exp. Eye Res. 30, 611 - 615.
- Fincham E.F. (1925)
 " The changes in the form of the crystalline lens in accommodation. "
 Trans. Optical Soc. U.K. 26, 5 239 - 269
- Fincham E.F. (1929)
 " The function of the lens capsule in the accommodation of the eye. "
 Trans. Optical Soc. U.K. 15, 3 101 - 117
- Fincham E.F. (1936)
 " Experiments on the influence of tension upon the form of the crystalline lens. "
 Trans. Optical Soc. U.K. 56, 138 - 147.
- Fincham E.F. (1937)
 " The mechanisms of accommodation. "
 Brit. J. Ophthalmol. 21 (monograph supplement 8) 1 - 80
- Fisher R.F. (1969a)
 " Elastic constants of the human lens capsule. "
 J. Physiol. 201, 1 - 19

- Fisher R.F. (1969b)
 " The significance of the shape of the lens and capsular energy changes in accommodation. "
 J. Physiol. 201, 21 - 47
- Fisher R.F. (1971)
 " The elastic constants of the human lens. "
 J. Physiol. 212, 147 - 180.
- Fisher R.F., & Pettet B.E. (1972)
 " The postnatal growth of the capsule of the human crystalline lens. "
 J. Anat. 112, 207 - 214.
- Fisher R.F. (1973a)
 " Presbyopia and the changes with age in the human crystalline lens. "
 J. Physiol. 228, 765-779.
- Fisher R.F. (1973b)
 in " The Human Lens in Relation to Cataract." Ciba Foundation Symposium, Pub: Elsevier, New York. Pgs 73 - 78
- Fisher R.F., & Wakely J. (1976)
 " The elastic constants and ultrastructural organisation of a basement membrane (lens capsule)
 Proc. R. Soc. Lond. 193, 335 - 358.
- Fisher R.F. (1977)
 " The force of contraction of the human ciliary muscle during accommodation. "
 J. Physiol. 270, 51 - 74
- Fisher R.F., & Hayes B.P. (1979)
 " Thickness and volume constants and ultrastructural organisation of basement membrane (lens capsule)."
 J. Physiol. 293, 229 - 245
- Fisher R.F. (1982)
 " The vitreous and lens in accommodation. "
 Trans. Ophthalmol. Soc. 102, 318.
- Fisher R.F. (1983)
 " Is The vitreous necessary for accommodation in man ? "
 Brit. J. Ophthalmol. 67, 206.
- Fisher R.F. (1986)
 " The ciliary body in accommodation. "
 Trans. Ophthalmol. Soc. U.K. 108, 208 - 219.
- Fisher R.F. (1988)
 " The mechanics of accommodation in relation to presbyopia "
 Eye 2, 646 - 649.

- Goodenough D.A. (1979)
 " Lens gap junctions: A structural hypothesis for nonregulated low resistance intercellular pathways."
 Invest. Ophthalmol. & Vis. Science. 18, 1104 - 1122.
- Goodenough D.A., Dick J.S.B. & Lyons J.E. (1980)
 "Lens metabolic cooperation: a study of mouse lens transport and permeability visualized with freeze-substitution autoradiography and electron microscopy."
 J, Cell Biol. 86, 576 - 589.
- Gullstrand A. (1924)
 in Appendixes to Helmholtz's " Treatise on Physiological Optics" Vol. 1 Translated from German and edited by Southall J.P.C., First published in English by The Optical Society of America. Pub: Dover, New York 1962.
 pgs 382 - 415
- Hanna C. & O'Brien J. (1961)
 " Cell production and migration in the epithelial layer of the lens. "
 Archiv. Ophthalmol. 66, 103 - 107
- Helmholtz H.von (1909 /1924)
 " Treatise on Physiological Optics. " (English Translation) Published in English by the Optical Soc. Am. Translated and edited by J.P.C. Southall (1924) from 3rd German Ed. 1909, Vol.1, Chapter 4, "Mechanism of Accommodation" 382 - 415
- Heyningen R. van (1971)
 " The human lens. 3: Some observations on the post-mortem lens"
 Exp. Eye Res. 13, 155 - 160.
- Hogan M.J., Alvaraldo J.A. and Wedell J.E. (1971)
 " Histology of the Human Eye: An Atlas and Textbook. "
 W.B. Saunders and Co. Chapter 12
- Howcroft M.J. & Parker J.A. (1977)
 " Aspheric curvatures for the human lens "
 Vis.Res. 1, 1217 - 1223
- Jongebloed W.L., Figueras M.J., Dijk F. Worst J.F.G. (1987)
 " A morphological description of human cataractous lenses by S.E.M. "
 Doc. Ophthalmol. 67, 197 - 207
- Kaufman P.L., Bito L.Z., & DeRousseau C.J. (1982)
 " The development of presbyopia in primates. "
 Trans. Ophthalmol. Soc. U.K. 102, 323 - 326.

- Kendall C.M. (1982)
 " Scanning electron microscopy of the primate crystalline lens. "
 (Final year project) The City University, London.
- Koretz J.F. & Handelsman G.H. (1982)
 " Model of the accommodative mechanism in the human eye "
 Vis. Res. 22, 917 - 924.
- Koretz J.F., & Handelsman G.H. (1983)
 " A model for accommodation in the young human eye : The affects of lens elastic anisotropy on the mechanism.
 Vis. Res. 23, 1679 - 1686
- Koretz J. Handelsman G.H. & Brown N.A.P. (1984)
 " Analysis of human crystalline lens curvature as a structure of function and accommodative state and age. "
 Vis. Res. 24, 10, 1141 - 1151.
- Koretz J.F., & Handelsman G.H. (1985)
 " Internal crystalline lens dynamics during accommodation, age related change. "
 Atti Fondazione G. Ronchi. 40, 409 - 416.
- Koretz J.F., & Handelsman G.H. (1986)
 " Modelling Age - related accommodative loss in the human eye. "
 Mathematical Modelling, 7, 1003 - 1014.
- Koretz J.F., Neider M.W., Kaufman P.L., Bertasso A.M., DeRousseau C.J., Bito L.Z. (1987a)
 " Slit-lamp Studies of the rhesus monkey eye. 1. Survey of the anterior chamber."
 Exp. Eye Res. 44, 307 - 318.
- Koretz J.F., Neider M.W., Kaufman P.L., Bertasso A.M., DeRousseau C.J., Bito L.Z. (1987b)
 " Slit lamp studies of the rhesus monkey eye: 2. Changes in crystalline lens shape, thickness and position during accommodation and ageing "
 Exp. Eye Res. 45, 317 - 326.
- Koretz J.F., Neider M.W., Kaufman P.L., Bertasso A.M., DeRousseau C.J., Bito L.Z. (1988a)
 " Slit lamp studies of the rhesus monkey eye: 3. The zones of discontinuity."
 Exp. Eye Res. 46, 871 - 880
- Koretz J.F. & Handelsman G.H. (1988b)
 " How the human eye focuses."
 Scientific American. July 88, 253, 1, 64 - 72.
- Kuszak J., Maisel H. & Harding C.V. (1978)
 " Gap junctions of chick lens fibre cells. "
 Exp. Eye. Res. 27, 495 - 498

- Kuszak J., Alcali J., & Maisel H. (1980)
 " The surface morphology of embryonic and adult chick lens
 fibre cells "
 Am. J. Anat. 159, 395 - 410.
- Kuszak J. & Rae J.L. (1982)
 " Scanning electron microscopy of the frog lens. "
 Exp. Eye Res. 35, 499 - 518
- Kuszak J., Bertram B.A., Macsai M.S., Rae J.L. (1984)
 "Sutures of the crystalline lens : A review "
 Scan. Elect. Microscopy. 3, 1369 - 1378.
- Kuszak J.R., Ennesser J.U., Umlas J., Macsai-Kaplan M.S. &
 Weinstein R.S. (1988)
 "The ultrastructure of fibre cells in primate lenses: A
 model for studying membrane senescence. "
 J. Ultrastruct. Res. 100, 60 - 74.
- Kuwabara T. (1968)
 " Microtubules in the lens"
 Arch. Ophthalmol. 79, 189 - 195.
- Kuwabara T. (1975)
 "The maturation of the lens cell: A morphological study."
 Exp. Eye Res. 20, 427 - 443.
- Leeson T.S. (1971)
 " Lens of the rat eye: an electron microscopic and freeze
 etch study. "
 Exp. Eye Res. 11, 78 - 82
- Lerche W., & Wulle K. G. (1969)
 " Electron microscopic studies on the development of the
 human lens. "
 Ophthalmologica 158, 296 - 309
- Maisel H., Harding C.V., Alcalá J.R. & Bradley R. (1981)
 " The morphology of the lens. "
 in "Molecular and Cellular Biology of the Eye Lens"
 ed. Bloemendal H., Pub: J.Wiley & Sons, New York.
- Mayer H.D., Hampton J.C. & Rosario B. (1961)
 " A simple method for removing the resin from epoxy-
 embedded tissue "
 J. Biophys. Biochem. Cytol. 9, 909 - 910.
- McCulloch C. (1954)
 " The zonule of Zinn: Its origin, course, insertion, and
 its relation to neighbouring structures. "
 Trans. Amer. Ophthalmol. Soc. 52, 525 - 585

- Neisel P. (1982)
 " Visible changes to the crystalline lens with age."
 Trans. Ophthalmol. Soc. U.K. 102, 327 - 329
- O'Neill W.D. & Doyle J.M. (1968)
 " A Thin shell deformation analysis of the human lens "
 Vis Res. 8, 193 - 206.
- Patnaik B. (1967)
 " A Photographic study of accommodative mechanisms :
 Changes in the lens nucleus during accommodation. "
 Inv. Ophthalmol. 6, 601 - 611.
- Pflugk A. von. (1906)
 " Uber die akkommodation des auges der taube, nebst
 bemerkungen aber die akkommodation des affen (Maccus
 Cynomolgus) und menschen. "
 Wiesbaden. Verlag von J.F. Bergmann. 1906 1 - 46
- Pflugk A. von. (1935)
 " What occurs in the eye during accommodation. "
 Brit. J. Physiol Opt. : April 1935
- Philipson (1973)
 in " The Human Lens in Relation to Cataract." Ciba
 Foundation Symposium. 1973. pg 67 - 78
- Rafferty N.S. and Goosens W. (1978a)
 " Growth and ageing of the lens capsule. "
 Growth 42, 375 - 389
- Rafferty N.S. & Goossens W. (1978b)
 " Cytoplasmic filaments in the crystalline lens of various
 species : Functional correlations. "
 Exp. Eye Res. 26, 177 - 190.
- Rafferty N.S. (1985)
 " Lens morphology " in " The Ocular Lens " ed Maisel
 Marcel Dekker New York Pgs 1 - 60
- Rafferty N.S. & Scholz D.L. (1989)
 " Comparative study of actin filaments patterns in lens
 epithelial cell. Are these determined by the mechanisms of
 lens accommodation ? "
 Cur. Eye Res. 8, 6 569 - 579
- Rohen J.W., Kaufman P.L., Eichhorn M., Goeckner P.A. & Bito
 L.Z. (1989)
 " Functional morphology of Accommodation in the Raccoon."
 Exp. Eye Res. 48, 523 - 537
- Ruskell G.L. (1981)
 Personal communication

- Sakuragawa M., Kuwabara T., Kinoshita J.H. Fukui H.N. (1975)
 " Swelling of lens fibres. "
 Exp. Eye Res. 21, 381 - 394.
- Salzmann M. (1912)
 " The Anatomy and Histology of the Human Eyeball in the Normal State. " (English translation)
 Translated E.V.L. Brown, Chicago 1912 Pgs 162 - 173
- Seland J.S. (1974)
 " Ultrastructural changes in the normal human lens capsule from birth to old age."
 Acta Ophthalmol. 52, 688 - 706
- Sivak J.G. (1980)
 " Accommodation in vertebrates . A contemporary survey. "
 in " Currents Topics in Eye Research" ed Zadunaissky J.A., & Davson H. Academic Press. Pgs 281 - 330
- Sivak J.C, Hilderbrand T.E., Lebert C.G., Myshak L.M., & Ryall L.A. (1986)
 " Ocular accommodation in chickens : corneal versus lenticular accommodation and effect of age. "
 Vis. Res. 26, 1865 - 1872
- Smith Priestly (1883)
 " On the growth of the crystalline lens."
 Trans. Ophthalmol. Soc. U.K. Vol 111
- Smith Priestly (1929)
 in the discussion that follows " The function of the lens capsule in the accommodation of the eye." Fincham 1929. Trans. Optical Soc. U.K. 56, 115 - 117.
- Tornqvist G. (1966)
 " Effect of topical carbachol on the pupil and refraction in young and presbyopic monkeys. "
 Invest Ophthalmol. 5, 186 - 195
- Tornqvist G. (1967)
 " The relative importance of the parasympathetic and sympathetic nervous systems for accommodation in monkeys. Invest. Ophthalmol. 6, 6, 612 - 617
- Trump B.J., Smuckler E.A., & Benditt E.P. (1961)
 " A method for staining epoxy sections for light microscopy."
 J. Ultrastruct. Res. : 3, 343 - 348.
- Tscherning M, (1904)
 " Physiologic Optics " Translated from french by C.Weiland, Pub: Keystone, Philadelphia U.S.A. 2nd Edition
 pgs 171 - 189

- Tscherning M. (1909)
 " Herman V Helmholtz et la theorie de L'accommodation. "
 Paris cited by Fincham E.F. (1937)
- Viggiano G. (1966)
 " Comportamento reologico degli omogenati di coetecchia e di lenti in toto "
 Boll. Soc. Ital. Biol. sper. 42, 2044 - 2046
- Wanko T. & Gavin M.A. (1958)
 " The fine structure of the lens epithelium. "
 Arch. Ophthalmol. 60, 868 - 879.
- Wanko T. & Gavin M.A. (1959)
 " Electron microscope study of lens fibres "
 J. Biophysics & Biochemical Cytol. 6, 97 - 101
- Wanko T. and Gavin M.A. (1961)
 " Cell surfaces in the crystalline lens "
 in " The Structure of the Eye " ed Smelser G.K.
 Academic Press Pages 221 - 233
- Weale R.A. (1962)
 " Presbyopia "
 Brit. J. Ophthalmol. 46, 660-668.
- Weale R.A. (1982)
 " A Biography of the Eye. " Chapter 7 "The crystalline lens" Pub: H.K. Lewis London. 185 - 237
- Willekens B. & Vrenson G. (1981)
 " The three dimensional organisation of the lens fibres in the rabbit. "
 Graef's Arch. Ophthalmol. 216, 275 - 289
- Willekens B. & Vrenson G. (1982)
 " Three dimensional Ultrastructure of the human lens fibre."
 Association for Eye Research. Poster 1982 suppl. pg 59
- Worgul B.W., Iwamoto T. & Mirriam G.R. (1977)
 " R.N.A.-containing cytoplasmic inclusions at the termini of maturing fibres in the rat lens. "
 Ophthalmol. Res. 9, 388 - 396.
- Young T. , (1801)
 " On the mechanisms of the eye. "
 Trans. Roy. Soc. 1801 cited by Fincham 1937
- Zeeman W.P.C. (1908)
 " Uber die form der hinteren linsenflache "
 Klin. Monatsbl. F. Augenheilk. :46, 83 - 86.